

GONADAL SEX DIFFERENTIATION OF RICE FIELD FROG *Hoplobatrachus rugulosus*
(Wiegmann, 1834)



A Dissertation Submitted in Partial Fulfillment of the Requirements
for the Degree of Doctor of Philosophy in Biological Sciences

Common Course

FACULTY OF SCIENCE

Chulalongkorn University

Academic Year 2020

Copyright of Chulalongkorn University

การเปลี่ยนแปลงสภาพเพศของอวัยวะสร้างเซลล์สืบพันธุ์ของกบนา *Hoplobatrachus rugulosus*
(Wiegmann, 1834)



วิทยานิพนธ์นี้เป็นส่วนหนึ่งของการศึกษาตามหลักสูตรปริญญาวิทยาศาสตรดุษฎีบัณฑิต
สาขาวิชาวิทยาศาสตร์ชีวภาพ ไม่สังกัดภาควิชา/เทียบเท่า
คณะวิทยาศาสตร์ จุฬาลงกรณ์มหาวิทยาลัย
ปีการศึกษา 2563
ลิขสิทธิ์ของจุฬาลงกรณ์มหาวิทยาลัย

ธฤชวรรณ ไตรจิตต์ : การเปลี่ยนแปลงสภาพเพศของอวัยวะสร้างเซลล์สืบพันธุ์ของกบนา *Hoplobatrachus rugulosus* (Wiegmann, 1834). (GONADAL SEX DIFFERENTIATION OF RICE FIELD FROG

Hoplobatrachus rugulosus (Wiegmann, 1834)) อ.ที่ปรึกษาหลัก : ผศ. ดร.จิรารัช กิตนะ, อ.ที่ปรึกษาร่วม : ผศ.

ดร.นพดล กิตนะ

กบนา *Hoplobatrachus rugulosus* เป็นกบที่มีการแพร่กระจายพันธุ์อยู่ในประเทศไทย และมีศักยภาพในการเป็นสัตว์ทดลองในงานวิจัยหลายด้าน ในการศึกษาเบื้องต้นพบรูปแบบของการเปลี่ยนแปลงสภาพเพศของกบชนิดนี้มีแนวโน้มที่จะเป็นแบบ undifferentiated เนื่องจากพบการเจริญของอวัยวะสร้างเซลล์สืบพันธุ์เป็นรังไข่เมื่อเมทาโมริโฟซิสสมบูรณ์ในกบทุกตัว อย่างไรก็ตามข้อมูลเรื่องรูปแบบของการเปลี่ยนแปลงสภาพเพศยังไม่ชัดเจน การศึกษาครั้งนี้จึงมีจุดประสงค์เพื่อศึกษาลำดับเหตุการณ์ของการเจริญและรูปแบบการเปลี่ยนแปลงสภาพเพศ รวมไปถึงศักยภาพในการสังเคราะห์สเตียรอยด์ในช่วงการเจริญของเนื้อเยื่ออวัยวะสร้างเซลล์สืบพันธุ์ โดยการศึกษาครั้งนี้ เอ็มบริโอกบนาได้มาจากการกระตุ้นให้เกิดการปฏิสนธิภายในห้องทดลอง ในสภาวะที่ได้รับแสงและอุณหภูมิตามธรรมชาติ ระยะการเจริญของกบนาระบุโดยใช้ระบบของ Gosner (1960) และบันทึกช่วงเวลาในแต่ละระยะของการเจริญ ผลการศึกษาพบว่ากบนาไม่มีระยะเวลาในการเจริญ 25-33 วัน จนกระทั่งเมทาโมริโฟซิสสมบูรณ์ อวัยวะสร้างเซลล์สืบพันธุ์สามารถสังเกตเห็นได้ภายใต้กล้องสเตอริโอ ตั้งแต่ระยะ Gosner 33 (9-12 วันหลังฟักจากไข่) ในขณะที่ความแตกต่างของอวัยวะสร้างรังไข่สามารถสังเกตเห็นได้ในช่วง 3-4 สัปดาห์หลังเมทาโมริโฟซิสสมบูรณ์ การศึกษาฮิสโตโลยีพบการสร้าง genital ridge เริ่มขึ้นในระยะ Gosner 25 (1-2 วันหลังฟักจากไข่) และการเปลี่ยนแปลงไปเป็นรังไข่ เริ่มขึ้นในระยะ Gosner 36 (13-17 วันหลังฟักจากไข่) โดยรังไข่ที่กำลังเจริญพบโอโอโกเนียปฐมภูมิเป็นจำนวนมาก ซึ่งจะเจริญไปเป็นโอโอไซต์ต่อไป ในขณะที่ชั้นเมดัลลาเกิดการสลายเพื่อสร้าง ovarian cavity โดยในช่วงเมทาโมริโฟซิส จะพบเฉพาะรังไข่เท่านั้น ส่วนการเปลี่ยนแปลงไปเป็นอวัยวะเพศจะเกิดขึ้นภายหลังในช่วง 1 สัปดาห์หลังเมทาโมริโฟซิสสมบูรณ์ โดยเกิดผ่านภาวะเพศกำกวม อวัยวะสร้างเซลล์สืบพันธุ์ในภาวะเพศกำกวมนี้ ประกอบด้วยเนื้อเยื่ออวัยวะที่กำลังเจริญ และเซลล์ไข่ระยะโอโอไซต์ ทั้งในภาวะที่ปกติและผิดปกติ พบอวัยวะที่เจริญเต็มที่ครั้งแรกในระยะ 6 สัปดาห์หลังเมทาโมริโฟซิสสมบูรณ์ จากข้อมูลดังกล่าวจึงสรุปได้ว่า รูปแบบของการเปลี่ยนแปลงสภาพเพศของกบนาเป็นแบบ undifferentiated โดยพบการเจริญของอวัยวะสร้างเซลล์สืบพันธุ์เพศเมียในช่วงที่กำลังเมทาโมริโฟซิส จากนั้นจึงพบอวัยวะสร้างเซลล์สืบพันธุ์ในภาวะเพศกำกวม และอวัยวะสร้างเซลล์สืบพันธุ์เพศผู้ในภายหลัง การศึกษาศักยภาพในการสังเคราะห์สเตียรอยด์ทำโดยศึกษาปริมาณการแสดงออก mRNA ของ cytochrome P450 17-hydroxylase/C17-20 lyase (CYP17) และ cytochrome P450 aromatase (CYP19) โดยวิธี quantitative real-time RT-PCR และการปรากฏอยู่ของ CYP17 mRNA ในเนื้อเยื่อโดยวิธี *in situ* hybridization ผลการศึกษาพบว่า ระดับของ CYP17 mRNA ในกลุ่มเพศผู้ระยะ 4-11 สัปดาห์หลังเมทาโมริโฟซิส มีระดับที่สูงกว่าทุกกลุ่ม ซึ่งสอดคล้องกับการปรากฏอยู่ของ CYP17 mRNA ในเนื้อเยื่ออวัยวะสร้างเซลล์สืบพันธุ์ โดยมีการแสดงออกแบบจำเพาะใน Leydig cells ในเนื้อเยื่ออวัยวะของทั้งในอวัยวะและภาวะเพศกำกวมของกบในช่วงอายุ 4-16 สัปดาห์หลังเมทาโมริโฟซิส แต่ไม่พบสัญญาณของ CYP17 mRNA ในทุกตัวอย่างรังไข่ การแสดงออกของ CYP19 mRNA ในกลุ่มเพศเมียระยะ 4-11 สัปดาห์หลังเมทาโมริโฟซิส พบว่ามีระดับสูงกว่าทุกกลุ่ม ซึ่งสอดคล้องกับการศึกษาฮิสโตโลยีที่พบโอโอไซต์ที่ล้อมรอบด้วยเซลล์ فولลิเคิลจำนวนมากเพิ่มขึ้น แสดงว่ารังไข่อาจมีการทำงานได้เต็มที่แล้ว ส่วนในกลุ่มภาวะเพศกำกวม ระยะ 4-11 สัปดาห์หลังเมทาโมริโฟซิส การแสดงออกของ CYP17 mRNA มีระดับที่สูง ในขณะที่การแสดงออกของ CYP19 mRNA มีแนวโน้มต่ำกว่า แสดงว่าเนื้อเยื่ออวัยวะของภาวะเพศกำกวม มีการเจริญดีและมีศักยภาพในการสังเคราะห์สเตียรอยด์ ในขณะที่เนื้อเยื่อรังไข่ของภาวะเพศกำกวม อาจไม่เกิดการ ทำงาน จากผลการศึกษาครั้งนี้พบว่า CYP17 และ CYP19 น่าจะมีบทบาทในระยะหลังจากอวัยวะสร้างเซลล์สืบพันธุ์ผ่านกระบวนการเปลี่ยนแปลงสภาพเพศไปแล้ว ซึ่งเป็นช่วงที่พบศักยภาพในการสังเคราะห์สเตียรอยด์ในอวัยวะสร้างเซลล์สืบพันธุ์มีความแตกต่างระหว่างเพศ ผลการศึกษานี้ทำให้ทราบข้อมูลพื้นฐานที่สำคัญสำหรับการศึกษาด้านชีววิทยาการเจริญในกบต่อไป

สาขาวิชา วิทยาศาสตร์ชีวภาพ

ปีการศึกษา 2563

ลายมือชื่อนิสิต

ลายมือชื่อ อ.ที่ปรึกษาหลัก

ลายมือชื่อ อ.ที่ปรึกษาร่วม

5772819623 : MAJOR BIOLOGICAL SCIENCES

KEYWORD: ANURAN, DEVELOPMENT, GONAD, INTERSEX, SEX DIFFERENTIATION, STEROIDOGENIC ENZYME

Thrissawan Trajitt : GONADAL SEX DIFFERENTIATION OF RICE FIELD FROG *Hoplobatrachus rugulosus* (Wiegmann, 1834).

Advisor: Asst. Prof. Dr. JIRARACH KITANA Co-advisor: Asst. Prof. Dr. NOPPADON KITANA

The rice field frog *Hoplobatrachus rugulosus*, a species widely distributed in Thailand, has potential to be a model in many fields of research. A preliminary study demonstrated that the gonadal differentiation in this frog showed tendency to be an undifferentiated type since all individuals had ovaries at complete metamorphosis. However, the information was still unclear. Therefore, this study aimed to investigate the chronology and pattern of gonadal sex differentiation as well as steroidogenic potential of gonadal tissues during development. The frog embryos were obtained by stimulating fertilization in laboratory under natural light and temperature conditions. Their developmental stage was identified using Gosner (1960) system. The time period during each stage of development was also recorded. *H. rugulosus* spent 25-33 days for development to complete metamorphosis. The gonad was firstly observed by stereomicroscope at Gosner stage 33 (9-12 days post hatch, dph), while the testis and ovary were distinguishable by morphology from 3-4 weeks after metamorphosis. Histological analysis showed that genital ridge formation began at stage 25 (1-2 dph) and ovarian differentiation began at stage 36 (13-17 dph). The developing ovary appeared with numerous primary oogonia which developed into oocytes, while the medulla regressed to form an ovarian cavity. During metamorphosis, only an ovary was observed. Testicular differentiation began later, during the first week after metamorphosis, and occurred via an intersex condition. The intersex gonads contained developing testicular tissue with both normal and atretic oocytes. The fully developed testis was firstly identified at 6 weeks after metamorphosis. Thus, the pattern of gonadal sex differentiation in *H. rugulosus* is an undifferentiated type, in which only female gonads are observed during metamorphosis and intersex and male gonads are observed later. For steroidogenic potential of gonad, the expression level of mRNA encoding cytochrome P450 17-hydroxylase/C17-20 lyase (CYP17) and cytochrome P450 aromatase (CYP19) were observed by quantitative real-time RT-PCR and localization of CYP17 mRNA in the tissues was observed by *in situ* hybridization. The results showed that CYP17 mRNA levels in male group at 4-11 weeks after metamorphosis showed a higher level than those of other groups. This result corresponded to their localization in the gonadal tissues that the CYP17 signals were specifically detected in Leydig cells of testicular tissue in both testes and intersex gonads at 4-16 weeks after metamorphosis but undetectable in all ovary samples. The CYP19 mRNA levels in female group at 4-11 weeks after metamorphosis was higher than those of other groups which corresponded with the histological results that the number of oocytes and follicular cells were increased, indicating potential steroidogenic function of the ovary. In intersex group at 4-11 weeks after metamorphosis, the level of CYP17 mRNA was high, whereas the level of CYP19 mRNA was relatively lower. It could be suggested that the testicular tissue of intersex gonad has developed and had steroidogenic function, while the ovarian tissue of intersex gonad may not function. Based on the present results, the role of CYP17 and CYP19 mRNA in sex differentiation in *H. rugulosus* may occur after the gonadal sex differentiated and the steroidogenic potential of the gonads exhibited sexual dimorphic pattern. These results provide a crucial basis for further research on developmental biology in anuran species.

Field of Study: Biological Sciences

Academic Year: 2020

Student's Signature

Advisor's Signature

Co-advisor's Signature

ACKNOWLEDGEMENTS

I would like to express my sincerest gratitude to my advisor, Assistant Professor Dr. Jirarach Kitana, I always appreciate her suggestions, guidance, patience, and encouragement throughout the doctoral study. Additionally, I would like to express my deepest appreciation to my co-advisor, Assistant Professor Dr. Noppadon Kitana for his encouragement, kind support, and invaluable guidance and suggestions.

I would like to thank the members of my thesis committee, Associate Professor Dr. Chatchawan Chaisuekul (Chairperson), Professor Dr. Suchinda Malaivijitnond, Assistant Professor Dr. Kanoktip Packdibamrung, Assistant Professor Dr. Wichase Khonsue, and Associate Professor Dr. Duangjai Boonkusol, for their time and comprehensive scientific suggestions.

Moreover, special thank is given to Professor Dr. Makoto Osada for his kind support and suggestions when I conducted part of my doctoral research in Japan. I also thank the members of the Aquacultural Biology Laboratory, Graduate School of Agricultural Science, Tohoku University, Japan for their kind support.

I would like to express my sincere appreciation to Assistant Professor Dr. Kazue Nagasawa, my role model teacher, for his attitude, opinions, comments and especially his inputs on the in situ hybridization technique and Assistant Professor Dr. Sukanya Jaroenporn for her excellent advice on the qrt-RT-PCR technique.

I would like to express my sincere gratitude to Assistant Professor Dr. Wichase Khonsue, the Amphibian and Reptile Research Unit, Chulalongkorn University for providing the frogs and frog culture facilities and Professor Dr. Somsak Panha, Animal Systematics Research Unit at Department of Biology, Faculty of Science, Chulalongkorn University for supporting laboratory equipment such as a high-resolution stereomicroscope for morphological study.

In addition, special thank is given to Dr. Phum Tachachartvanich, Dr. Tongchai Thitiphuree, Dr. Patchara Danaisawadi, Dr. Panupong Thammachoti, Dr. Ruttapon Srisonchai, Dr. Parin Jirapatrasilp and Mr. Taratorn Fainanta for their kindness and helpful guidance.

I would like to thank the members of the BioSentinel Laboratory, Department of Biology, Faculty of Science, Chulalongkorn University, including Mr. Khattapan Jantawongsri for his assistance in frog agriculture and several laboratory techniques, Dr. Rangsimma Pewphong, Mr. Rachata Maneein, Miss Yupaporn Visoot, Mr. Patchara Sittishevapark, Mr. Suthirote Meesawat, Mr. Worapat Sawatwong, Miss Lalita Srion, Miss Chanyapatch Saenthetthanyawat, Miss Sadanan Summat, Miss Kotchanun Bunjerdluk and current undergraduate students for their help in laboratory work and for their support in various ways throughout this study.

In addition, appreciation is also extended to the Aquacultural Biology Laboratory, Graduate School of Agricultural Science, Tohoku University, Japan; Animal Systematics Research Unit, Chulalongkorn University; Primate Research Unit and The National Primate Research Center of Thailand, Chulalongkorn University for providing excellent facilities and the Graduate School of Dentistry, Tohoku University, Japan and the Small Animal Teaching Hospital, Faculty of Veterinary Science, Chulalongkorn University for providing mammalian tissue samples on my work. I also acknowledge the scholarship from the Development and Promotion of Science and Technology Talents Project (DPST). A part of this doctoral research was funded by the 90th Anniversary of Chulalongkorn University Fund (Ratchadaphiseksomphot Endowment Fund), Research Assistantship Fund from Faculty of Science, Chulalongkorn University and Overseas Research Experience Scholarship for Graduate Student from the Graduate School, Chulalongkorn University.

I have always been appreciative of the Biological Sciences Program and Department of Biology, Faculty of Science, Chulalongkorn University, where I have earned a lot of knowledge and life experience. I would like to extend my sincere appreciation to all the faculty members of the department who have helped, given me lessons, taught me in many ways, without them I would not be who I am today.

Above all and importantly, I would like to express my greatest gratitude to my beloved family for their support, unconditional understanding, and encouragement through my life.

Thrissawan Traijitt



จุฬาลงกรณ์มหาวิทยาลัย
CHULALONGKORN UNIVERSITY

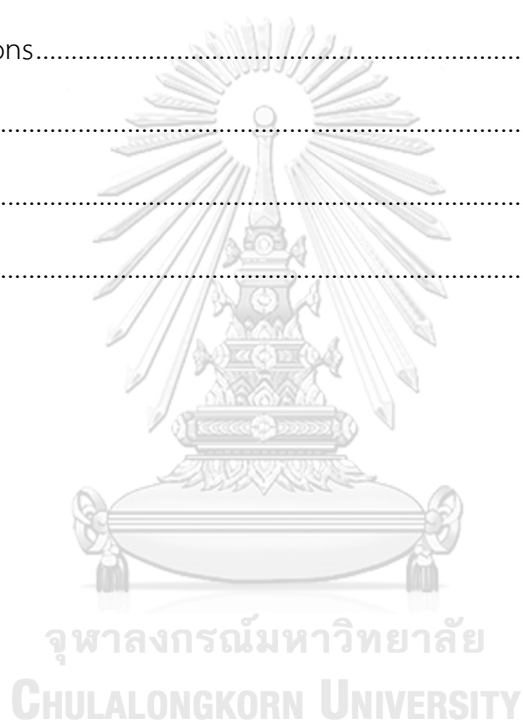
TABLE OF CONTENTS

	Page
ABSTRACT (THAI)	iii
ABSTRACT (ENGLISH)	iv
ACKNOWLEDGEMENTS	v
TABLE OF CONTENTS	vii
LIST OF TABLES	xi
LIST OF FIGURES	xiii
CHAPTER I General Introduction	1
1.1 Objectives	5
1.2 Scope of the study	5
CHAPTER II Literature Reviews	7
2.1 Somatic development in amphibians	7
2.2 Gonadal development in anuran amphibians	16
2.2.1 Sex determination	16
2.2.2 Development of undifferentiated gonad	18
2.2.3 Sex differentiation	20
2.2.4 Stage of ovarian differentiation	26
2.2.5 Stage of testicular differentiation	29
2.3 Sex steroid hormone synthesis during gonadal development in anurans	32
2.4 The rice field frog <i>H. rugulosus</i> (Wiegmann, 1834)	36
2.4.1 Classification and distribution of <i>H. rugulosus</i>	36
2.4.2 Description of adult <i>H. rugulosus</i>	38

2.4.3 Description of <i>H. rugulosus</i> tadpole	40
2.4.4 Morphological variation and phylogenetic relationship of <i>H. rugulosus</i> ...	43
2.4.5 Cytogenetics of <i>H. rugulosus</i>	46
2.4.6 Reproductive biology in <i>H. rugulosus</i>	47
CHAPTER III Chronological Changes in Somatic Development of the Rice Field Frog	
<i>Hoplobatrachus rugulosus</i> (Wiegmann, 1834).....	49
3.1 Introduction.....	49
3.2 Materials and methods.....	51
3.3 Results	52
3.3.1 Embryo (stages 1-20, Table 3.1, Figure 3.2).....	53
3.3.2 Hatchling (stages 21-24, Table 3.2, Figure 3.4).....	57
3.3.3 Tadpole (stages 25-41, Table 3.3, Figures 3.3 and 3.5).....	58
3.3.4 Metamorph (stages 42-46, Table 3.4, Figure 3.5)	63
3.4 Discussion and conclusion	64
CHAPTER IV Pattern of Gonadal Sex Differentiation in the Rice Field Frog	
<i>Hoplobatrachus rugulosus</i> (Wiegmann, 1834).....	69
4.1 Introduction.....	69
4.2 Materials and methods.....	71
4.2.1 Animal procurement.....	71
4.2.2 Morphological study.....	72
4.2.3 Histological study.....	72
4.3 Results	73
4.3.1 Gonad morphological sex differentiation	73
4.3.2 Gonad histological sex differentiation and development.....	74

1) Genital ridge formation: Gosner stages 25 (1-2 dph.) – 26 (1-3 dph.)...	74
2) Development of indifferent gonad: Gosner stages 27 (3-5 dph) – 35 (11-17 dph)	74
3) Ovarian differentiation: Gosner stage 36 (12-20 dph.) – 4 weeks after metamorphosis.....	78
4) Development of the intersex gonad: one week after metamorphosis	88
5) Testicular differentiation: 1–6 weeks after metamorphosis.....	97
4.4 Discussion and conclusion	101
Chapter V Steroidogenic Potential of Gonad during Sex Differentiation in the Rice Field Frog <i>Hoplobatrachus rugulosus</i> (Wiegmann, 1834)	109
5.1 Introduction.....	109
5.2 Materials and methods.....	111
5.2.1 Animal procurement.....	111
5.2.2 Immunohistochemistry.....	111
5.2.3 <i>In situ</i> hybridization.....	113
1) RNA extraction and complementary DNA (cDNA) synthesis.....	113
2) cDNA cloning of CYP17 and CYP19 genes	114
3) RNA probe preparation.....	117
4) hybridization	119
5.2.4 Quantitative real-time reverse transcription polymerase chain reaction (qrt-RT-PCR).....	120
5.3 Results	124
5.3.1 Localization of CYP17 and CYP19 enzymes in <i>H. rugulosus</i> gonad by immunohistochemistry.....	124
5.3.2 Cloning of <i>CYP17</i> , <i>CYP19</i> , and β - <i>actin</i> cDNA.....	132

5.3.3 Localization of <i>CYP17</i> and <i>CYP19</i> mRNA in <i>H. rugulosus</i> gonad by an <i>in situ</i> hybridization	135
5.3.4 <i>CYP17</i> and <i>CYP19</i> mRNA expressions in <i>H. rugulosus</i> gonad by quantitative real-time RT-PCR (qrt-RT-PCR).....	141
5.4 Discussion and conclusion	147
Chapter VI General Discussion and Conclusion.....	156
Conclusion.....	162
Recommendations.....	170
Appendix	172
REFERENCES	187
VITA.....	204



LIST OF TABLES

	Page
Table 2.1 Comparison of developmental stage numbers when observed by different staging systems (Altig and McDiarmid, 2007).....	8
Table 2.2 Comparison of developmental stages between Gosner staging system (1960) in <i>Rana</i> and Nieuwkoop and Faber (1994) in <i>Xenopus</i> (Simmons and Horowitz, 2007).....	14
Table 3.1 Description of developmental stages 1-20 of <i>H. rugulosus</i> embryo according to morphological characteristics in Figure 3.2. Stage = stage of embryonic development according to Gosner (1960); TL = total length of embryo; age = developmental period; haf = hours after fertilization	54
Table 3.2 Description of developmental stages 21-24 of <i>H. rugulosus</i> according to the morphological characteristics in Figure 3.3. Stage = stage of embryonic development according to Gosner (1960); TL = total length of embryo; age = developmental period; haf = hours after fertilization.....	57
Table 3.3 Description of developmental stages 25-41 of <i>H. rugulosus</i> according to the morphological characteristics in Figure 3.3 and 3.5. Stage = stage of tadpole development according to Gosner (1960); TL = total length of tadpole; age = developmental period; dph = days post hatch	60
Table 3.4 Description of developmental stages 42-46 of <i>H. rugulosus</i> according to the morphological characteristics in Figure 3.6. Stage = stage of tadpole development according to Gosner (1960); TL = total length of tadpole or froglet; age = developmental period; dph = days post hatch	63
Table 3.5. Comparison of staging characteristics of tadpole in anuran species.....	67
Table 4.1 Comparison of the somatic (Gosner stage) and gonadal stages of ovarian development in <i>H. rugulosus</i> following the criteria of Ogielska and Kotusz (2004).....	103

Table 4.2 Comparison of the somatic (Gosner stage) and gonadal stages of testicular development in <i>H. rugulosus</i> using criteria adjusted from Haczkiwicz and Ogielska (2013) and Ogielska and Kotusz (2004).....	105
Table 5.1 Primers used to amplify <i>CYP17</i> , <i>CYP19</i> and β - <i>actin</i> cDNAs	116
Table 5.2 Primers used for qrt-RT-PCR analysis	123
Table 5.3 Semi-quantitative scores of relative fold change of <i>CYP17</i> and <i>CYP19</i> mRNA.....	146



LIST OF FIGURES

	Page
Figure 1. 1 Research framework of studying gonadal sex differentiation in the rice field frog <i>H. rugulosus</i>	6
Figure 2.1 Schematic representation of embryonic development at stages 1 to 20, showing number of Gosner stage at the top left corner and the textual important key morphological characteristics of each stage (Gosner, 1960).....	11
Figure 2.2 Schematic representation of tadpole development at stages 21 to 38, showing number of Gosner stage at the top left corner and the textual important key morphological characteristics of each stage (Gosner, 1960).....	12
Figure 2.3 Schematic representation of tadpole development at stages 39 to 46, showing number of Gosner stage at the top left corner and the textual important key morphological characteristics of each stage (Gosner, 1960).....	13
Figure 2.4 Schematic representation of the development of undifferentiated gonad of amphibian (Ogielska, 2009). (A) Migration of pPGCs across basal lamina to the genital ridge; (B) proliferation of the epithelial cells and invasion to the interior of the gonad, PGCs are present in the genital ridge; (C) rearrangement of the epithelial cells to form the cortex containing PGCs and the medulla; (D) the undifferentiated gonad at the period before sex differentiation showing invasion of mesenchymal cells into the space between the cortex and the medulla. The gray areas represent coelomic epithelium, the dark lines represent basal lamina. C: cortex, m: medulla, PGC: primordial germ cell, pPGC: presumptive primordial germ cell, Mch: mesenchymal cell.....	20
Figure 2.5 Schematic representation of gonadal development in amphibian (Viertel and Richter, 1999). Development of undifferentiated gonad shows in (A), (B), and (C). (A) Genital ridge formation; (B) proliferation of coelomic epithelial cell in the indifferent gonad; (C) separation of cortex and medulla part. Development of ovary shows in (D), (E), and (F). (D) Cortex and medulla separated by mesenchymal tissue; (E) ovarian cavity formation in the medulla	

part; (F) development of follicles. Development of testis shows in (G), (H), and (I). (G) Cortex and medulla part closely associated; (H) differentiation of cortex into surface epithelium; (I) differentiation of medulla into testicular rete and seminiferous tubules. B: basal lamina, CE: coelomic epithelial cell, CI: inner epithelial mass, CS: surface epithelium, CX: cortex, ED: rudimentary efferent duct, F: follicular cells, GS: secondary gonium, M: medulla, ME: mesenchymal tissue, O: oogonium, OC: ovarian cavity, OD: oocyte in diplotene stage, OE: early oocyte (leptotene-pachytene), PGC: primordial germ cell, R: testicular rete, SC: spermatocyte, SG: spermatogonium, ST: seminiferous tubule..... 24

Figure 2.6 Patterns of gonadal sex differentiation in some anuran amphibians according to the definition of Witschi (1929) and Flament (2016)..... 26

Figure 2.7 Schematic representation of ovarian development in anurans showing 10 stages of ovarian differentiation (Ogielska, 2009). Stage I–III: undifferentiated gonad; stage IV: sexual differentiation; stage V: first nests of meiocyte; stage VI: first diplotene oocytes; stages VII–IX: increasing number of diplotene oocytes and decreasing number of oogonia and nests; stage X: fully developed ovary. Arrows indicate germ patches. 29

Figure 2.8 Schematic representation of testicular development in anuran showing 10 stages of testicular differentiation (Ogielska, 2009). Stage I–III: undifferentiated gonad; stage IV: early testis; stage V: primary spermatogonia form aggregations; stage VI: primary spermatogonia rearrange into sex cords; stage VII: formation of sex cords; stage VIII: active spermatogenesis begins; stage IX: active spermatogenesis; stage X: fully developed testis..... 31

Figure 2.9 Steroidogenic pathway in vertebrates (Häggström and Richfield, 2014)..... 33

Figure 2.10 Morphological character of the rice field frog *H. rugulosus* (Wiegmann, 1834) 37

Figure 2.11 Comparison of adult female and male rice field frog *H. rugulosus*. (A) Lateral view of female frog; (B) lateral view of male frog showing vocal sac

(arrow); (C) ventral view of female frog; (D) ventral view of male frog showing paired lateral vocal sacs at the angle of submandibular region	39
Figure 2.12 Morphological characteristics of <i>H. rugulosus</i> tadpole at stage 38 in (A) lateral view; (B) dorsal view; (C) ventral view.....	41
Figure 2.13 The mouth part with keratin teeth of <i>H. rugulosus</i> tadpole stage 38: (A) representative stereomicroscope photograph of oral disc and (B) schematic representation of the mouth part structure with LTRF as 2:3+3/3+3:2	43
Figure 2.14 Phylogenetic relationships between <i>Hoplobatrachus</i> species. Numbers at the nodes are NJ bootstrap values. The tree was analyzed using <i>Cyt b</i> and reported by Yu et al., 2015	45
Figure 3.1 Two layers of jelly envelope (arrows) surrounding the egg of <i>H. rugulosus</i>	52
Figure 3.2 Micrographs of <i>H. rugulosus</i> at different embryonic phases (stages 1-20) showing Gosner stage number (top left corner) and the distinct key morphological characteristics according to Gosner (1960)	56
Figure 3.3 Micrographs of <i>H. rugulosus</i> at different hatchling phases (stages 21-24) and a tadpole phase (stage 25) showing Gosner stage number (top left corner) and the distinct key morphological characteristics according to Gosner (1960).....	58
Figure 3.4 Micrographs of <i>H. rugulosus</i> hind limb bud at stage 29 showing the position for the measurement of the proportion between the leg length (L) and the leg diameter (D).....	59
Figure 3.5 Micrographs of <i>H. rugulosus</i> at different tadpole phases (stages 26-41) showing Gosner stage number (top left corner), the distinct key morphological characteristics according to Gosner (1960) and the characteristics of hind limb bud for classification of the stage of tadpole (lower figure of each panel). D: diameter of hind limb buds, L: length of hind limb buds	62

- Figure 3.6** Micrographs of *H. rugulosus* at different metamorph phases (stages 42-46) showing Gosner stage number (top left corner) and the distinct key morphological characteristics according to Gosner (1960). Solid line: position of mouth angle; dash line: position of nostril and eye 64
- Figure 4.1** Representative stereomicroscope photographs of the gonad morphology and location in *H. rugulosus* showing (A) the developing gonads at stage 33 (arrow heads), (B) ovaries at 4 weeks after metamorphosis with numerous ovarian sacs (arrow heads), and (C) oval elongate-shaped testes at 4 weeks after metamorphosis (arrow heads) 73
- Figure 4.2** (Left) Somatic development, (Middle) gonad histology, and (Right) schematic representation of the gonads in *H. rugulosus* at (A) stage 25 and (B) stage 26, showing the genital ridge formation. D: diameter of hind limb bud, L: length of hind limb bud, PGC: primordial germ cell, SC: somatic cell, YP: yolk platelet 74
- Figure 4.3** (Left) Somatic development, (Middle) gonad histology, and (Right) schematic representation of the gonads in *H. rugulosus* at (A) stage 27, (B) stage 28 and (C) stage 29, showing the indifferent gonad formation. G: gonocyte, SC: somatic cell 76
- Figure 4.4** (Left) Somatic development, (Middle) gonad histology, and (Right) schematic representation of the gonads in *H. rugulosus* at (A) stage 30, (B) stage 31, (C) stage 32 and (D) stage 33, showing the indifferent gonad formation. Cx: cortex, G: gonocyte, M: medulla , SC: somatic cell 77
- Figure 4.5** (Left) Somatic development, (Middle) gonad histology, and (Right) schematic representation of the gonads in *H. rugulosus* at (A) stage 34 and (B) stage 35, showing the indifferent gonad with an increased number of gonocytes and somatic cells. Cx: cortex, G: gonocyte, M: medulla, SC: somatic cell..... 78
- Figure 4.6** (Left) Somatic development, (Middle) gonad histology, and (Right) schematic representation of the gonads in *H. rugulosus* at (A) stage 36, (B) stage 37, (C) stage 38 and (D) stage 39, showing the ovarian differentiation with the

presence of ovarian cavity and primary oogonia in the cortex. Cx: cortex, M: medulla, OC: ovarian cavity, PG: primary oogonia, SC: somatic cell 81

Figure 4.7 (Left) Somatic development, (Middle) gonad histology, and (Right) schematic representation of the gonads in *H. rugulosus* at (A) stage 40 and (B) stage 41, showing the ovarian differentiation with the presence of ovarian cavity and the cortex composed of primary oogonia and cyst of secondary oogonia (at leptotene and pachytene stage). Cx: cortex, M: medulla, OC: ovarian cavity, PG: primary oogonia, SC: somatic cell, SG: cyst with secondary oogonia 82

Figure 4.8 (Left) Somatic development, (Middle) gonad histology, and (Right) schematic representation of the gonads in *H. rugulosus* at (A) stage 42, (B) stage 43, (C) stage 44, (D) stage 45 and (E) stage 46, showing the developing ovary with germ cells at different stages. DiO: diplotene oocyte, F: follicle, OC: ovarian cavity, PG: primary oogonia, SG: cyst with secondary oogonia 84

Figure 4.9 (Left) Somatic development, (Middle) gonad histology, and (Right) schematic representation of the gonads in *H. rugulosus* at (A) 1 week, (B) 2 weeks and (C) 3 weeks after metamorphosis, showing the developing ovary with numerous diplotene oocytes surrounded by follicular cells. ePC: early primary oocyte (leptotene-pachytene), DiO: diplotene oocyte, F: follicle, OC: ovarian cavity, PG: primary oogonia 86

Figure 4.10 (Left) Somatic development, (Middle) gonad histology, and (Right) schematic representation of the gonads in *H. rugulosus* at (A) 4 weeks, (B) 5 weeks and (C) 6 weeks after metamorphosis, showing the developing ovary with a number of diplotene oocytes. DiO: diplotene oocyte, F: follicle, GP: germ patch, OC: ovarian cavity 87

Figure 4.11 (Left) Somatic development, (Middle) gonad histology, and (Right) schematic representation of the gonads in *H. rugulosus* at (A) 1 week, (B) 2 weeks and (C) 3 weeks after metamorphosis, showing the intersex gonad with regressed ovarian cavity, diplotene oocytes and degenerating oocytes at the innermost area, and early seminiferous tubules (containing spermatogonia and

some spermatogonial cysts) in the outermost area of the cortex. C: sex cord, DiO: diplotene oocyte, DO: degenerating oocyte, F: follicle, RC: regressed cavity, Spg: spermatogonia..... 91

Figure 4.12 (Left) Somatic development, (Middle) gonad histology, and (Right) schematic representation of the gonads in *H. rugulosus* at (A) 4 weeks, (B) 5 weeks and (C) 6 weeks after metamorphosis, showing the intersex gonad with testis-ova at the innermost area and testicular tissue at the outermost area of the cortex. C: sex cord, F: follicle, RC: regressed cavity, Spc: spermatocyte, Spg: spermatogonium, Spz: spermatozoa, ST: seminiferous tubule, TO: testis-ovum 93

Figure 4.13 Comparison of gonad morphology and histology in juvenile male *H. rugulosus* at (A, B) 5 and (C, D) 7 weeks after metamorphosis. Representative (A) stereomicroscope photograph of the testes morphology; (B) histology photomicrograph of A, the intersex gonad with oocytes, gonial cysts and groups of meiocytes; (C) stereomicroscope photograph of the gonad at 7 weeks with a mixed appearance of male gonad and lobular structure of female gonad (arrows); (D) histology photomicrograph of C, the ovary. DiO: diplotene oocyte, DO: degenerating oocyte, F: follicle, GP: germ patch, OC: ovarian cavity, Spg: spermatogonia, TO: testis-ovum..... 94

Figure 4.14 Photomicrograph of the gonads of *H. rugulosus* at (A) 4 weeks, (B) 5 weeks, (C) 6 weeks, (D) 7 weeks, (E) 8 weeks, (F) 10 weeks and (G) 13 weeks after metamorphosis, showing the variety of intersex gonad at different age. The intersex gonad contained testis-ovum at the innermost area and testicular tissue at the outermost area of the cortex. C: sex cord, DO: degenerating oocyte, F: follicle, L: Leydig cell, RC: regressed cavity, Spc: spermatocyte, Spg: spermatogonium, Spz: spermatozoa, ST: seminiferous tubule, TO: testis-ovum 96

Figure 4.15 (Left) Somatic development, (Middle) gonad histology, and (Right) schematic representation of the gonads in *H. rugulosus* at (A) 4 weeks, (B) 5 weeks and (C) 6 weeks after metamorphosis, showing the testis with seminiferous tubules containing spermatogonium, group of spermatocytes,

spermatozoa, Sertoli cell, and Leydig cells. L: Leydig cell, Spc: spermatocyte, Spg: spermatogonium, Spz: spermatozoa, ST: seminiferous tubule..... 99

Figure 4.16 Photomicrograph of the gonads in *H. rugulosus*, showing the intersex gonad (A) at higher magnification of Figure 4.12C with testis-ovum surrounded with follicle next to seminiferous tubules with spermatogenic cells at several stages, (B) the testis at higher magnification of Figure 4.13C, containing seminiferous tubules with spermatogonia, groups of spermatocytes, spermatozoa, Sertoli cells and Leydig cells between the tubules, (C) the structure of seminiferous tubule with spermatogenic cells at every stage. F: follicle, L: Leydig cell, Ser: Sertoli cell, Spc I: primary spermatocyte, Spc II: secondary spermatocyte, Spg I: primary spermatogonium, Spg II: secondary spermatogonium, Spt: spermatid, Spz: spermatozoa, ST: seminiferous tubule, TO: testis-ovum..... 100

Figure 4.17 Summary diagram representing the chronology of gonadal development in *H. rugulosus*..... 108

Figure 5.1 Amplicons of the partial sequence of *CYP17*, *CYP19* and β -actin cDNA from *H. rugulosus* that were electrophoresed in a 1.5% agarose gel and stained with SYBR® Safe DNA dye showed the product size at 799 bp for *CYP19*, 699 bp for *CYP17*, and 158 bp for β -actin. M1: 1 kb DNA ladder, M2: 100 bp DNA ladder..... 116

Figure 5.2 Vector map of pGEM-T Easy (Promega, Madison, USA) 118

Figure 5.3 Recombinant plasmids harbouring the *CYP17* and *CYP19* genes were confirmed by restriction analysis, electrophoresed in a 1.5% agarose gel, and stained with SYBR® Safe DNA dye. M1: 1 Kb molecular weight marker, M2: 100 bp molecular weight marker, lanes 1-2: recombinant plasmids harbouring the *CYP17* (linearized by *NcoI* and *Sall*, respectively) showed a single band at 3,700 bp, lanes 3-4: recombinant plasmids harbouring the *CYP19* (linearized by *NcoI* and *Sall*, respectively) showed a single band at 3,800 bp. 118

- Figure 5.4** Determination of newly synthesized RNA probe for *in situ* hybridization in a 1.5% agarose gel stained with SYBR® Safe DNA dye. The RNA probe size are 699 bp for *CYP17* (lanes 1-2) and 799 bp for *CYP19* (lanes 3-4). M1: 1 Kb molecular weight marker, M2: 100 bp molecular weight marker, lanes 1-2: *CYP17* anti-sense and sense RNA probe, respectively, lanes 3-4: *CYP19* anti-sense and sense RNA probe, respectively. 119
- Figure 5.5** Amplification of partial sequence of *CYP17*, *CYP19* and β -*actin* cDNA from *H. rugulosus* showing lanes 1-3 PCR product size at 230 bp for *CYP17*, 174 bp for *CYP19*, and 158 bp for β -*actin*, respectively 123
- Figure 5.6** Photomicrographs of immunohistochemical staining for CYP17 enzyme by a polyclonal anti-CYP17/CYP17A1 antibody (LS-B13802) showing (A) immunoreaction of CYP17 enzyme in the Leydig cells of mouse testis (arrows), (B) *H. rugulosus* testis without specific immunoreaction of CYP17 enzyme, (C, D) negative control of mouse and *H. rugulosus* testis, respectively, (E, F) H&E staining in mouse and *H. rugulosus* testis, respectively 126
- Figure 5.7** Photomicrographs of immunohistochemical staining for CYP17 enzyme by a monoclonal anti-CYP17A1 antibody (sc-374244) with chromogenic detection by DAB (A, B) and Vector VIP peroxidase substrate kit (C, D) showing (A, C) immunoreaction of CYP17 enzyme in the Leydig cells of dog testis (arrows), (B, D) *H. rugulosus* testis without detectable immunoreaction of CYP17 enzyme, (E, F) negative control of dog and *H. rugulosus* testis, respectively, (G, H) H&E staining in dog and *H. rugulosus* testis, respectively 128
- Figure 5.8** Photomicrographs of immunohistochemical staining for CYP19 enzyme by a polyclonal anti-CYP19/aromatase antibody (LS-B2816) showing (A) nonspecific immunoreaction of CYP19 enzyme in cat ovary, (B) *H. rugulosus* ovary without detectable immunoreaction of CYP19 enzyme, (C, D) negative control of cat and *H. rugulosus* ovary, respectively, (E, F) H&E staining in cat and *H. rugulosus* ovary, respectively 130

- Figure 5.9** Photomicrographs of immunohistochemical staining for CYP19 enzyme by a monoclonal anti-CYP19 antibody (sc-374176) showing (A) mouse ovary without detectable immunoreaction of CYP19 enzyme, (B) *H. rugulosus* ovary without detectable immunoreaction of CYP19 enzyme, (C, D) negative control of mouse and *H. rugulosus* ovary, respectively, (E, F) H&E staining in mouse and *H. rugulosus* ovary, respectively 131
- Figure 5.10** Nucleotide and deduced amino acid sequence of *CYP17* cDNA of *H. rugulosus* (GenBank Accession No. MW017204). The primer sequences used for qrt-RT-PCR are underlined 133
- Figure 5.11** Nucleotide and deduced amino acid sequence of *CYP19* cDNA of *H. rugulosus* (GenBank Accession No. MW017205). The primer sequences used for qrt-RT-PCR are underlined 134
- Figure 5.12** Nucleotide and deduced amino acid sequence of β -actin cDNA of *H. rugulosus*. The primer sequences used for qrt-RT-PCR are underlined 134
- Figure 5.13** Photomicrographs of the *in situ* hybridization for *CYP17* mRNA in *H. rugulosus* testis at 16 weeks after metamorphosis: (A) *CYP17* mRNA localization in the testis hybridized with anti-sense probe showing the signal of *CYP17* mRNA that specifically expressed in the Leydig cells (blue signal), (B) the tissue at high magnification of inset in A, (C) the tissue hybridized with sense probe showing no positive signal presented, (D) the tissue stained with H&E. L: Leydig cell, Spg: spermatogonium, Spz: spermatozoa, ST: seminiferous tubule 136
- Figure 5.14** Photomicrographs of the *in situ* hybridization for *CYP17* mRNA of *H. rugulosus* ovary at 16 weeks after metamorphosis. (A) *CYP17* mRNA localization in the ovary hybridized with anti-sense probe showing false positive signals in an oocyte, (B) the tissue hybridized with sense probe showing false positive signals in some oocytes, (C) the tissue stained with H&E 137
- Figure 5.15** Photomicrographs of the *in situ* hybridization for *CYP17* mRNA in *H. rugulosus* gonad at 4 to 6 weeks after metamorphosis. *CYP17* mRNA localization in the gonad hybridized with anti-sense probe showing the signal of

CYP17 mRNA in the Leydig cells (blue signal) of testicular tissue at (A) 4 weeks (intersex gonad), (B) 4 weeks (testis), (C) 5 weeks, and (E) 6 weeks after metamorphosis. (D) and (F) the tissue at high magnification of inset in (C) and (E), respectively..... 138

Figure 5.16 Photomicrographs of the *in situ* hybridization for *CYP17* mRNA in *H. rugulosus* testis at 7 to 12 weeks after metamorphosis. *CYP17* mRNA localization in the testicular tissue hybridized with anti-sense probe showing the signal of *CYP17* mRNA in the Leydig cells (blue signal) at (A) 7 weeks, (B) 8 weeks, (C) 9 weeks, (D) 10 weeks, (E) 11 weeks and (F) 12 weeks after metamorphosis 139

Figure 5.17 Photomicrographs of the *in situ* hybridization for *CYP17* mRNA in *H. rugulosus* testis at 13 to 16 weeks after metamorphosis. *CYP17* mRNA localization in the testicular tissue hybridized with anti-sense probe showing the signal of *CYP17* mRNA in the Leydig cells (blue signal) at (A) 13 weeks, (B) 14 weeks, (C) 15 weeks and (D) 16 weeks after metamorphosis 140

Figure 5.18 Photomicrographs of the *in situ* hybridization for *CYP19* mRNA of *H. rugulosus* ovary at 16 weeks after metamorphosis. *CYP19* mRNA localization in the ovary (A) hybridized with anti-sense probe showing false positive signals in some oocytes, (B) the tissue hybridized with sense probe showing false positive signals in some oocytes, (C) the tissue stained with H&E 141

Figure 5.19 Quantification of *CYP17* mRNA in the *H. rugulosus* gonad during the gonadal development period (Gosner stages 25-46 and 1-11 weeks after metamorphosis) showing bar charts of fold changes in expression relative to st 25-35 group. Data were normalized with β -actin. Error bars represent SEM at each group. The different letters above each bar indicate significant differences between groups ($p < 0.05$). st: Gosner stage, wks: weeks after metamorphosis 143

Figure 5.20 Quantification of *CYP19* mRNA in the *H. rugulosus* gonad during the gonadal development period (Gosner stages 25-46 and 1-11 weeks after metamorphosis) showing bar charts of fold changes in expression relative to st

25-35 group. Data were normalized with β -actin. Error bars represent SEM at each group. The different letters above each bar indicate significant differences between groups ($p < 0.05$). st: Gosner stage, wks: weeks after metamorphosis 145

Figure 6.1 Summary diagram of somatic and gonadal development in *H. rugulosus* 158

Figure 6.2 Schematic representation of ovarian development in *H. rugulosus* showing the developmental period with important histological evidences. *Stage 25, the genital ridge*: PGC with yolk platelet inside cytoplasm (yellow labeled cell). *Stage 35, the indifferent gonad*: numerous gonocytes (yellow labeled cells) in the cortex. *Stage 36, the developing ovary*: ovarian cavity formation (green labeled area). *Stage 42, the developing ovary*: diplotene oocytes surrounding by follicular cells (pink labeled cells). *One week after metamorphosis, ovary*: numerous diplotene oocytes and follicular cells (pink labeled cells). *Four weeks after metamorphosis, fully developed ovary*: mostly diplotene oocytes surrounding by follicular cells (pink labeled cells). The expression of *CYP17* and *CYP19* mRNA were represented as shaded bars at the bottom of figure. The score of gradient shade in the bar corresponded to the results in figure 5.21, 5.22. and Table 5.3 Cx: cortex, DiO: diplotene oocyte, ePC: early primary oocyte (leptotene-pachytene), F: follicle, G: gonocyte, GP: germ patch, M: medulla, OC: ovarian cavity, PG: primary oogonia, PGC: primordial germ cell, SC: somatic cell, SG: cyst with secondary oogonia, YP: yolk platelet..... 165

Figure 6.3 Schematic representation of testicular development in *H. rugulosus* showing the developmental period with important histological evidences. *Stage 25, the genital ridge*: PGC with yolk platelet inside cytoplasm (yellow labeled cell). *Stage 35, the indifferent gonad*: numerous gonocytes (yellow labeled cells) in the cortex. *Stage 36, the developing ovary*: ovarian cavity formation (green labeled area). *Stage 42, the developing ovary*: diplotene oocytes surrounding by follicular cells (pink labeled cells). *One week after metamorphosis, 1) intersex gonad*: group of spermatogonia at the outermost area (blue labeled area) and diplotene oocytes and degenerating oocyte at the

innermost area. Six weeks after metamorphosis, intersex: seminiferous tubule containing spermatogonia, and spermatozoa at the outermost area (blue labeled area) and testis-ova at the innermost area, 2) *testis*: seminiferous tubule containing spermatogonia, spermatocytes, and spermatozoa. The expression of *CYP17* and *CYP19* mRNA were represented as shaded bar at the bottom of figure. The score of gradient shade in the bar corresponded to the results in figure 5.21, 5.22. and Table 5.3. The *CYP17* mRNA was highly expressed since 4 weeks after metamorphosis and localized in the interstitial tissue of the testis and intersex gonad (dark blue labeled area). Cx: cortex, DiO: diplotene oocyte, DO: degenerating oocyte, F: follicle, G: gonocyte, M: medulla, OC: ovarian cavity, PG: primary oogonia, PGC: primordial germ cell, RC: regressed cavity, SC: somatic cell, SG: cyst with secondary oogonia, Spg: spermatogonia, Spc: spermatocyte, Spz: spermatozoa, TO: testis-ovum, YP: yolk platelet. 168

CHAPTER I

General Introduction

Sex development in amphibians has been studied for decades in several species, however, it is still not clear in some points. Research and data from the past revealed that they have species-specific variation. The process of sex development can be derived from the occurrence of sex determination and sex differentiation. Sex of amphibians is mostly determined by genetic factors (genetic sex determination: GSD). A few studies suggested that sex of amphibians can be determined by environmental factors (environmental sex determination: ESD) such as temperature (Hayes, 1998; Eggert, 2004; Nakamura, 2010). The GSD in amphibians normally occurs after fertilization which is directly controlled by sex determining gene (Nakamura, 2009; Phuge and Gramapurohit, 2013). The sex differentiation process continues during metamorphosis, but the microscopic observable sexual differences of gonad may occur at different developmental stages among species (Gramapurohit et al., 2000). The embryonic development of anuran amphibian has normally been described as a developmental staging system. Gosner's staging system is one of the standard systems that has been recommended by several researchers for using in developmental study in anuran species. In Gosner's staging system, the developmental period of frog has been divided into 4 phases including embryo (stages 1-20), hatchling (stages 21-24), tadpole (stages 25-41), and metamorph (stages 42-46) (Altig and McDiarmid, 1999). However, the developmental period in each stage varies among species (Altig and McDiarmid, 1999). The beginning of gonadal development in amphibians is the formation of primordial gonad. It usually occurs in a tadpole at stage before feeding begins (Gosner stage 24) (Ogielska, 2009). Then the primordial gonad develops into the indifferent gonad and then differentiates into male or female gonad. There are some variations in sex differentiation in gonad of

amphibians. The sex differentiation of gonad starts at the different somatic development stage. Moreover, the patterns of sex differentiation also vary.

Patterns of gonadal sex differentiation in anurans can be categorized into three patterns/types based on population sex ratio at complete metamorphosis including 1) differentiated type: indifferent gonad directly differentiates into ovary or testis. Female and male gonads differentiate after complete metamorphosis, 2) semi-differentiated type or an intermediate type: the indifferent gonad begins to develop into ovary or remains in the undifferentiated form while testis differentiates later through an intersex phase, ovary and intersex gonad can be found after complete metamorphosis, and 3) undifferentiated type: the indifferent gonad develops into ovary after complete metamorphosis, testicular development occurs later after the intersex gonad has differentiated (Witschi, 1929a; Gramapurohit et al., 2000; Saidapur et al., 2001; Ogielska, 2009; Phuge and Gramapurohit, 2013; Flament, 2016). To determine a pattern and chronology of gonadal sex differentiation, morphological and histological studies are suitable methods for tracing the evidence of gonadal tissue formation. Furthermore, during gonadal tissue formation, some cells may produce endogenous steroids which have been suggested to influence sex differentiation in amphibians. It has been reported that sex steroids can completely change the sex into male or female or induce intersex gonad (Hayes, 1998; Nakamura, 2010). Therefore, to examine steroidogenic function of gonad together with function in germ cell production, understanding in the steroidogenic activity in the gonad during the developmental period is very important.

The role of steroid hormones in sex differentiation in anurans has been discussed for a long time. The mechanisms of steroidogenesis are still not conclusive because of interspecific variation. Sex steroids, estrogens and androgens were reported to have crucial role during sex differentiation in anurans (Maruo et al., 2008; Nakamura, 2009; Phuge and Gramapurohit, 2013). Estrogens always play a role in feminization, while androgens play a role in masculinization as it is known in

mammals. However, the role of androgens depends on anuran species (Ogielska, 2009). The steroidogenesis in gonad occurs during the process of gonadal sex differentiation. According to the steroidogenic pathway of vertebrates, there are some steroidogenic enzymes involved in sex steroid synthesis including 3 β -hydroxysteroid dehydrogenase (3 β -HSD), cytochrome P450 17 β hydroxylase/C17-20 lyase (CYP17), 17 β -hydroxysteroid dehydrogenase (17- β HSD), cytochrome P450 aromatase (CYP19), and 5 α -reductase (5 α Red1). The study in some anuran species showed sexually dimorphic patterns of some enzymes and their mRNA expression. CYP17 is the enzyme that converts pregnenolone into dehydroepiandrosterone (DHEA) and progesterone into androstenedione (AE). CYP19 (cytochrome P450 aromatase) is the enzyme that converts testosterone into estradiol (E2). The expression of *CYP17* and *CYP19* mRNA were found at different levels and patterns between males and females. The gonadal activity of *CYP19* are detected at high level during ovarian development which represents feminization of gonad, while *CYP17* may have a major role in testicular development (Maruo et al., 2008; Nakamura, 2009). The research in *Glandirana/Rana rugosa* using immunohistochemical technique to localize CYP17 and CYP19 enzyme in gonadal tissues showed that CYP17 was found in somatic cells of the indifferent gonad of early stage tadpole and interstitial cells of the testis of adult frog (Sakurai, 2008). Another study also showed that CYP19 was found in gonadal somatic cells of the female tadpole and ovarian somatic cells at complete metamorphosis (Isomura et al., 2011). Furthermore, the expression and localization of *CYP17* and *CYP19* mRNA were also reported in some anurans. Likely, *CYP17* trends to express at a high level during male gonad development in *G. rugosa* (Iwade et al., 2008; Maruo et al., 2008), *Lithobates/R. sylvaticus* (Navarro-Martín et al., 2012), and *Xenopus leavis* (Piprek et al., 2018), whereas *CYP19* trends to express at a high level during female gonad development in *G. rugosa* (Iwade et al., 2008; Maruo et al., 2008), *L. sylvaticus* (Navarro-Martín et al., 2012), *Silurana/X. tropicalis* (Navarro-Martín et al., 2012) and *X.*

leavis (Mawaribuchi et al., 2014; Piprek et al., 2018). Therefore, *CYP17* and *CYP19* are good candidates for studying the steroidogenic potential in gonad during the gonadal development in anurans.

The rice field frog *Hoplobatrachus rugulosus* is a native frog that widely distributed in wetlands throughout Thailand and also in central and southern China to Myanmar, Lao People's Democratic Republic, Vietnam, Cambodia and peninsular Malaysia (Diesmos et al., 2004; Frost et al., 2006). This species can be raised in farms and used as an alternative protein source in many countries (Pariyanonth, 1985; Tokur et al., 2008). Also, it can be manipulated in laboratory and provides a large number of offspring in a short period of time. Therefore, it has been used as an experimental animal in many fields of biological research (Khonsue and Thirakhupt, 2001; Schmalz and Zug, 2002; Bain and Truong, 2004; Ratanasaeng et al., 2008; Hasan et al., 2012). In environmental research, the abnormalities in its somatic development and reproductive system have been used for evaluating the effect of environmental changes and xenobiotic contamination (Katawutpoonphan, 2008; Ruamthum et al., 2011; Trachantong et al., 2013; Tang et al., 2020). However, basic knowledge about its normal development especially in reproductive system is still limited. A preliminary study demonstrated that the gonadal sex differentiation in this frog showed a tendency to be an undifferentiated type since all individuals had ovaries after complete metamorphosis (Traijitt et al., 2010). However, additional information on gonadal development after metamorphosis as well as its chronological changes is still needed to confirm this finding and to examine the process that will be occurred in order to develop the male. Therefore, chronology and pattern of gonadal sex differentiation in *H. rugulosus* were studied using morphological and histological approaches. In addition, localization and expression level of mRNA of the steroidogenic enzymes were studied using qualitative *in situ* hybridization and quantitative real-time RT-PCR (qrt-RT-PCR) to demonstrate steroidogenic potential of gonadal tissues during developmental process. The results from this study could be

crucial to validate the potential use of *H. rugulosus* as a model for developmental biology and environmental research in anuran amphibian.

1.1 Objectives

1. To examine the chronology of gonadal sex differentiation in *H. rugulosus*
2. To determine a pattern of gonadal sex differentiation in *H. rugulosus* based on morphology and histology of the gonads
3. To examine steroidogenic potential of gonadal tissues during the development of *H. rugulosus*

1.2 Scope of the study

The frog embryos in this research were obtained by artificial fertilization at Amphibian and Reptile Research Unit, Chulalongkorn University, under natural light and water temperature. To achieve the objectives, the gonadal development of *H. rugulosus* was studied as described in the research scheme in Figure 1.1.

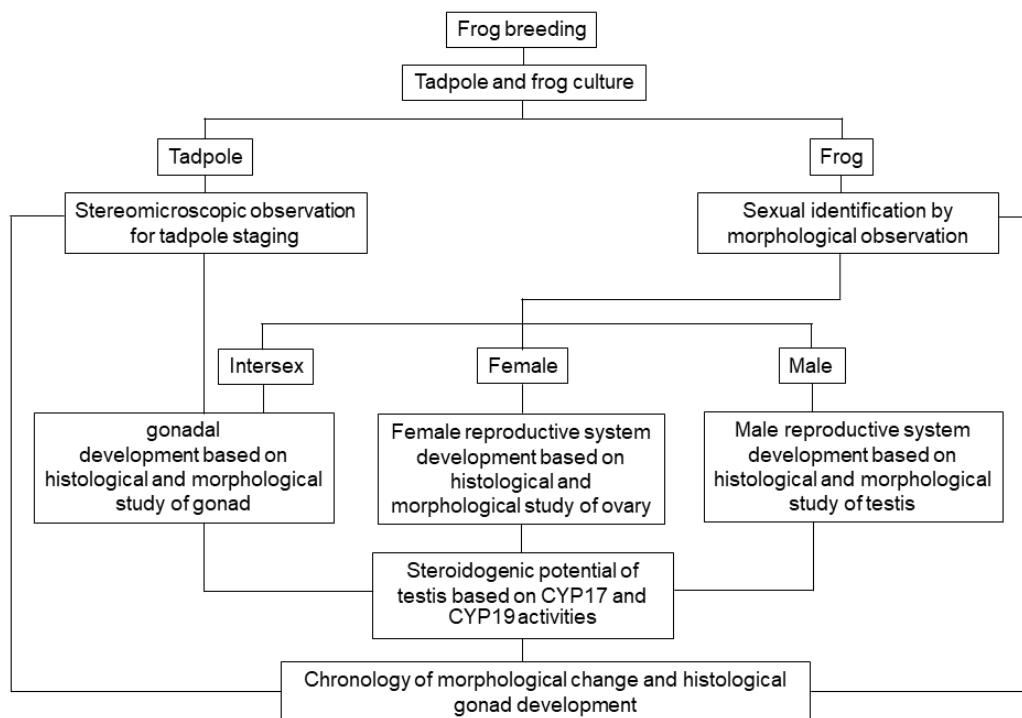


Figure 1. 1 Research framework of studying gonadal sex differentiation in the rice field frog *H. rugulosus*



CHAPTER II

Literature Reviews

2.1 Somatic development in amphibians

Amphibians have several compelling characteristics that make them to be an interesting animal model in many fields of research. In terms of evolution, they are intermediate between fishes and amniotes (Duellman and Trueb, 1994). Their life history, ecology, and behavior are also interesting since they spend parts of life in two different kinds of habitat, in an aquatic environment when they are larvae and in a terrestrial environment when they transform into froglets through metamorphosis process. Moreover, anuran amphibians have adaptive radiation since they have a wide range of morphological and physiological adaptation. Therefore, they can inhabit a wide range of habitat and have high diversity (Duellman and Trueb, 1994; Burggren and Warburton, 2007). These points of view make them a suitable choice for studying physiology, developmental biology, and cell and molecular biology (Burggren and Warburton, 2007; Burlibaşa and Gavrilă, 2011). Amphibians are also widely acknowledged as a key model in environmental ecotoxicology. They can be a specific species that serve as sentinel species for environmental pollution studies (Burlibaşa and Gavrilă, 2011; West, 2018). Furthermore, they can be easily bred and cultured in the laboratory. Also, their egg size and embryo size are physically large and have distinct characteristics which easily to be observed. Therefore, they are good models to study developmental biology and applied biology. To conduct the experiment on anurans, understanding on their embryonic development is important. Staging tables are needed and can serve as tools that facilitate studying embryonic development in anurans.

Staging is the identification of the morphological landmarks that are crucial for comparing the sequence of events in a developmental continuum (Altig and McDiarmid, 1999). More than 45 staging tables have been established (Duellman and

Trueb, 1994). However, only 4 staging tables were frequently cited including Shumway (1940), Taylor and Kollros (1946), Gosner (1960), and Nieuwkoop and Faber (1967). A comparison in the characters to each staging system by Altig and McDiarmid (1999) was reported in Table 2.1. However, Altig and McDiarmid (2007) did not recommend translating the Gosner staging system from other systems. Identification of the developmental stage should be performed in the specimens.

Table 2.1 Comparison of developmental stage numbers when observed by different staging systems (Altig and McDiarmid, 2007)

Gosner, 1960	Nieuwkoop and Faber, 1956, 1967	Shumway, 1940	Taylor and Kollros, 1946	Gosner, 1960	Nieuwkoop and Faber, 1956, 1967	Shumway, 1940	Taylor and Kollros, 1946
1	1	-	-	26	48	-	I
2	1	2	-	27	49	-	II
3	2	3	-	28	50	-	III
4	3	4	-	29	51	-	IV
5	4	5	-	30	52	-	V
6	5	6	-	31	53	-	VI
7	6	7	-	32	53+	-	VII
8	7	8	-	33	53++	-	VIII
9	9	9	-	34	54	-	IX
10	10	10	-	35	54+	-	X
11	11	11	-	36	54++	-	XI
12	12	12	-	37	55	-	XII
13	13	13	-	38	56+	-	XIII
14	14	14	-	39	56	-	XIV
15	17	15	-	40	56+	-	XV-XVII
16	19	16	-	41	58	-	XVIII-XIX
17	23	17	-	42	59	-	XX
18	26	18	-	43	61	-	XXI
19	30	19	-	44	62	-	XXII
20	32	20	-	45	63	-	XXIII-XXIV
21	35	21	-	46	66	-	XXV
22	41	22	-				
23	43	23	-				
24	44	24	-				
25	46	25	-				

Shumway staging table described the stage of embryonic development in *R. pipiens* which were modified based on the study in *L. sylvaticus* by Pollister and Moore (1937). They reported the external morphology of *L. sylvaticus* since fertilization (stage 1) until external gill development (stage 23), cross sections of eye and ear development, and age of each stage at different temperature. Later, the

staging table of *R. pipiens* (Shumway, 1940) was published the external morphology since fertilization (stage 1) until operculum closure was complete (stage 25). Shumway staging system was different from those defined by Pollister and Moore (1937) in some points such as at stage 7 (the fifth cleavage occurred instead of what appears to be the seventh cleavage), and adding 2 stages after external gill development, stage 24 and 25 (operculum formation). Stages 1-25 were indicated as prefeeding stages.

Next, twenty-five postfeeding stages of *R. pipiens* were established by Taylor and Kollros (1946). This staging system included the entire period from the end of embryonic life to complete metamorphosis. They were divided into 4 groups of stage including 1) the limb bud stages (stages I-V; separated by the proportion of the length and diameter of limb bud), 2) the paddle stages (stages VI-X; separated by the transformation of a paddle and indentation of paddle margin), 3) the foot stages or premetamorphic stages (stages XI-XVII; separated by more development of hind limb and differentiation of the toe), and 4) the metamorphic stages (stages XVIII-XXV; separated by regression of the cloacal tail piece). Stage XXV, the tail was completely resorbed indicating the fully developed juvenile stage.

Later, the complete staging system of *Bufo valliceps* was established by Limbaugh and Volpe (1957). This staging system was designed based on the study in several toad species by Gosner and Black (1958) including *B. terrestris terrestris*, *B. t. americanus*, *B. t. copei*, *B. woodhousei fowleri* and the study by Volpe (1959) in *B. quercicus*. The Limbaugh and Volpe staging system consisted of 46 stages using Arabic numerals which were equal to Taylor and Kollros table excepted stage 40 (included stages XV-XVII of Taylor and Kollros) and 41 (included stages XVII-XIX of Taylor and Kollros). The reduction in the number of larval stages made this system a desirable simplification. Therefore, this adoption was suitable for general use and strongly recommended. Then, Gosner (1960) tried to generalize the staging table based on Limbaugh and Volpe system and presented as the illustrations and short

textual comments in each stage (Figure 2.1-2.3) (Limbaugh and Volpe, 1957). The Gosner staging system can be applied in all taxa of anuran, it is considered as an important tool for studying of interspecific comparison (Altig and McDiarmid, 1999).



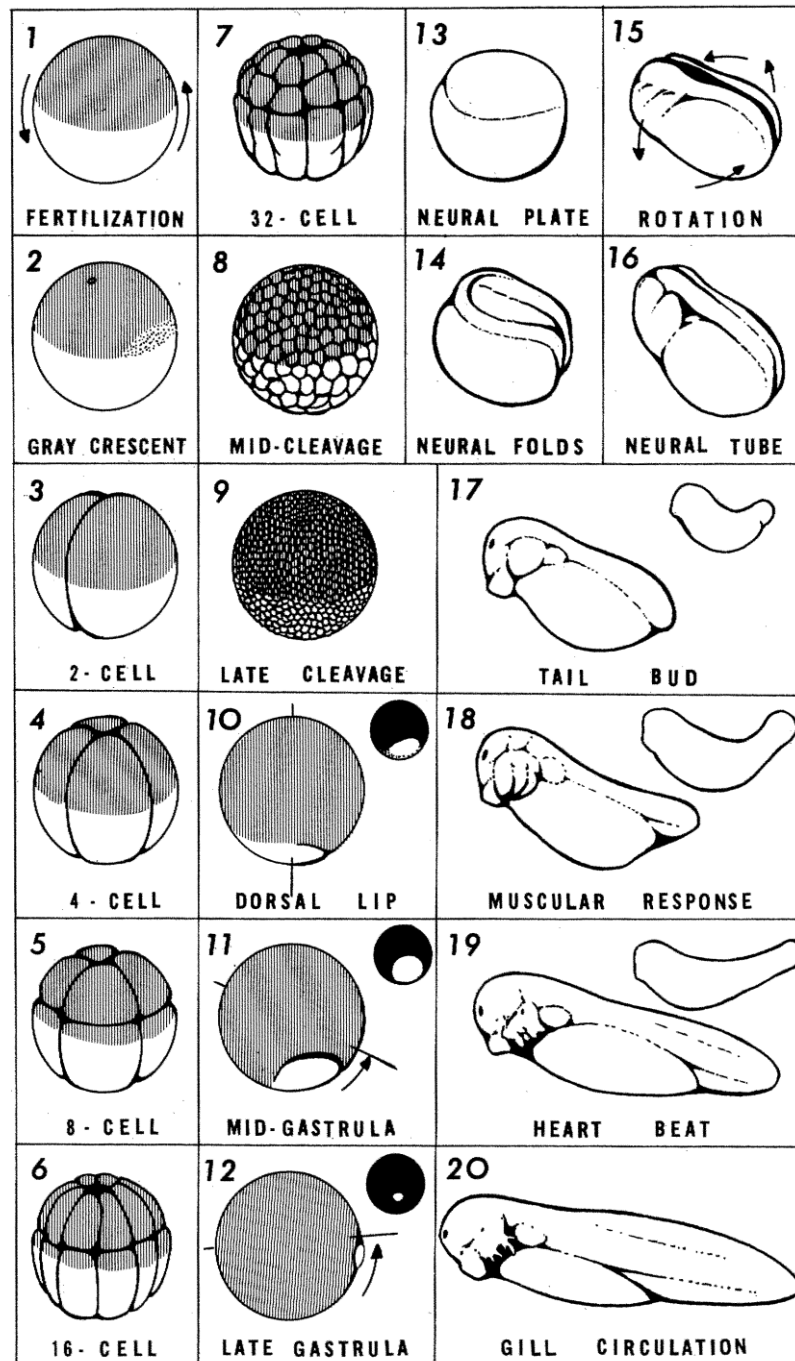


Figure 2.1 Schematic representation of embryonic development at stages 1 to 20, showing number of Gosner stage at the top left corner and the textual important key morphological characteristics of each stage (Gosner, 1960)

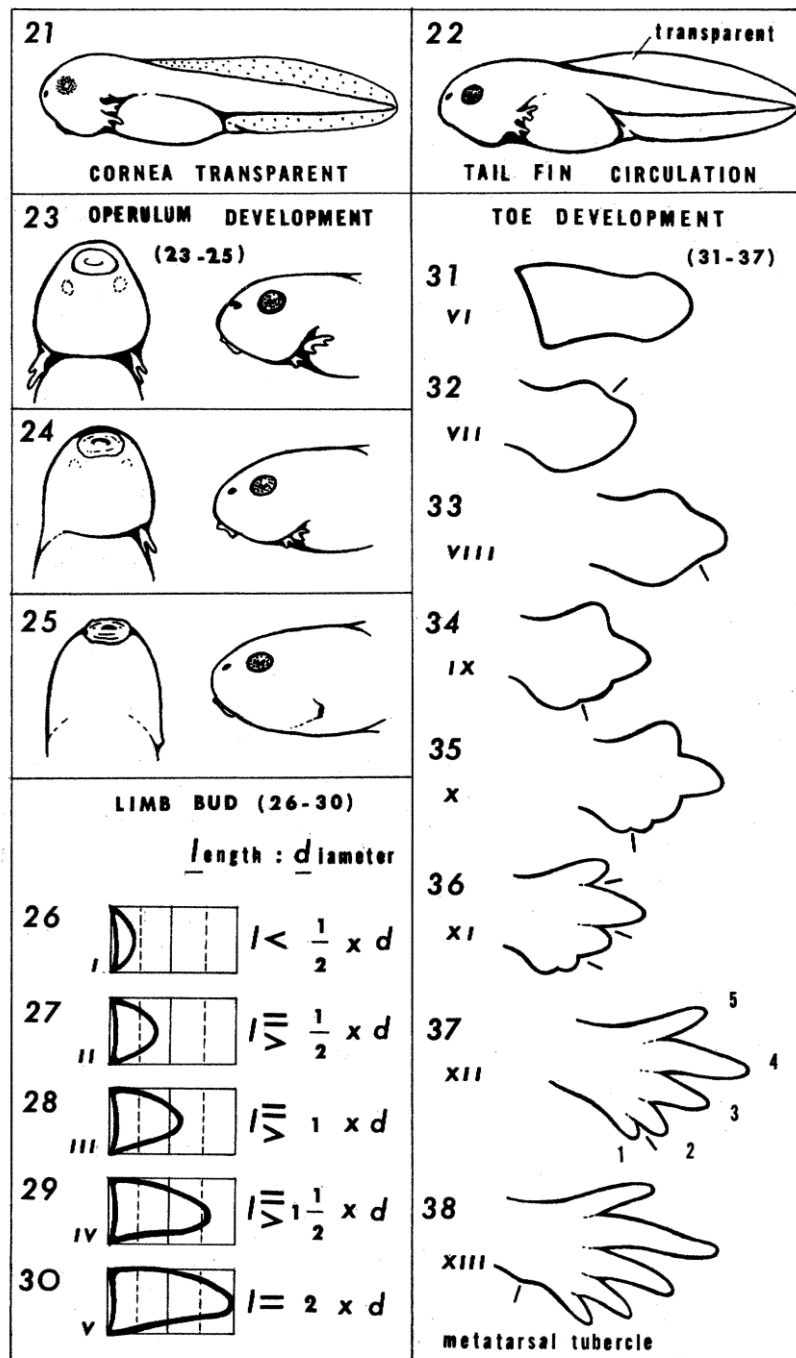


Figure 2.2 Schematic representation of tadpole development at stages 21 to 38, showing number of Gosner stage at the top left corner and the textually important key morphological characteristics of each stage (Gosner, 1960)

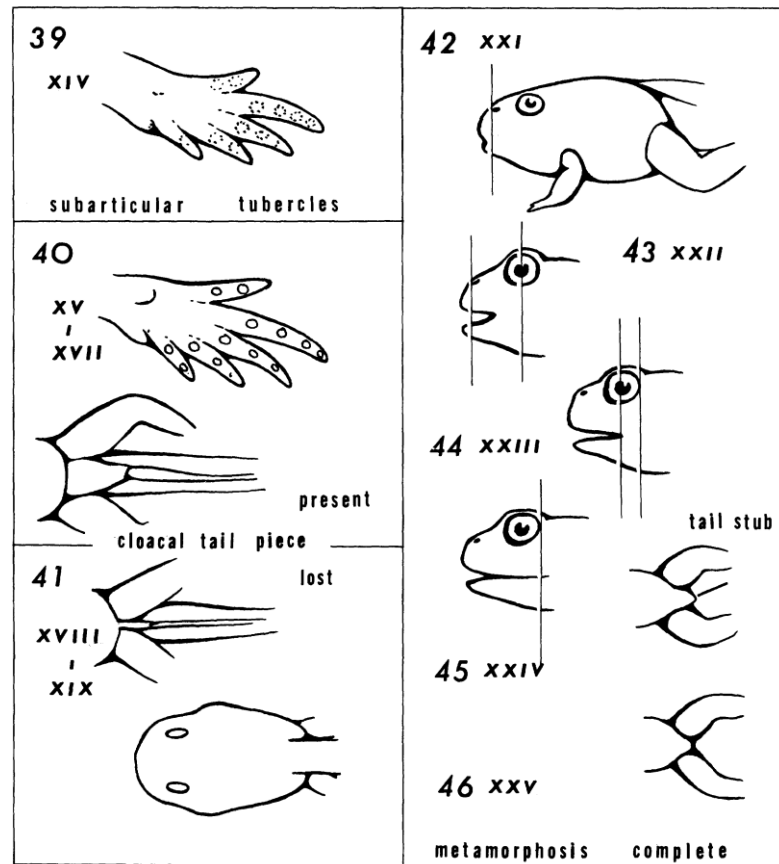


Figure 2.3 Schematic representation of tadpole development at stages 39 to 46, showing number of Gosner stage at the top left corner and the textual important key morphological characteristics of each stage (Gosner, 1960)

The staging system by Nieuwkoop and Faber (1967) was later modified for using in *X. laevis*, a valuable model for several biological research. This staging system consisted of 66 stages (Nieuwkoop and Faber, 1967) which were increased in developmental resolution, especially in embryonic/prefeeding stages and hatchling stages as shown in Table 2.2. Since *X. laevis* tadpole has transparent body, it can be used for staging purposes (Simmons and Horowitz, 2007). However, the occurrence of some external morphological characteristics may not correspond to internal development. In *Xenopus*, changes in skeletal morphology during metamorphosis had poorly correlated with changes in external morphology (Trueb and Hanken, 1992). Also, the development of ear vesicle is more rapid than changes in external

morphology (Simmons and Horowitz, 2007). Due to several specific characteristics of *Xenopus*, Nieuwkoop and Faber system has been recommended for the study of developmental stages only in *Xenopus*.

Table 2.2 Comparison of developmental stages between Gosner staging system (1960) in *Rana* and Nieuwkoop and Faber (1994) in *Xenopus* (Simmons and Horowitz, 2007)

Developmental phase	Gosner stage	<i>Rana</i> Criteria	NF stage	<i>Xenopus</i> Criteria
Embryonic/ prefeeding	1–19	Rapid cell division, gastrulation, neural plate and tube formation, tail budding, beginning of muscular function	1–34	Rapid cell division, gastrulation, neural plate and tube formation, tail budding, beginning of muscular function
Hatchling	20–25	Transition to feeding and free-swimming tadpole; disappearance of external gills	35–45	Transition to feeding and free-swimming tadpole; lateral line system externally visible
Early larval	26–30	Development of hind limb buds	46–53	Development of hind limb and fore limb buds
Late larval	31–41	Lengthening of hind limbs, differentiation and lengthening of toes, appearance of metatarsal and subarticular tubercles; disappearance of cloacal tail piece	54–61	Appearance of fingers; differentiation of toes; shortening of tentacles
Metamorphic climax	42–46	Emergence and differentiation of fore limbs; resorption of tail; remodeling of head	62–66	Resorption of tail; remodeling of head; appearance of adult skin

However, Altig and McDiarmid (1999) recommended using the staging table by Gosner (1960). It has also been used as one of the standard systems and strongly recommended by several researchers (Altig and McDiarmid, 1999; Shimizu and Ota, 2003; Del Pino et al., 2004; Sayim and Kaya, 2008; Saha and Gupta, 2011; Pfalzgraff et al., 2015). Although the staging systems were modified as short textual comments for describing their morphological changes and simple comparing among species, there was interspecific variation in developmental patterns and plasticity of growth (Altig and McDiarmid, 1999). Therefore, to increase the value of data, the total length and size of tadpole in the species of interest should be considered.



2.2 Gonadal development in anuran amphibians

2.2.1 Sex determination

In vertebrates, at least two mechanisms of sex determination are reported including genetic sex determination (GSD) and environmental sex determination (ESD) or some combination of these two factors (Nakamura, 2009). In GSD, the sex of an individual is directly determined into male or female by chromosomal factors at the ambient condition without external influences. In ESD, the sex of an individual is determined by environmental factors. For example, in some species of reptiles, the sex of an individual is determined by the incubation temperature of the eggs. This mechanism is called temperature-dependent sex determination (TSD) (Hayes, 1998; Nakamura, 2009). In amphibians, the sex of an individual is generally determined by GSD in normal condition. However, in some species, the temperature of rearing water results in bias sex ratio, thus, it is likely controlled by genetic factors and may also be influenced by environmental factors (Hayes, 1998).

There were 2 systems of sex chromosome reported in amphibians including XX/XY (male heterogametic XY) and ZZ/ZW (male homogametic ZZ). In amphibians, Y and W chromosomes have various stages of evolution ranging from undetectable, heterochromatin bands, late replicating bands, different two forms of Y chromosome to well differentiated sex chromosomes (Ogielska, 2009). According to phylogenetic analysis, male homogametic system (ZZ/ZW) was the ancestral state. After that, they have evolutionarily evolved into male heterogametic system (XX/XY) (Flament, 2016). The basic system of sex chromosomes in amphibian seems to be ZZ/ZW (Ogielska, 2009). Up to now, *G. rugosa* is only one species that has coexistence of XX/XY and ZZ/ZW systems. They are separated by geography, the population in western Japan have XX/XY system and the population in northeastern Japan have ZZ/ZW system (Nakamura, 2009; Nakamura, 2013). Recently, at least 3 chromosomes coexist (YZ, YW, and ZZ males and ZW and WW females) in the same population and can be found in

S. tropicalis. It is suggested that there is an ongoing process of homologous transition (Roco et al., 2015; Scharl, 2015). Most of amphibians had no morphologically distinct sex chromosomes, only 4% in 1,500 species studied had distinguishable sex chromosomes (Hayes, 1998; Eggert, 2004; Flament, 2016).

The study in genes involved in gonadal sex differentiation have been established on the basis in mammals. In XX/XY sex-determining system, Y chromosome is known to carry the which express the testicular differentiation. Y-linked *Sry* gene is the sex-determining gene that trigger formation of testis. In case of female (XX), *Sry* gene is not found. Whereas the female development initiated. Other genes such as *SF1*, *WT1*, *Sox9*, *Mis*, *Dmrt1*, *Dax1* were found during mammalian gonadal formation. Expression of *Sox9* and *Mis* (or *Amh*, anti-Mullerian hormone) was found in Sertoli cells during testicular differentiation. Whereas expression of *Dax1* was found in ovarian differentiation and this gene can inhibit *Sox9* and *Mis* transcription (Eggert, 2004). Expression of some Sox gene in *X. laevis* was found differently to that of mammal, *xSox12* and *Sox3* genes expressed mainly in ovary. Whereas *xSox18* expressed in testis but not found in ovary. Expression of *Dax1* was also found differently from that of mammal, it expressed in testis but declined in ovary. Expression of *Dmrt1* was found in testis (Eggert, 2004). During the sex differentiation period, *SF1* protein is higher expressed in ovary than the testis in *R. catesbeiana* (Mayer et al., 2002). In the ZZ/ZW sex-determining system, W-linked gene named *dm-W* and *DMY/dmrt1bY* genes were considered as sex determining genes. In *X. laevis*, both *dm-W* and *dmrt1* mRNA were expressed in primordial gonads during the sex determination period. The immunohistochemical analysis showed localization of *dm-W* and *dmrt1* in somatic cells surrounding primordial germ cells of ZW gonads (Flament, 2016). This indicates that *dm-W* and *dmrt1* have a role in ovarian differentiation. Although sex-linked genes have been described, the sex determining genes in amphibians are still unknown. The difference among species

demonstrated that there was no common ancestral sex determining genes in amphibians (Ogielska, 2009).

2.2.2 Development of undifferentiated gonad

In amphibians, sex determination can occur since fertilization after male and female pronuclei fusion. Gonadal development occurs later during larval development stage. The gonads begin to develop from undifferentiated stage. Then the somatic cells of gonad differentiate according to function of sex determining genes and germ cells are then transform into oogonia and spermatogonia.

In anurans, the gonadal development begins with genital ridge formation which two longitudinal folds of coelomic epithelium are formed at the dorsal part of body cavity along both sides of the gut mesentery. The primordial germ cells (PGCs) migrate across the mesentery and distribute along the length of the genital ridge, then the PGCs rearrange. Distribution of PGCs results in partition of gonadal tissue into 1) *pars progonolis*—the anterior part without PGCs, this part will transform into fat body, 2) *pars gonolis*—central part with accumulation of PGCs, this part will develop into the proper gonad, and 3) *pars epigonolis*—posterior part without PGCs, this part will degenerate (Witschi, 1929b; Ogielska, 2009). The genital ridge formation usually starts when the tadpole develops to the stage that feeding begins (Gosner stage 24) (Ogielska, 2009). The epithelial cells proliferate and develop into the somatic part of gonad which will be transformed into the cortex and the medulla later. The medulla is formed by interruption of epithelial cells to the basal membrane and migration of them into the interior of the genital ridge. The PGCs develop into gonidia which are located in the cortex. Somatic cells of undifferentiated gonad will develop into follicular cells in future ovary or seminiferous tubule, *rete testis* and efferent ducts in future testis. The undifferentiated gonad is attached to body cavity wall by mesogonium (Ogielska, 2009). In addition, some groups of somatic cells originate from mesonephros then invade into the space between the cortex and the medulla and develop into theca cells in future ovary and Leydig cells

in future testis. These cells have important roles in steroid hormone production (Ogielska, 2009).

For the development of germ cells, Ogielska (2009) has summarized the nomenclature and differentiation of germ cells based on the definition from Nieuwkoop and Sutasurya (1979) and Witschi (1929a) as follows:

1) Presumptive primordial germ cells (pPGCs) are the germ cells during extragonadal period and before active migration. They are localized in the endoderm.

2) Primordial germ cells (PGCs) are the germ cells during migration and accumulation in the indifferent gonad. In the indifferent gonad, there are two morphologically distinct kinds of germ cells; PGCs and gonial cells. To distinguish from PGCs, Ogielska (2009) recommended to name the smaller cell without yolk platelets as a gonial cell. The PGCs are large cells with a spherical or ovoid nucleus and yolk platelets. When PGCs reach to genital ridge, yolk platelets are depleted by vitellolysis then they develop to gonial cells.

3) Oogonia or spermatogonia are the germ cells that found after the gonadal sex differentiation. The difference between oogonia or spermatogonia cannot be identified by their morphology (Figure 2.4).

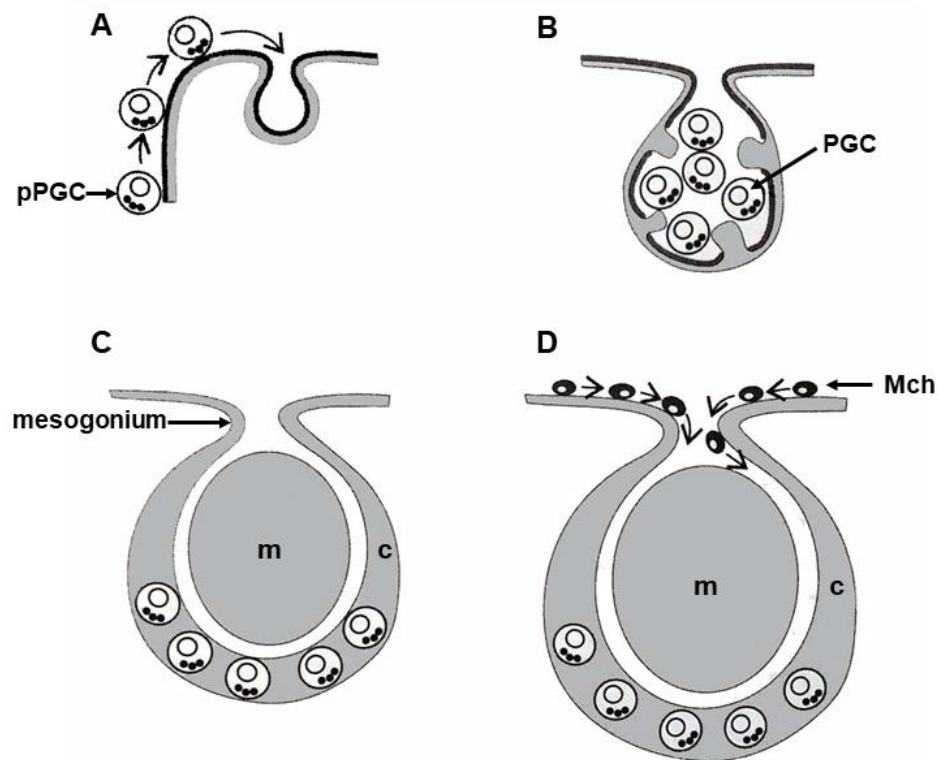


Figure 2.4 Schematic representation of the development of undifferentiated gonad of amphibian (Ogielska, 2009). (A) Migration of pPGCs across basal lamina to the genital ridge; (B) proliferation of the epithelial cells and invasion to the interior of the gonad, PGCs are present in the genital ridge; (C) rearrangement of the epithelial cells to form the cortex containing PGCs and the medulla; (D) the undifferentiated gonad at the period before sex differentiation showing invasion of mesenchymal cells into the space between the cortex and the medulla. The gray areas represent coelomic epithelium, the dark lines represent basal lamina. C: cortex, m: medulla, PGC: primordial germ cell, pPGC: presumptive primordial germ cell, Mch: mesenchymal cell

2.2.3 Sex differentiation

Sex differentiation in anuran amphibians is believed to begin after genetic sex determination at fertilization. This process occurs during metamorphosis but initiates at different stages among species. A common pattern of gonadal development in

amphibians was reported by Viertel and Richter (1999) which shown in Figure 2.5. The process of development initiates when the somatic cells of gonad form genital ridges which appear as longitudinal bilateral thickening tissues and are attached by mesogonium (Figure 2.5A). The PGCs emigrate from the endoderm to the forming gut. The somatic and germ line cells proliferate continuously and rearrange into 2 layers including cortex (outer layer) and medulla (inner layer). The PGCs are located in the cortex of the undifferentiated gonad (Figure 2.5C). Then the gonad goes through the sexual differentiation phase. Female and male gonads can be distinguished by the amount of medullary tissue and the number and size of germ cells. The ovaries are larger than the testis and have wrinkled surfaces.

The developing ovary (Figures 2.5D-F) contains well-developed cortex while the medulla is less developed. The cortex is separated from the medulla by acellular collagenous layer. Proliferation of PGCs occurs then the PGCs develop into oogonia and primary oocytes which located in the cortex. The medulla degenerates and loses its sex cord pattern. The cortex increases in size and number of cells whereas the medulla regresses to form the ovarian cavity. The connective tissues of medulla become a thin membranous layer lining the ovarian cavity. The oogonia proliferate and form cluster in the oogonial nest containing about 16 gonial cells. The primary oocytes enter prophase of meiotic cell division during the larval period. At complete metamorphosis, the ovary contains oogonia, leptotene, zygotene, pachytene, and diplotene oocytes. The oocytes are surrounded by follicular cells which become steroid-producing follicular epithelium.

The developing testis (Figures 2.5G-F), by contrast with ovary, contains well-developed medulla while the cortex is less developed. The germinal epithelium degenerates and becomes a simple peritoneal surface. The cluster of PGCs become spermatogonia surrounding with follicular cells. Then they are dispersed through the compact medullary tissue. The number of tubule is increased at the center of medulla. Then they differentiate into seminiferous tubules. Spermatogenesis occurs

and cluster of gonads surrounding with follicular cells appears. There are two types of spermatogonia in the premetamorphic larvae including a primary single spermatogonia and cluster of secondary spermatogonia. The secondary spermatogonia enter meiosis and become primary spermatocytes at late metamorphosis. In some anurans, seminiferous tubules are formed at late metamorphosis and completed after metamorphosis. The medullary cord near the hilus becomes rete testis. The cords at the anterior part become the vas efferentes which connected to opisthonephric tubules, then opened to the Wolffian duct. However, the efference tubule can connect directly to Wolffian duct in some anurans. The follicular cells become steroid-producing Sertoli cells and the interstitial cells become steroid-producing Leydig cells.



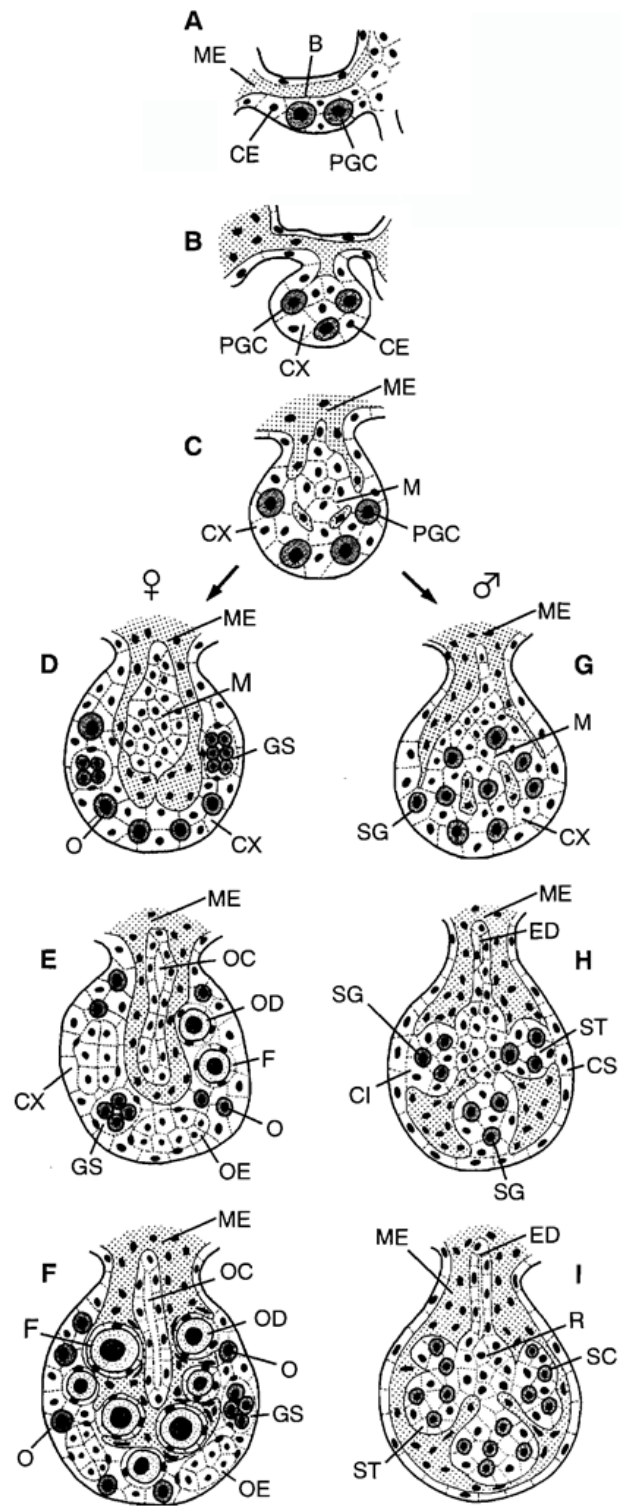


Figure 2.5 Schematic representation of gonadal development in amphibian (Viertel and Richter, 1999). Development of undifferentiated gonad shows in (A), (B), and (C). (A) Genital ridge formation; (B) proliferation of coelomic epithelial cell in the indifferent gonad; (C) separation of cortex and medulla part. Development of ovary shows in (D), (E), and (F). (D) Cortex and medulla separated by mesenchymal tissue; (E) ovarian cavity formation in the medulla part; (F) development of follicles. Development of testis shows in (G), (H), and (I). (G) Cortex and medulla part closely associated; (H) differentiation of cortex into surface epithelium; (I) differentiation of medulla into testicular rete and seminiferous tubules. B: basal lamina, CE: coelomic epithelial cell, CI: inner epithelial mass, CS: surface epithelium, CX: cortex, ED: rudimentary efferent duct, F: follicular cells, GS: secondary gonium, M: medulla, ME: mesenchymal tissue, O: oogonium, OC: ovarian cavity, OD: oocyte in diplotene stage, OE: early oocyte (leptotene-pachytene), PGC: primordial germ cell, R: testicular rete, SC: spermatocyte, SG: spermatogonium, ST: seminiferous tubule

The patterns of gonadal sex differentiation have been observed in several species of anuran. They can be divided into three types (Witschi, 1929b; Gramapurohit et al., 2000; Ogielska, 2009; Piprek et al., 2010; Phuge and Gramapurohit, 2013) (Figure 2.6). 1) *Differentiated type*, the gonadal development begins with formation of indifferent gonad then the ovaries and testes develop simultaneously. Female and male gonads differentiate after metamorphosis. 2) *Semi-differentiated type*, the gonadal development also begins with indifferent gonad. Ovaries and intersex gonads can be found after metamorphosis (Flament, 2016). 3) *Undifferentiated type*, the gonadal development also starts with indifferent gonad, then ovaries develop in all individuals at metamorphosis. Testicular development occurs later through the process of oocyte degeneration after the intersex gonads have differentiated (Ogielska, 2009; Phuge and Gramapurohit, 2013). Ogielska (2009) suggested that the differentiated and undifferentiated type may be grouped as differentiated type if the sex differentiation is considered based on the time of testicular differentiation, not the sequence of somatic development. The semi-differentiated type is not a common type and can be found in very few species such as *Rhacophorus arboreus* (Tanimura and Iwasawa, 1989) and *R. curtipes* (Gramapurohit et al., 2000). The presence of diplotene oocytes (testis-ova) in testis can be found in some period of developing testis in species of the family Ranidae and Rhacophoridae (Ogielska, 2009). Therefore, the testis-ova is not the distinct characteristic that was observed only in the semi-differentiated type. Although the patterns of sex differentiation have been studied in many species, the distinction between undifferentiated and semi-differentiated type is still unclear (Phuge and Gramapurohit, 2013).

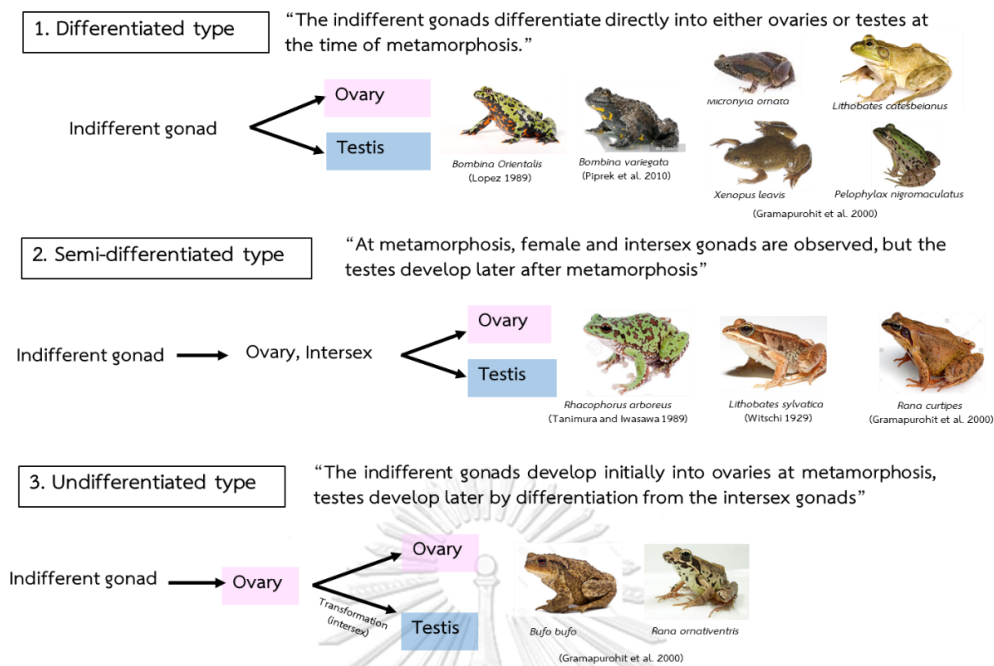


Figure 2.6 Patterns of gonadal sex differentiation in some anuran amphibians according to the definition of Witschi (1929) and Flament (2016)

2.2.4 Stage of ovarian differentiation

The stage of ovarian differentiation in anurans has been described by Ogielska and Kotusz (2004) in which 12 species were observed (*R. lessonae*, *R. ridibunda*, *R. temporaria*, *R. arvalis*, *R. pipiens*, *R. catesbeiana*, *Bombina bombina*, *Hyla arborea*, *B. bufo*, *B. viridis*, *X. laevis*, *Pelobates fuscus*). The process of ovarian differentiation was suggested in the unified pattern which could be divided into 10 stages as follows (Figure 2.7):

- **Stage I** (undifferentiated gonad): PGCs immigrate from the forming gut into genital ridges. The PGCs are localized inside the genital ridges in one or a few rows. Then they are grouped. The PGCs at this stage are large when compared with somatic cells and composed of yolk platelets. For all 12 species, stage I of ovarian differentiation was found in tadpole at Gosner stages 24–25.

- **Stage II** (undifferentiated gonad): the PGCs divide and vitellolysis is complete. The germ cells are considered to be called primary gonia. The primary oogonia appear as a single cell.

- **Stage III** (undifferentiated gonad): the somatic cells divide mitotically and migrate into the central part of the gonad. At this stage, the gonad composes of medulla with somatic cells filling a primary gonadal cavity and cortex containing a few PGCs. The medulla forms metameric knots then it will be ovarian sacs (lobes).

- **Stage IV** (sexual differentiation): the somatic cells of metameric knots are disappeared and secondary ovarian cavity is formed. The mitotic activity of the primary oogonia is high. Some of the primary oogonia form cytoplasmic bridges. The nest of secondary oogonia is formed. Each nest is separated by somatic prefollicular cells. Blood vessels and mesenchyme cells invaded the ovarian cortex.

- **Stage V** (first nests of meiocyte): progonad part of an ovary differentiates into fat body. The ovary increases in size because of enlargement of the lumen and the thickening of the cortex. The secondary oogonia enter meiosis. The cortex composes of primary oogonia and nests of secondary oogonia or meiocytes.

- **Stage VI** (first diplotene oocytes): the ovary increases in size. The fat body more separates from the gonad proper. First diplotene oocytes appear in the cortex. The prefollicular cells become oocyte follicles. At this stage, the cortex composes of diplotene oocytes, nests of meiocytes, and nests of secondary oogonia. The single primary oogonia appear at outermost layer of the cortex.

- **Stage VII** (the number of diplotene oocytes increases and the number of oogonia and nests decreases): the nest of Pachytene oocytes no longer exists. They become diplotene oocytes and their follicles. The diplotene cells protrude into the ovarian cavity. The cavity decreases in size and changes its shape into a flat space.

- **Stage VII-IX** (further growth of diplotene oocytes and thin area of oogonia): the number of diplotene oocyte increases and the ovary increases in size continuously. The fat body appears as several finger-like processes. The area of primary oogonia at the external parts of the cortex are decrease. The thickness of the cortex increases gradually and becomes about 10-fold as thick as in ovarian Stage II. The number of ovarian sacs is different among species.

- **Stage X** (fully developed ovary): the ovary composes of diplotene oocytes with rudimental patches of oogonia. In juvenile ovaries, diplotene oocytes are previtellogenic.

In female frog, the diplotene oocytes appear at all classes of differentiation including previtellogenic, vitellogenic, and mature. Each diplotene oocyte is surrounded by a follicle which composed of a layer of follicular cells and theca. The theca composes of connective tissue, fibers of smooth muscle, small blood vessels, and nerves. The oogonia locate at the outermost area of the cortex and form germ patches.

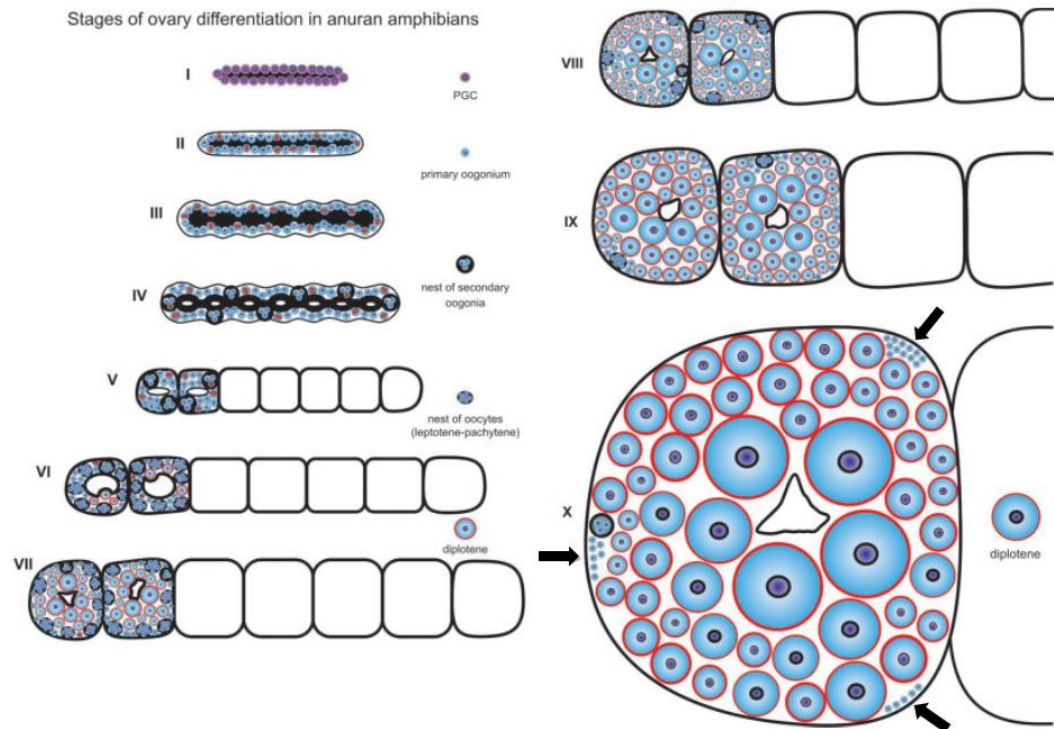


Figure 2.7 Schematic representation of ovarian development in anurans showing 10 stages of ovarian differentiation (Ogielska, 2009). Stage I–III: undifferentiated gonad; stage IV: sexual differentiation; stage V: first nests of meiocyte; stage VI: first diplotene oocytes; stages VII–IX: increasing number of diplotene oocytes and decreasing number of oogonia and nests; stage X: fully developed ovary. Arrows indicate germ patches.

จุฬาลงกรณ์มหาวิทยาลัย
CHULALONGKORN UNIVERSITY

2.2.5 Stage of testicular differentiation

The stage of testicular development in anurans has been described based on the study of Ogielska and Bartmańska (1999), Ogielska (2009), and Haczkiwicz and Ogielska (2013). Testicular development can be divided into 10 stages. Stages I–III, the stages of undifferentiated gonad are already described in stages I–III of the ovarian differentiation (see pages 26–27). The earliest morphological characters of testis differentiation were observed in tadpoles at Gosner stages 27–28 (4–5 week-old tadpole). At that time an undifferentiated gonad composed of 6–9 metameres which

will differentiate into a testis. The development at stages IV-X are described as follows (Figure 2.8):

- **Stage IV** (early testis): the cortex degenerates. The knots of the medulla are compact. The gonia (primary spermatogonia) migrate into the medulla. The space between cortex and medulla is invaded by mesenchymal cells. The mesenchyme then develop into connective tissue and Leydig cells. The testis begins to develop from the proximal part while the distal part will regress.

- **Stage V** (primary spermatogonia form aggregations): primary spermatogonia aggregate into a group of 3– 8 cells surrounded by mesenchymal cells.

- **Stage VI** (primary spermatogonia rearranged into sex cords): the spermatogonia together with Sertoli cells arrange into seminiferous cord surrounded by mesenchymal cells and collagen fibers. The medullar cells begin to develop into rete testis.

- **Stage VII** (formation of sex cords): seminiferous cords increase in size. Rete testis is conspicuous. Interstitial tissue and the tunica albuginea begin to differentiate.

- **Stage VIII** (active spermatogenesis begins): the first dark primary and cluster of secondary spermatogonia appear. The developing seminiferous cord joins the rete testis. The tunica albuginea is well developed and the amount of interstitial tissue increases.

- **Stage IX** (active spermatogenesis): meiosis starts and the seminiferous cords become seminiferous tubules with a lumen inside. The seminiferous tubules contain primary spermatogonia, cysts of secondary spermatogonia, and cysts of early spermatocyte. The rete testis becomes connected to the seminiferous tubules by short canals.

- **Stage X** (fully developed testis): the seminiferous tubules are well-developed. They are elongated and convoluted blind sacs, which become connected to the rete testis and ductuli efferentes.

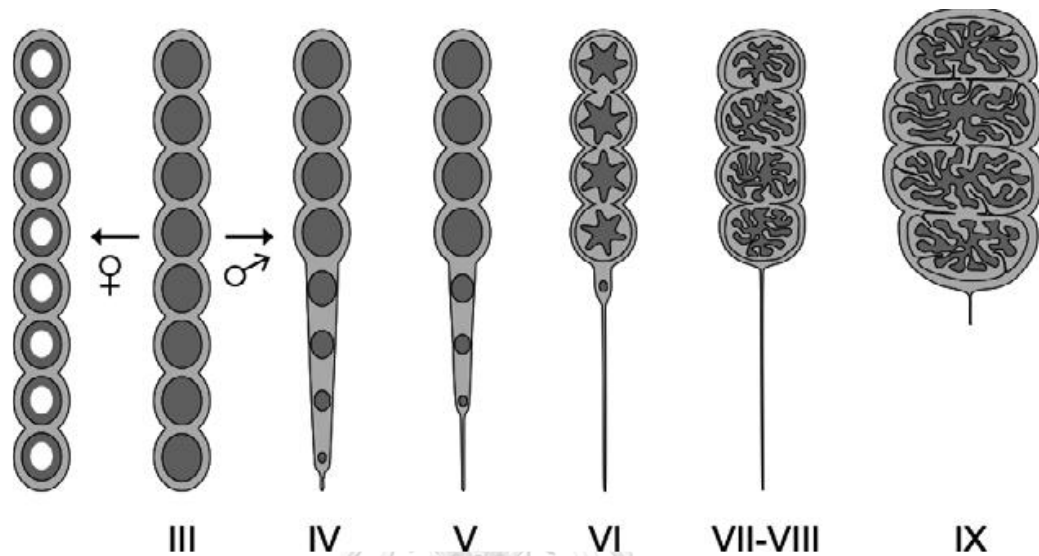


Figure 2.8 Schematic representation of testicular development in anuran showing 10 stages of testicular differentiation (Ogielska, 2009). Stage I–III: undifferentiated gonad; stage IV: early testis; stage V: primary spermatogonia form aggregations; stage VI: primary spermatogonia rearrange into sex cords; stage VII: formation of sex cords; stage VIII: active spermatogenesis begins; stage IX: active spermatogenesis; stage X: fully developed testis

2.3 Sex steroid hormone synthesis during gonadal development in anurans

Sex steroid hormones are important factors for sex differentiation in amphibians. To explain the influence of sex steroids, a number of studies usually focused on the effect of exogenous steroids. Exposure to exogenous steroids could induce sex differentiation and sex reversal in amphibians (Hayes, 1998; Piprek et al., 2012; Flament, 2016). Role of endogenous steroid hormone during gonadal development in amphibians have been investigated, however, there were little knowledge and still unclear (Hayes, 1998; Flament, 2016). Study in key enzymes of steroidogenesis could provide crucial information. According to steroidogenesis, the process starts from cholesterol as a precursor via a series of enzyme-catalyzed reactions. Several enzymes and genes have been studied about the expression pattern during gonadal development in vertebrates such as StAR, CYP11A1, 3 β -HSD, CYP17, 17- β HSD, CYP19, and 5 α Red1. Firstly, StAR (steroidogenic acute regulating protein) is a protein required for transferring cholesterol from the outer mitochondrial membrane to the inner membrane, where CYP11A1 located. CYP11A1 (cytochrome P450 side-chain cleavage enzyme) is the enzyme that converts cholesterol into pregnenolone. 3 β -HSD (3 β -hydroxysteroid dehydrogenase) is the enzyme that converts pregnenolone into progesterone and dehydroepiandrosterone (DHEA) into androstenedione (AE). CYP17 (cytochrome P450 17 β hydroxylase/C17-20 lyase) is the enzyme that converts pregnenolone into DHEA and progesterone into AE. 17- β HSD (17 β -hydroxysteroid dehydrogenase) is the enzyme that converts AE into testosterone. CYP19 (cytochrome P450 aromatase) is the enzyme that converts testosterone into estradiol (E2). 5 α Red1 (5 α -reductase) is the enzyme that converts testosterone into 5 α -dihydrotestosterone (5 α DHT) (Norris and Carr, 2013) (Figure 2.9).

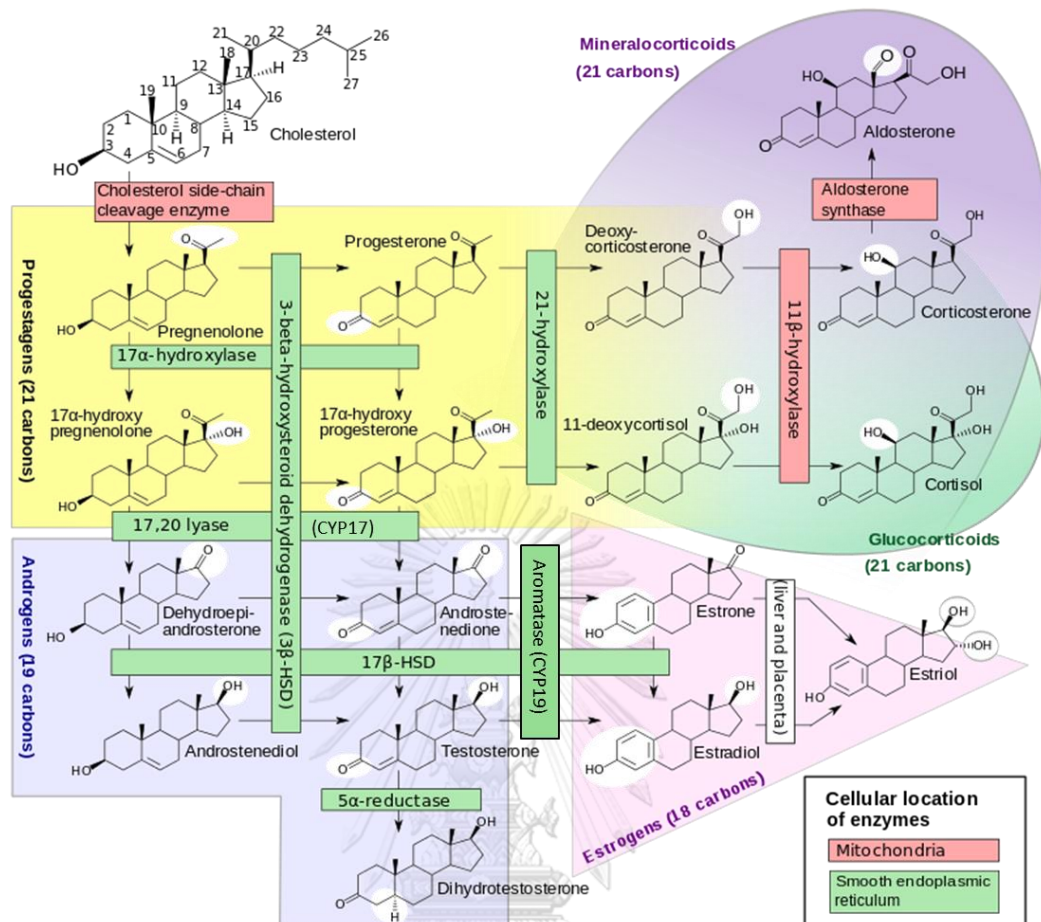


Figure 2.9 Steroidogenic pathway in vertebrates (Hägström and Richfield, 2014)

In previous studies, the activity of steroidogenic enzymes was observed during gonadal development in *G. rugosa*. Immunoreactivity of CYP17 enzyme was found in somatic cells of the indifferent gonad in males since Shumway stage 25 and Taylor and Kollros (TK) stage I and interstitial cells of the adult testis. Localization of 3 β -HSD and 17- β HSD enzyme were detected in somatic cells of the indifferent gonad of both sexes and interstitial cells of the adult testis. The activity of CYP17 enzyme was examined in the homogenate gonad and testis of frog, steroid hormone production was measured by HPLC chromatograms and detected using a liquid scintillation counter. The conversion rate of progesterone to androstenedione (AE) in the indifferent gonad of males was higher than females (Sakurai et al., 2008). Localization of CYP19 (aromatase) was found in somatic cells of the indifferent gonad of females

at TK stage I, a stage before sex determination in *G. rugosa*. The immunoreactivity was also found in ovarian somatic cells at TK stage XXV, a stage at complete metamorphosis. The activity of CYP19 enzyme was measured by HPLC analysis, conversion of testosterone to 17 β -estradiol was found since TK stage I and conversion rate in female was higher than males (Isomura et al., 2011).

Apart from steroidogenic enzymes, the expression of mRNA encoding those enzymes were also investigated. In *G. rugosa*, the expression of *CYP11A1*, *CYP17*, and *3 β -HSD* mRNA in the gonadal tissues were examined in both quantitative (qRT-PCR analysis) and qualitative (*in situ* hybridization) aspects. The level of *CYP17* mRNA expression was found much higher in the male gonads than in female gonads at TK stages II-III and extremely high in adult testis, but low in adult ovary. The expression patterns of *CYP11A1* and *3 β -HSD* mRNA were found without sexual dimorphism during gonadal sex differentiation but the adult testis and ovary were more expressed when compared to the larval stage. The results from *in situ* hybridization showed that localization of *CYP17* mRNA was found in somatic cells of an indifferent gonad of the tadpole at TK stage I and Leydig cells of the testis in 3 months after metamorphosis (Iwade et al., 2008). In addition, Maruo et al. (2008) also studied in *G. rugosa* and reported that the expression level of *17- β HSD8* mRNA was undetectable in the indifferent gonad before the onset of sex determination. *CYP17* mRNA expression was found in indifferent gonads in both sexes and much higher in male gonads. *CYP19* mRNA expression was much higher in female gonads. While expression patterns of *CYP11A1*, *3 β -HSD*, *17- β HSD12*, *5 α Red1*, and *StAR* mRNA were found without sexual dimorphism during gonadal sex differentiation (Maruo et al., 2008). Therefore, in *G. rugosa*, *CYP17* mRNA may have a crucial role in testicular development and *CYP19* mRNA may have a crucial role in ovarian development (Iwade et al., 2008; Sakurai et al., 2008; Isomura et al., 2011).

Furthermore, the evaluation of *CYP17*, *CYP19*, and *foxl2* mRNA expression was also investigated in *L. sylvaticus*. Transcription factor forkhead box L2 (*foxl2*) is a

protein that regulates *CYP19* transcription. *CYP19* mRNA was higher expressed in presumptive female larvae since Gosner stage 30 and adult females, contrasted with presumptive males and adult male groups. *foxl2* mRNA level was upregulated in presumptive female and adult females. *CYP17* mRNA level was higher in presumptive male than female. However, only the results of sexually dimorphic patterns of *CYP19* mRNA level in *L. sylvaticus* were recommended for using in the prediction phenotypic sex of *S. tropicalis* because it was highly different in expression level between sexes. The difference in *CYP19* mRNA level was found in presumptive *L. sylvaticus* larvae at Nieuwkoop and Faber (NF) stage 50 (Navarro-Martin et al., 2012). In *X. leavis*, sexually dimorphic patterns of *CYP19* mRNA level occurred just after sex determination. During sex differentiation, ovarian cavities were formed in the ZW gonad and mass of *Cyp17a1* and *Cyp19a1* positive cells were found. This mass-in-line structure disappears in the ZZ testis (Mawaribuchi et al., 2014).

One of the methods to demonstrate the activity pattern of endogenous steroid is treating the larvae with the reagent that block endogenous steroid production (Hayes, 1998). In *B. bufo* and *R. dalmatina*, acceleration in ovarian development occurred when treating tadpoles with androsten-3 one 17 β -carbossilic acid (inhibitor of 5- α -reductase) (Zaccanti et al., 1994). In *L. catesbeianus*, female to male sex reversal occurred when treating with aromatase inhibitor 4- hydroxy-androstenedione (Yu et al., 1993). Treating tadpole with fadrozole (aromatase inhibitor) could induce masculinization of gonad in *X. leavis* (Miyata and Kubo, 2000) and *S. tropicalis* (Duarte et al., 2009). In *S. tropicalis*, intersex gonads were found for 15% of their population (Duarte et al., 2009).

Overall, it can be implied that estrogens may be involved in female gonad development and *CYP19* has a major role in ovarian differentiation which represents feminization of gonad. While androgens may be involved in male gonad development and *CYP17* related to testicular development in some anuran species.

2.4 The rice field frog *H. rugulosus* (Wiegmann, 1834)

2.4.1 Classification and distribution of *H. rugulosus*

Kingdom Animalia

Phylum Chordata

Class Amphibia

Order Anura

Family Dicroglossidae

Subfamily Dicroglossinae

Genus *Hoplobatrachus*

Species *Hoplobatrachus rugulosus*

Common name: rice field frog, rugose frog, East Asian bullfrog, Chinese edible frog, Chinese bullfrog, Chinese tiger frog, I-san field frog, Taiwanese frog, common lowland frog

- Synonym: - *R. chinensis* (Osbeck, 1765)
- *R. rugulosa* (Wiegmann, 1834)
 - *R. tigrina* var. *pantherina* (Steindachner, 1867)
 - *Hydrostentor pantherinus* (Steindachner, 1867)
 - *R. esculenta chinensis* (Wolterstorff, 1906)
 - *R. burkilli* (Annandale, 1910)
 - *R. tigrina* var. *burkilli* (Boulenger, 1918)
 - *R. rugulosa* (Annandale, 1918)
 - *R. tigrina rugulosa* (Smith, 1930)
 - *R. tigrina* var. *pantherina* (Boulenger, 1920)
 - *R. tigrina rugulosa* (Smith, 1930)
 - *R. tigrina rugulosa* (Fang and Chang, 1931)

- *R. tigrina pantherina* (Taylor and Elbel, 1958)
- *R. (Euphlyctis) rugulosa* (Dubois, 1981)
- *Euphlyctis tigrina rugulosa* (Poynton and Broadley, 1985)
- *Limnonectes (Hoplobatrachus) rugulosus* (Dubois, 1987)
- *Tigrina rugulosa* (Fei, Ye, and Huang, 1990)
- *H. rugulosus* (Dubois, 1992)
- *H. nensis* (Ohler, Swan, and Daltry, 2002)

Information from Amphibian Species of the World 6.0, an Online Reference and National Center for Biotechnology Information (NCBI) (Downloaded on 28 October 2020)



Figure 2.10 Morphological character of the rice field frog *H. rugulosus* (Wiegmann, 1834)

H. rugulosus distributes from central and southern China to Myanmar, Thailand, Lao People's Democratic Republic, Vietnam, Cambodia and peninsular Malaysia (Diesmos et al., 2004; Frost et al., 2006). It inhabits wet areas such as rice fields, irrigation infrastructure, fishponds, ditches, floodplain wetlands, and forest pools (Diesmos et al., 2004). In terms of conservation status, International Union for

Conservation of Nature and Natural Resources (IUCN) classified *H. rugulosus* as a least concern species (Diesmos et al., 2004). This species is the only one member of the genus *Hoplobatrachus* found in Thailand (Chan-ard, 2003; Pansook et al., 2012). In Thailand, this frog is a valuable commercial animal because it is alternative protein source (Pariyanonth, 1985; Tokur et al., 2008). It is an interesting species to study for both commercial and scientific purposes.

2.4.2 Description of adult *H. rugulosus*

Morphological characters of adult *H. rugulosus* in Thailand were described by Flower (1899) as follows. The dorsal part of head, body, and limbs are olive-brown or pale olive-green with very dark greenish-brown or black spots. Skin on the back is either spotless or with large dark spots. Spots on legs may become broad dark transverse bars. There is no vertebral line in this species (Figure 2.10). The ventral part of body and limbs are pure silver white. The skin surface between the dorsal and the ventral body parts is an irregular space of lemon-yellow with greenish-brown spots. The lips, chin, and underneath of head are lemon-yellow with some distinct dark spots. Adult male *H. rugulosus* has paired lateral vocal sacs which are dark gray and shaded with pink. *H. rugulosus* eyes have dark brown iris with a narrow golden ring round the black pupil (Figure 2.11). Snout vent length of adult frog was about 142 millimeters.

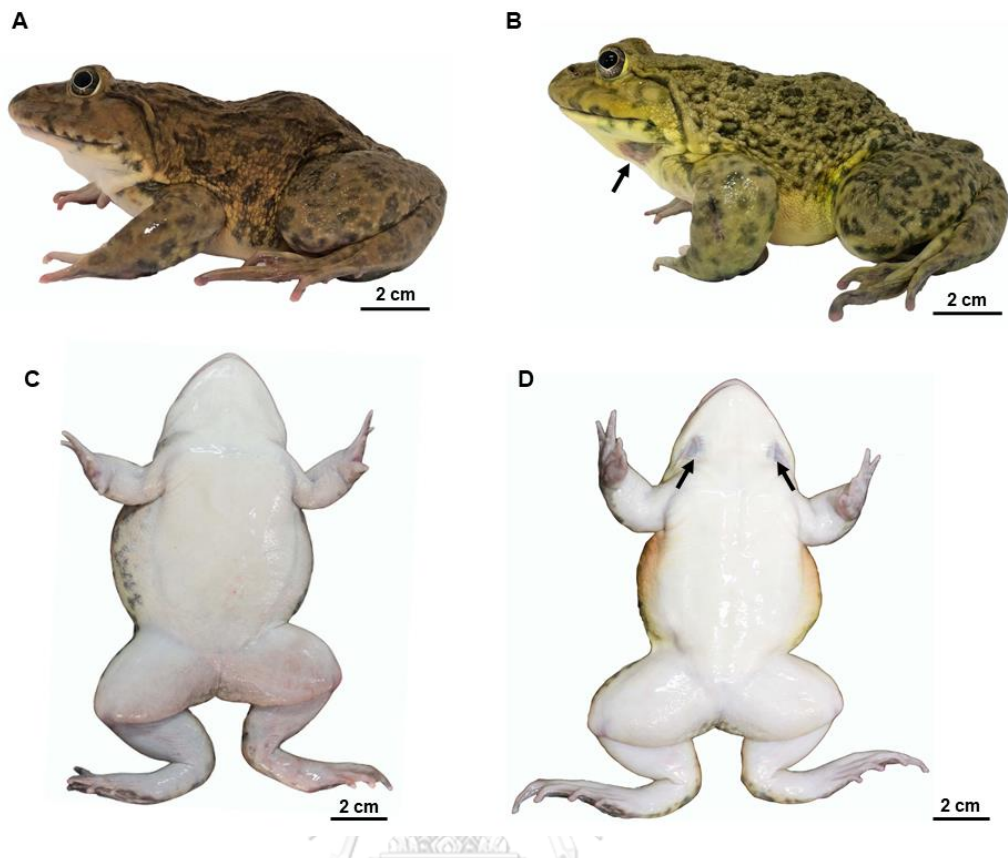


Figure 2.11 Comparison of adult female and male rice field frog *H. rugulosus*. (A) Lateral view of female frog; (B) lateral view of male frog showing vocal sac (arrow); (C) ventral view of female frog; (D) ventral view of male frog showing paired lateral vocal sacs at the angle of submandibular region

2.4.3 Description of *H. rugulosus* tadpole

Morphological characters of *H. rugulosus* tadpole in Thailand were described by Flower (1899), Danaisawat et al. (2010), and Aran et al. (2012) as follows. The proportion of body length and tail length is 1:2. Nostrils locate near to the eye than to tip of the snout. Eyes locate dorsolateral position. Mouth part locates at the ventral subterminal of head portion. The spiracle opens on the left side, directs backward and upward (posterodorsal position), and locates nearer to the anus than tip of snout. Anus opening locates medially, a vent tube is parallel with the ventral margin of the fin. Tail length is longer than tail height for 3.5-4 times. The upper crest is convex and slightly wider than the lower. Tip of the tail is a slender shape. Color pattern of the tadpole is yellowish-brown, mottled with darker brown. Dark brown crescent-shaped is marked above each nostril. Ventral part of the body is white and iridescent. The tail is yellow and mottled with brown. A horizontal dark line is present along the medial of the basal third of the tail (Figure 2.12). The tadpole size at stage 37 was reported by Aran et al. (2012). The range of body length was 15.99-17.18 millimeters. The range of tail length was 26.64-27.65 millimeters.

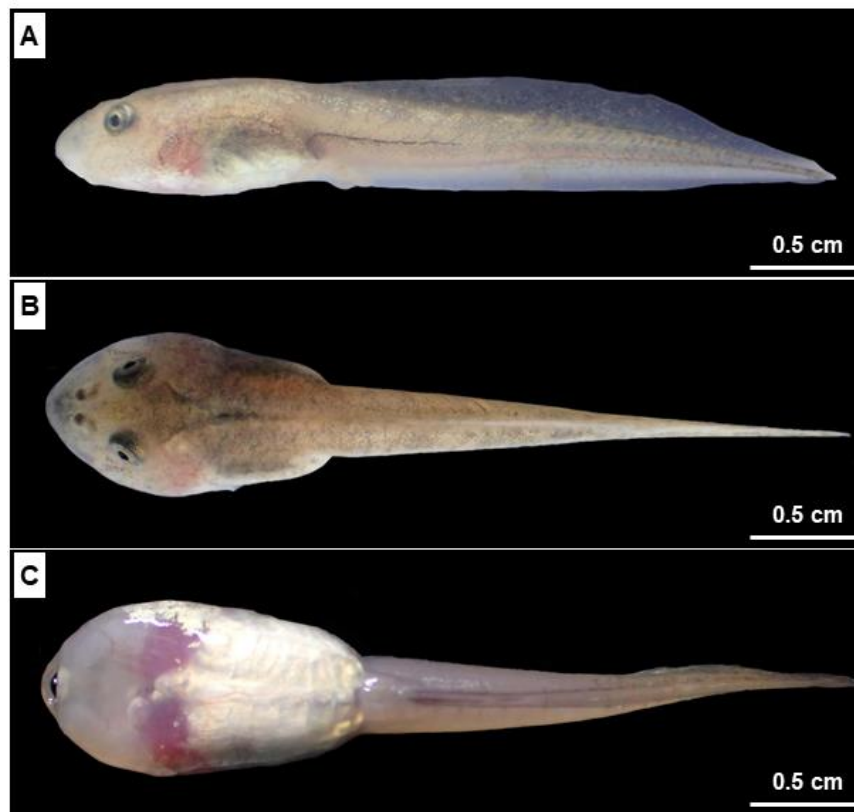


Figure 2.12 Morphological characteristics of *H. rugulosus* tadpole at stage 38 in (A) lateral view; (B) dorsal view; (C) ventral view

Mouth morphology of tadpole at stage 38 is a useful character for species identification. The morphology of oral apparatus of *H. rugulosus* is correlated with its mode of feeding since *Hoplobatrachus* is a carnivore and has cannibalism behavior (Altig and McDiarmid, 1999). Mouth part of *H. rugulosus* locates at ventral subterminal of the head portion. The mouth part structure composes of distinctive soft part and keratinized part (Figure 2.13). The anterior and posterior labia around the mouth opening are a soft part, while jaws (also called beak) at the mouth opening and droplet-like labial teeth a keratinized part. The labial teeth are biserial form with two tooth row per ridge which was a unique characteristic for discoglosids (Altig and McDiarmid, 1999). The anterior labium consists of two uninterrupted teeth rows and three interrupted teeth rows. The posterior labium is characterized by three interrupted teeth rows and two uninterrupted teeth rows. This labial characteristic of

H. rugulosus, can be defined with the labial tooth row formula (LTRF) as 2:3+3/3+3:2. The margin of the anterior and posterior labia is surrounded by a continuous row of large and blunted marginal papillae. These papillae are indistinct in the angles of the mouth. Keratinized jaw sheaths, with pitch-black and serrated cutting edge, can be observed. The upper beak with a medial projection is thinner than the lower beak. The lower beak have two strong projections which are compatible with the medial projection of the upper beak. The keratinized jaw sheaths start shedding at stage 41 and disappear at stage 42.

The LTRF of *H. rugulosus* in this study was similar to the LTRF of previous study in *H. rugulosus* in Khon Kaen Province, northeastern Thailand (Aran et al., 2012), and in *H. tigerinus* (synonym) in Songkhla Province, southern Thailand (Manthey and Grossmann, 1997) and in Bangkok, Thailand (Flower, 1899). Unlike, in *H. chinensis* (synonym) in Thanh Hoa Province, Vietnam which the LTRF was $2^2: 2^2+2^2/4^2+4^2: 1^2$ (Grosjean et al., 2004). The structure of mouthpart has been used as an important character for identification of the tadpole species (Duellman and Trueb, 1994). Therefore, the difference of LTRF in *H. rugulosus* in Thailand and *H. chinensis* (synonym) in Vietnam could be due to different population. This corresponds to the molecular studies which implied that *H. rugulosus* may be a cryptic species complex. The *H. rugulosus*, bred type was determined as sister clade to the wild type (Yu et al., 2015).

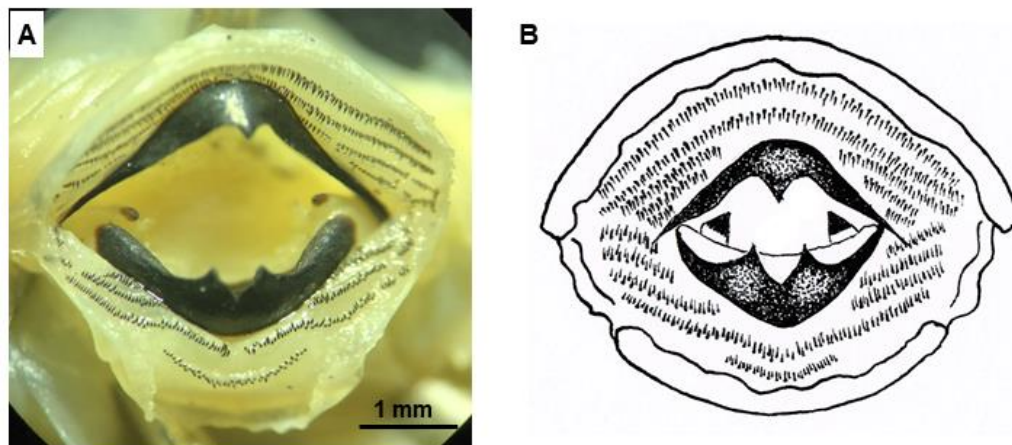


Figure 2.13 The mouth part with keratin teeth of *H. rugulosus* tadpole stage 38: (A) representative stereomicroscope photograph of oral disc and (B) schematic representation of the mouth part structure with LTRF as 2:3+3/3+3:2

2.4.4 Morphological variation and phylogenetic relationship of *H. rugulosus*

H. rugulosus have been broadly distributed from the Indian subpeninsula to eastern Asia. The geographic variation was reported in *H. rugulosus* from Myanmar, Thailand, Hong Kong, and Taiwan. Some morphological characteristics showed minor differences between localities but did not show a relationship to the patterns of geographic variation. The population of eastern frogs had larger size and have more rugose skin pattern than the western frogs. Spotted bellies were usually found in Taiwan frogs and the spotting decreased in the population at the westward location to Myanmar. Myanmar frogs have immaculate (Schmalz and Zug, 2002). Later, this species was considered as a cryptic species complex. The phylogenetic relationship was observed based on the genetic variation of mitochondrial gene (*Cyt b*) and nuclear gene (*NCX1*, *Rag1*, *Rhod*, and *Try*). *H. rugulosus* in Thailand was considered as bred type and the population in China was wild type and the bred type was suggested to be a sister clade to the wild type (Figure 2.14) (Yu et al., 2015). In Thailand, phylogenetic relationship of *H. rugulosus* was observed based on the

genetic variation of *Cyt b. H. rugulosus* population in Thailand could be classified into 2 clades. The mountain ranges and the Isthmus of Kra may play a role in hindering gene flow of *H. rugulosus* populations in Thailand (Pansook et al., 2012).



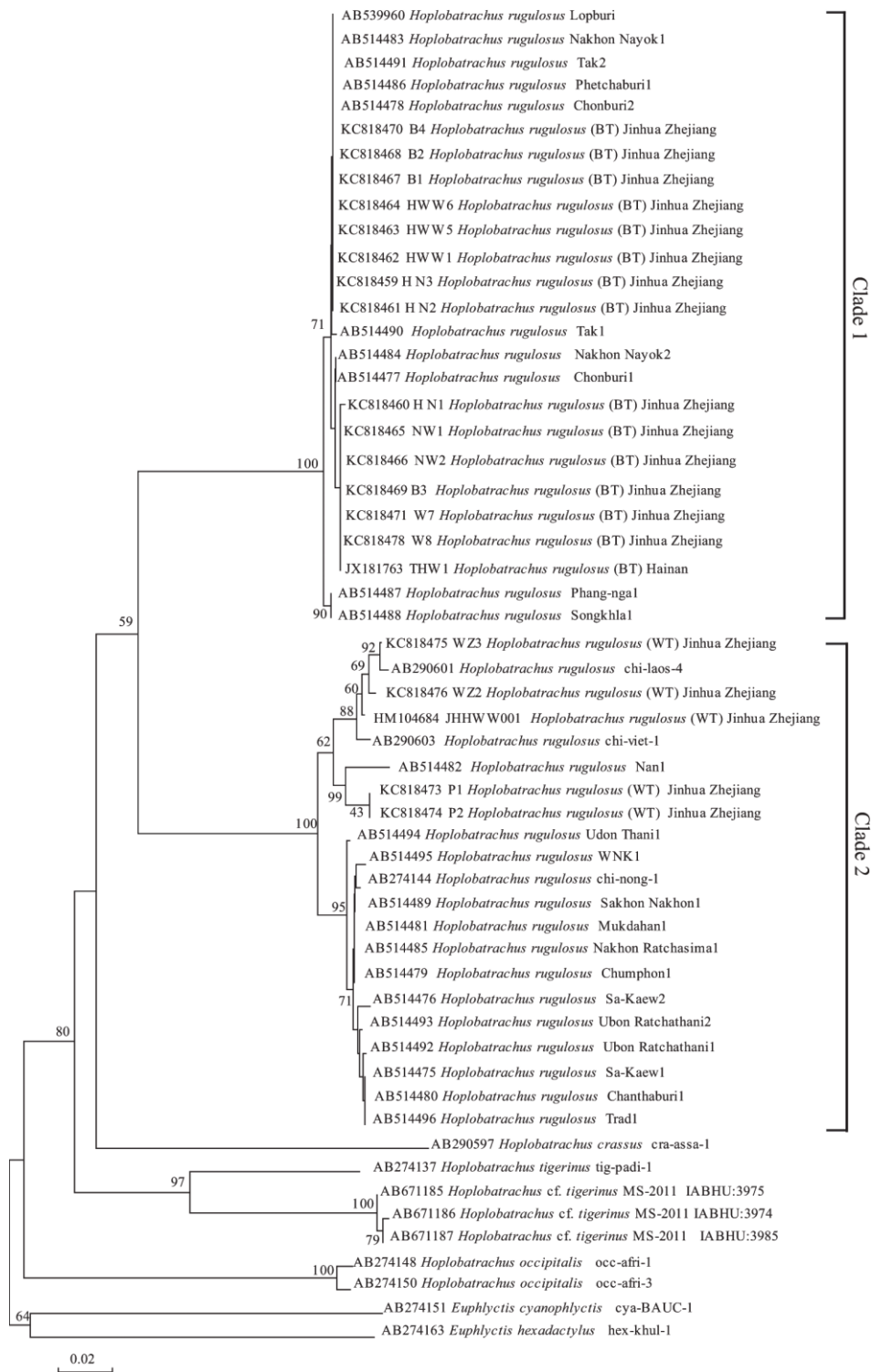


Figure 2.14 Phylogenetic relationships between *Hoplobatrachus* species. Numbers at the nodes are NJ bootstrap values. The tree was analyzed using *Cyt b* and reported by Yu et al., 2015

2.4.5 Cytogenetics of *H. rugulosus*

In Thailand, the studying of chromosome in *H. rugulosus* /*R. rugulosa* was observed in specimens from Phetchaburi province by Chockchaichomnankit (2000). The karyotype was examined by conventional staining technique. The karyotype was $2n$ (diploid) =26 with 5 pairs of large chromosomes (4 pairs of metacentric and 1 pair of submetacentric type) and 8 pairs of small chromosomes (4 pairs of metacentric and 4 pairs of submetacentric type). The nucleolar organizer regions were examined by G-band and C-band staining and showed that 13 pairs of their chromosomes are homomorphic, there was no different between sexes. It was suggested that the sex chromosome in this species have not yet evolutionarily developed. Later, the karyotype of *H. rugulosus* specimens from Nakhon Nayok and Prachin Buri province were observed by conventional staining technique by Donsakul (2009). The karyotype was $2n$ (diploid) =26 with 5 pairs of large chromosomes 8 pairs of small chromosomes (10 pairs of metacentric and 3 pairs of submetacentric type). Recently, the karyotype of *H. rugulosus* specimens from Ubon Ratchathani province was observed by conventional staining technique by Kakampuy and Supanuam (2018). Their karyotype was $2n$ (diploid) =26 with 1 pair of large metacentric, 3 pairs of large submetacentric, 2 pairs of medium metacentric, 2 pairs of small metacentric and 6 pairs of small submetacentric chromosome (Kakampuy and Supanuam, 2018). The result from this work suggested that there was no difference in sex chromosome. However, the number of chromosomes in each type are different may be because of the difference of the standard criterion for indicating the chromosome type. The sex chromosome of *H. rugulosus* has been reported as both XX/XY and ZZ/ZW (Banerjee and Chakrabarti, 2003). This report was misleading according to the use of the scientific name *H. rugulosus* as a synonyme of *R. rugulosa*. The species in the original study of Nishioka and Hanada (1994) was *R. rugosa*.

2.4.6 Reproductive biology in *H. rugulosus*

The developing oocytes during the ovarian development and seasonal variation in *H. rugulosus/R. tigerina* was examined by histological and ultrastructural study (TEM) by Sretarugsa et al. (2001). In adult frog, the developing oocytes can be classified into 6 stages including stage I-II oocyte (previtellogenic stage), stage III-IV oocyte (vitellogenic stage) and stage V-VI oocyte (vitellogenic and fully growth stages). The ovarian formation occurred in 1-month-old frog. The 2-4-month-old frogs contained only stage I oocyte. The female frogs reached to maturity stage at the age of 12 months. Their ovary contained oocytes at every stage.

The annual testicular activity in *H. rugulosus/R. rugulosa* was examined in the population from culture farm in Taiwan by Yu et al. (1993). The primary spermatogonia proliferated during November to December. Every stage of spermatogenesis could be found year round however the number of spermatozoa were highest during April to June. Leydig cells began to proliferate in late March and abundant in April to July. The seasonal changes in plasma androgen levels were correlated to Leydig cells proliferation and spermatogenesis. The structure of the testis and seasonal variation in *H. rugulosus/R. tigerina* were observed in a population in Thailand by Sretarugsa et al. (1997). Spermatogenic cells could be classified into 12 stages based on nuclear characteristics including stage 1 (primary spermatogonia), stage 2 (secondary spermatogonia), stages 3-7 (primary spermatocytes: leptotene, zygotene, pachytene, diplotene, and metaphase 1 spermatocytes), stage 8 (secondary spermatocytes), stage 9 (early spermatids), stage 10 (round spermatids), stage 11 (late spermatids) and stage 12 (spermatozoa). The testicular formation could be detected in 1-month-old frogs. The testis of 2-month-old frogs was found containing hollow sex cords. In 3-month-old frogs, the sex cords differentiated into seminiferous tubules containing primary spermatogonia. In 4-month-old frogs, spermatozoa were firstly detected in the testis. The testis reached to fully mature stage when the frogs are at the end of 6 months of age. Later, spermatogenic

process was classified into 14 stages based on studying in ultrastructure by Manochantr et al. (2003). This study reported in more detail than the study of Sretaruḡsa et al. (1997). The primary spermatocytes were divided into 6 stages (leptotene, zygotene, pachytene, diplotene, diakinesis, and metaphase) and the spermatid was divided into 4 stages.



CHAPTER III

Chronological Changes in Somatic Development of the Rice Field Frog *Hoplobatrachus rugulosus* (Wiegmann, 1834)

3.1 Introduction

More than eighty years ago, the staging table of embryo and larva development in amphibian had been published by several researchers in different species of anuran. In 1940, the study of twenty-five prefeeding stages of *R. pipiens* was published by Shumway (1940) after the publication of the temperature influenced egg development in *L. sylvaticus* (Moore, 1939). Then the study of twenty-five postfeeding stages of *R. pipiens* was published by Taylor and Kollros (1946). However, the number of the postfeeding stages is not consecutive with Shumway's table. Limbaugh and Volpe (1957) reported the complete staging table of *B. valliceps* which composed of 46 stages. In 1960, Gosner tried to simplify the staging table from the previous work of Shumway (1940), Taylor and Kollros (1946), Limbaugh and Volpe (1957) and adopted this table to use in other species based on the studies in larvae of toad species, *B. t. americanus* and *B. woodhousei fowle* (Gosner and Black, 1958). Gosner's staging system was later adjusted and used as a supplement with other staging systems in identification of embryonic stage in a number of anuran species. Currently, staging table by Gosner has been used as one of standard system and strongly recommended by several researchers (Altig and McDiarmid, 1999; Shimizu and Ota, 2003; Del Pino et al., 2004; Sayim and Kaya, 2008; Saha and Gupta, 2011; Pfalzgraff et al., 2015).

In Thailand, more than 175 species of amphibian fauna are found. There were several reports of their morphological and ecological data but the studies on life history and embryonic development are scarce. The rice field frog *H. rugulosus* is an anuran amphibian in the family Dicroglossidae, the only one member of the genus *Hoplobatrachus* found in Thailand (Chan-ard, 2003; Pansook et al., 2012). This frog is

a native frog that widely distributed throughout wet lands in Thailand and also in central and southern China to Myanmar, Lao People's Democratic Republic, Vietnam, Cambodia, and peninsular Malaysia (Diesmos et al., 2004; Frost et al., 2006). Recently, it was reported that this frog may be a cryptic species by molecular technique (Yu et al., 2015). Taxonomic studies as well as life history of this species is still needed to be done in different populations throughout their distribution range. *H. rugulosus* has been used as an experimental animal for basic biological studies in Thailand such as in taxonomic diversity and geographic variation (Khonsue and Thirakhupt, 2001; Schmalz and Zug, 2002; Bain and Truong, 2004; Hasan et al., 2012), physiology (Ratanasaeng et al., 2008), behavior (Wei et al., 2011) and pathology (Satetasit et al., 2009; Sailasuta et al., 2011). Furthermore, it has also been used in studies of environmental endocrine disrupting effects on the metamorphosis and gonadal development (Ruamthum et al., 2011; Trachantong et al., 2013). *H. rugulosus* tadpole is suitable to be an experimental animal for many studies because it could be cultured and manipulated in laboratory, it has a short period of metamorphosis, and the body size and organs are large enough to observe the morphological characters by naked eyes and under stereomicroscope. However, the information of normal embryonic and larval development in this species has never been documented. Therefore, in this study the morphological characters during the embryonic and larval development were studied in *H. rugulosus* by photomicrography and described according to Gosner staging system (Gosner, 1960). The period of time during development in *H. rugulosus* was presented as the table of chronological normal development from the stage at fertilization to complete metamorphosis.

3.2 Materials and methods

Animal procurement was carried out at Amphibian and Reptile Research Unit, Faculty of Science, Chulalongkorn University. In this study, *H. rugulosus* (bred type) were originally obtained from northern Thailand which represented a single clade of *H. rugulosus* populations (Pansook et al., 2012). The adult frogs were stimulated for fertilization during breeding period (April to July) then, the data were collected during April to August. Six pairs of adult male and female *H. rugulosus* were used as breeder. The study on somatic development during metamorphosis of *H. rugulosus* were done in two breeding periods between April to July of 2015 and 2018. Fertilization was stimulated by injection of GnRH analogue (Suprefact, Frankfurt am Main, Germany) to induce spermination, ovulation, and mating as reported in Pariyanonth (1985). Subcutaneous injection of 10 µg/1 kg body weight GnRH analogue was done in the area of abdomen using 27Gx1/2” needle. Each brood of tadpoles was raised in a 100L plastic containers under natural light and temperature conditions (water temperature 27.5–28.1 °C). Water was changed every day to remove waste and maintain oxygen level. Tadpoles and froglets were fed with commercial fish pellets once a day. The morphological changes since fertilization until complete metamorphosis were carefully observed under stereomicroscope according to the definition of characteristics in each stage of tadpole (Gosner, 1960) and photographed by Olympus DP72 camera on an Olympus SZX16 stereomicroscope with Image Stacking Cell-D Auto-montage software (Olympus Life Science, Tokyo, Japan). Tadpoles at Gosner stages 18-46 were euthanized by immersion in 0.25% of ethyl 3-aminobenzoate methanesulfonate (MS-222) aqueous solution before observation. The tadpole of 8-16 individuals at each stage were observed to collect the data of developing time. The range of total length (TL) of the embryo and tadpole at stages 1-25 was measured using Image Stacking Cell-D Auto-montage software and the TL of tadpole and froglet at stages 26-46 was measured using a digital Vernier caliper. During the observation period, the early-stage embryos

(after fertilization to Gosner stage 20) were studied at every 15 minutes intervals in the first 24 hours. After the early stage, observation was done every hour for the Gosner stages 21-25 (day 2 onward) and every day for the Gosner stages 26-46. The experimental protocol was approved by the Animal Care and Use Committee of Faculty of Science, Chulalongkorn University (Protocol Review No. 1623002).

3.3 Results

The clutch size from six pairs of breeders ranged from 600-1,800 eggs. The eggs were laid in water as large clumps. There were 2 layers of jelly envelope surrounding the egg (Figure 3.1). The range of diameter of the spherical egg without envelope was 2.012-2.166 millimeters (n=8). The animal pole was dark-brownish pigmented and the vegetal pole was white. According to the Gosner staging system, developmental period of frog has been divided into 4 phases including embryo (stages 1-20), hatchling (stages 21-24), tadpole (stages 25-41), and metamorph (stages 42-46). The ages of each stage were determined as well as their morphological characteristics as follows:

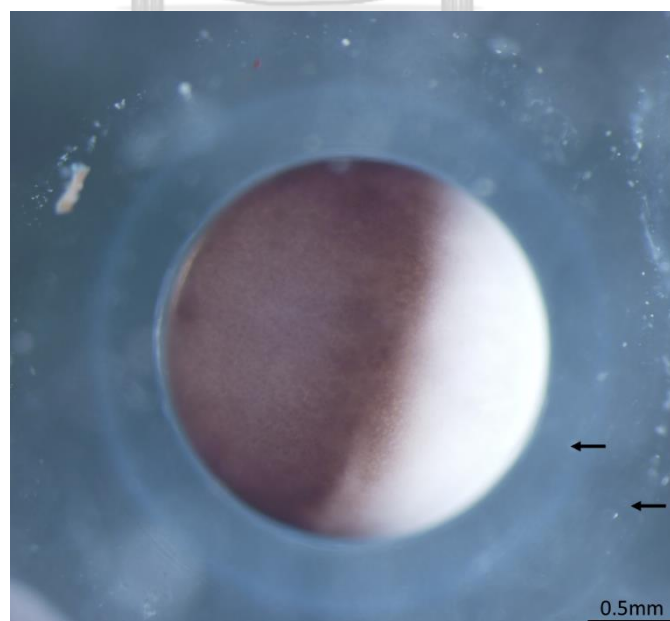


Figure 3.1 Two layers of jelly envelope (arrows) surrounding the egg of *H. rugulosus*

3.3.1 Embryo (stages 1-20, Table 3.1, Figure 3.2)

The embryo phase began with fertilization (stage 1), then the fertilized egg entered mitotic cell division which determined the beginning of stage 2. The embryonic cells underwent multiple rounds of cleavage and became blastula without increasing the cell size (stages 3-9). Gastrulation occurred at stages 10-12. Neurulation was observed at stages 13-16. Tail bud development began at stage 17. Muscular response firstly occurred at stage 18. External gills began to develop at stage 19. Hatching began at stage 20.



Table 3.1 Description of developmental stages 1-20 of *H. rugulosus* embryo according to morphological characteristics in Figure 3.2. Stage = stage of embryonic development according to Gosner (1960); TL = total length of embryo; age = developmental period; haf = hours after fertilization

Stage	Description	range of TL (mm)	range of age
1 (n=16)	Fertilization stage: The animal pole (pigmented area) was on top while the vegetal pole was in the lower part. This position will allow the egg to go through the next stage of development.	2.012-2.166	0-10 mins after fertilization
2 (n=16)	1-cell stage: The gray crescent was observed between the animal pole and vegetal pole of the fertilized egg, opposite to the sperm penetration point. The upper part of the fertilized egg became flat.	2.044-2.088	
3 (n=16)	2-cell stage: The embryo entered the mitotic cell division which is the beginning of cleavage. The embryonic cell meridional divided into 2 equal blastomeres. The first cleavage furrow originated at the animal pole and proceeded to the vegetal pole.	2.013-2.118	
4 (n=16)	4-cell stage: The embryonic cells meridional divided into 4 equal blastomeres. The second cleavage furrow was perpendicular to the first one and passed from the animal pole to the vegetal pole.	2.073-2.102	10-25 mins after fertilization
5 (n=16)	8-cell stage: The embryonic cells meridional divided into 8 blastomeres. The third cleavage furrow was lateral to the second one. The cleavage at the animal pole was faster than the vegetal pole.	2.098-2.138	
6 (n=10)	16-cell stage: At the animal pole, the embryonic cells meridional divided into 16 blastomeres. At the vegetal pole, the cleavage delayed.	2.023-2.114	
7 (n=10)	32-cell stage: The embryonic cells latitudinal divided into 32 blastomeres. The cleavage still delayed at the vegetal pole.	2.097-2.160	0.5-1 haf
8 (n=10)	Midcleavage/morula: The embryonic cells divided into more than 64 blastomeres. The size of blastomeres in the animal pole was smaller than in the vegetal pole.	2.090-2.169	

Stage	Description	range of TL (mm)	range of age
9 (n=10)	Late cleavage/blastula: The cell proliferation continued without the increase in size of the blastula. The blastomeres were divided into many smaller cells. The pigmented area at the animal pole extended over the vegetal pole, this process called epiboly.	2.125-2.162	2-5 haf
10 (n=10)	Dorsal lip: Involution of the cells from the animal pole toward the vegetal pole occurred. The dorsal lip appeared indicating the beginning of gastrulation.	2.135-2.259	
11 (n=10)	Yolk plug: The surface at the animal pole extended over the vegetal pole and the exposed area of the vegetal pole was reduced, yolk plug presented. The embryo began to be oval in shape and its position began to change creating anterior and posterior axes.	2.012-2.254	
12 (n=10)	Late gastrula: Small protruding yolk plug was present.	2.173-2.224	
13 (n=10)	Neural plate: The embryo became elongated. The dorsal area became flattening and formed a thick plate called neural plate.	2.195-2.375	3-7 haf
14 (n=10)	Neural fold: Neural fold was observed as the elevation of two ridges along the dorsal surface of the body and between these two ridges was neural groove.	2.248-2.560	
15 (n=10)	Elongation and rotation: The neural groove became narrow. The neural fold approached each other. The embryo elongated and rotated.	3.028-3.115	
16 (n=10)	Neural tube: Neural tube formed by closing of the neural fold. The embryo began to develop a head. Gill plates were observed.	3.741-4.164	5-9 haf
17 (n=10)	Tail bud: Tail bud developed at the posterior end of the embryo. Adhesive gland (oral sucker) developed.	4.260-4.455	
18 (n=10)	Muscular response, olfactory pits visible: Muscular response was noticeable. The embryo wriggled by spontaneous muscular movement. The vitelline membrane became thin and expanded. The olfactory pit developed at the ventral part of the head. The gill plates protruded.	4.302-4.707	11-13 haf
19 (n=10)	Gill buds, heart beat: External gill bud began to develop. Heartbeat was observed below the gills.	5.034-5.638	13-17 haf
20 (n=10)	Gill circulation, tail elongation: The external gill plate divided into several ridges and increased in size to form external gill filaments. Gill circulation was also observed. The tail elongated. Hatching began. The violent wiggling of embryo caused the surrounding gelatinous membrane to rupture then the embryo spurted out from the membrane.	6.036-6.284	17-21 haf

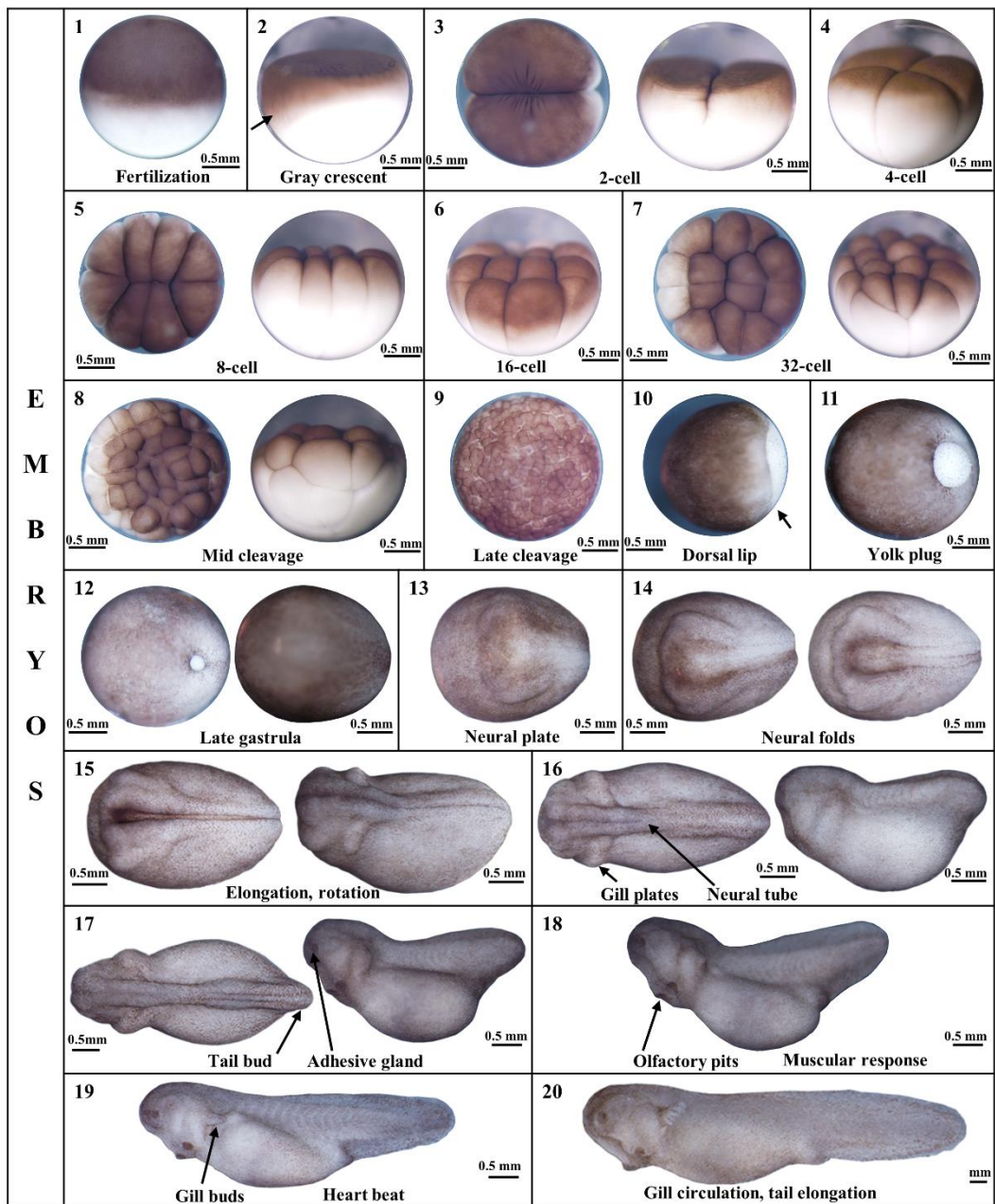


Figure 3.2 Micrographs of *H. rugulosus* at different embryonic phases (stages 1-20) showing Gosner stage number (top left corner) and the distinct key morphological characteristics according to Gosner (1960)

3.3.2 Hatchling (stages 21-24, Table 3.2, Figure 3.4)

In *H. rugulosus*, the hatchling phase began during stages 20-21. Then stages 22-24 were the stages of external gill development, pigmentation, and mouthpart development.

Table 3.2 Description of developmental stages 21-24 of *H. rugulosus* according to the morphological characteristics in Figure 3.3. Stage = stage of embryonic development according to Gosner (1960); TL = total length of embryo; age = developmental period; haf = hours after fertilization

Stage	Description	range of TL (mm)	range of age
21 (n=10)	Cornea transparent, mouth opening: The eyes of the tadpole developed. The cornea was transparent. The opening of the mouth part was observed. The tadpole was active and could swim spontaneously.	6.482-6.701	15-23 haf
22 (n=10)	Tail fins transparent, fin circulation: Dorsal and ventral tail fins became transparent and the capillary circulation was observed. Epidermis became transparent. The edge of the mouth became round. Pigmentation initially appeared in the dorsal part of the head and body.	6.705-7.113	21-26 haf
23 (n=10)	Operculum covering gill bases, labia and teeth differentiation: Labia and teeth differentiated, and adhesive gland degenerated. Operculum covered external gill bases. The external gills fully developed. Gut also developed and the body trunk appeared asymmetrical when it was observed at the ventral aspect. Pigmentation pattern in epidermis also appeared as yellowish-brown at the head, tail, and dorsal part of the trunk, mottled with black at the dorsal part of the tail and the body trunk. Iridescent speckles appeared at the dorsal area of the head and very distinct at the skin area above the eyes.	7.177-8.323	31-35 haf
24 (n=10)	External gill atrophy, operculum closure on right: The external gills reduced. The operculum folds covered the external gills and closed on the right side while the external gills on the left side remained. Iridescent pigment slightly appeared in the skin of the belly.	9.803-10.327	36-44 haf

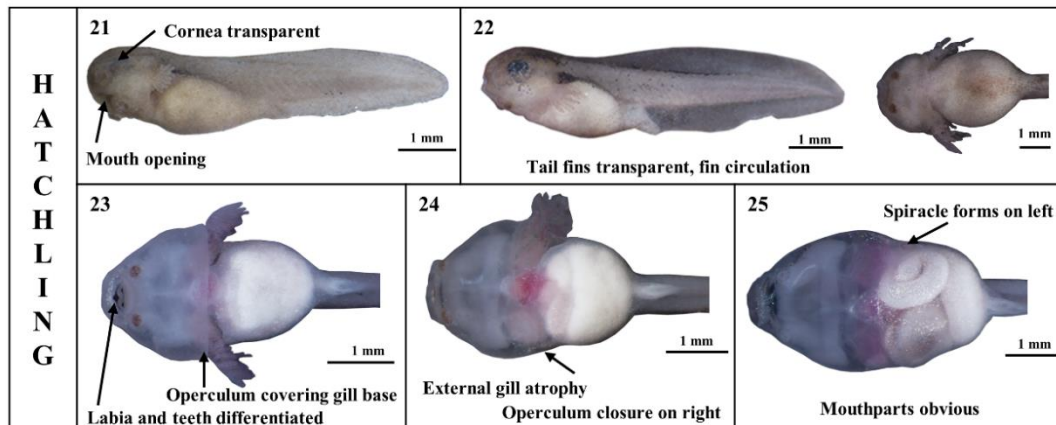


Figure 3.3 Micrographs of *H. rugulosus* at different hatchling phases (stages 21-24) and a tadpole phase (stage 25) showing Gosner stage number (top left corner) and the distinct key morphological characteristics according to Gosner (1960)

3.3.3 Tadpole (stages 25-41, Table 3.3, Figures 3.3 and 3.5)

The tadpole phase was the longest phase of developmental period. The external gills disappeared at stage 25 (within 1-2 dph or 58-88 hours). Stages 26-30 were the stages of hind limb bud development classified by the proportion of the leg length and the leg diameter which were evaluated by the according to the position of hind limb bud in Figure 3.4. Stages 31-39 were the stages of toe differentiation and development classified by the indentation of toe forming and toe separation. Stage 40 was identified by the presence of foot tubercles and stage 41 was the stage of forelimb formation.

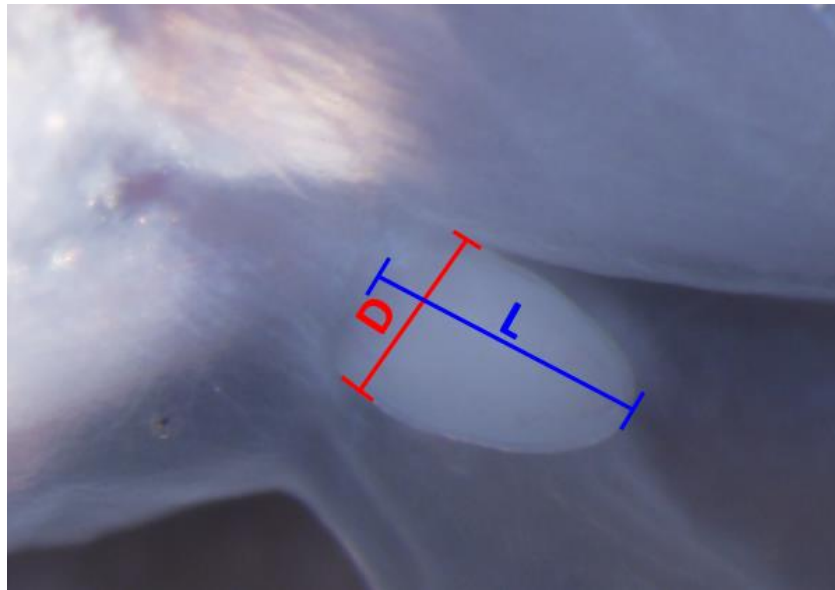


Figure 3.4 Micrographs of *H. rugulosus* hind limb bud at stage 29 showing the position for the measurement of the proportion between the leg length (L) and the leg diameter (D)



Table 3.3 Description of developmental stages 25-41 of *H. rugulosus* according to the morphological characteristics in Figure 3.3 and 3.5. Stage = stage of tadpole development according to Gosner (1960); TL = total length of tadpole; age = developmental period; dph = days post hatch

Stage	Description	range of TL (mm)	range of age
25 (n=8)	Mouthpart obvious, spiracle on left: Mouthpart shifted to upper position and located at the tip of the head. Operculum completely formed. The left external gill atrophy and spiracle formation were observed.	10.734-12.639	1-2 dph
26 (n=8)	Hind limb bud development I: Developing hind limb buds were first visible. The length (L) of limb buds was shorter than half of its diameter (D) ($L < \frac{1}{2} D$). Iridescent pigmentation was observed on the tail.	11.900-13.557	2-3 dph
27 (n=8)	Hind limb bud development II: The hind limb buds increased in size. The length of the limb buds was equal or longer than half of its diameter ($L \geq \frac{1}{2} D$).	12.984-15.592	3-5 dph
28 (n=8)	Hind limb bud development III: The hind limb buds elongated. The length of the limb buds was equal or longer than its diameter ($L \geq D$).	13.060-14.845	4-6 dph
29 (n=8)	Hind limb bud development IV: The hind limb buds elongated. The length of the limb buds was equal or longer than one and a half of its diameter ($L \geq 1\frac{1}{2} D$).	18.773-21.943	6-8 dph
30 (n=8)	Hind limb bud development V: The hind limb buds elongated. The length of the limb buds was equal to two times of its diameter ($L = 2D$).	22.121-25.157	7-9 dph
31 (n=8)	Toe differentiation and development—foot paddle: Foot paddle developed with slight indentation of the paddle margin.	24.510-27.470	8-10 dph
32 (n=8)	Toe differentiation and development—the first indentation: The foot paddle showed indentation of the 4 th and the 5 th toes.	22.091-25.160	8-11 dph
33 (n=8)	Toe differentiation and development—the second indentation: The foot paddle showed indentation between the 5 th – 4 th and the 4 th – 3 rd toes.	23.570-28.530	9-12 dph
34 (n=8)	Toe differentiation and development—the third indentation): The foot paddle margin showed indentation between the 5 th – 4 th , the 4 th – 3 rd , and the 3 rd – 2 nd toes.	26.190-29.883	10-13 dph

Stage	Description	range of TL (mm)	range of age
35 (n=8)	Toe differentiation and development—the fourth indentation: The foot paddle margin showed indentation between all five toes. Knee joint began to develop.	29.267-33.227	11-15 dph
36 (n=8)	Toe differentiation and development—the 3rd - 5th toes separated: The 3 rd - 5 th toes separated. The margin of the 5 th toe web was directed toward the tip of the 2 nd toe.	32.650-36.930	13-17 dph
37 (n=8)	Toe differentiation and development—all toe separated: The toes elongated and all toe separated. The margin of the 5 th toe web was directed toward the tip of the 1 st toe.	36.033-38.740	14-18 dph
38 (n=8)	Toe differentiation and development—metatarsal tubercles: The hind limbs increased in size. Inner metatarsal tubercles appeared at the lateral side of metatarsal area above the 1 st toe. The oral structure clearly developed and could be used as important characteristics to identify the tadpole species.	36.873-40.721	17-21 dph
39 (n=8)	Toe differentiation and development—subarticular patch: Subarticular patches appeared as light patches at the inner surface of the toes.	37.840-41.597	19-22 dph
40 (n=8)	Foot tubercles, vent tube presented: The hind limbs well developed. Foot tubercles were observed beneath the joint on the toes. Vent tube presented and not reduced yet.	39.100-44.853	19-23 dph
41 (n=8)	Forelimb visible, mouthpart atrophy, vent tube lost: Forelimb development was observed under the covering by an operculum. The mouth part became atrophied. The keratinized jaw sheaths started shedding. Cloacal tail piece reduced and vent tube completely lost.	46.137-51.547	20-26 dph

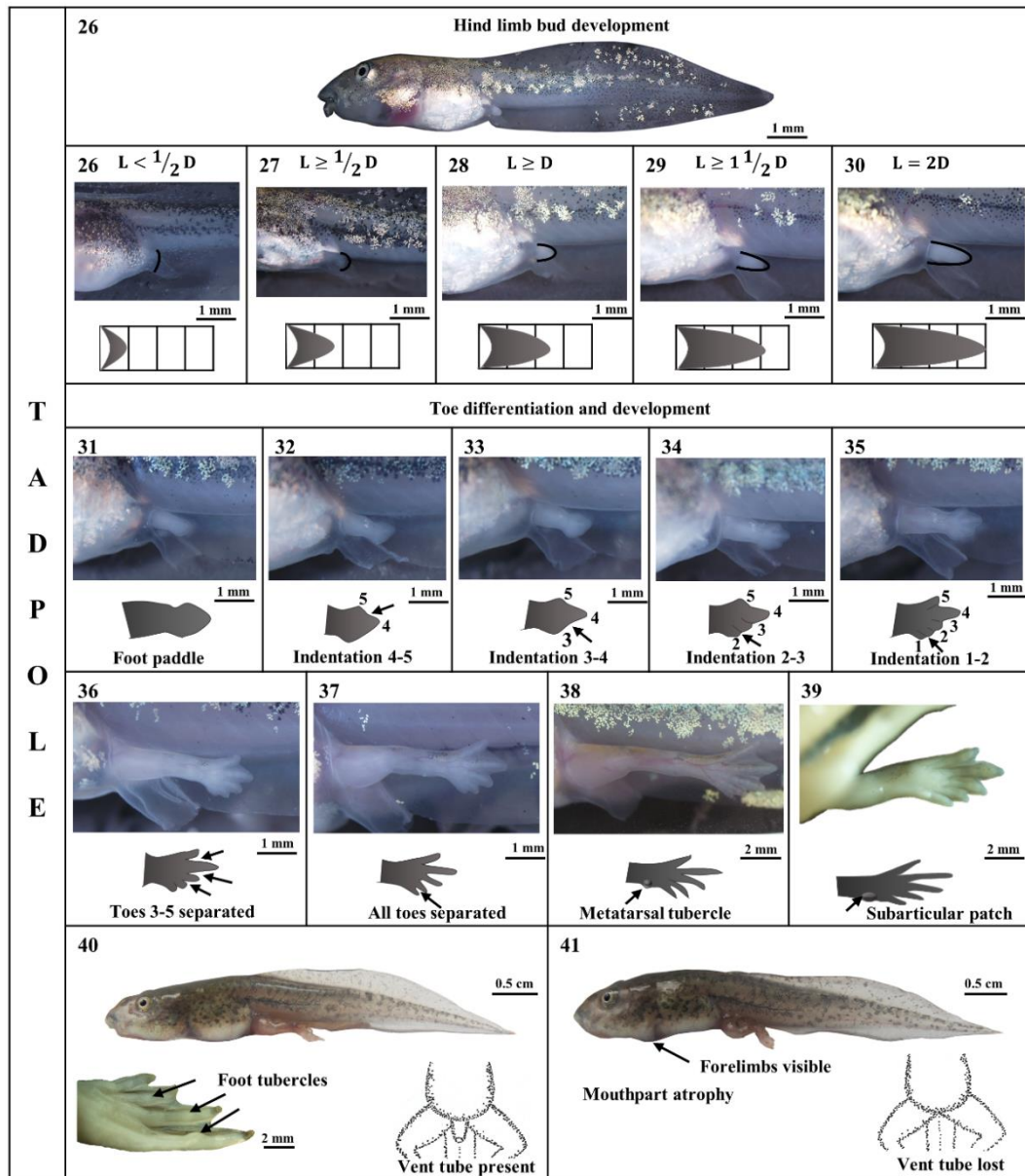


Figure 3.5 Micrographs of *H. rugulosus* at different tadpole phases (stages 26-41) showing Gosner stage number (top left corner), the distinct key morphological characteristics according to Gosner (1960) and the characteristics of hind limb bud for classification of the stage of tadpole (lower figure of each panel). D: diameter of hind limb buds, L: length of hind limb buds

3.3.4 Metamorph (stages 42-46, Table 3.4, Figure 3.5)

The metamorph phase is the phase that the tadpole changed their physical appearance for terrestrial habitat. The metamorphs at stages 42-45 were identified by the development of mouth and the metamorphs at stages 43-46 were identified by the progress of tail degeneration.

Table 3.4 Description of developmental stages 42-46 of *H. rugulosus* according to the morphological characteristics in Figure 3.6. Stage = stage of tadpole development according to Gosner (1960); TL = total length of tadpole or froglet; age = developmental period; dph = days post hatch

Stage	Description	range of TL (mm)	range of age
42 (n=8)	Forelimbs emerge, mouth angle anterior to nostrils: The forelimb emerged. The shape of the mouth was changed. From the lateral view, the end of the mouth angle was located anterior to the nostril. The keratinized jaw sheaths spurted out from the mouth part.	44.196-50.373	20-26 dph
43 (n=8)	Mouth angle located between nostril and eye: From the lateral view, the end of the mouth angle located between the nostril and the anterior end of the eye. The eyeballs began protruding. The tail became atrophied.	40.867-43.627	22-26 dph
44 (n=8)	Mouth angle located beneath eye, tail greatly reduced: From the lateral view, the end of the mouth angle reached to the middle point of the eye. The tail began to reduce. Dorsal and ventral fins gradually disappeared.	31.020-34.692	23-27 dph
45 (n=8)	Mouth angle located posterior to eye, tail stub: From the lateral view, the end of the mouth angle was posterior to the eye. The tail greatly reduced and remained as a small tail stub.	24.462-26.887	24-28 dph
46 (n=8)	Tail resorbed / complete metamorphosis: The tadpole became froglet. The tail completely reduced.	19.188-20.847	25-33 dph

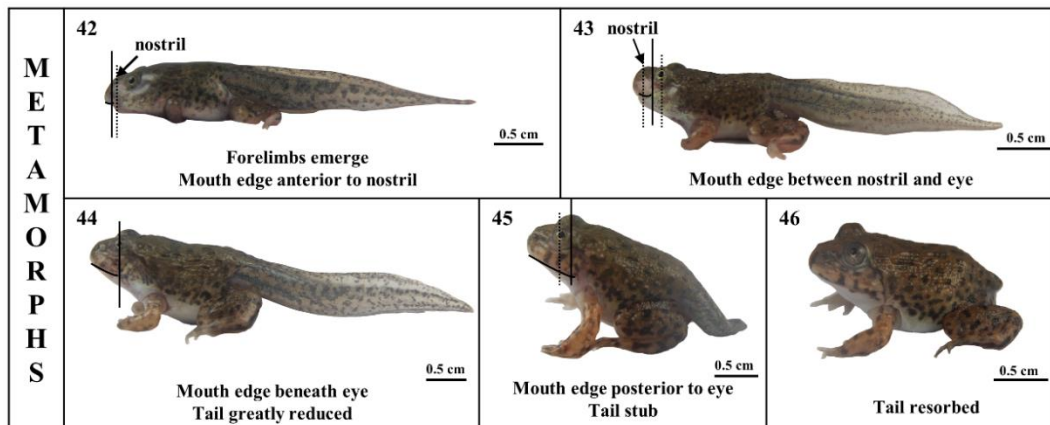


Figure 3.6 Micrographs of *H. rugulosus* at different metamorph phases (stages 42-46) showing Gosner stage number (top left corner) and the distinct key morphological characteristics according to Gosner (1960). Solid line: position of mouth angle; dash line: position of nostril and eye

3.4 Discussion and conclusion

Anuran is a widely distributed group of amphibians that can be found in several kinds of habitat. Because their embryonic development occurs in aquatic habitat, adaptation of jelly coat formation is necessary in this group of amphibians. There was a report about interspecific variation of jelly coat patterns that correlated with their environmental conditions (Duellman and Trueb, 1994). In this study, the eggs of *H. rugulosus* were surrounded by 2 layers of jelly coat and laid in the form of large clump in lentic habitats. This pattern was normally found in *Rana* species (Duellman and Trueb, 1994). The clutch size of *H. rugulosus* was 600-1,800 eggs and the range of egg diameter was 2.012-2.166 millimeters, approximately. The difference in clutch size may be influenced by maternal effect and the female size correlated with the number of egg production (Bernardo, 1996). *H. rugulosus* is a large frog, the female weighed approximately 340-460 grams and can produce a large number of eggs per clutch. It is known that the female conditions can influence oviposition site, population size, clutch structure, egg site, energy content, and pigment in the ovum.

The pattern of development, ecomorphology, and other factors were the next important factors (Altig and McDiarmid, 2007).

According to the study by Gosner in 1960, *B. valliceps* and *R. pipiens* were used as animal models to describe the stage characteristics of anuran development (Gosner, 1960). In this study, the morphological characteristics of *H. rugulosus* used for classifying the stage were similar to the characteristics in Gosner staging system. The morphological characters of anuran tadpole are various and different among species which corresponded to their ecomorphological diversity (Altig and McDiarmid, 1999). Some key characteristics are observable at different periods during developmental timeline. Some examples are shown in Table 3.5. *H. rugulosus* tadpoles have various kinds of aquatic habitat such as paddy fields, irrigation infrastructure, fishponds, floodplain wetlands, forest pools, pools, ponds, and other wet areas (Diesmos et al., 2004). The tadpole has specific characters that are suitable for living in their habitats including adhesive glands, spiracle opening position, eye position, and mouth part position. The adhesive glands developed before hatchling stage (stage 17). The tadpole used the glands to attach to the substrate after hatching from jelly coat when it inhabited the flowing-water environment. The position of spiracle opening in stage 25 appeared on the left side of the body is a specific characteristic in each taxon in the anuran. The spiracle characteristics depended on the opercular fold fusion. In *H. rugulosus*, operculum fused in the right side prior to that of the left side. Therefore, at stage 24 the tadpole had external gills just only at the left side during the development of lung inside the body. When the lung developed, the left opercular fold fused and formed the spiracle as well. Similarly, position of the eyes also correlated with their aquatic habitat. *H. rugulosus* eyes located at dorsolateral position. This was suitable for living in both lentic and lotic systems. Mouth part of anuran is one of key characteristics used to identify species during embryonic development. *H. rugulosus* had mouth part located at the ventral subterminal of the head portion. The characteristics of the oral apparatus of

H. rugulosus was correlated with its mode of feeding since this frog is a carnivore and has cannibalism behavior (Altig and McDiarmid, 1999).

Several studies reported that the developmental period of anuran was different between species. Metamorphosis of *R. leptoglossa* was completed within 68-72 days (Saha and Gupta, 2011) while that of *Polypedates (P.) teraiensis* was 58 days (Chakravarty et al., 2011). In Madagascar, metamorphosis of *Mantidactylus betsileanus* was completed within 89 days (Scheld et al., 2013). There were reports of different developmental periods of the same species that lived in different areas. Metamorphosis of *Microhyla (M) ornata* in Japan was completed within 40 days (Shimizu and Ota, 2003) while that of *M. ornata* in India was 49 days (Narzary and Bordoloi, 2013). In this study, *H. rugulosus* tadpole took 58-88 hrs for development to stage 25 which was quite fast compared to other species in anuran group. The study of Grosjean et al (2004) suggested that the adaptation of *Hoplobatrachus* could explain the population succession in this genus. The adult frogs could breed in temporary flooded or flooded areas and the tadpoles had fast development. In this study, metamorphosis of *H. rugulosus* was completed within 30.8 days \pm 2.86 SD or 25-33 days. The rapid rate of development in this species may provide benefits for escaping from some stress conditions such as predators (Calsbeek and Kuchta, 2011), dryness (Gomez-Mestre et al., 2013), and diseases (Warne et al., 2011) which were also reported in other frog species. Developmental period depended on species intrinsic factors and environmental conditions (Duellman and Trueb, 1994). The environmental factors including temperature (Liamtong et al., 2019; Tang et al., 2020), diet (Somsueb and Boonyaratpalin, 2001; Ding et al., 2015), salinity of water (Nakkrasae et al., 2016), population density (Wei et al., 2014), and number of predators (Chakravarty et al., 2011) can influence the tadpole development. The intrinsic factors especially hormone regulation play a role in frog metamorphosis including thyroid hormone, prolactin, thyroid stimulating hormone, aldosterone, corticosterone, and corticoid (Duellman and Trueb, 1994).

Table 3.5. Comparison of staging characteristics of tadpole in anuran species

Species	<i>R. pipiens</i> (Shumway, 1940)	<i>Hyla arborea</i> (Sayim and Kaya, 2008)	<i>Mantidactylus betsileanus</i> (Scheild et al., 2013)	<i>M. ornata</i> (Shimizu and Ota, 2003)	<i>M. ornata</i> (Narzary and Bordoloi, 2013)	<i>P. teraiensis</i> (Tamuly and Dey, 2014)	<i>R. leptoglossa</i> (Saha and Gupta, 2011)	<i>H. rugulosus</i> (This study)
Characters								
Fifth cleavage (Stage 7)	irregular	regular	N/A	irregular	irregular	irregular	regular	irregular
Rotation (Stage 15)	ciliary rotation	No ciliary rotation	N/A	N/A	N/A	ciliary rotation	ciliary rotation	ciliary rotation
Tail bud (Stage 17)	No arched form	Arched form	No arched form	Arched form	Arched form	No arched form	No arched form	No arched form
External gill	Present	Present	Absent	Present	Present	Present	Present	Present
Hatchling	Stage 20	Stages 20-21	Stages 23-25	Stage 21	Stage 20	Stage 20	Stages 20-21	Stages 20-21
Days of development	N/A	N/A	89 days	40 days	49 days	58 days	68-72 days	25-33 days

In conclusion, in Thailand, more than 175 species of amphibians were listed but the study of developmental stages and metamorphosis of frogs was limited. This study is the first report which provides the staging table with time data in normal development of *H. rugulosus* under natural light and temperature in the laboratory during breeding season (April to July). *H. rugulosus* developed since the first cell division until morula stage (Gosner stage 9) within 1-2 haf. Gastrulation (Gosner stage 10) began in 2-5 haf. The process of neurulation (Gosner stage 13) started after 3-7 haf. The embryos hatched from the membrane coats (Gosner stages 20-21) in 17-23 haf. The gill buds developed (Gosner stage 19) in 13-17 haf and disappeared (Gosner stage 25) in 1-2 dph. The hind limbs began to develop (Gosner stage 26) in 2-3 dph and their development completed (Gosner stage 40) in 19-23 dph. The forelimb appeared (Gosner stage 41) in 20-26 dph. The tail started to degenerate (Gosner stage 43) after 22-26 dph and fully resorbed (Gosner stage 46) in 25-33 dph.

Therefore *H. rugulosus* spend 25-33 dph for development until complete metamorphosis.

The information of the developmental rate and somatic stages of *H. rugulosus* in this study is one of the important life history characters that will be crucial for developmental research of this species in the future. The result may also be useful for applying in other taxa that have a similar ecomorphological pattern but the interspecific difference should be considered. It is also useful in term of using *H. rugulosus* as an experimental animal for environmental toxicology research such as teratogenicity tests. Furthermore, these findings can be applied for frog farming, for example to find suitable condition factors that can increase commercial benefits.



CHAPTER IV

Pattern of Gonadal Sex Differentiation in the Rice Field Frog

Hoplobatrachus rugulosus (Wiegmann, 1834)

4.1 Introduction

Sex differentiation is a diverse, e.g. protandric hermaphroditism, protogynous hermaphroditism, heterogametic sexual system (Tsai et al., 2011; Aneesh et al., 2018; Kottarathil and Kappalli, 2019; Pewphong et al., 2020) and crucial process of animal development. In amphibians, genetic sex determination generally occurs after fertilization, which is directly influenced by sex-determining genes (Hayes, 1998; Eggert, 2004; Nakamura, 2010) and environmental temperature (Eggert, 2004). Sex differentiation continues during metamorphosis, but observable differences may vary among different species. Sexual differentiation and development in amphibians have been studied for decades in several species, including *Lithobates catesbeianus*/*R. catesbeiana* (Swingle, 1925), *R. temporaria* (Witschi, 1929b), *R. ornativentris* (Iwasawa, 1969), *Pelophylax nigromaculatus*/*R. nigromaculata* and *R. japonica* (Shirane, 1986), *B. japonicus formosus* (Tanimura and Iwasawa, 1987), *Bombina orientalis* (Lopez, 1989), *Rhacophorus arboreus* (Tanimura and Iwasawa, 1989), *Pelophylax ridibundus*/*R. ridibunda* (Ogielska and Wagner, 1990), *X. laevis* (Kelley, 1996), *G. rugosa* (Nakamura, 2009), *R. curtipes* (Gramapurohit et al., 2000), *Bombina variegata* (Piprek et al., 2010), *Euphlyctis cyanophlyctis* (Phuge and Gramapurohit, 2013), *Scinax fuscovarius* (Goldberg, 2015), and *Dendropsophus labialis* (Pinto Erazo et al., 2016). The different sex differentiation processes can be categorized into different patterns. Anuran species can be divided into three sex differentiation patterns, or types (Witschi, 1929a; Gramapurohit et al., 2000; Saidapur et al., 2001; Eggert, 2004; Ogielska, 2009; Piprek et al., 2010; Phuge and Gramapurohit, 2013).

The first is the *differentiated type*, in which gonadal development begins with the formation of indifferent gonads, which develop into ovaries or testes. Female

and male gonads differentiate after metamorphosis. This pattern is common and has been reported in *Bombina orientalis* (Lopez, 1989), *Bombina variegata* (Piprek et al., 2010), *Lithobates catesbeianus*, *M. ornata*, *Pelophylax nigromaculatus*, *X. leavis* (Gramapurohit et al., 2000), and others. The second is the *semi-differentiated type*, in which the ovaries and intersex gonads can be found after metamorphosis (Flament, 2016). This type is uncommon and has only been found in a few species, e.g. *L. sylvaticus* (Witschi, 1929a), *Rhacophorus arboreus* (Tanimura and Iwasawa, 1989), and *R. curtipes* (Gramapurohit et al., 2000). The third is the *undifferentiated type*, in which the indifferent gonads develop into ovaries after metamorphosis. Testicular development occurs later, after the intersex gonads have differentiated (Flament, 2016). This pattern was reported in *B. bufo* and *R. ornativentris* (Gramapurohit et al., 2000). While it is known that anurans undergo sexual differentiation via these three patterns, the distinction between the undifferentiated and semi-differentiated types is still not clear.

The rice field frog, *H. rugulosus*, is a frog native to Thailand and is widely distributed throughout the wetlands from south-central China to the Thai-Malay Peninsula (Diesmos et al., 2004). This frog is an economically important food species and has the potential to be an experimental species in many fields of research (Pariyanonth, 1985; Diesmos et al., 2004; Tokur et al., 2008). As an experimental animal, *H. rugulosus* also plays a key role in many fields, such as biodiversity and geographic variation (Khonsue and Thirakhupt, 2001; Schmalz and Zug, 2002; Bain and Truong, 2004; Hasan et al., 2012) and the taxonomic study of phylogenetic relationships (Pansook et al., 2012) and cryptic species complexes (Yu et al., 2015). In physiology, this species has been used as a model for studying reproductive systems (Ratanasaeng et al., 2008), including the effects of environmental endocrine disruptors (Ruamthum et al., 2011; Trachantong et al., 2013). Although there have been a number of reports using *H. rugulosus*, there is still no information about the species' gonadal development.

The preliminary study demonstrated that ovarian differentiation in this species may occur earlier than testicular differentiation (Trajitt et al., 2010), and so could be categorized into either the undifferentiated or semi-differentiated type. Therefore, in this study, the process of gonadal sex differentiation in *H. rugulosus* was studied chronologically using morphological and histological approaches to clarify its pattern of gonad development.

4.2 Materials and methods

4.2.1 Animal procurement

Four pairs of adult male and female *H. rugulosus* were obtained from the Amphibian and Reptile Research Unit, Chulalongkorn University and used as the breeders for artificial fertilization. These frogs were originally obtained from a northern Thailand population that represents a single clade (Pansook et al., 2012). Subcutaneous injection of a GnRH analogue (Suprefact, Frankfurt am Main) was used to induce spermination, ovulation, and mating as reported in Pariyanonth (1985). All tadpoles were raised in 100-L plastic containers under natural light (12L: 12D) and a water temperature of 27.5–28.1°C. Water was renewed daily to remove waste and maintain the oxygen level. Tadpoles and frogs were fed with commercial fish pellets once daily. The somatic stage of each individual was examined under a stereomicroscope and estimated according to the Gosner staging system (Gosner, 1960). The age and morphological characteristics of each stage were reported in chapter III. The samples at each stage were euthanized in 0.25% (w/v) MS-222 (tricaine methanesulfonate) and photographed. The experimental protocol was approved by the Animal Care and Use Committee of Faculty of Science, Chulalongkorn University (Protocol Review No. 1623002).

4.2.2 Morphological study

After reaching stage 25 (1-2 dph), sixteen tadpoles were randomly sampled at each stage until stage 46, when metamorphosis was completed (25-33 dph). After this, 8-14 frogs were collected weekly until four months after metamorphosis. After euthanization, the gonads of each sample were dissected and the morphological characters of the gonad were examined under a stereomicroscope and photographed.

4.2.3 Histological study

Sixteen individuals of each tadpole stage (stages 25–46) and 8–14 individuals for each week after metamorphosis to the adult stage were fixed in Davidson's fixative for 24–48 hours. The gonad-kidney complex was carefully dissected, then dehydrated in an alcohol series (70, 90, 95, and 100% (v/v) ethanol). The tissues were then cleared in xylene and embedded in a paraffin block following the standard procedure (Kiernan, 1999) before being serially sectioned at 6- μ m thickness and stained with periodic acid and Schiff reagent (PAS stain) and hematoxylin. PAS stain was used to demonstrate the basement membrane such as the boundary of the germ cell group and the boundary of the seminiferous cord. Slides of gonad tissues were examined under light microscopy and photographed (Carl Zeiss-Axio Scope A1). The histological data on the developmental stages of the gonad were compared to the results of the external and gonad morphology and reported as the chronology of gonadal development for this species. The pattern of gonadal sex differentiation was examined according to the definitions of Witschi (1929), Ogielska (2009), and Flament (2016).

4.3 Results

4.3.1 Gonad morphological sex differentiation

The gonads of *H. rugulosus* were observed under light stereomicroscopy starting at stage 33 (8-12 dph), appearing as strands of a long white structure lining the anteromedial region of the kidneys (Figure 4.1A). During metamorphosis, the gonads increased in size but were still not differentiated between sexes until 3 to 4 weeks after metamorphosis. The gonads were covered by a peritoneum, which was fused together and attached the gonad to the dorsal cavity wall. In the female, the gonad expanded and formed a multiple-lobed structure composed of ovarian sacs (Figure 4.1B), which was distinct in juvenile females until adults. The shape of the ovary gradually changed due to the production of oocytes. For males, under the peritoneum, the connective tissue capsule (tunica albuginea) was formed surrounding the developing testis. The distinctive character of the testes was their long oval shape with a smooth surface (Figure 4.1C). Finger-like fat bodies were present at the cephalic end of both the ovary and testis.

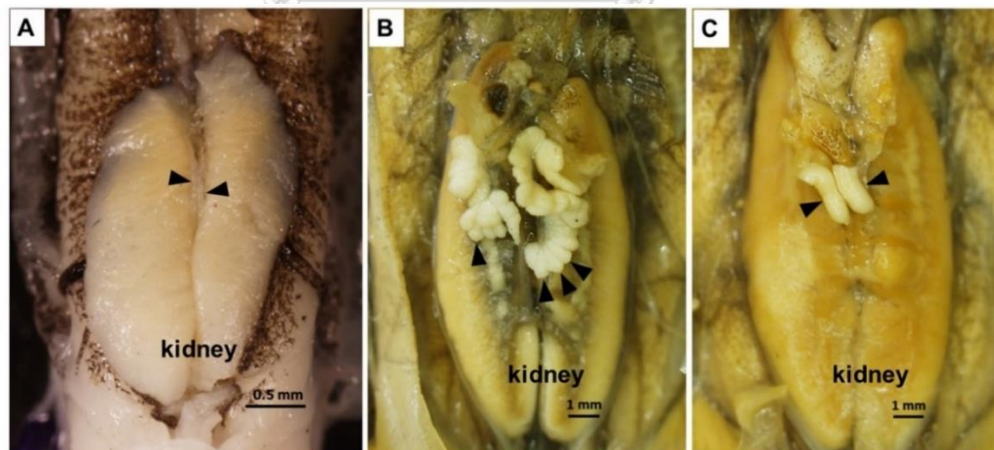


Figure 4.1 Representative stereomicroscope photographs of the gonad morphology and location in *H. rugulosus* showing (A) the developing gonads at stage 33 (arrow heads), (B) ovaries at 4 weeks after metamorphosis with numerous ovarian sacs (arrow heads), and (C) oval elongate-shaped testes at 4 weeks after metamorphosis (arrow heads)

4.3.2 Gonad histological sex differentiation and development

1) Genital ridge formation: Gosner stages 25 (1-2 dph.) – 26 (1-3 dph.)

The genital ridge was noticeable by histology at stage 25. Two thickenings of the germinal epithelium formed ventral to the dorsal mesentery at the anteromedial region of the kidneys. At this stage, the genital ridge was composed of 1–2 large primordial germ cells (PGCs) per cross section and surrounded by somatic cells (Figure 4.2). The distinctive character of the PGCs was their large irregular cell shape with a prominent and pale-stained spherical nucleus and yolk platelets in the cytoplasm.

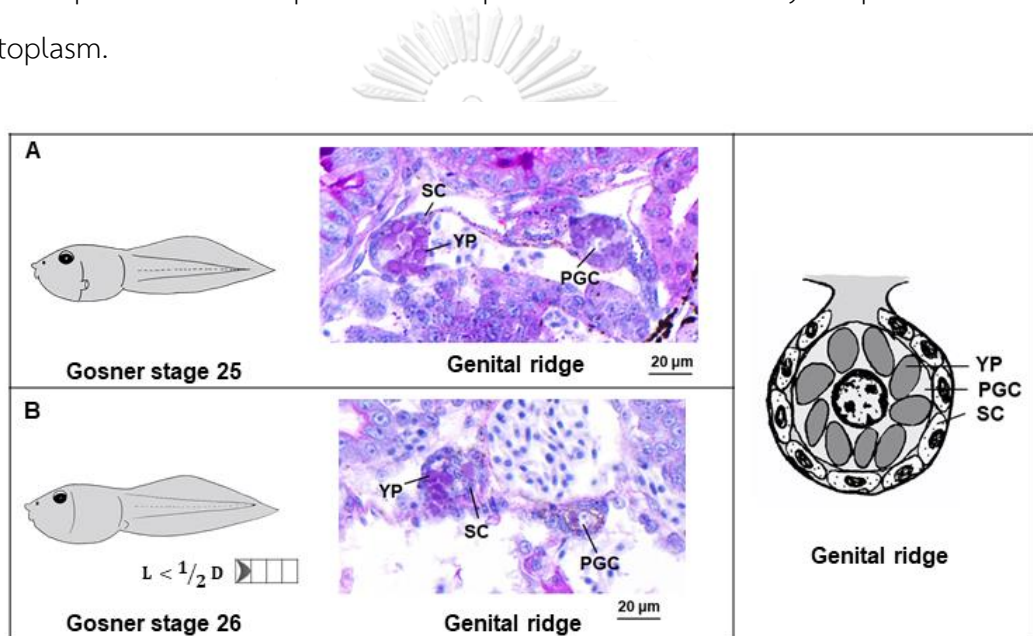


Figure 4.2 (Left) Somatic development, (Middle) gonad histology, and (Right) schematic representation of the gonads in *H. rugulosus* at (A) stage 25 and (B) stage 26, showing the genital ridge formation. D: diameter of hind limb bud, L: length of hind limb bud, PGC: primordial germ cell, SC: somatic cell, YP: yolk platelet

2) Development of indifferent gonad: Gosner stages 27 (3-5 dph) – 35 (11-17 dph)

Starting at stage 27, the size of the genital ridge increased after the proliferation of PGCs and somatic cells. It developed into the indifferent embryonic gonad protruding into the coelomic cavity. Once the yolk platelets in the PGCs were

depleted (Figure 4.3), the germ-line cells became gonocytes. The indifferent gonad gradually increased in size with increasing numbers of gonocytes and somatic cells until stage 34 (Figure 4.5). During this period, the gonocytes were large spherical cells with a spherical nucleus. At stage 30, the gonad tissue began to separate into two layers of cortex—a peripheral region with gonocytes—and the medulla, an internal region consisting of dark blue stained somatic cells (Figure 4.4).



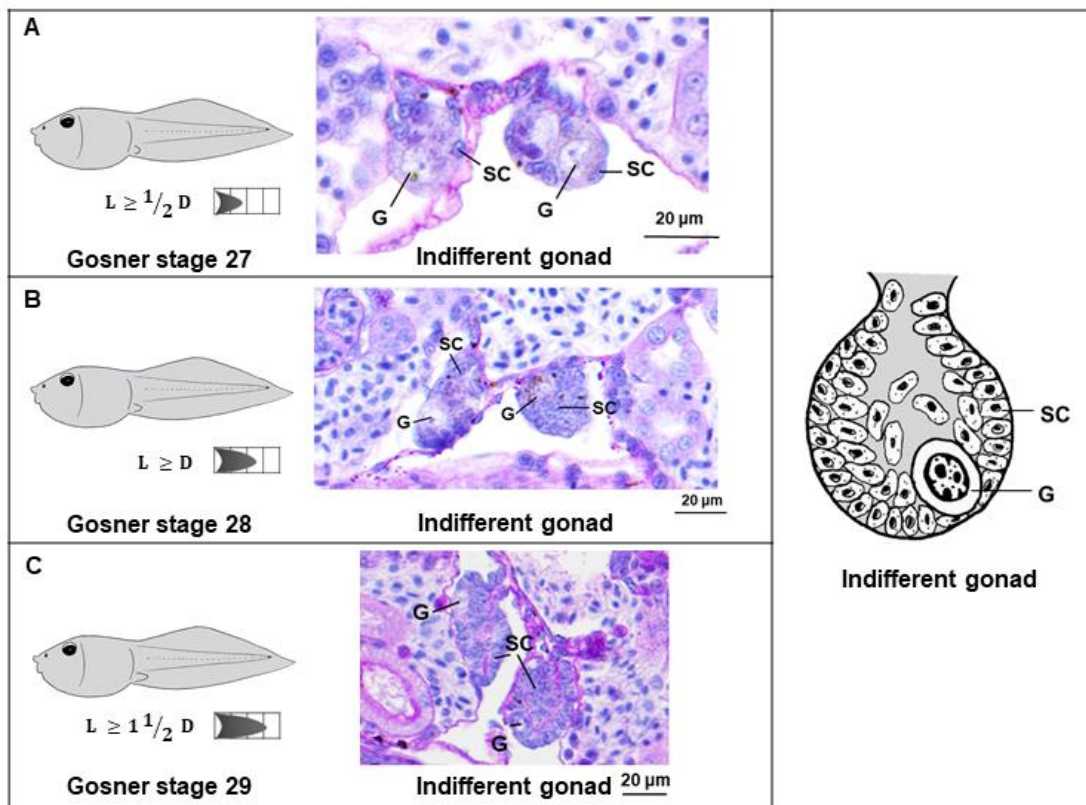


Figure 4.3 (Left) Somatic development, (Middle) gonad histology, and (Right) schematic representation of the gonads in *H. rugulosus* at (A) stage 27, (B) stage 28 and (C) stage 29, showing the indifferent gonad formation. G: gonocyte, SC: somatic cell

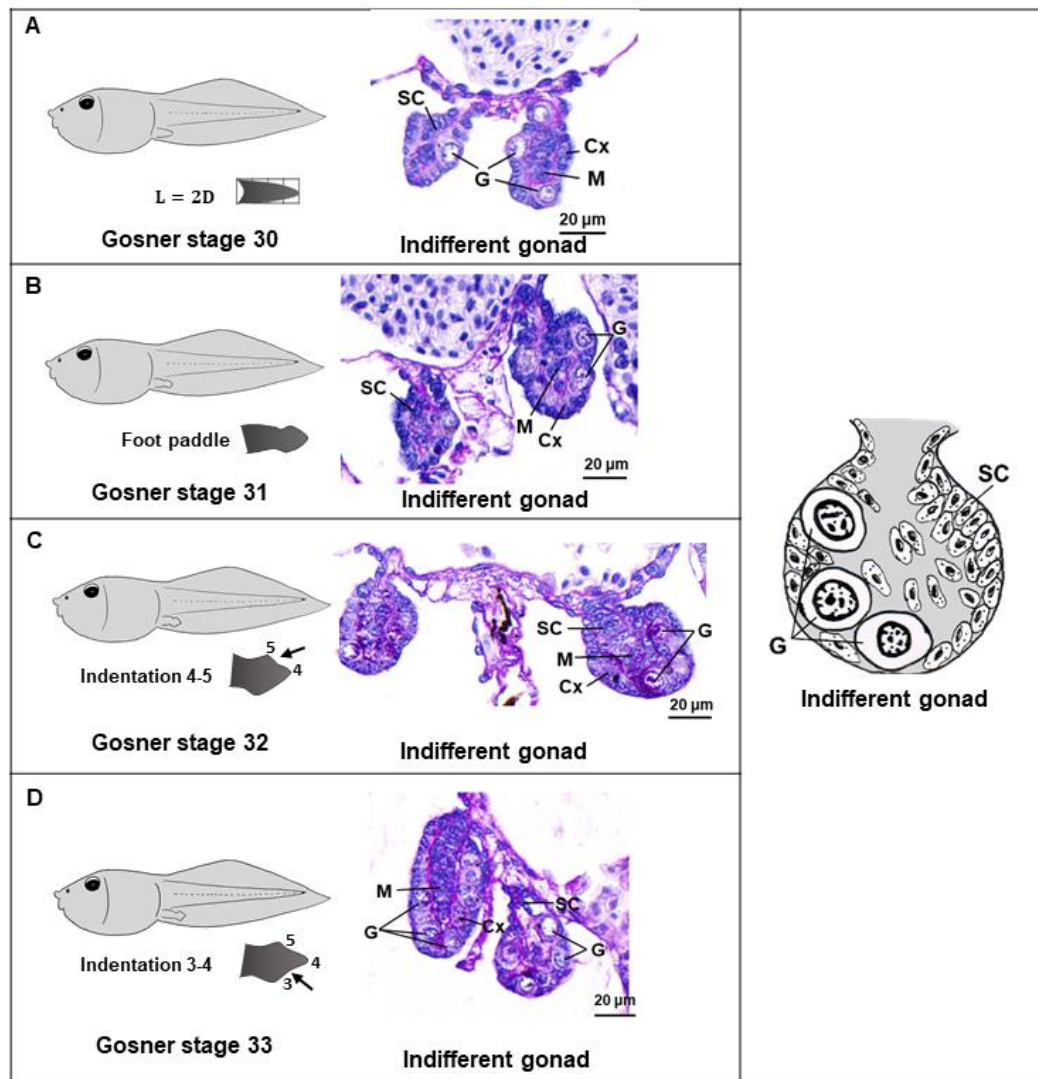


Figure 4.4 (Left) Somatic development, (Middle) gonad histology, and (Right) schematic representation of the gonads in *H. rugulosus* at (A) stage 30, (B) stage 31, (C) stage 32 and (D) stage 33, showing the indifferent gonad formation. Cx: cortex, G: gonocyte, M: medulla, SC: somatic cell

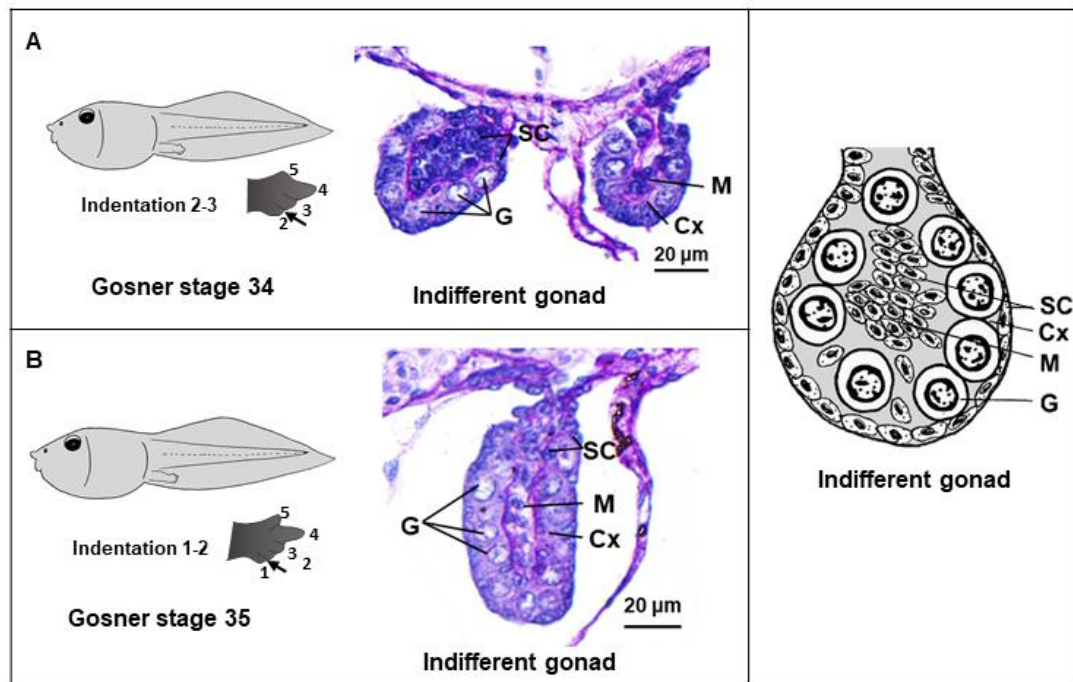


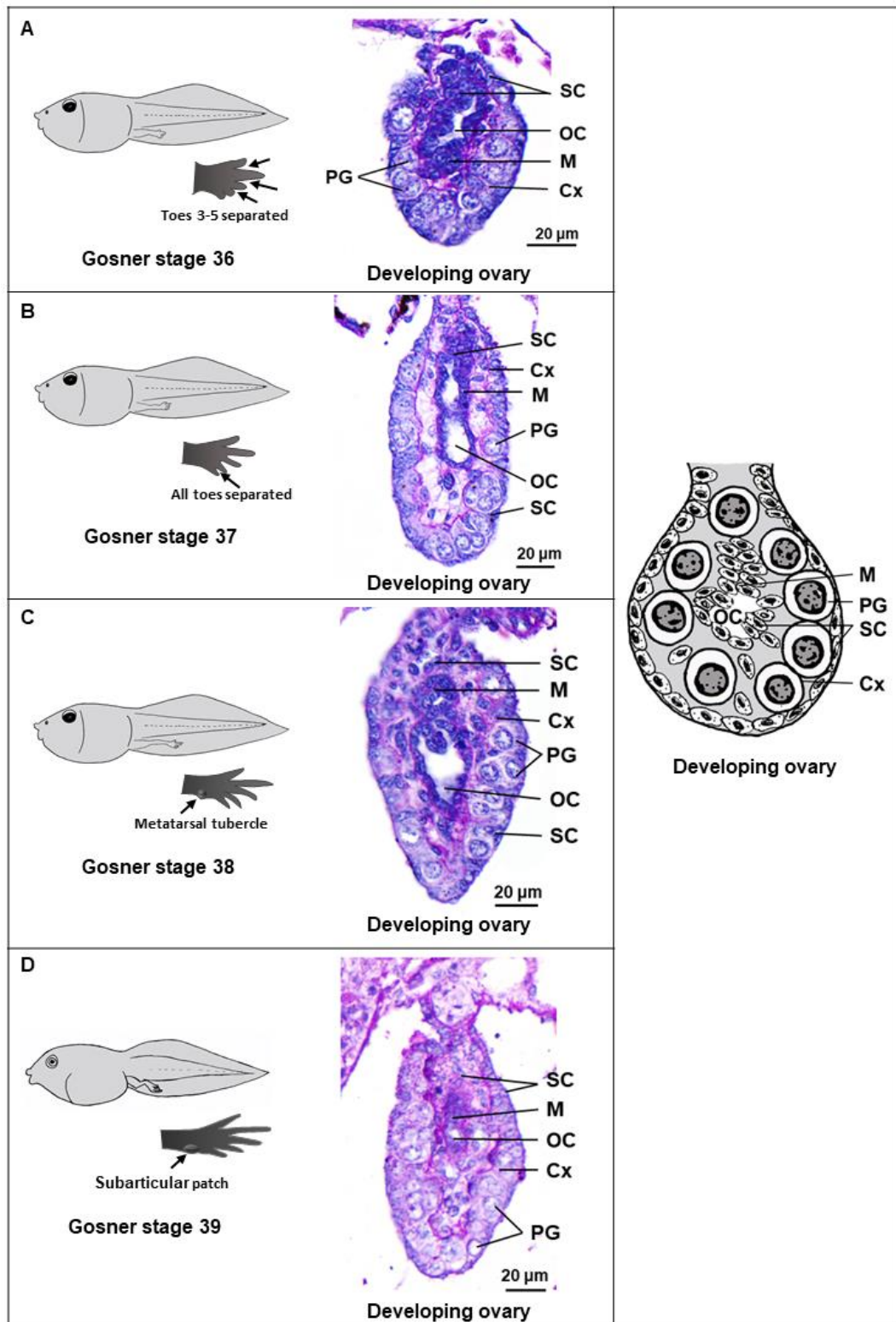
Figure 4.5 (Left) Somatic development, (Middle) gonad histology, and (Right) schematic representation of the gonads in *H. rugulosus* at (A) stage 34 and (B) stage 35, showing the indifferent gonad with an increased number of gonocytes and somatic cells. Cx: cortex, G: gonocyte, M: medulla, SC: somatic cell

3) Ovarian differentiation: Gosner stage 36 (12-20 dph.) – 4 weeks after metamorphosis

Starting at stage 36, the developing gonad expanded and gonocytes (primary oogonia from now) was spherical in shape with a pale stained cytoplasm and a spherical nucleus. Some of the primary oogonia divided mitotically and stayed aggregated into a cluster called the secondary oogonia, surrounded by a cyst. The cyst was composed of developing germ cells at the same stage of cell division. The medulla at this stage was less developed and regressed into an ovarian cavity. This is the first stage at which the gonad was clearly distinguishable as an ovary based on the appearance of the ovarian cavity and location of the single primary oogonia and cysts, which were confined to the cortex (Figure 4.6A). Since stage 40, the cortex then developed and increased in size. Secondary oogonia entered the first meiotic

prophase and formed nests of meiocytes at the leptotene and pachytene stages (Figure 4.7). At stage 42 (20-26 dph.), diplotene oocytes were seen for the first time (Figure 4.8A), and the diplotene oocytes were large spherical cells with a pink or purple stained cytoplasm and a spherical nucleus consisting of several nucleoli. The oocyte was surrounded by flat follicular cells with an oval nucleus. The medulla region of the ovary regressed continuously, and the ovarian cavity enlarged (Figure 4.8). The ovary increased in size and number of diplotene oocytes. At stage 46, the ovary was found in all individuals. Therefore, there were 100% of female at complete metamorphosis.





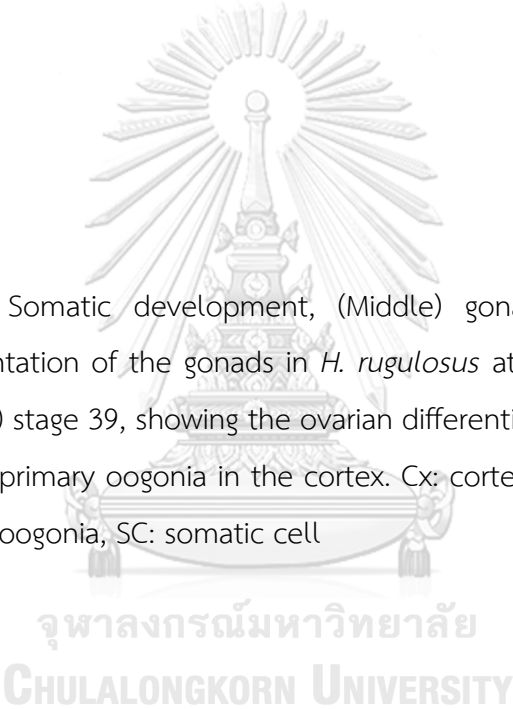


Figure 4.6 (Left) Somatic development, (Middle) gonad histology, and (Right) schematic representation of the gonads in *H. rugulosus* at (A) stage 36, (B) stage 37, (C) stage 38 and (D) stage 39, showing the ovarian differentiation with the presence of ovarian cavity and primary oogonia in the cortex. Cx: cortex, M: medulla, OC: ovarian cavity, PG: primary oogonia, SC: somatic cell

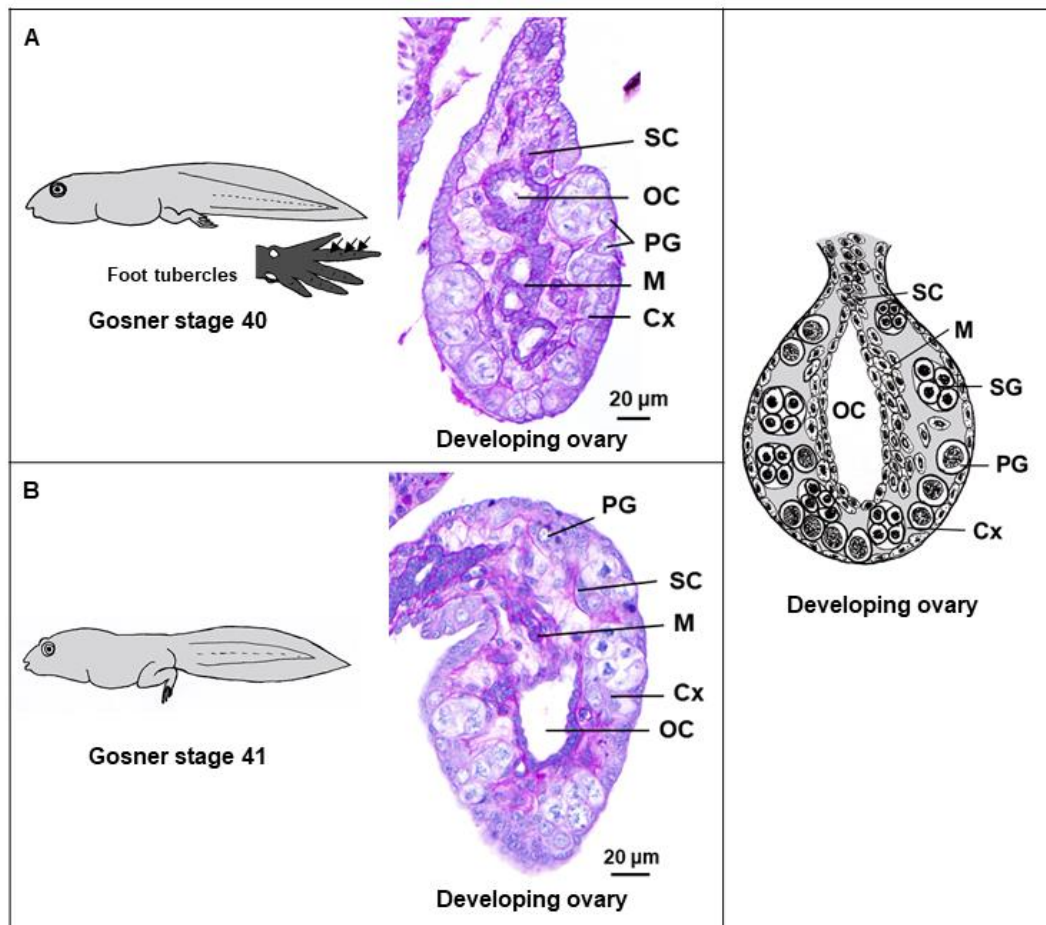
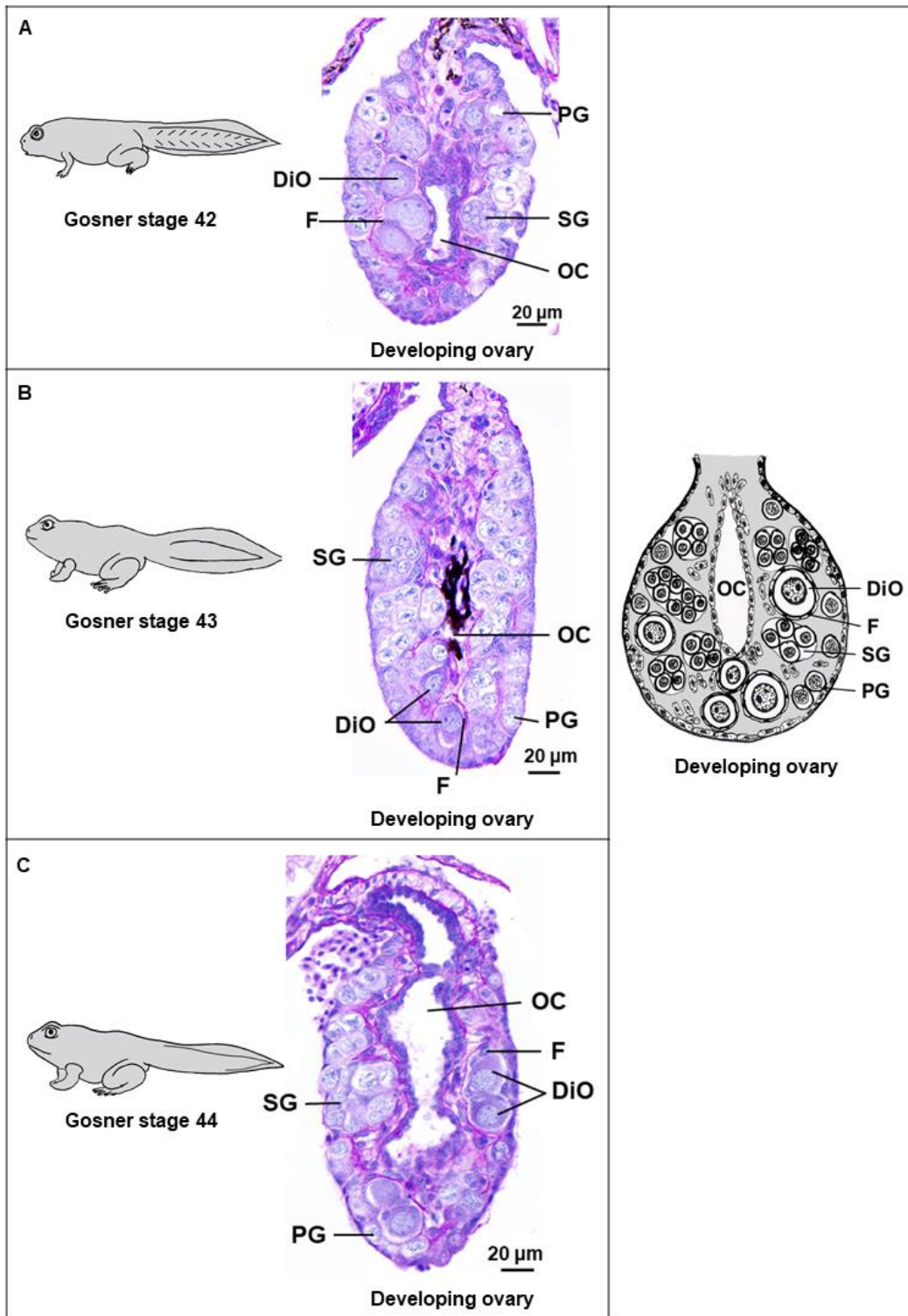


Figure 4.7 (Left) Somatic development, (Middle) gonad histology, and (Right) schematic representation of the gonads in *H. rugulosus* at (A) stage 40 and (B) stage 41, showing the ovarian differentiation with the presence of ovarian cavity and the cortex composed of primary oogonia and cyst of secondary oogonia (at leptotene and pachytene stage). Cx: cortex, M: medulla, OC: ovarian cavity, PG: primary oogonia, SC: somatic cell, SG: cyst with secondary oogonia



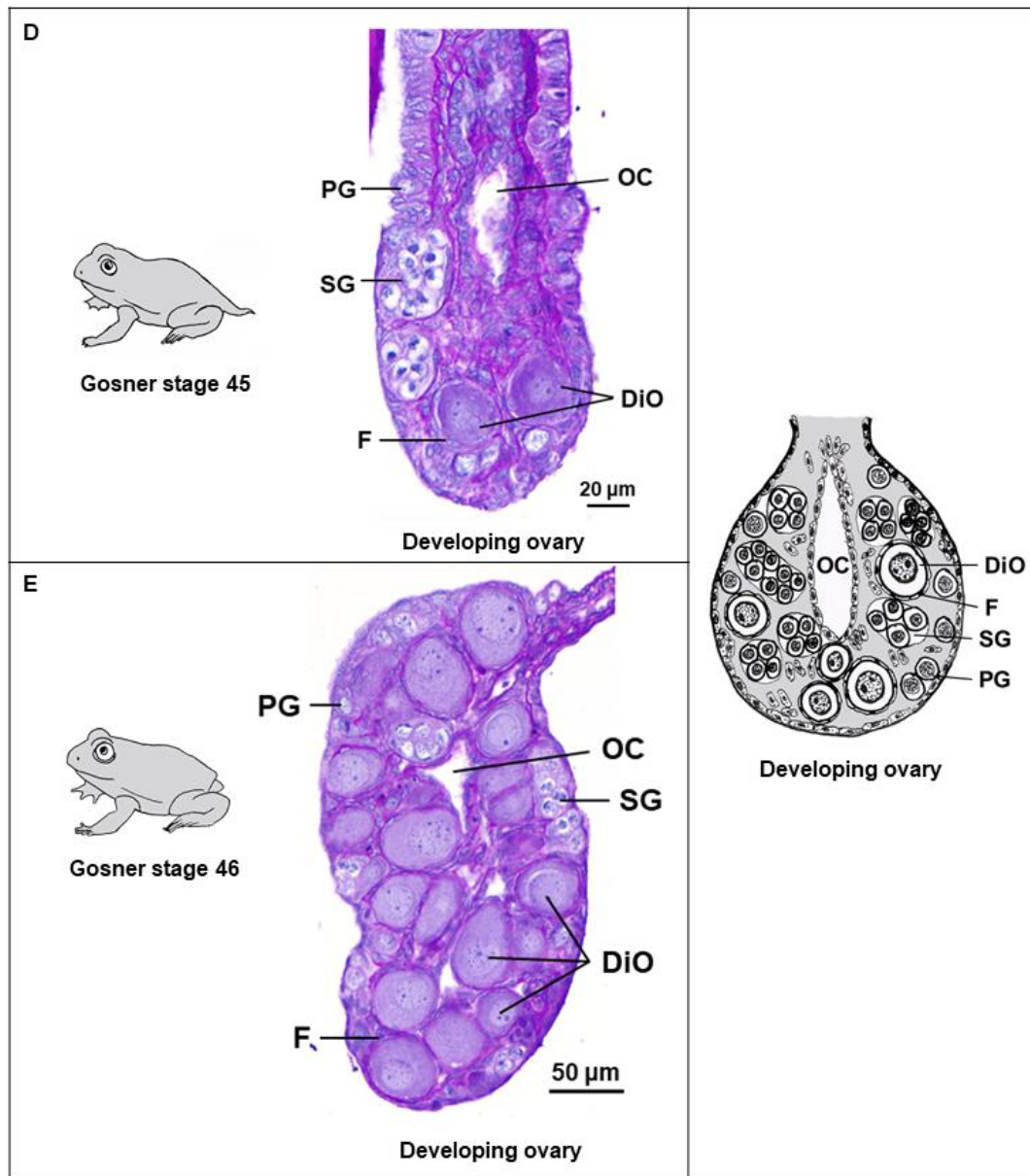


Figure 4.8 (Left) Somatic development, (Middle) gonad histology, and (Right) schematic representation of the gonads in *H. rugulosus* at (A) stage 42, (B) stage 43, (C) stage 44, (D) stage 45 and (E) stage 46, showing the developing ovary with germ cells at different stages. DiO: diplotene oocyte, F: follicle, OC: ovarian cavity, PG: primary oogonia, SG: cyst with secondary oogonia

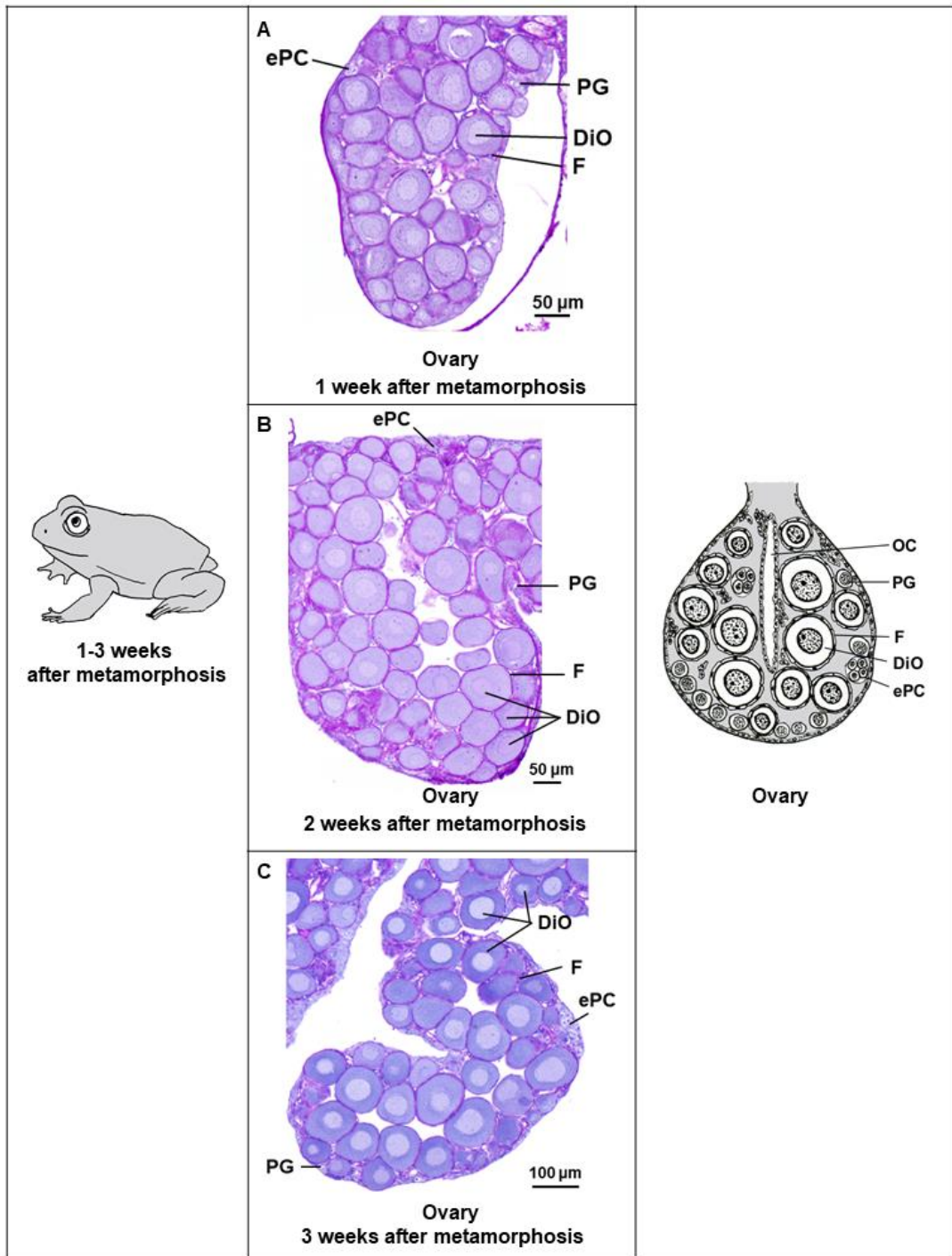


Figure 4.9 (Left) Somatic development, (Middle) gonad histology, and (Right) schematic representation of the gonads in *H. rugulosus* at (A) 1 week, (B) 2 weeks and (C) 3 weeks after metamorphosis, showing the developing ovary with numerous diplotene oocytes surrounded by follicular cells. ePC: early primary oocyte (leptotene-pachytene), DiO: diplotene oocyte, F: follicle, OC: ovarian cavity, PG: primary oogonia

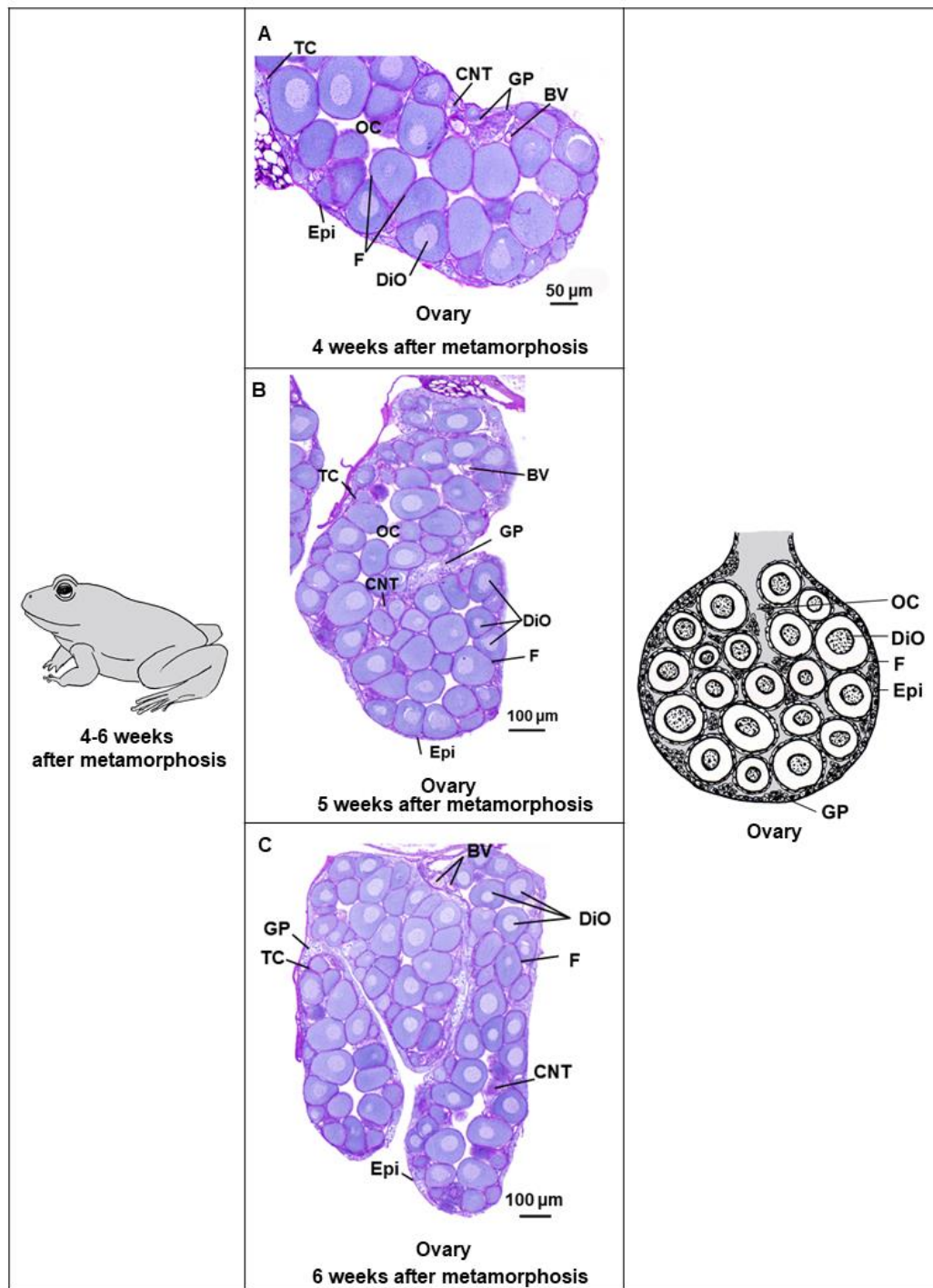


Figure 4.10 (Left) Somatic development, (Middle) gonad histology, and (Right) schematic representation of the gonads in *H. rugulosus* at (A) 4 weeks, (B) 5 weeks and (C) 6 weeks after metamorphosis, showing the developing ovary with a number of diplotene oocytes. DiO: diplotene oocyte, F: follicle, GP: germ patch, OC: ovarian cavity

The development of the ovary continued until 4 weeks after metamorphosis, when the ovary consisted of numerous diplotene oocytes surrounded by flattened follicular cells that looked like a simple squamous epithelial lining. The diplotene oocytes developed from the outermost layer towards the innermost layer of the cortex. The secondary oogonia entered meiosis and formed a cyst of leptotene-pachytene oocytes. Therefore, earlier-stage developing germ cells were found in parts of the outermost area, such as single primary oogonia and cysts containing secondary oogonia or leptotene-pachytene meiocytes (Figure 4.9). A group of them was enveloped by loose connective tissue forming the germ patch. At 4-6 weeks after metamorphosis, the ovary reached at fully developed stage which composed of the different groups of somatic cells/tissues also developed, such as theca cells, connective tissues, epithelial tissues, and blood vessels (Figure 4.10).

4) Development of the intersex gonad: one week after metamorphosis

One week after metamorphosis, some individuals (36.4%) began to develop intersex gonads after a long period (starting at stage 36) of ovarian development. The histological character of the intersex gonad resembled both a developing ovary and a developing testis. The diplotene oocytes were usually found in the innermost area of the cortex. The primary oogonia and cysts with meiocytes were still observed during this stage in the outermost area of the cortex. The ovarian cavity regressed. Some diplotene oocytes showed abnormal characters, which indicated atresia, such as hyperbasophilic cytoplasm, vacuolation, and an irregular nuclear shape. The others were normal during the diplotene stage. Later, the outermost area of the cortex was replaced by developing testicular tissue with evidence of forming seminiferous tubules (Figure 4.11). These findings implied that the transformation of the gonadal sex had occurred and the ovary had seemingly transformed into the testis. During the development of the testis, the diplotene oocytes were found inside the testicular tissue and called testis-ova (Figure 4.12).

Additionally, in terms of the external morphology, the intersex gonad was a long cylindrical organ, indistinguishable from the testis in Figure 4.1C. Although the external morphology showed a testis-like character, the histology revealed ovarian tissue mixed together with the developing testicular tissue. The intersex gonads were still observed in some individuals until the adult stage at 16 weeks after metamorphosis (mature). In juvenile males at 5 weeks after metamorphosis, diplotene oocytes were presented at the innermost area surrounded by the area of testicular formation, with a seminiferous tubule containing spermatogonia and cysts of spermatogenic cells present at every stage (Figure 4.13B). However, the degree of intersex tissue occupying the gonad varied among individuals, from 1 to 12 diplotene oocytes per cross section (Figure 4.14). In some individuals, the external morphology was similar to that of the testis, but small ovarian sacs were still present (Figure 4.13C). The histology of the above-mentioned gonads revealed a mixture of ovarian tissue containing numerous diplotene oocytes and some degenerating oocytes in the testicular tissue. They had a thickening connective tissue layer that surrounded the outermost area of the cortex. This character was similar to that of the tunica albuginea, which is normally formed in the developing male gonad. The outer surface was smooth. This character was not found in females at the same stage of development (Figure 4.13D).

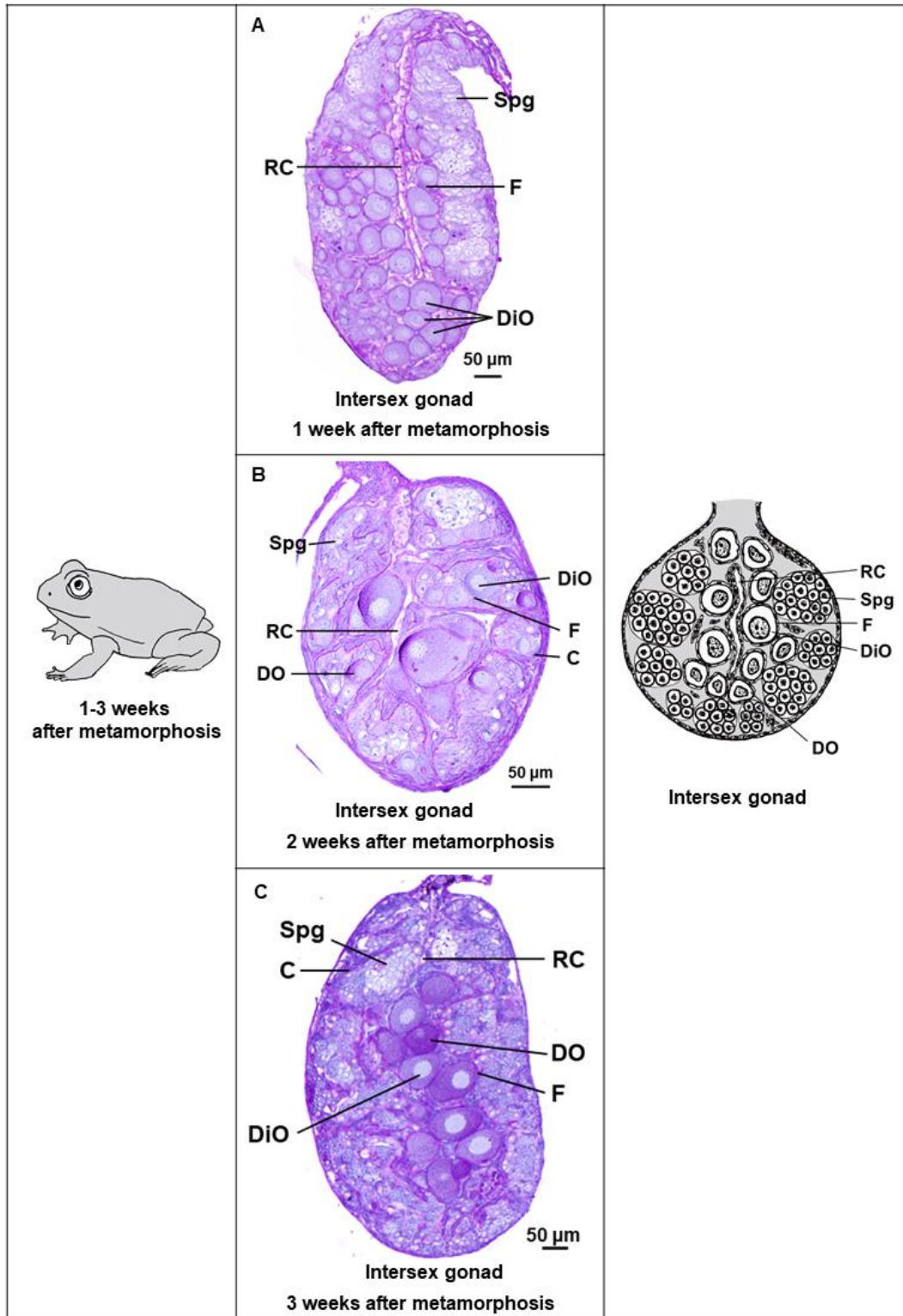


Figure 4.11 (Left) Somatic development, (Middle) gonad histology, and (Right) schematic representation of the gonads in *H. rugulosus* at (A) 1 week, (B) 2 weeks and (C) 3 weeks after metamorphosis, showing the intersex gonad with regressed ovarian cavity, diplotene oocytes and degenerating oocytes at the innermost area, and early seminiferous tubules (containing spermatogonia and some spermatogonial cysts) in the outermost area of the cortex. C: sex cord, DiO: diplotene oocyte, DO: degenerating oocyte, F: follicle, RC: regressed cavity, Spg: spermatogonia

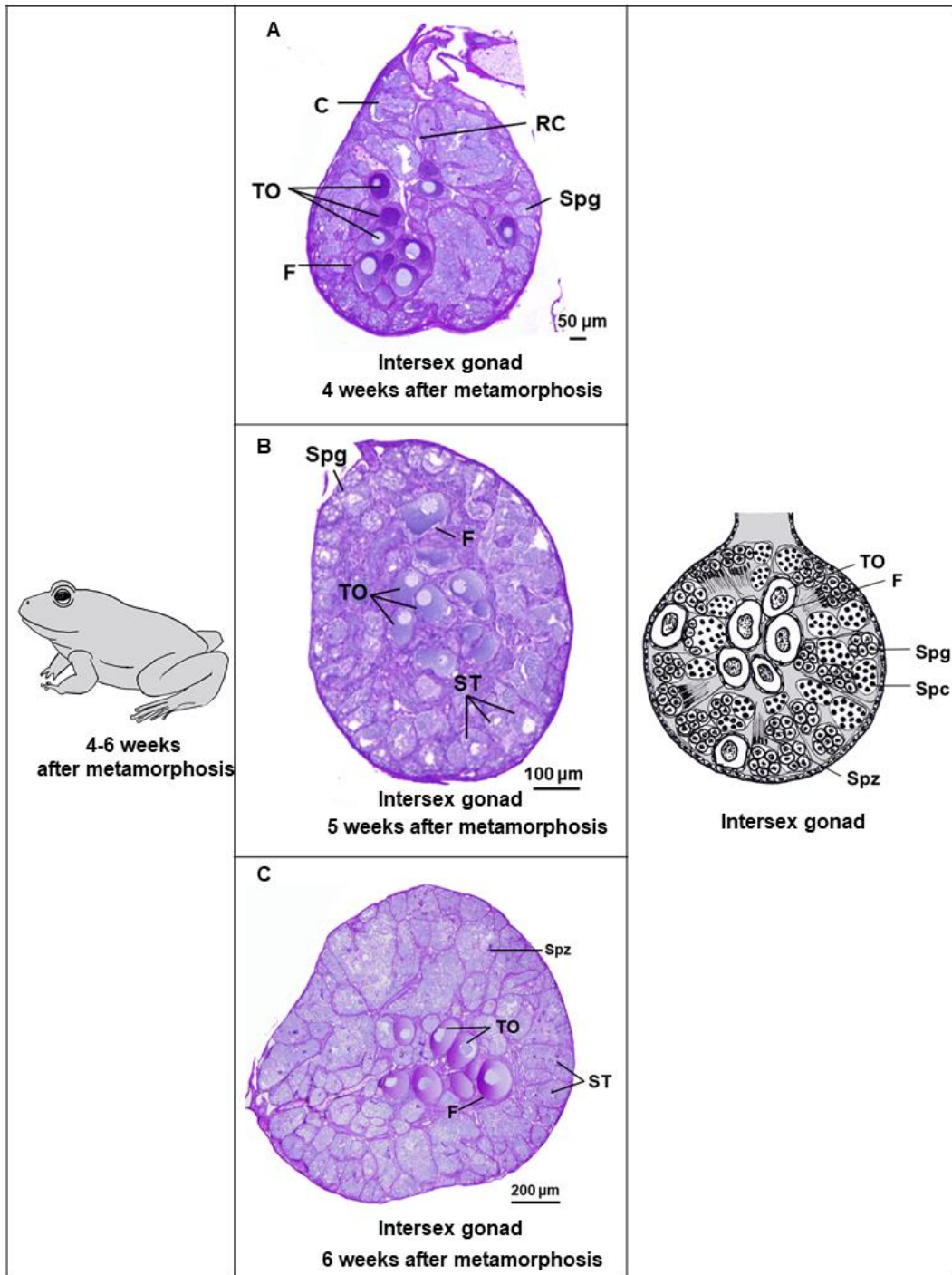


Figure 4.12 (Left) Somatic development, (Middle) gonad histology, and (Right) schematic representation of the gonads in *H. rugulosus* at (A) 4 weeks, (B) 5 weeks and (C) 6 weeks after metamorphosis, showing the intersex gonad with testis-ova at the innermost area and testicular tissue at the outermost area of the cortex. C: sex cord, F: follicle, RC: regressed cavity, Spc: spermatocyte, Spg: spermatogonium, Spz: spermatozoa, ST: seminiferous tubule, TO: testis-ovum

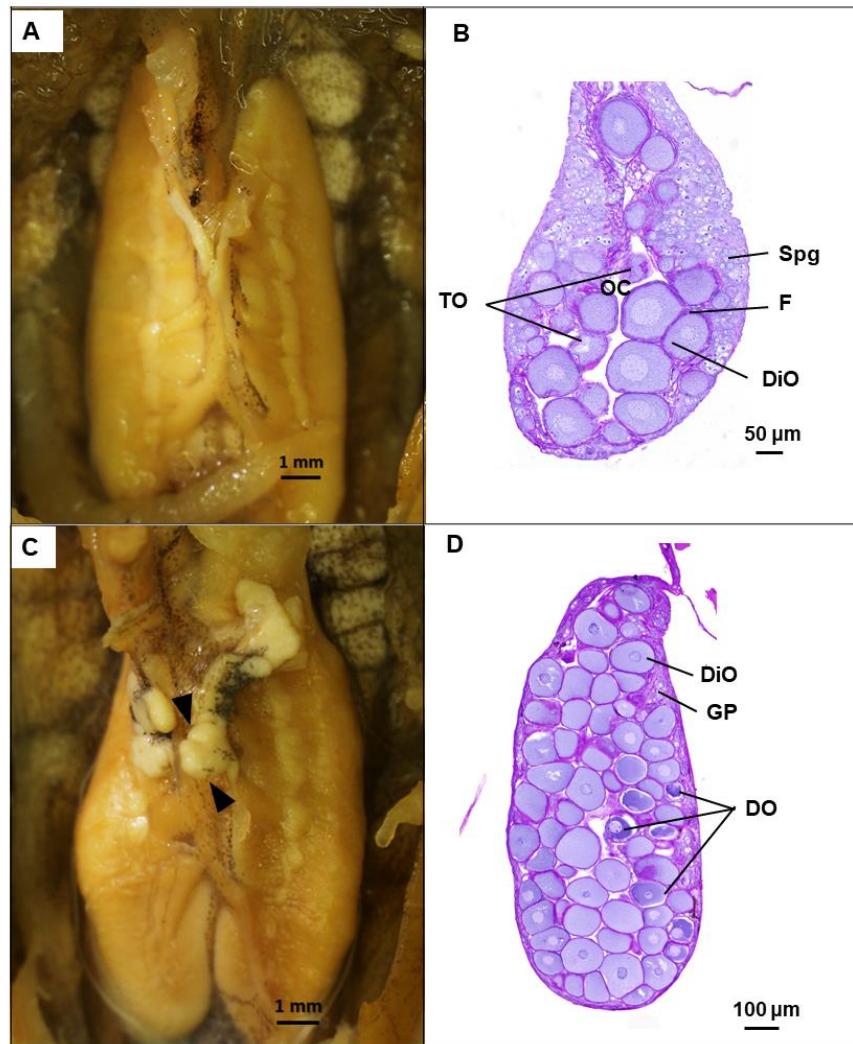
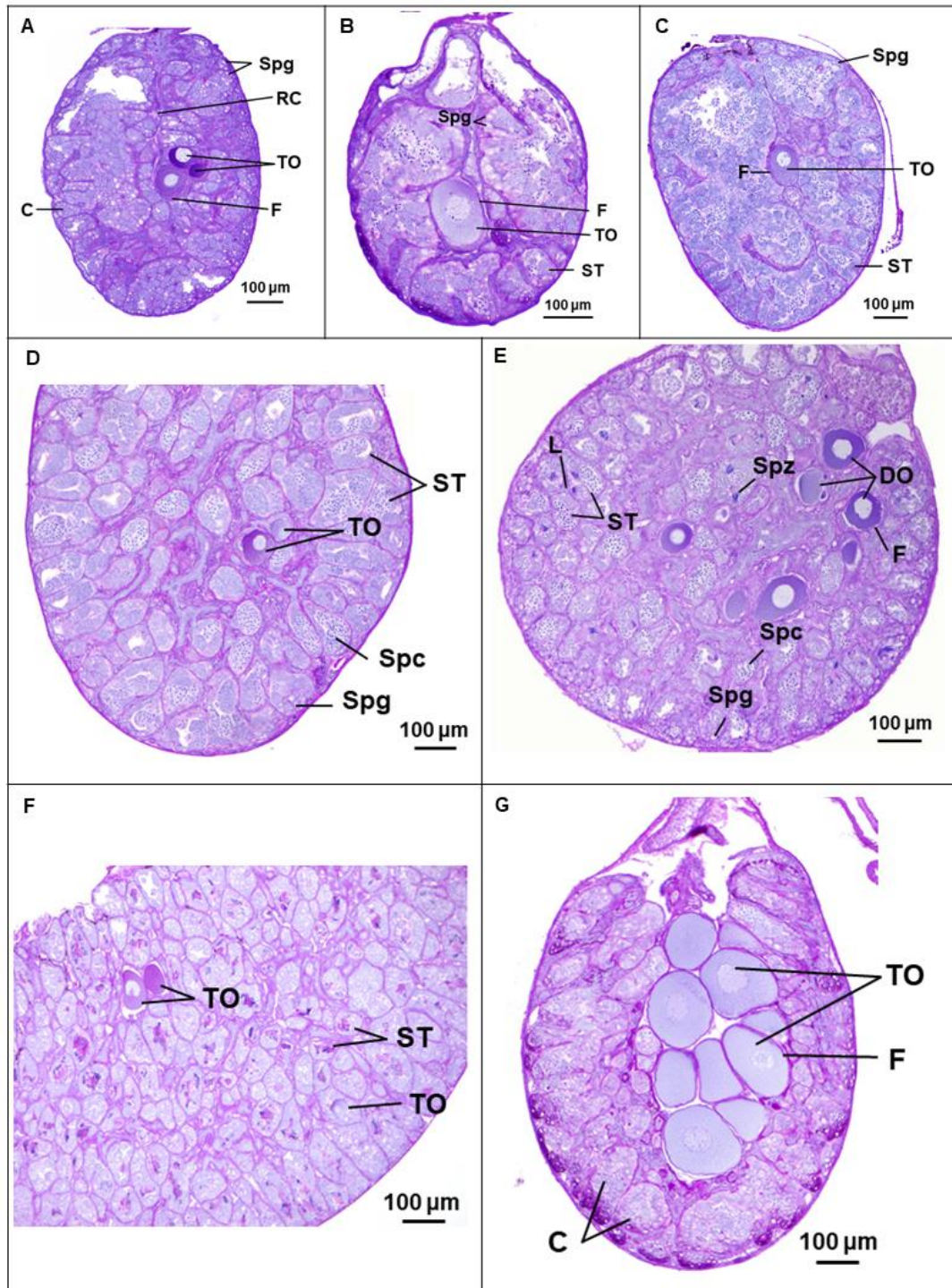


Figure 4.13 Comparison of gonad morphology and histology in juvenile male *H. rugulosus* at (A, B) 5 and (C, D) 7 weeks after metamorphosis. Representative (A) stereomicroscope photograph of the testes morphology; (B) histology photomicrograph of A, the intersex gonad with oocytes, gonial cysts and groups of meiocytes; (C) stereomicroscope photograph of the gonad at 7 weeks with a mixed appearance of male gonad and lobular structure of female gonad (arrows); (D) histology photomicrograph of C, the ovary. DiO: diplotene oocyte, DO: degenerating oocyte, F: follicle, GP: germ patch, OC: ovarian cavity, Spg: spermatogonia, TO: testis-ovum



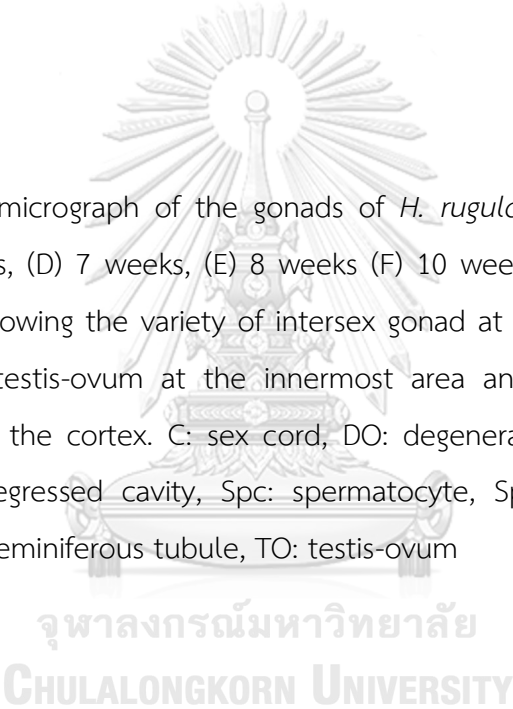
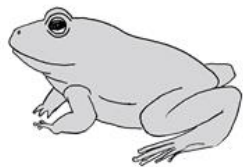


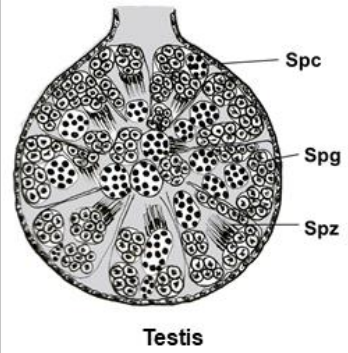
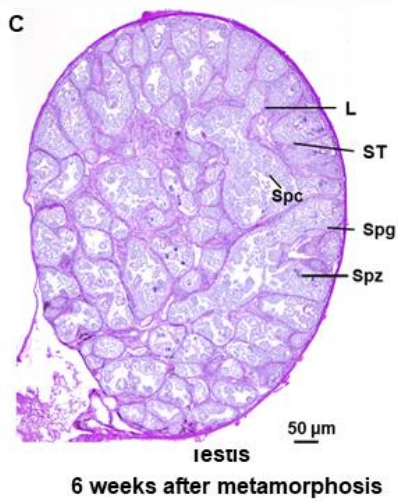
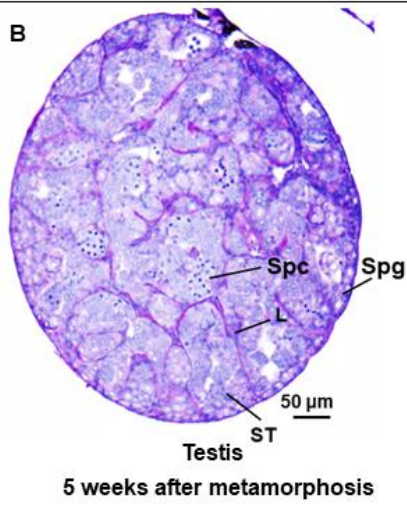
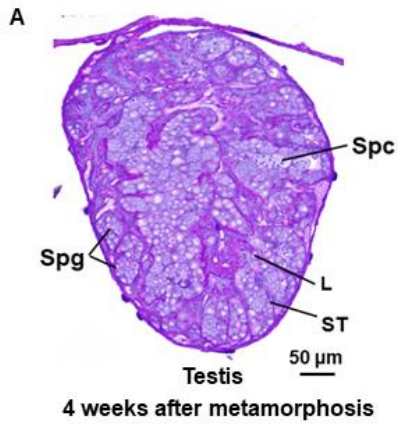
Figure 4.14 Photomicrograph of the gonads of *H. rugulosus* at (A) 4 weeks, (B) 5 weeks, (C) 6 weeks, (D) 7 weeks, (E) 8 weeks (F) 10 weeks and (G) 13 weeks after metamorphosis, showing the variety of intersex gonad at different age. The intersex gonad contained testis-ovum at the innermost area and testicular tissue at the outermost area of the cortex. C: sex cord, DO: degenerating oocyte, F: follicle, L: Leydig cell, RC: regressed cavity, Spc: spermatocyte, Spg: spermatogonium, Spz: spermatozoa, ST: seminiferous tubule, TO: testis-ovum

5) Testicular differentiation: 1–6 weeks after metamorphosis

After the intersex gonad was observed (one week after metamorphosis), the testicular differentiation seemed to occur continuously. At 2–4 weeks after metamorphosis, the seminiferous cord was composed of dividing gonocytes (spermatogonia). Clusters of germ cells at different stages of spermatogenesis were found, including spermatogonia, secondary spermatogonia, and primary spermatocytes during prophase. Up to 6 weeks after metamorphosis, the testis was found to be well-developed and contain cysts of spermatogenic cells at every stage inside the seminiferous tubule (Figure 4.15). The spermatogenic cell types—including spermatogonium, spermatocyte, spermatid, and spermatozoa—were easily identifiable. Some mesenchymal cells differentiated into Leydig cells in the intertubular space (Figure 4.16). Other somatic cells developed into connective tissues and blood vessels. After this period, the testis became large and the number of seminiferous tubules increased. The rete testis developed and became connected to the seminiferous tubules when they reached the age of 6-9 weeks after metamorphosis (Table 4.2)



4-6 weeks after metamorphosis



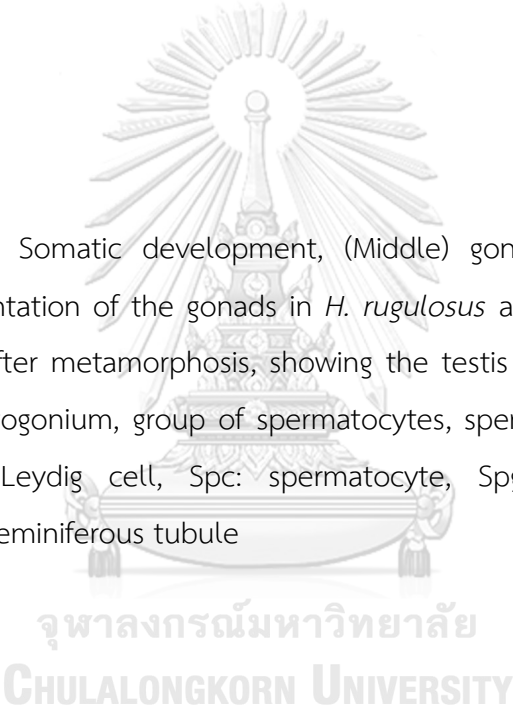


Figure 4.15 (Left) Somatic development, (Middle) gonad histology, and (Right) schematic representation of the gonads in *H. rugulosus* at (A) 4 weeks, (B) 5 weeks and (C) 6 weeks after metamorphosis, showing the testis with seminiferous tubules containing spermatogonium, group of spermatocytes, spermatozoa, Sertoli cell, and Leydig cells. L: Leydig cell, Spc: spermatocyte, Spg: spermatogonium, Spz: spermatozoa, ST: seminiferous tubule

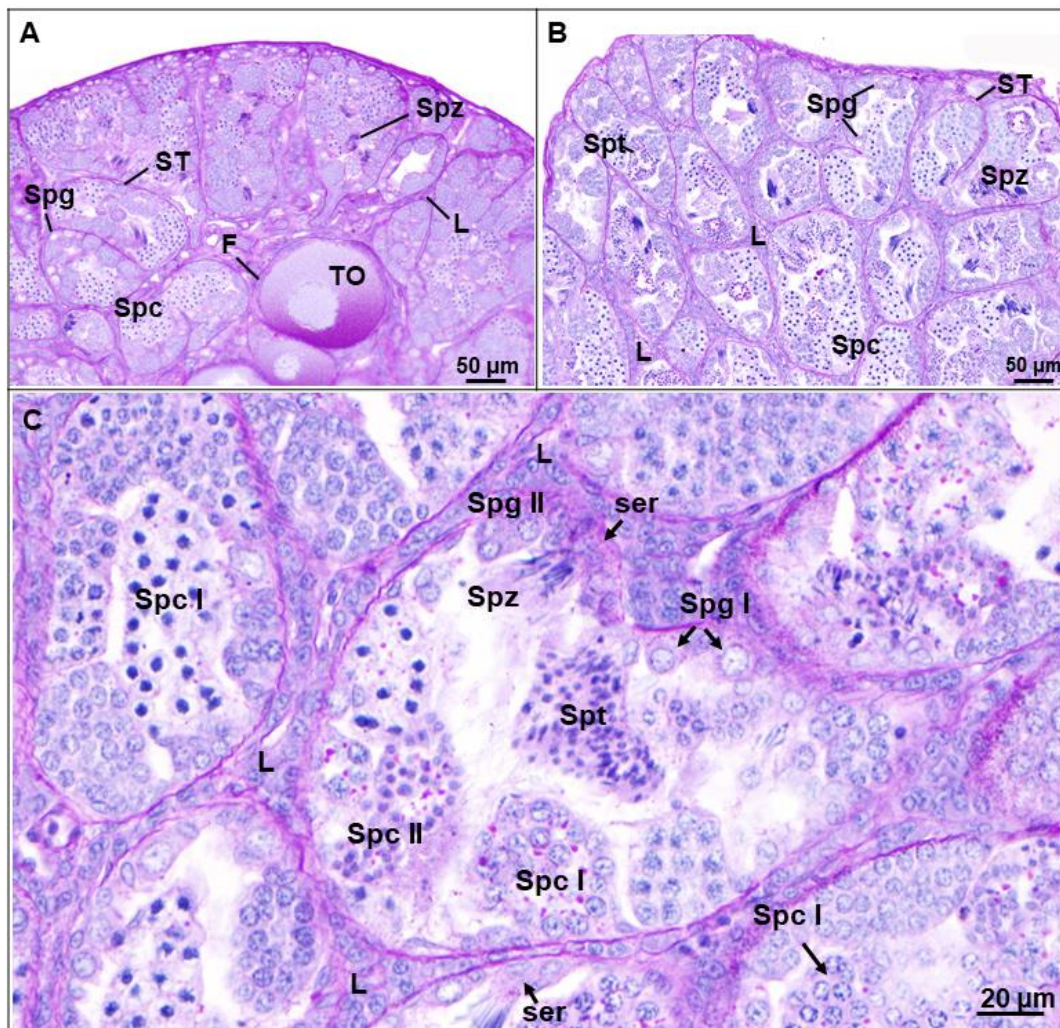


Figure 4.16 Photomicrograph of the gonads in *H. rugulosus*, showing the intersex gonad (A) at higher magnification of Figure 4.12C with testis-ovum surrounded with follicle next to seminiferous tubules with spermatogenic cells at several stages, (B) the testis at higher magnification of Figure 4.13C, containing seminiferous tubules with spermatogonia, groups of spermatocytes, spermatozoa, Sertoli cells and Leydig cells between the tubules, (C) the structure of seminiferous tubule with spermatogenic cells at every stage. F: follicle, L: Leydig cell, Ser: Sertoli cell, Spc I: primary spermatocyte, Spc II: secondary spermatocyte, Spg I: primary spermatogonium, Spg II: secondary spermatogonium, Spt: spermatid, Spz: spermatozoa, ST: seminiferous tubule, TO: testis-ovum

4.4 Discussion and conclusion

Hoplobatrachus rugulosus exhibited an undifferentiated type of gonadal sex differentiation, and all of the indifferent gonads differentiated initially into ovaries (100%) during metamorphosis, and later the ovaries of more than one-third of the frogs transformed into testes, as evident by the seminiferous cord formation, presence of testis-ova, and atretic oocytes in the tissue. During this period, a prolonged intersex condition and testis-ova was found starting at one week after metamorphosis until the individuals reached maturity (16 weeks after metamorphosis). The intersex condition found was similar to that reported in some other anurans that undergo this type of gonadal differentiation (Gramapurohit et al., 2000; Saidapur et al., 2001; Eggert, 2004; Flament, 2016), including *B. bufo*, *R. curtipes*, and *R. ornativentris* (Gramapurohit et al., 2000); *Hyla japonica* (Nakamura, 2009); *Euphlyctis cyanophlyctis* (Phuge and Gramapurohit, 2013); and *Scinax fuscovarius* (Goldberg, 2015).

In *H. rugulosus*, the first evidence of ovarian differentiation appears at Gosner stage 36. Several studies have reported that it can occur at various Gosner stages among undifferentiated species, such as stage 25 in *R. curtipes* (Gramapurohit et al., 2000), stage 26 in *Scinax fuscovarius* (Goldberg, 2015), stage 27 in *Euphlyctis cyanophlyctis* (Phuge and Gramapurohit, 2013), and stages 31–35 in *R. temporaria* (Ogielska and Kotusz, 2004). At this point, Ogielska and Kotusz (2004) studied 12 species of anuran (*R. lessonae*, *R. ridibunda*, *R. temporaria*, *R. arvalis*, *R. pipiens*, *R. catesbeiana*, *Bombina bombina*, *Hyla arborea*, *B. bufo*, *B. viridis*, *Xenopus laevis*, *Pelobates fuscus*) and reported that their ovarian differentiation is independent of somatic development, and that tadpole age is a more important factor. Female *H. rugulosus* reached maturity at 16 weeks after metamorphosis, as evidenced by the presence of ripe diplotene oocytes (full of yolk) and signs of spawning.

According to the Ogielska and Kotusz (2004), the pattern of female gonadal differentiation in 12 species of anurans, as described using the morphology and

histology of developing ovaries, separated ovarian differentiation into 10 stages. Stages I–III involve an undifferentiated gonad and stages IV–X are ovarian. By comparing the rate of somatic development with the rate of ovarian differentiation, Ogielska and Kotusz (2004) derived three types of female gonad development. The first is a *basic rate*, in which ovarian differentiation occurs during metamorphosis. The second is an *accelerated rate*, in which ovarian differentiation occurs before metamorphosis at the earlier tadpole stage. The third is the *retarded rate*, in which ovarian differentiation occurs after metamorphosis. Based on these criteria, *H. rugulosus* has a basic rate of ovarian differentiation (Table 4.1), like several other amphibian species, including *R. temporaria* (Ogielska and Kotusz, 2004), *Bombina orientalis* (Lopez, 1989), and *Rhacophorus arboreus* (Tanimura and Iwasawa, 1989). The rate of gonadal differentiation is known to be different among amphibian species (Storrs-Méndez and Semlitsch, 2010; Goldberg, 2015; Pinto Erazo et al., 2016). It should be noted that the pathways that control the development of the body and gonad vary among species, and might also be affected by environmental conditions, such as season, temperature, diet, or population density (Ogielska, 2009).

Table 4.1 Comparison of the somatic (Gosner stage) and gonadal stages of ovarian development in *H. rugulosus* following the criteria of Ogielska and Kotusz (2004)

Gonadal stage	Characteristic of gonad	Somatic stage
I	PGCs migrate into the genital ridge.	25–26
II	Gonocyte present separately as a single cell in the indifferent gonad.	27–34
III	Somatic cells migrate to the medial part. Gonad composed of cortex and medulla. Gonocyte division present in the cortex.	35
IV	Sexual differentiation begins. Medulla degenerates and ovarian cavity develops.	36
V	Secondary oogonia enters meiosis. Cortex composed of primary oogonia and nests of secondary oogonia.	37–41
VI	First diplotene oocytes present. Cortex composed of primary oogonia, nests of secondary oogonia, nests of meiocytes and diplotene oocytes.	42–45
VII	Diplotene oocytes increase in number and size and protrude into the ovarian cavity, which changes shape into a narrow space.	46 (metamorphosis complete)
VIII	Ovary composed of almost only diplotene oocytes. The outermost area filled with primary oogonia, nests of secondary oogonia while the nests of meiocytes decrease.	1 week after metamorphosis
IX	Fat body becomes finger-like shaped. Primary oogonia, nests of secondary oogonia and meiocytes at the outermost area of the cortex are presented as a thin area.	2 weeks after metamorphosis
X	Fully developed ovary, the cortex is composed mostly of diplotene oocytes. Germ patches present in the outermost area of the cortex.	4 weeks after metamorphosis

The testicular differentiation of species with differentiated gonad development begins with a centralization of the germ cells in the indifferent gonad. The germinal epithelium in the cortex degenerates while germ cells migrate to the central medulla to form sex cords, which then develop into seminiferous tubules. Testicular differentiation in undifferentiated species occurs through the process of gonad transformation from ovary into testis (Witschi, 1921). Witschi (1921) also observed gonad transformation in *R. curtipes*. In these cases, the transformation of the ovary occurs at an early stage. Gonocytes at the same stage of cell division are

present as the sex cord forms in the ovarian sac. The sex cord appears as a highly compact group of gonocytes. Spermatogonia migrate from the cortex to the central part of the gonad. Then, the cortex degenerates and the central region develops into the testis (Witschi, 1929a) (Table 4.2). Recently, it was accepted that the testis in this group of amphibian develops from the intersex gonad (Flament, 2016).



Table 4.2 Comparison of the somatic (Gosner stage) and gonadal stages of testicular development in *H. rugulosus* using criteria adjusted from Haczkiwicz and Ogielska (2013) and Ogielska and Kotusz (2004)

Gonadal stage	Characteristic of gonad	Somatic stage
i	PGCs migrate into the genital ridge.	25–26
ii	Gonocyte present separately as a single cell in the indifferent gonad.	27–34
iii	Somatic cells migrate to the medial part. Gonad composed of cortex and medulla. Gonocyte division present in the cortex.	35
iii a	Correspond to the ovarian development stage IV (Table 1)	36
iii b	Correspond to the ovarian development stage V (Table 1)	37–41
iii c	Correspond to the ovarian development stage VI (Table 1)	42–45
iii d	Correspond to the ovarian development stage VII (Table 1)	46 (metamorphosis complete)
Gonadal stages iv–vii develop via an intersex condition		
iv	The outermost layer composed of primary spermatogonia surrounded by some somatic cells and groups of 2–4 dividing gonocytes. The innermost layer composed of diplotene oocytes.	1 week after metamorphosis
v	The outermost layer composed of primary spermatogonia aggregated into groups of 3–8 cells surrounded by mesenchymal cells. The innermost layer composed of diplotene oocytes.	1 week after metamorphosis
vi	The outermost layer composed of primary spermatogonia arranged into seminiferous cord and surrounded by mesenchymal cells. Rete testis development begins. The innermost layer composed of diplotene oocytes.	2 weeks after metamorphosis
vii	The outermost layer composed of seminiferous cords increasing in size. Interstitial tissue and the tunica albuginea begin to differentiate. The innermost layer composed of diplotene oocytes and degenerating oocytes.	3–4 weeks after metamorphosis
viii	Spermatogenesis begins. Primary spermatogonia and cysts of secondary spermatogonia present. The seminiferous cord joins the rete testis. The tunica albuginea is well developed, and the amount of interstitial tissue increases. Testis-ova may be present.	4–5 weeks after metamorphosis
ix	Seminiferous tubules develop containing primary spermatogonia, cysts of secondary spermatogonia, and cysts of early spermatocyte. The rete testis becomes connected to the seminiferous tubules. Testis-ova may be present.	6–9 weeks after metamorphosis
x	Fully developed testis, the seminiferous tubule is composed of cysts of spermatogenic cells at every stage. Testis-ova may be present.	10 weeks after metamorphosis

Gonad transformation in the present study was different from that in the above-mentioned reports on *H. rugulosus*. The intersex condition was first found in the gonad when the diplotene oocytes were developed, at one week after metamorphosis. The cluster of gonocytes was first present in the cortex, after which the sex cords were formed. The testicular tissue in the intersex gonad was found in the outermost area of the cortex and became fully developed, which was characterized by complete spermatogenesis. The diplotene oocytes were found at the innermost area of the cortex. Based on the examination of the intersex gonads found in every developmental stage from 1–16 weeks after metamorphosis, it was hypothesized that the gonad transformation occurred from the outermost area towards the innermost area of the gonad, the testis-ova were pushed into the medial region by the development of sex cords in the outermost area, the testis-ova degenerated before vitellogenesis, and the ovarian cavity disappeared. In this study, the testis-ova were still found (approximately 1–3 oocytes/cross section) in the mature testis.

The rates of testicular differentiation and somatic development were compared using the criterion for ovary development from Ogielska and Kotusz (2004) based on the basic, accelerated, and retarded rates of development (Goldberg, 2015; Pinto Erazo et al., 2016). In *H. rugulosus*, the first sign of testicular differentiation was observed one week after metamorphosis, and so it exhibited a retarded rate. This result is similar to that for *Scinax fuscovarius* (Goldberg, 2015), *Bombina variegata* (Piprek et al., 2010), and *Euphlyctis cyanophlyctis* (Phuge and Gramapurohit, 2013).

Reproductive organ development has been used as a biomarker assessing the endocrine disrupting effects for more than 40 years (Haider, 1980; Hayes, 1998). Several studies have reported the abnormal intersex condition of the gonad. However, the intersex gonad is likely normal in some species, such as *B. americanus* and *Hyla versicolor* (Storrs-Méndez and Semlitsch, 2010). In *H. rugulosus*, intersex gonads were also found during gonadal development when testis was transformed

to ovary. Therefore, it is important to know that the gonad intersex condition in this species can not be precisely interpreted as an abnormal reproductive development character when it is used as animal model to determine hormone-like contaminants in the environment.

In conclusion, this study is the first report to describe the normal gonadal development of *H. rugulosus* from the first stage of sex differentiation to the maturation stage. Gonadal development in this frog began at stage 25. The first sign of sex differentiation was observed at stage 36, which was the beginning of ovarian differentiation. The gonads of all individuals developed an ovary during metamorphosis, indicating that the sexual development was undifferentiated. The intersex gonads were observed one week after metamorphosis, when testicular tissue formation occurred inside the gonads of some individuals in which some of the ovarian tissue was degraded. The presence of intersex gonads and testis-ova during this period was prolonged in some individuals until they reached maturation at 6 weeks after metamorphosis (Figure 4.17). In group of females, during 1-3 weeks after metamorphosis, the ovaries increased in size and number of diplotene oocytes without the area of testicular tissue and maintained the ovary structure until they reached at fully developed stage (4 weeks after metamorphosis). Comparing the rate of gonadal differentiation with the rate of somatic development revealed that ovarian differentiation in *H. rugulosus* occurred at a basic rate, whereas testicular differentiation occurred at a retarded rate. The results from our study are crucial for further understanding sexual development of this anuran, as well in using the intersex condition as a biomarker for reproductive environmental toxicology analysis of this species.

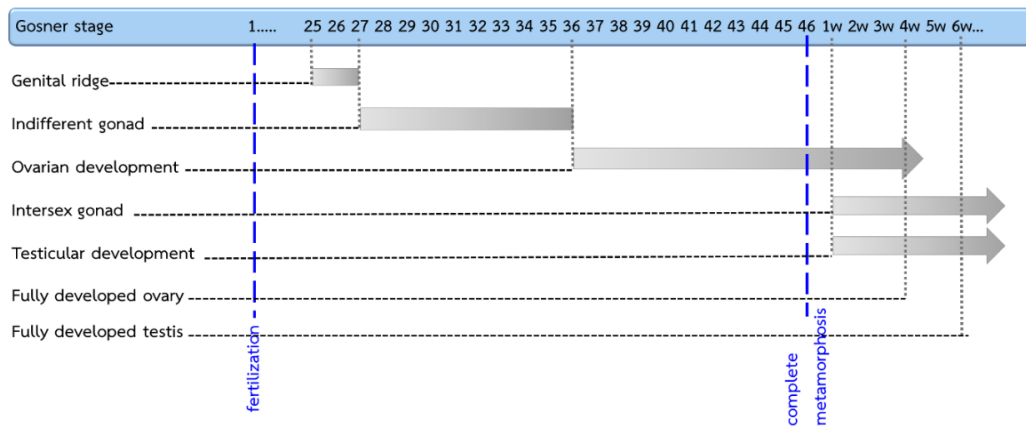


Figure 4.17 Summary diagram representing the chronology of gonadal development in *H. rugulosus*



Chapter V

Steroidogenic Potential of Gonad during Sex Differentiation in the Rice Field Frog *Hoplobatrachus rugulosus* (Wiegmann, 1834)

5.1 Introduction

In amphibian, sex is determined by genetic factors (genetic sex determination, GSD) which occurred at fertilization, environmental factors such as temperature and environmental hormones (environmental sex determination, ESD), or a combination of these two factors (Hayes, 1998; Eggert, 2004; Nakamura, 2009). During the larval developmental period, sex differentiation occurs and could be regulated by hormones. Endogenous steroids can influence normal gonadal sex differentiation in amphibians (Hayes, 1998; Nakamura, 2009; Ogielska, 2009). The prior study (chapter IV) has shown that the pattern of gonadal sex differentiation of *H. rugulosus* exhibited an undifferentiated type, in which the gonad developed into ovary at complete metamorphosis in all individuals, then the testis developed later through the intersex condition. However, the key factors that control mechanism for gonadal sex differentiation in this species is still unknown.

In anurans, the fact that sex steroids play a crucial role during gonadal development have been generally recognized. Males and females could produce different sex steroid hormones and showed different steroidogenic activity in the endocrine organs. However, the role of endogenous steroid is still not clear (Hayes, 1998). Several anuran species have been used as an animal model to investigate this aspect. The Japanese wrinkled frog *G. rugosa* is a species that has a lot of information on the role of the sex steroids during gonadal development and it is closely related to *H. rugulosus*. The gonad of *G. rugosa* has been investigated for the localization of steroidogenic enzymes such as 3β -hydroxysteroid dehydrogenase (3β -HSD), cytochrome P450 17β hydroxylase/C17–20 lyase (CYP17), 17β -hydroxysteroid dehydrogenase (17β -HSD), cytochrome P450 aromatase (CYP19), at the protein and

mRNA level in the tissues by immunohistological technique and *in situ* hybridization, respectively. The immunoreactivity of CYP17 enzyme was observed in somatic cells of the indifferent gonad of the males but not in the females and it was also observed in the Leydig cells of the testis in the adult male *G. rugosa* (Sakurai et al., 2008). Localization of *CYP17* mRNA was also observed in somatic cells of an indifferent gonad of the tadpole and in Leydig cells of the testis of this frog species (Iwade et al., 2008). Immunopositive signals of 3β -HSD enzyme were observed in somatic cells of the indifferent gonad of males and females at different somatic stages and in the Leydig cells of the testis in the adult frogs (Sakurai et al., 2008). Immunoreactivity of 17β -HSD enzyme was found in the indifferent gonad of male and testis in the adult frogs (Sakurai et al., 2008). The immunoreactivity of CYP19 enzyme was observed in gonadal somatic cells of the females, but not in the indifferent gonad of the males, and positive signals for CYP19 enzyme were also localized in ovarian somatic cells at metamorphosis (Isomura et al., 2011). Furthermore, the study of the expression pattern of genes encoding steroid-metabolizing enzyme was also observed by qrt-RT-PCR. In *G. rugosa*, *CYP 17* mRNA expression was found much higher in the male gonad. In contrast, the expression level of *CYP19* was much higher in female gonad compared with the male (Maruo et al., 2008; Nakamura, 2009). Nevertheless, expression levels of *CYP11A1*, *3\beta*-HSD, *17\beta*-HSD, *5\alpha*Red1, and *StAR* were similarly found without sexual dimorphism during gonadal sex differentiation. Interestingly, from these reports, it is suggested that CYP17, the enzyme that converts pregnenolone into dehydroepiandrosterone (DHEA) and converts progesterone into androstenedione (AE), may play a crucial role in testicular development. Moreover, CYP19, the enzyme that converts testosterone into estradiol, has a major influence on ovarian development (Iwade et al., 2008; Sakurai et al., 2008; Isomura et al., 2011).

Therefore, studying the expression pattern of CYP17 and CYP19 enzymes at different periods during gonadal development in *H. rugulosus* might help to clarify

the influence of these key enzymes on the phase of development. In this study, localization of CYP17 and CYP19 enzymes and their mRNA were observed by immunohistochemistry and *in situ* hybridization techniques, respectively. The level of CYP17 and CYP19 mRNA were observed as a quantitative study by qrt-RT-PCR in *H. rugulosus* at every stage during the sex differentiation period.

5.2 Materials and methods

5.2.1 Animal procurement

Four pairs of adult male and female *H. rugulosus* were used as breeders for artificial fertilization by subcutaneous injection of GnRH analog (Suprefact, Frankfurt am Main, Germany) to induce spermination, ovulation, and mating according to a protocol of Pariyanonth (1985). All tadpoles were raised in 100L plastic containers under natural light (12L: 12D) and a water temperature of 27.5–28.1°C. Water was changed every day to remove waste and maintain oxygen level. Tadpoles and frogs were fed with commercial fish pellets once a day. The morphological stage of all individuals was estimated according to the Gosner staging system (Gosner, 1960) under a stereomicroscope. The tadpole at stages 25–46 and frog at 1 week after metamorphosis to adult (16 weeks after metamorphosis) were euthanized in 0.25% (w/v) MS-222 (tricaine methanesulfonate) and examined. The experimental protocol was approved by the Animal Care and Use Committee of Faculty of Science, Chulalongkorn University (Protocol Review No. 1623002).

5.2.2 Immunohistochemistry

Localization of CYP17 (a representative key enzymes for androgen production), and CYP19 (a representative female-specific steroidogenic enzymes), were investigated in gonadal tissues to demonstrate steroidogenic potential of the tissues during on gonadal development. The gonad-kidney complex from 8 individuals per each stage of the tadpole (stages 25-46) and frog (1 week after metamorphosis) and

the gonad from 8 individuals per each week of the frog at 2 weeks after metamorphosis to adult (16 weeks after metamorphosis) were examined. The tissues were carefully dissected and fixed in 4% buffered paraformaldehyde at 4 °C overnight. The tissues were dehydrated through a graded series of ethanol (70%, 90%, 95%, and 100% v/v) and embedded in paraffin. Paraffin sections were done at 6 µm thickness. Then the tissue sections were deparaffinized, hydrated and incubated in 3% (v/v) H₂O₂-methanol for 10 minutes to inactivate endogenous peroxidase then washed in distilled water. Next, the sections were immersed in 1% (w/v) zinc sulfate and heated in a microwave oven with a high-power setting for 15 minutes for antigen retrieval. The sections were rinsed in distilled water then washed in 0.1% (v/v) Tween-20 in Tris-buffered saline (TBS-T) to prevent nonspecific binding and incubated with blocking reagent, normal goat serum (IHC HRP detection kit, Millipore Corporation, Billerica, USA), for 1 hour at room temperature. In this study, there were 2 kinds of primary antibodies used for each specific enzyme. Anti-CYP17/CYP17A1 antibody, a rabbit polyclonal anti-human IgG antibody (LifeSpan Biosciences, Seattle, USA, code LS-B13802), and anti-CYP17A1 antibody, a mouse monoclonal anti-human IgG antibody (Santa Cruz Biotechnology, Santa Cruz, USA, code sc-374244), were used for *CYP17* enzyme localization. Anti-CYP19/aromatase antibody, a rabbit polyclonal anti-human antibody (LifeSpan Biosciences, Seattle, USA, code LS-B2816), and anti-CYP19 antibody, a mouse monoclonal anti-human IgG antibody (Santa Cruz Biotechnology, Santa Cruz, USA, code sc-374176), were used for *CYP19* enzyme localization. The sections were incubated with diluted primary antibodies (1: 100, 1:500, and 1:1,000) for 1 hour at room temperature in a moist chamber. After washing in TBS-T, the sections were then incubated with biotinylated goat anti-mouse IgG and goat anti-rabbit IgG (IHC HRP detection kit, Millipore Corporation, Billerica, USA) for 30 minutes at room temperature. Then the sections were washed with TBS-T and incubated with Streptavidin HRP for 30 minutes at room temperature. Peroxidase activity was demonstrated by an incubation with 0.3% (w/v)

3,3'-diaminobenzidine-4 HCl (DAB; Sigma-Aldrich, St Louis, USA) and 3% hydrogen peroxide. In some experiments, peroxidase activity was also observed by Vector VIP peroxidase substrate kit (Vector Laboratories, Burlingame, USA). The sections were rinsed in distilled water and continued through the process of dehydration, clearing and mounting with Permount mounting media. Sections of mammals (mouse ovary, mouse testis, cat ovary, and dog testis) were used as positive control by the same immunostaining protocol. For negative control, the mammalian and frog tissues were incubated without the primary antibody and processed through the same protocol. The mouse ovary and mouse testis were obtained from the Graduate School of Dentistry, Tohoku University, Japan and the cat ovary and dog testis were obtained from the Small Animal Teaching Hospital, Faculty of Veterinary Science, Chulalongkorn University.

5.2.3 *In situ* hybridization

Since there was no information on *CYP17* and *CYP19* mRNA of *H. rugulosus* in the NCBI database. Thus, the method for *in situ* hybridization had to start from the generation of *H. rugulosus* *CYP17* and *CYP19* cDNA by the cloning method.

1) RNA extraction and complementary DNA (cDNA) synthesis

Total RNA was prepared from mature testis and ovary of the adult *H. rugulosus* to clone *CYP17* and *CYP19* cDNA, respectively. The mature testis and ovary were rapidly dissected, cut into small pieces, and stored in RNAlater stabilization solution (ThermoFisher Scientific, Waltham, USA) for RNA preservation. Total RNA was extracted using RNeasy mini kit (Qiagen, Tokyo, Japan) according to the manufacturer's instructions. Then total RNA was treated with DNase I (Qiagen, Tokyo, Japan) on a spin column for 15 minutes at 25 °C. The quantity of RNA was measured by spectrophotometry with a NanoDrop ND-1000 instrument (ThermoFisher Scientific, Waltham, USA) and RNA integrity was evaluated by electrophoresis on a 1% (w/v) agarose gel. Then total RNA (1µg) was transcribed to cDNA using high-capacity cDNA

reverse-transcription kits (Applied Biosystems, Tokyo, Japan) according to the manufacturer's protocol.

2) cDNA cloning of CYP17 and CYP19 genes

To obtain a partial sequence of *CYP17*, *CYP19*, and β -actin cDNAs, double-strand cDNAs were synthesized using degenerate primers (Table 5.1). β -actin was used to standardize the level of *CYP17* and *CYP19* mRNAs. Since there was no data of *H. rugulosus* *CYP17*, *CYP19*, and β -actin in the NCBI, the primers for *CYP17*, *CYP19*, and β -actin synthesis were designed using the highly conserved regions of *CYP17*, *CYP19*, and β -actin from other anuran and vertebrate species. The primers used for first strand *CYP17* cDNA synthesis were designed based on the sequence of human *Homo sapiens* (GenBank Accession No. NM_000102.3), chicken *Gallus gallus* (GenBank Accession No. NM_001001901.2), turtle *Chelydra serpentina* (GenBank Accession No. AY533546.1), frog *Xenopus laevis* (GenBank Accession No. AF325435.1), frog *Rana dybowskii* (GenBank Accession No. AF042278.1), frog *Glandirana rugosa* (GenBank Accession No. AB284119.2), frog *Nanorana parkeri* (GenBank Accession No. XM_018553412.1) and rainbow trout *Oncorhynchus mykiss* (GenBank Accession No. NM_001124747.1). For *CYP19* cDNA synthesis, the primers were designed based on the sequence of human *Homo sapiens* (GenBank Accession No. M18856.1), chicken *Gallus gallus* (GenBank Accession No. AH002431.2), frog *Sulurana tropicalis* (GenBank Accession No. AB244215.1), frog *Xenopus laevis* (GenBank Accession No. AB031278.1), frog *Glandirana rugosa* (GenBank Accession No. AB178482.2) and fish *Cyprinus carpio* (GenBank Accession No. EU375455.1). The primers for β -actin cDNA synthesis were also designed from nucleotide sequence of frog *Hymenochirus curtipes* (GenBank Accession No. JP287064.1), frog *Physalaemus pustulosus* (GenBank Accession No. AY226144.1), frog *Xenopus laevis* (GenBank Accession No. AF079161.1) and frog *Sulurana tropicalis* (GenBank Accession No. NM_213719.1). The sequences of each gene were aligned using the clustal W program. Then the conserved regions were detected and selected for primer design using Primer 3 program (Rozen and Skaletsky, 2000). After primer design, the PCR reaction was carried out for 35 cycles under the following conditions: denaturation at 95 °C for 30 seconds, annealing at 50

°C for 30 seconds (the optimum annealing temperature for *CYP17*, *CYP19*, and β -*actin*; unpublished data), and extension at 72 °C for 1 minute. The *H. rugulosus* cDNA template for amplification was obtained from 1 individual then aliquoted into 3 sample tubes for amplification of *CYP17*, *CYP19*, and β -*actin*. The PCR products were examined with gel electrophoresis on 1.5% (W/V) agarose gel. A photograph was taken under UV light with AB-6932GXES digital camera (ATTO, Tokyo, Japan). The DNA fragment size of *CYP17*, *CYP19*, and β -*actin* were 699 base pair (bp), 799 bp, and 158 bp, respectively (Figure 5.1). These PCR products were purified using a QIA quick gel extraction kit (Qiagen, Germantown, USA), cloned into pGEM®-T Easy Vector (Promega, Madison, USA), and sequenced by Macrogen, Inc. (Seoul, Republic of Korea). The cDNA sequences were translated into deduced amino acid sequences by the ExpASY program (<https://web.expasy.org/translate>). Then the deduced amino acid sequences were aligned using the clustal W program comparing with the amino acid database of *CYP17*, *CYP19*, and β -*actin* of other anuran species in GenBank. In addition, the similarity and identity were calculated by LALIGN (http://www.ch.embnet.org/software/LALIGN_form.html).



Table 5.1 Primers used to amplify *CYP17*, *CYP19* and β -actin cDNAs

Gene		Sequence	Size
<i>CYP17</i>	Forward	5'-ACA GCT TGG TGG ACA TCT TT-3'	699 bp
	Reverse	5'-CTT CTC CGA GAC ACA CGC GT-3'	
<i>CYP19</i>	Forward	5'-GGA TGA ATG AAA ATG GGA TTA-3'	799 bp
	Reverse	5'-GTT CCT TTC TTC ACA TAA TAG-3'	
β -actin	Forward	5'-GGW ATT GCW GAY AGA ATG CAG A-3'	158 bp
	Reverse	5'-TGC TTG CTG ATC CAC ATC TG-3'	

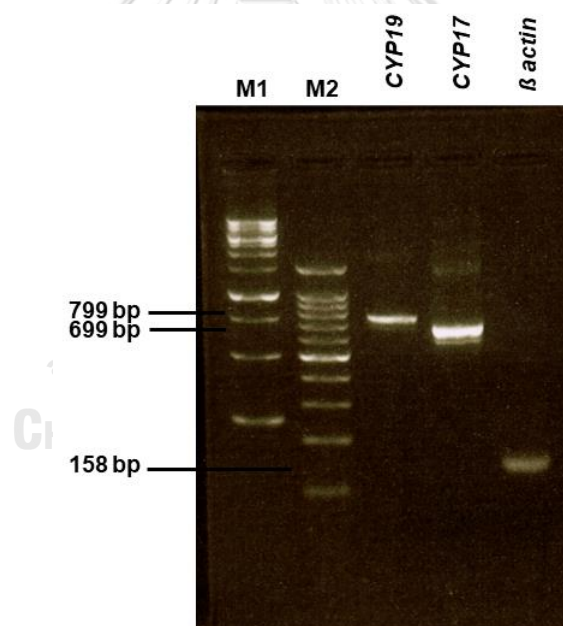


Figure 5.1 Amplicons of the partial sequence of *CYP17*, *CYP19* and β -actin cDNA from *H. rugulosus* that were electrophoresed in a 1.5% agarose gel and stained with SYBR® Safe DNA dye showed the product size at 799 bp for *CYP19*, 699 bp for *CYP17*, and 158 bp for β -actin. M1: 1 kb DNA ladder, M2: 100 bp DNA ladder.

3) RNA probe preparation

A 699-bp cDNA *CYP17* fragment and a 799-bp cDNA *CYP19* fragment were subcloned into the pGEM T-easy vector (Promega, Madison, USA) (Figure 5.2). The DNA constructs were then linearized with *NcoI* and *Sall*. The recombinant plasmids harbouring the *CYP17* and *CYP19* genes were examined with gel electrophoresis on 1.5% (W/V) agarose gel. A photograph was taken under UV light with AB-6932GXES digital camera (ATTO, Japan) (Figure 5.3) Then the restriction enzymes were inactivated using phenol (1:1). The linear plasmid harboring the gene of interest were precipitated using absolute ethanol (2 times of the gene product volume), 10% NaOAc, and glycogen and incubated at 4 °C overnight, then centrifuged (15,300 xg). The pellets of the product were used for the RNA probe synthesis. Sense and antisense RNA probes for *CYP17* and *CYP19* were individually transcribed *in vitro* using Digoxigenin-labeled (Roche, Mannheim, Germany) and SP6 or T7 RNA polymerase (Promega, Madison, USA) mixed with RNasin (Promega, Madison, USA) and transcription buffer, then incubated at 37 °C for 2 hours in a heated block containing water. The RNA probes were examined with gel electrophoresis on 1.5% (W/V) agarose gel. A photograph was taken under UV light with AB-6932GXES digital camera (ATTO, Japan) (Figure 5.4).

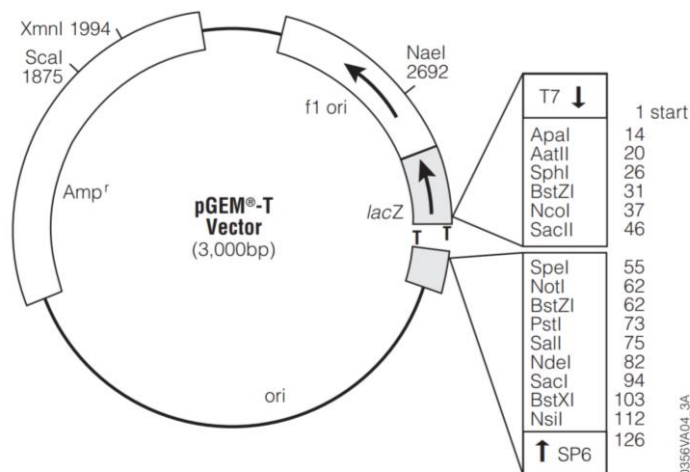


Figure 5.2 Vector map of pGEM-T Easy (Promega, Madison, USA)

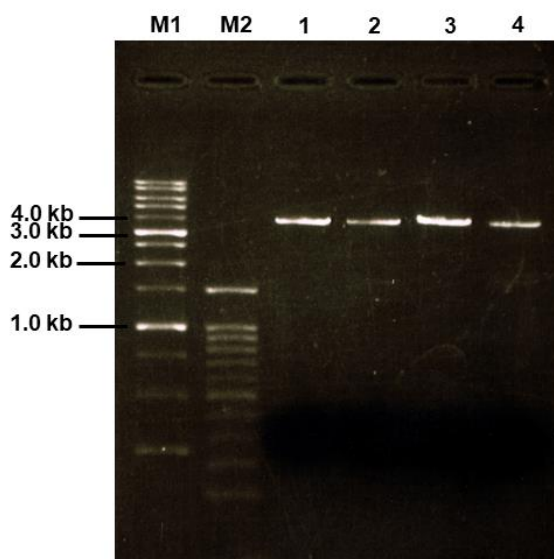


Figure 5.3 Recombinant plasmids harbouring the *CYP17* and *CYP19* genes were confirmed by restriction analysis, electrophoresed in a 1.5% agarose gel, and stained with SYBR® Safe DNA dye. M1: 1 Kb molecular weight marker, M2: 100 bp molecular weight marker, lanes 1-2: recombinant plasmids harbouring the *CYP17* (linearized by *NcoI* and *Sall*, respectively) showed a single band at 3,700 bp, lanes 3-4: recombinant plasmids harbouring the *CYP19* (linearized by *NcoI* and *Sall*, respectively) showed a single band at 3,800 bp.

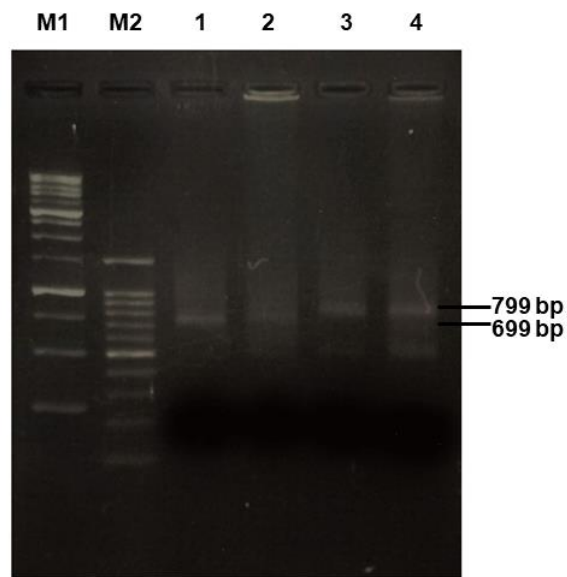


Figure 5.4 Determination of newly synthesized RNA probe for *in situ* hybridization in a 1.5% agarose gel stained with SYBR® Safe DNA dye. The RNA probe size are 699 bp for *CYP17* (lanes 1-2) and 799 bp for *CYP19* (lanes 3-4). M1: 1 Kb molecular weight marker, M2: 100 bp molecular weight marker, lanes 1-2: *CYP17* anti-sense and sense RNA probe, respectively, lanes 3-4: *CYP19* anti-sense and sense RNA probe, respectively.

4) hybridization

The gonad-kidney complex from 6 individuals per each stage of the tadpole (stages 42-46) and frog (1 week after metamorphosis) and the gonad from 6 individuals per each week of the frog at 2 weeks after metamorphosis to adult (16 weeks after metamorphosis) were examined. The tissues were fixed in 4% buffered paraformaldehyde at 4 °C overnight. The tissues were dehydrated through a graded series of ethanol (70%, 90%, 95%, and 100% v/v) and embedded in paraffin. Paraffin sections were done at 6 µm thickness. The sections were attached to Frontier glass slides (Matsunami Glass, Osaka, Japan). *In situ* hybridization was performed according to the method described by Nagasawa et al. (2019). The sections were deparaffinized, hydrated, permeabilized with proteinase K (5 µg/mL) (Roche, Mannheim, Germany) for 10 minutes at room temperature and acetylated by 0.25%

v/v acetic anhydride and 1.35%v/v triethanolamine. Then the sections were incubated with prehybridization buffer (50% formamide, 2x saline sodium citrate (SSC) pH 4.5) at 70°C for 30 minutes. Then the sections were incubated with hybridization mixture (0.5 µg/mL RNA probe, 50% formamide, 2x SSC pH 4.5, 20 µg/mL transfer RNA (tRNA), 50 µg/mL heparin, 10% sodium dodecyl sulfate (SDS), and 25% dextran sulfate) at 70°C for 16 hours. After hybridization, the slides were washed 3 times in 0.2x SSC solution at 70°C for 20 minutes. To reduce background signal, nonspecific binding probes were digested by RNase A solution (20 µg/mL) (Sigma-Aldrich Japan, Tokyo, Japan) at 37°C for 30 minutes. The slides were washed 3 times in 0.2x SSC solution at 70°C for 20 minutes. Before the antibody reaction, the non-specific binding was blocked using Blocking One (Nacalai Tesque, Kyoto, Japan) for 30 minutes at room temperature. Hybridized DIG-labeled probes were visualized using alkaline phosphatase-conjugated digoxigenin antibody (anti-DIG-AP Fab fragments, diluted 1:500). A mixture of nitro blue tetrazolium chloride (NBT)/5-bromo-4-chloro-3-indolyl phosphate, toluidine salt (BCIP) solution was used for color development of the anti-Digoxigenin-AP Fab fragments at room temperature in the dark. After *in situ* hybridization, each sample was counterstained by eosin then mounted in Softmount media (Wako Pure Chemical Industries, Tokyo, Japan) and observed under a BX-53 microscope (Olympus, Tokyo, Japan) and the image was taken with a DP73 Olympus digital camera (Olympus, Tokyo, Japan).

5.2.4 Quantitative real-time reverse transcription polymerase chain reaction (qrt-RT-PCR)

The qrt-RT-PCR analysis was used to detect the steroidogenic potential of gonad-kidney complex and gonad at different stages. The expression of *CYP17* and *CYP19* mRNA during sex differentiation were examined. The gonad-kidney complex from at least 6 individuals per each stage of the tadpole (stages 25-46) and frog (1 week after metamorphosis) and the gonad from at least 6 individuals per each week of the froglet at 2-11 weeks after metamorphosis were used in this analysis. After

ethanasia, the tissues were immediately dissected, cut into small pieces, and stored in RNA*later* stabilization solution (ThermoFisher Scientific, Waltham, USA) for RNA preservation. Total RNA was extracted using TRIzol reagent according to the manufacturer's instructions (Invitrogen, Waltham, USA). The total RNA was used as the template for double-stranded cDNA synthesis using Tetro™ cDNA Synthesis Kit following the manufacturer's protocol (Bioline, London, UK).

Based on the partial sequence of *CYP17* and *CYP19* mRNA (from the method 3.2.), the primers for real-time RT-PCR analysis (Table 5.2) were designed using the Primer 3 program (Rozen and Skaletsky, 2000). The specificity of primers was tested by sequencing analysis. PCR products were purified using PCR Clean-Up System (Promega, Madison, USA), and sequenced by Macrogen, Inc. (Seoul, Republic of Korea). Then the sequencing data from forward primer and reverse primer were aligned using clustal W program. The same regions were selected and presented as nucleotide of PCR product from these primers. The nucleotide of PCR products was aligned using the clustal W program comparing with the database from method 3.2 (GenBank Accession No. MW017204 for *CYP17* and MW017205 for *CYP19*). The identity of PCR products was calculated by LALIGN (http://www.ch.embnet.org/software/LALIGN_form.html). The results revealed that there were 100% identity to the partial sequences of *H. rugulosus CYP17* (MW017204) and *CYP19* (MW017205). Therefore, the primers were specific to the target sequenced and suitable for qrt-RT-PCR analysis.

For the qrt-RT-PCR analysis, SensiFAST SYBR Hi-ROX Kit (Bioline, London, UK) was used according to the manufacturer's protocol which consisted of denaturation at 95 °C for 2 minutes followed by 40 cycles at 95 °C for 5 seconds, 55 °C for 10 seconds and 72 °C for 10 seconds, then 95 °C for 15 seconds, 60°C for 1 minute and 95 °C for 15 minutes, ending with the step at 25°C. To confirm the amplification specificity, the melting curve analysis was performed for each gene to check for single amplification. Amount of PCR product were indicated by real-time detection of

the SYBR Green fluorescence intensity and measured at the end of each extension phase. Then the products were quantified with the StepOnePlus™ Software v2.3 (Applied Biosystems, Carlsbad, USA) according to the manufacturer's instructions. The cycle threshold (Ct) values were determined from the exponential phase of PCR amplification by the StepOnePlus™ Software. *β-actin* were used as endogenous reference gene. The number of cycles target genes of each age group were normalized with *β-actin*. Then the amount of PCR product were calculated by the $2^{-\Delta Ct}$ method (Schmittgen and Livak, 2008). The expression levels of each target mRNA were statistically analyzed with the Kruskal-Wallis test. A value of $P < 0.05$ was set as a significance level. Statistical analysis was performed using SPSS software program version 22 (International Business Machines Corp., New York, USA). The relative fold change of each gene was evaluated by semi-quantitative scoring method.



Table 5.2 Primers used for qrt-RT-PCR analysis

Gene		Sequence	Size
<i>CYP17</i>	Forward	5'-GTCCCGTATCACCATTGCTC-3'	230 bp
	Reverse	5'-GCGTATACCAGCTCCAAAGG-3'	
<i>CYP19</i>	Forward	5'-AAGCGATTCTGGCACAAC-3'	174 bp
	Reverse	5'-CGCTTCCCATGCATCAAAGT-3'	

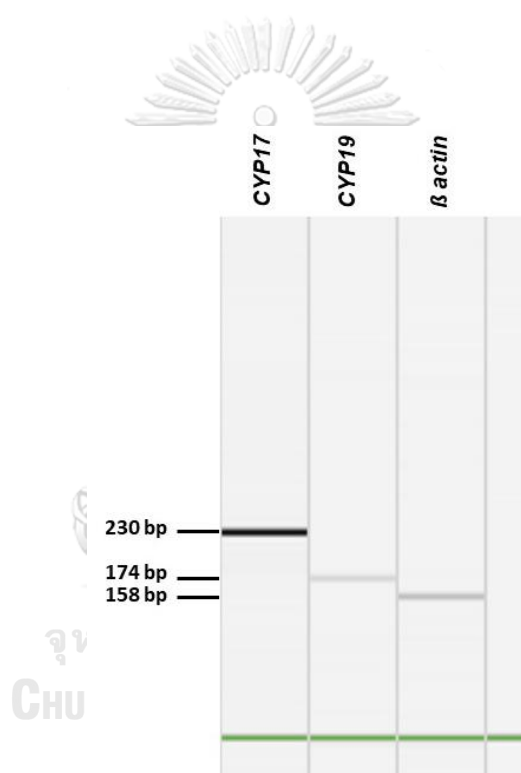


Figure 5.5 Amplification of partial sequence of *CYP17*, *CYP19* and β -actin cDNA from *H. rugulosus* showing lanes 1-3 PCR product size at 230 bp for *CYP17*, 174 bp for *CYP19*, and 158 bp for β -actin, respectively

5.3 Results

5.3.1 Localization of CYP17 and CYP19 enzymes in *H. rugulosus* gonad by immunohistochemistry

In this study, commercial anti-human antibodies had been used and tried out for suitable conditions of CYP17 and CYP19 enzyme localization in *H. rugulosus* gonad tissues. The results showed that there was no evidence of specific cross-reactivity of CYP17 and CYP19 antiserum with *H. rugulosus* tissues.

For CYP17 enzyme, two kinds of commercial antibodies including an anti-CYP17/CYP17A1 antibody (LS-B13802) and an anti-CYP17A1 antibody (sc-374244) were used. The immunopositive signals for the anti-CYP17/CYP17A1 antibody (LS-B13802) were tested using mouse testis as a positive control tissue. The LS-B13802 antibody had a slight cross-reactivity to Leydig cells of mouse testis (Figure 5.6A) but no detectable cross-reactivity in *H. rugulosus* testis (Figure 5.6B). Then the anti-CYP17A1 antibody (sc-374244) was tested. A dog testis was freshly prepared and used as a positive control tissue. The immunoreactivity of CYP17 enzyme presented as brown signals in the Leydig cells of dog testis when detected by DAB (Figure 5.7A). However, evidence for cross-reactivity of this antibody with CYP17 enzyme was not found in *H. rugulosus* testis (Figure 5.7B). After changing the chromogenic detection method for positive signal to Vector VIP peroxidase substrate kit, evidence of cross-reactivity was obviously presented as red-purple signals in the Leydig cells of dog testis (Figure 5.7C). However, cross-reactivity of the antibody and CYP17 enzyme was still undetectable in *H. rugulosus* testis (Figure 5.7D). Thereby, CYP17 enzyme localization could not be detected in *H. rugulosus* gonad by these two antibodies.

Mouse

H. rugulosus

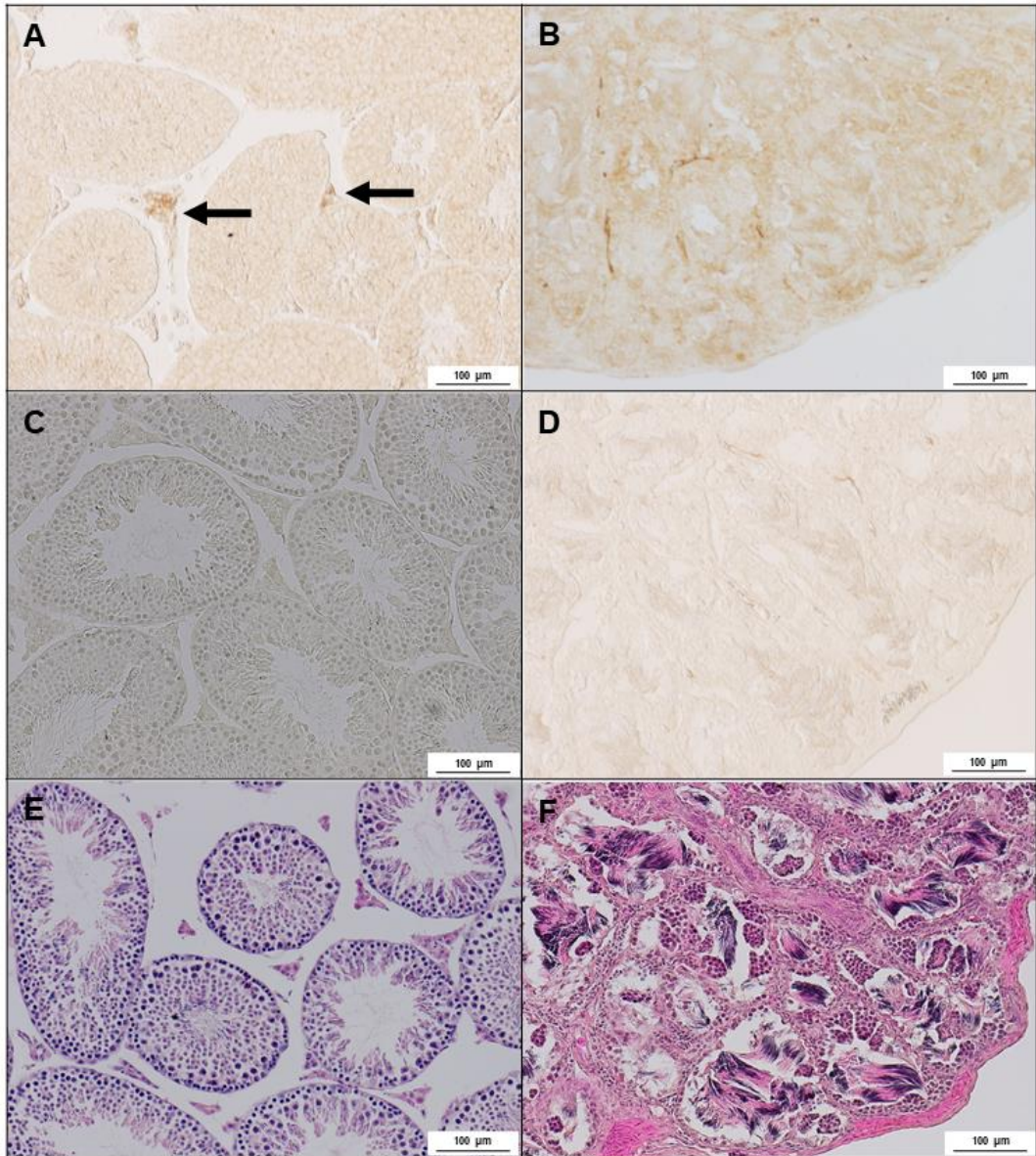
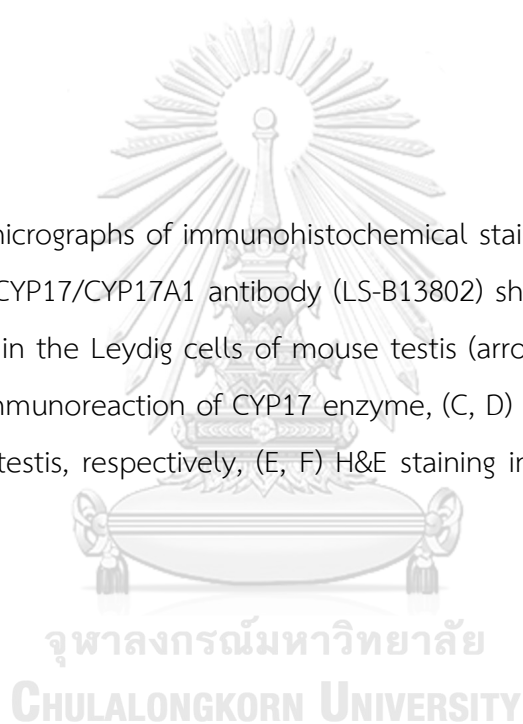


Figure 5.6 Photomicrographs of immunohistochemical staining for CYP17 enzyme by a polyclonal anti-CYP17/CYP17A1 antibody (LS-B13802) showing (A) immunoreaction of CYP17 enzyme in the Leydig cells of mouse testis (arrows), (B) *H. rugulosus* testis without specific immunoreaction of CYP17 enzyme, (C, D) negative control of mouse and *H. rugulosus* testis, respectively, (E, F) H&E staining in mouse and *H. rugulosus* testis, respectively



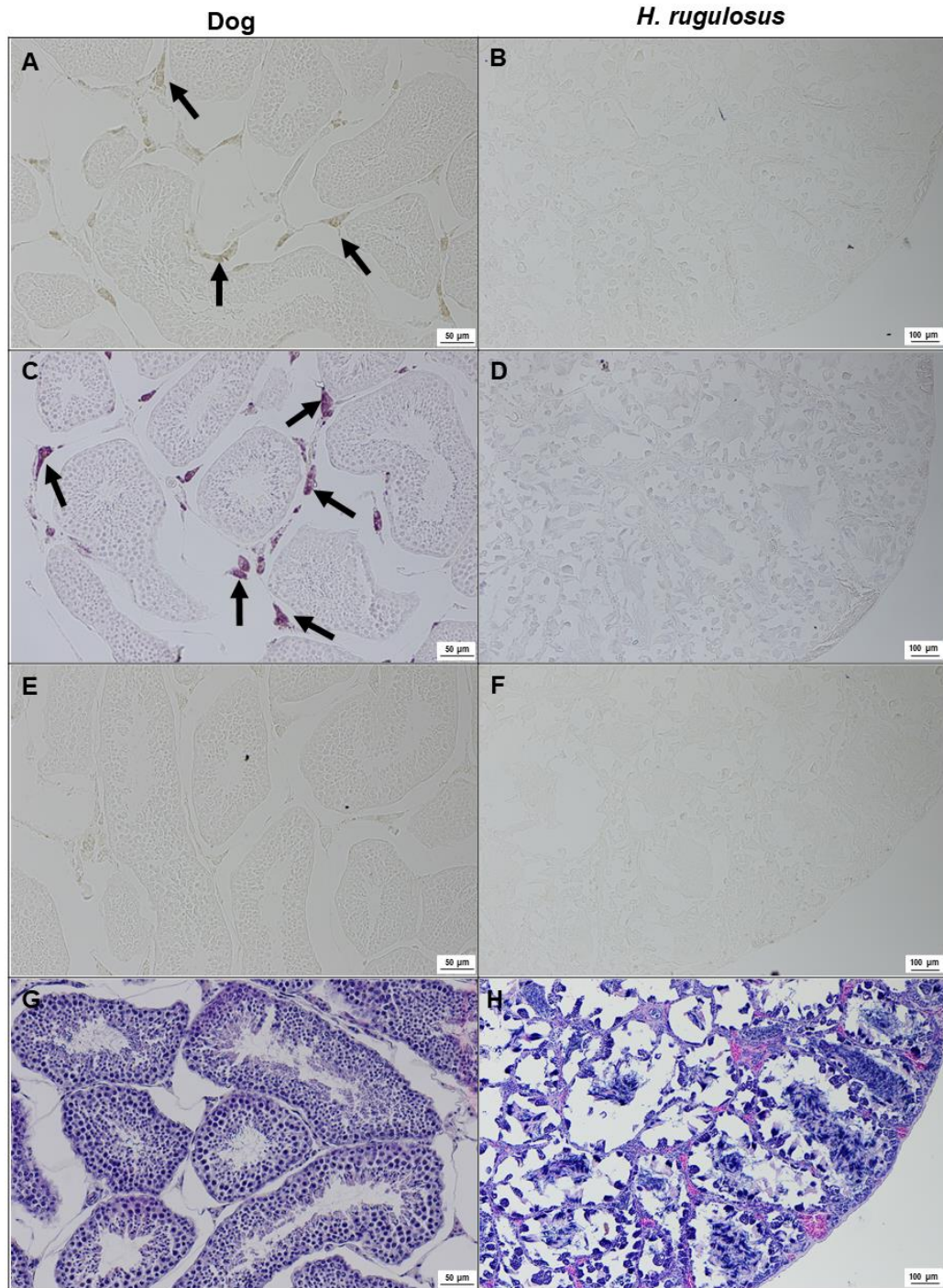
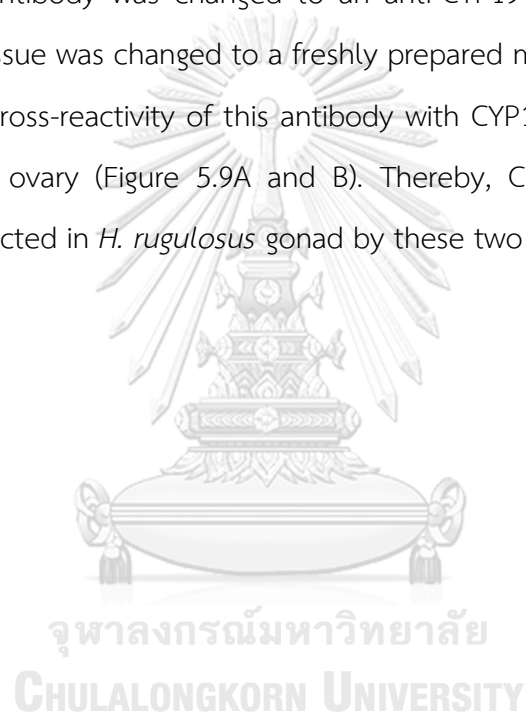


Figure 5.7 Photomicrographs of immunohistochemical staining for CYP17 enzyme by a monoclonal anti-CYP17A1 antibody (sc-374244) with chromogenic detection by DAB (A, B) and Vector VIP peroxidase substrate kit (C, D) showing (A, C) immunoreaction of CYP17 enzyme in the Leydig cells of dog testis (arrows), (B, D) *H. rugulosus* testis without detectable immunoreaction of CYP17 enzyme, (E, F) negative control of dog and *H. rugulosus* testis, respectively, (G, H) H&E staining in dog and *H. rugulosus* testis, respectively

For CYP19 enzyme, two kinds of commercial antibodies including an anti-CYP19/aromatase antibody (LS-B2816) and an anti-CYP19 antibody (sc-374176) were used. The immunopositive signals for an anti-CYP19/aromatase antibody (LS-B2816) were tested using cat ovary as a positive control tissue. The results showed that non-specific signals were found in cat ovary. The immunoreactive signals presented as brown color areas with no specificity to any cell types (Figure 5.8A). Meanwhile, the immunoreactivity of CYP19 enzyme was undetectable in *H. rugulosus* ovary (Figure 5.8B). Then the antibody was changed to an anti-CYP19 antibody (sc-374176) and positive control tissue was changed to a freshly prepared mouse ovary. There was no evidence of any cross-reactivity of this antibody with CYP19 enzyme in both mouse and *H. rugulosus* ovary (Figure 5.9A and B). Thereby, CYP19 enzyme localization could not be detected in *H. rugulosus* gonad by these two antibodies.



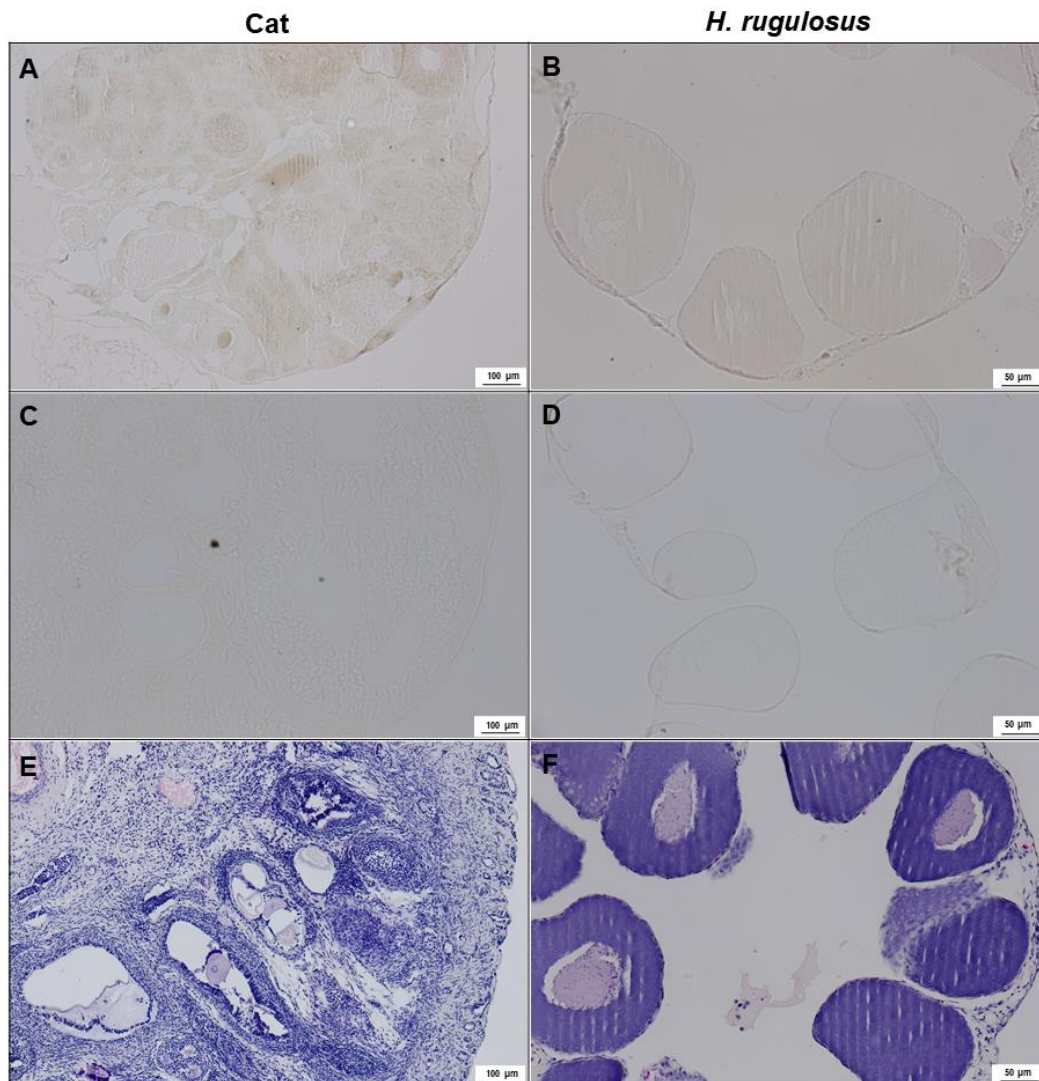


Figure 5.8 Photomicrographs of immunohistochemical staining for CYP19 enzyme by a polyclonal anti-CYP19/aromatase antibody (LS-B2816) showing (A) nonspecific immunoreaction of CYP19 enzyme in cat ovary, (B) *H. rugulosus* ovary without detectable immunoreaction of CYP19 enzyme, (C, D) negative control of cat and *H. rugulosus* ovary, respectively, (E, F) H&E staining in cat and *H. rugulosus* ovary, respectively

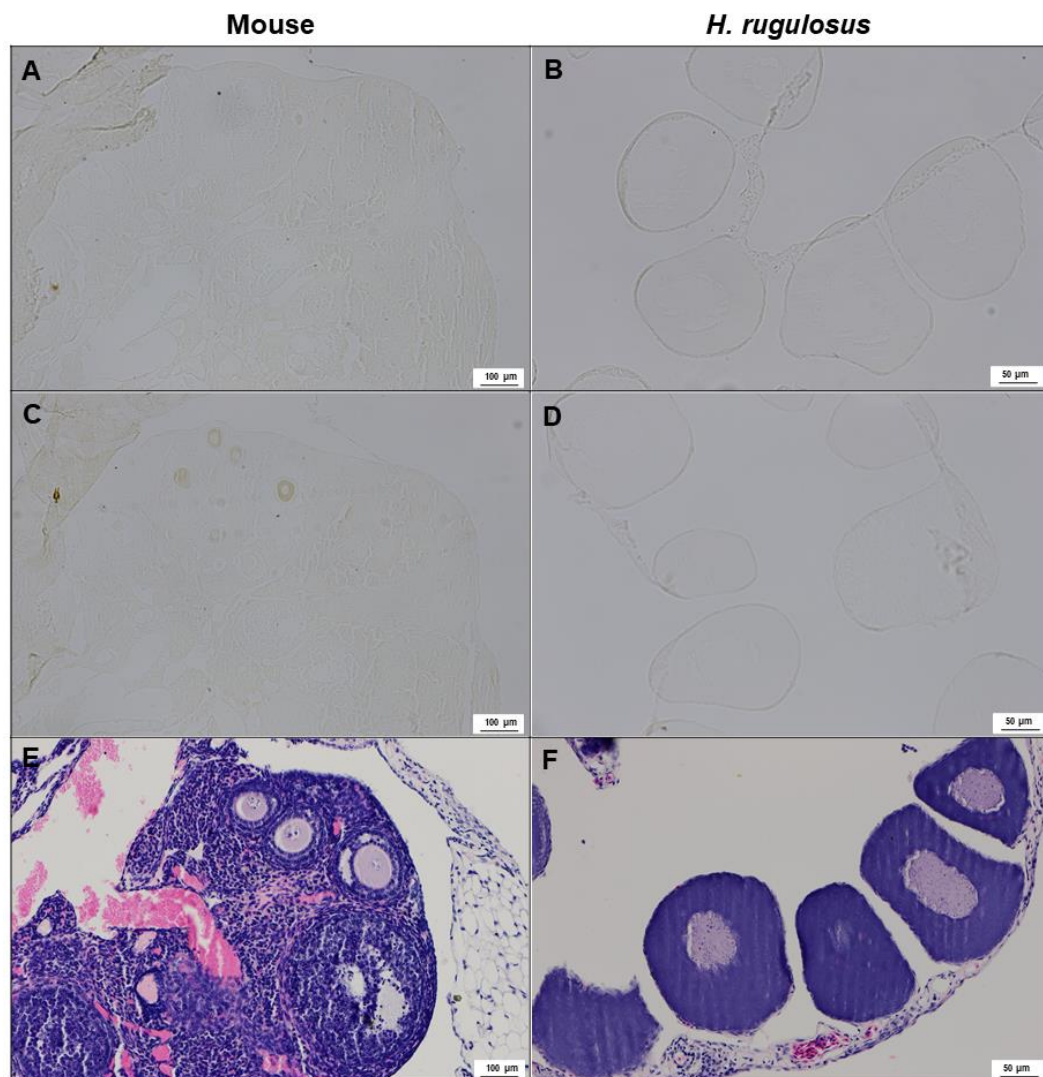


Figure 5.9 Photomicrographs of immunohistochemical staining for CYP19 enzyme by a monoclonal anti-CYP19 antibody (sc-374176) showing (A) mouse ovary without detectable immunoreaction of CYP19 enzyme, (B) *H. rugulosus* ovary without detectable immunoreaction of CYP19 enzyme, (C, D) negative control of mouse and *H. rugulosus* ovary, respectively, (E, F) H&E staining in mouse and *H. rugulosus* ovary, respectively

From these experiments, it indicates that these anti-human antibodies cannot specifically cross-react to gonadal tissue of *H. rugulosus* for both CYP17 and CYP19 enzyme. Due to non-cross reactivity of the antibodies, the immunohistochemistry could not be conducted for studying the steroidogenic potential in *H. rugulosus* gonadal tissue. Therefore, *in situ* hybridization was considered for further investigation on the presence of steroidogenic enzyme mRNA in *H. rugulosus* gonadal tissues.

5.3.2 Cloning of CYP17, CYP19, and β -actin cDNA

The partial sequence of *H. rugulosus* CYP17 cDNA (GenBank Accession No. MW017204) is 699 bp long and contains open reading frame of 457 bp that begins with the first start codon at position 243 and encode 152 amino acids (Figure 5.10). Among the anuran CYP17, the deduced amino acid sequence of *H. rugulosus* showed 94.2% identity and 98.8% similarity with frog *Nanorana parkeri*, 94.8% identity and 97.7% similarity with frog *Glandirana rugosa* and 82.6% identity and 94.2% similarity with frog *Xenopus laevis*. The deduced amino acid sequence was 75.3% identity and 88.8% similarity with chicken *Gallus gallus*, 70.5% identity and 85.0% similarity with rainbow trout *Oncorhynchus mykiss* and 58.7% identity and 80.8% similarity with human *Homo sapiens*.

```

ACAGCTGGTGGACATCTTCCGCTGTCTTCAGATATTTCCAAACAAGCATTTAGACATCTTGAGGCGAGTCAGTGGCAGCTGGAGATCAAC 90
TTCTGCATAGAAATTAAGAACAACAAGGATGGSTTTTCTGGTGAACCTGTCAATGACTTGITGGATGCTCTTCTGAAAGCCAAATTA 180
GCATGGAAAACAACAACAGCAACATAOCACAAGATGTGGGGCTCACGGAGGATCACATCTCATGACTGTAGGGGATATATTTGGAGGG 270
M E N N N S N I P Q D V G L T E D H I L M T V G D I F G A 89
GAGTGGAGACCACATCTACAGTGTAAAAATGGGCTATTGCATATTTACTACACTATCCAGAGGTCCAGAAGAAAATTGAGGAGAGCTGG 360
G V E T T S T V L K W A I A Y L L H Y P E V Q K K I Q E E L 119
ATGCAAGGTTGGGTGTGGAAGATATCCACTCTCAGTGACAGGAAAATCCCTTCATTATACAGAGGCTAOCATCTCTGAAGTGCCTGGAA 450
D A K V G C G R Y P L L S D R K I L H Y T E A T I S E V L R 149
TTCGTCCCGTATCACCATTCCTCATCCCGCAAGTAGCTTTAAAAAGATCCAGTATTGGAGAATACACCATTCCTAAAGAAGCCCGGTGG 540
I R P V S P L L I P H V A L K D S S I G E Y T I P K E A R V 179
TTATTAOCTCTGGTCTCTACACCATGATGAGAAGGAATGGGTAAATCCAAATCTCTTCAATCCAGATCGATTCTTGGATGAAAATGGAA 630
V I N L W S L H H D E K E W V N P N L F N P D R F L D E N G 209
AOCGGGTCTACTCCOCAAAGTCAGAGTTAOUTTCCCTTTGGAGCTGGTATACGGGTGTGTCTGGAGAG 699
N R V Y S P S Q S Y L P F G A G I R V C L G E 232

```

Figure 5.10 Nucleotide and deduced amino acid sequence of *CYP17* cDNA of *H. rugulosus* (GenBank Accession No. MW017204). The primer sequences used for qrt-RT-PCR are underlined

The partial sequence of *H. rugulosus CYP19* cDNA (GenBank Accession No. MW017205) is 799 bp long and contains open reading frame of 795 bp that begins with the first start codon at position 3 and encoded 265 amino acids (Figure 5.11). Among the anuran *CYP19*, the deduced amino acid sequence of *H. rugulosus* showed 91.7% identity and 98.1% similarity with frog *Glandirana rugosa*, 83.8% identity and 95.5% similarity with frog *Xenopus laevis* and 82.6% identity and 94.7% similarity with frog *Sulurana tropicalis*. The deduced amino acid sequence was 71.3% identity and 89.8% similarity with chicken *Gallus gallus*, 52.1% identity and 84.2% similarity with common carp *Cyprinus carpio* and 68.3% identity and 89.8% similarity with human *Homo sapiens*.

```

GGATGAATGAAAAATGGATTATATTTAACAGCAATCCATCACTGTGGAAAGGTGATTGCAOCCCTTCTTCAOCCGAGCTTTGTCTGGGCOCG 90
  M N E N G I I F N S N P S L W K V I R P F F T R A L S G P 29
GACTTATCCAGACTACAGAACACTGCATTAAGTCAOCCAAGCGATTCTGGCACAACTGTGTGATGTTAOCATCAGCAGGGGAATGTAA 180
  G L I Q T T E H C I K S T K R F L A Q L C D V T N Q Q G N V 59
ATGTGCTCAAGCTCATGAGACTCATCATGTTAGACAOCCTTAACAAOCTCTTCTAAGAAATTOCTACAGATGAAAAATGAAATGTGTTTGA 270
  N V L K L M R L I M L D T S N N L F L R I P T D E N E I V L 89
AGATCCAGAAAATACTTTGATGCATGGCAAGCCCTTATCCTGAAAOCCTGCACATTTCTTTTAAATTTTCTGGCTCTACAAGAAGTATGAGA 360
  K I Q K Y F D A W E A L I L K P D I F F K F S W L Y K K Y E 119
AATCAGOCAATGATTTGAAGAGGCTGTGAAATTTCTCAITGAACAAAAGCGACGGGAGCTTTCAGCTTCAGACAAACTGGATGAGCATC 450
  K S A N D L K E A V E I L I E Q K R R E L S A S D K L D E H 149
TTGATTTTGCCTCAGAGTTAATCTTTGCACAGAACTGTGGAGATCTAACAGCTGAGAATGTAAOCCAAAGCATACTGGAATGTGATTG 540
  L D F A S E L I F A Q N R G D L T A E N V N Q S I L E M L I 179
CTGCOCCAGACACCATGTGGTGTCTCTCTACTTCATGCTAAOCCATCACTCAGCATOCCAAAGCTGAAGAGATGATTCTGGAAGAAA 630
  A A P D T M S V S L Y F M L T L I T Q H P K A E E M I L E E 209
TCCATGCTGTGTGGTGAOCCGAGAAGTACAGAGTAGOGACATGCAAAAOCTTAAAGTTCTGGAGAACTTTATCTATGAAGCATGAGGT 720
  I H A V V G D R E V Q S S D M Q N L K V L E N F I Y E S M R 239
ACCAGCCTGTGGTAGACTTAGTCATGCGCAAGGCTCTGGAGGATGAOCTAATTGATGCCTATTATGTGAAGAAAGGAC 799
  Y Q P V V D L V M R K A L E D D V I D G Y Y V K K G 265

```

Figure 5.11 Nucleotide and deduced amino acid sequence of *CYP19* cDNA of *H. rugulosus* (GenBank Accession No. MW017205). The primer sequences used for qrt-RT-PCR are underlined

The partial sequence of *H. rugulosus* β -actin cDNA is 158 bp long and contains open reading frame of 141 bp that begins with the first start codon at position 16 and encodes 47 amino acids (Figure 5.12). Among the anuran β -actin, the deduced amino acid sequence of *H. rugulosus* showed 100% identity and 100% similarity with frog *Sulurana tropicalis*, frog *Xenopus laevis*, and frog *Rana japonica*; and 100% identity and 100% similarity with human *Homo sapiens*.

```

GGTATTGCTGATAGAAATGCAGAAGGAAATCACTGCOOCTGGCOOCTAGCACAAATGAAAATTAAGATCATTGCAOCCOCTGAGCGCAAGTAC 90
  M Q K E I T A L A P S T M K I K I I A P P E R K Y 30
TCTGTCTGGATTGGTGGCTOCCATCTTGGOCTOCCCTCTCCACCTTCCAACAGATGTGCATCAGCAAGCA 158
  S V W I G G S I L A S L S T F Q Q M W I S K 52

```

Figure 5.12 Nucleotide and deduced amino acid sequence of β -actin cDNA of *H. rugulosus*. The primer sequences used for qrt-RT-PCR are underlined

5.3.3 Localization of *CYP17* and *CYP19* mRNA in *H. rugulosus* gonad by an *in situ* hybridization

CYP17 and *CYP19* mRNA probes for *H. rugulosus* were synthesized and used for the *in situ* hybridization technique. Tissue distribution patterns of *CYP17* mRNA were firstly analyzed in testis of adult *H. rugulosus*. The results showed that the specific expression of *CYP17* mRNA was strongly detected in the Leydig cells in the intertubular space (Figure 5.15A and B). Conversely, there was no signals presented when the sense probes were used in the testis (Figure 5.15C). The frog ovary was then observed and the *CYP17* mRNA signal was detected non-specifically. In addition, after repeating the experiment, false positive signals were observed in the frog ovary when using both anti-sense and sense probes (Figure 5.16A and B, respectively). The false positive signals showed as inconsistency of blue signals presented in cytoplasm and nucleus of some oocytes.

Since *CYP17* mRNA detection in ovaries presented many non-specific binding signals, the detection results were focused on the developing testes and the intersex gonads. In the intersex gonads, no specific signals were detected at 1 and 3 weeks after metamorphosis. While at 4 weeks after metamorphosis, the *CYP17* mRNA signals were specifically detected in the intersex gonad at the outer layer of cortex, the area of testicular tissue formation. The hybridization signals were found in the intertubular tissue (Figure 5.15A). The hybridization signals could not be detected in the testis at 4 weeks after metamorphosis (Figure 5.17B). Then at the age of 5 weeks, *CYP17* mRNA were specifically expressed in the Leydig cells of the developing testis and the signals were found in every week until 16 weeks after metamorphosis (Figure 5.17-5.19).

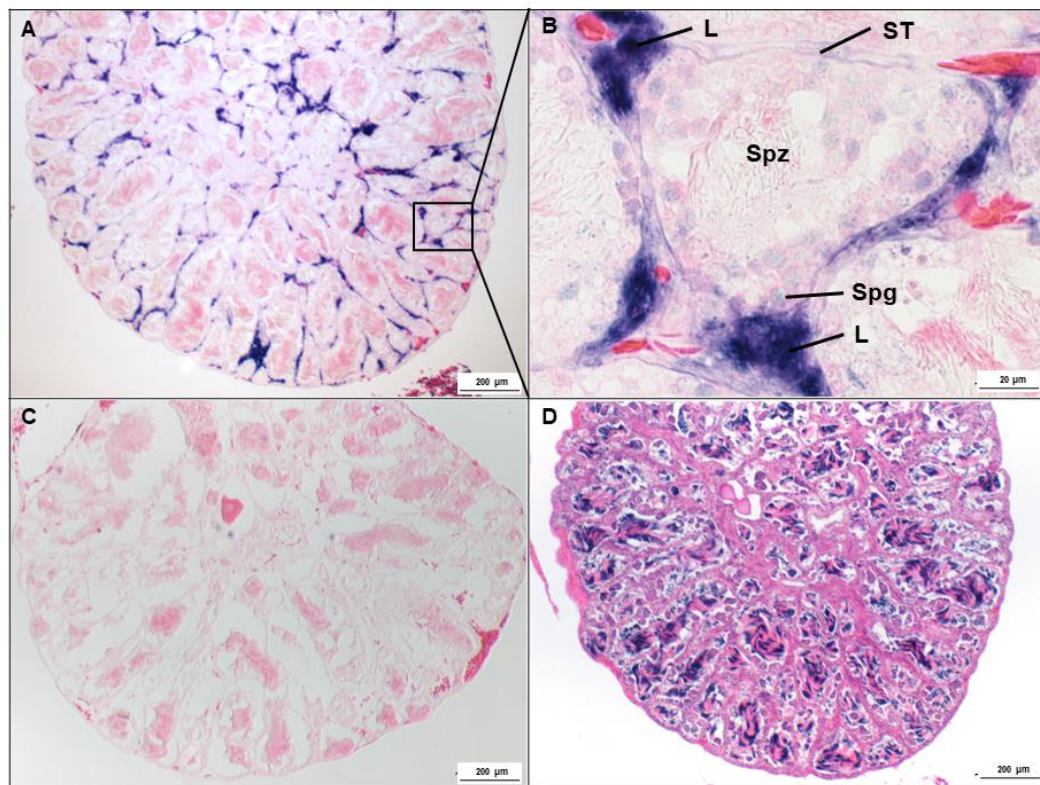


Figure 5.13 Photomicrographs of the *in situ* hybridization for *CYP17* mRNA in *H. rugulosus* testis at 16 weeks after metamorphosis: (A) *CYP17* mRNA localization in the testis hybridized with anti-sense probe showing the signal of *CYP17* mRNA that specifically expressed in the Leydig cells (blue signal), (B) the tissue at high magnification of inset in A, (C) the tissue hybridized with sense probe showing no positive signal presented, (D) the tissue stained with H&E. L: Leydig cell, Spg: spermatogonium, Spz: spermatozoa, ST: seminiferous tubule

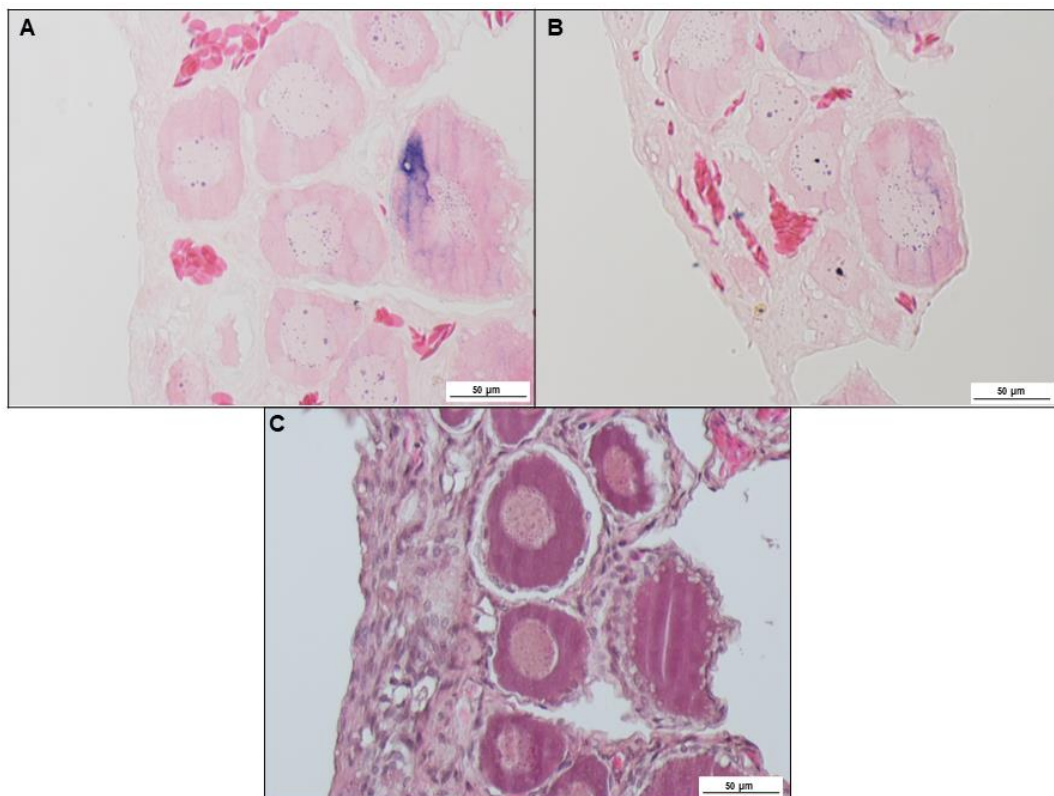


Figure 5.14 Photomicrographs of the *in situ* hybridization for *CYP17* mRNA of *H. rugulosus* ovary at 16 weeks after metamorphosis. (A) *CYP17* mRNA localization in the ovary hybridized with anti-sense probe showing false positive signals in an oocyte, (B) the tissue hybridized with sense probe showing false positive signals in some oocytes, (C) the tissue stained with H&E

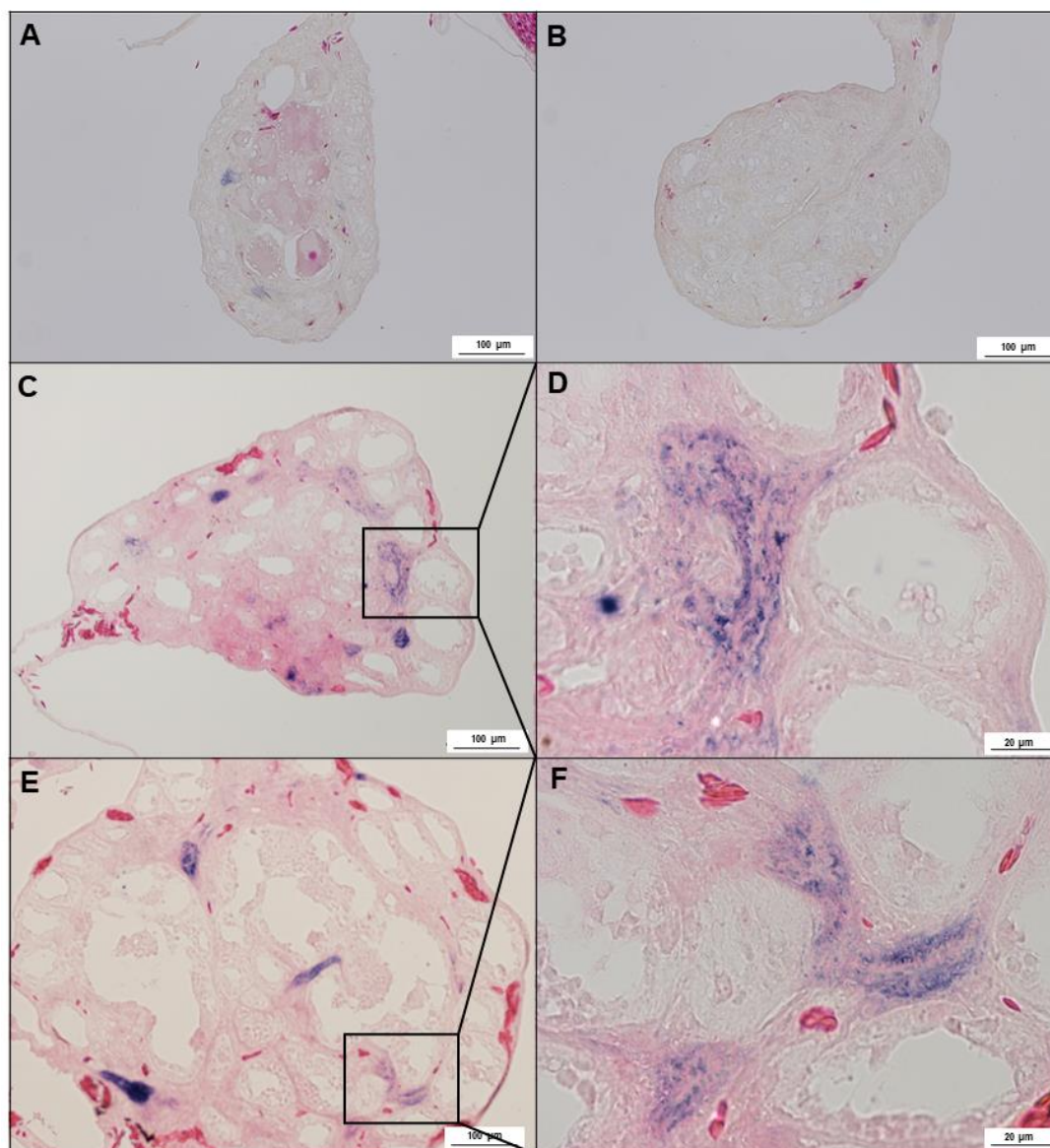


Figure 5.15 Photomicrographs of the *in situ* hybridization for *CYP17* mRNA in *H. rugulosus* gonad at 4 to 6 weeks after metamorphosis. *CYP17* mRNA localization in the gonad hybridized with anti-sense probe showing the signal of *CYP17* mRNA in the Leydig cells (blue signal) of testicular tissue at (A) 4 weeks (intersex gonad), (B) 4 weeks (testis), (C) 5 weeks, and (E) 6 weeks after metamorphosis. (D) and (F) the tissue at high magnification of inset in (C) and (E), respectively

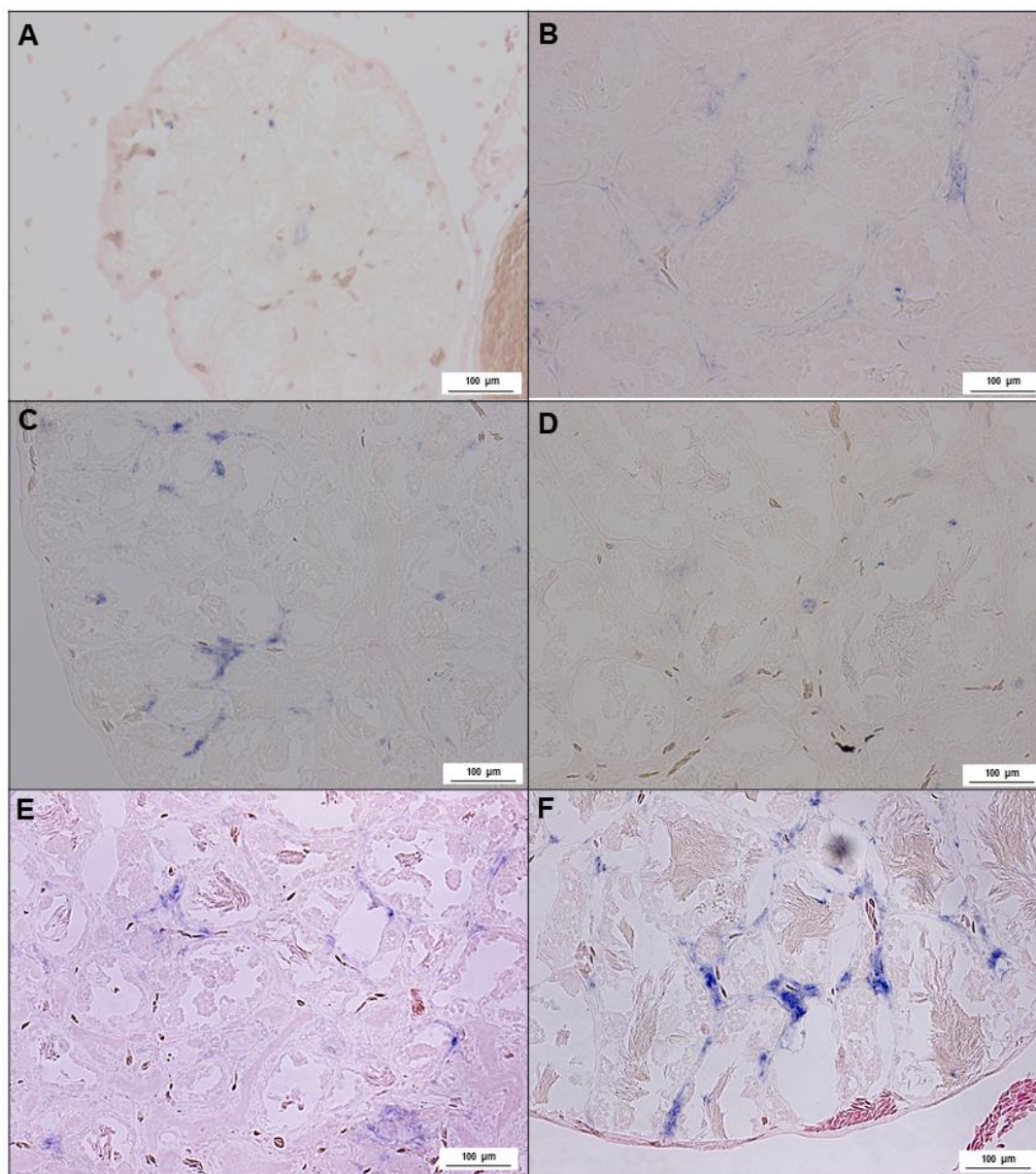


Figure 5.16 Photomicrographs of the *in situ* hybridization for *CYP17* mRNA in *H. rugulosus* testis at 7 to 12 weeks after metamorphosis. *CYP17* mRNA localization in the testicular tissue hybridized with anti-sense probe showing the signal of *CYP17* mRNA in the Leydig cells (blue signal) at (A) 7 weeks, (B) 8 weeks, (C) 9 weeks, (D) 10 weeks, (E) 11 weeks and (F) 12 weeks after metamorphosis

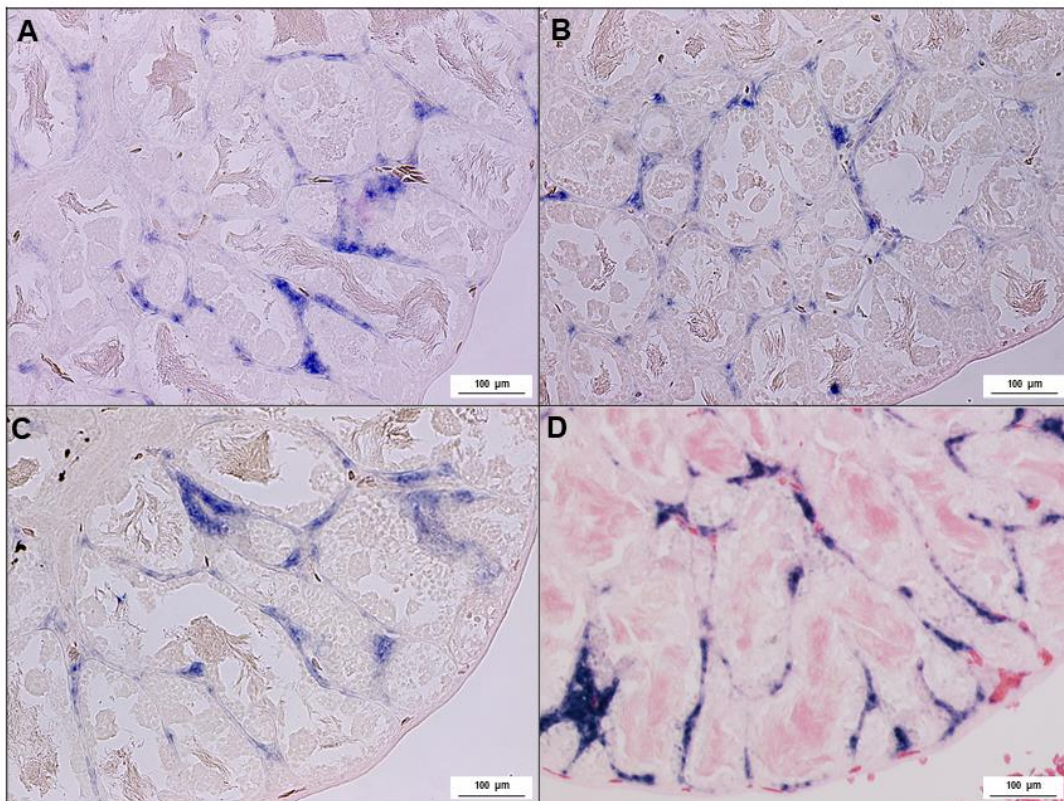


Figure 5.17 Photomicrographs of the *in situ* hybridization for *CYP17* mRNA in *H. rugulosus* testis at 13 to 16 weeks after metamorphosis. *CYP17* mRNA localization in the testicular tissue hybridized with anti-sense probe showing the signal of *CYP17* mRNA in the Leydig cells (blue signal) at (A) 13 weeks, (B) 14 weeks, (C) 15 weeks and (D) 16 weeks after metamorphosis

Localization for *CYP19* mRNA expression was performed by an *in situ* hybridization. The tissue distribution patterns of *CYP19* mRNA were firstly analyzed in ovary of the adult frog. The result revealed that *CYP19* mRNA signal was not specifically detected in the ovary. In addition, false positive signals were observed in the frog ovary when using both anti-sense and sense probes (Figure 5.20A and B, respectively). From this results, *CYP19* mRNA expressions were not specifically detected in gonadal tissue of *H. rugulosus* by *in situ* hybridization. Therefore, this technique cannot completely explain the expression pattern of steroidogenic activity

during the development of *H. rugulosus*. qrt-RT-PCR was then considered as a technique for observing the steroidogenic synthesis in *H. rugulosus* gonad.

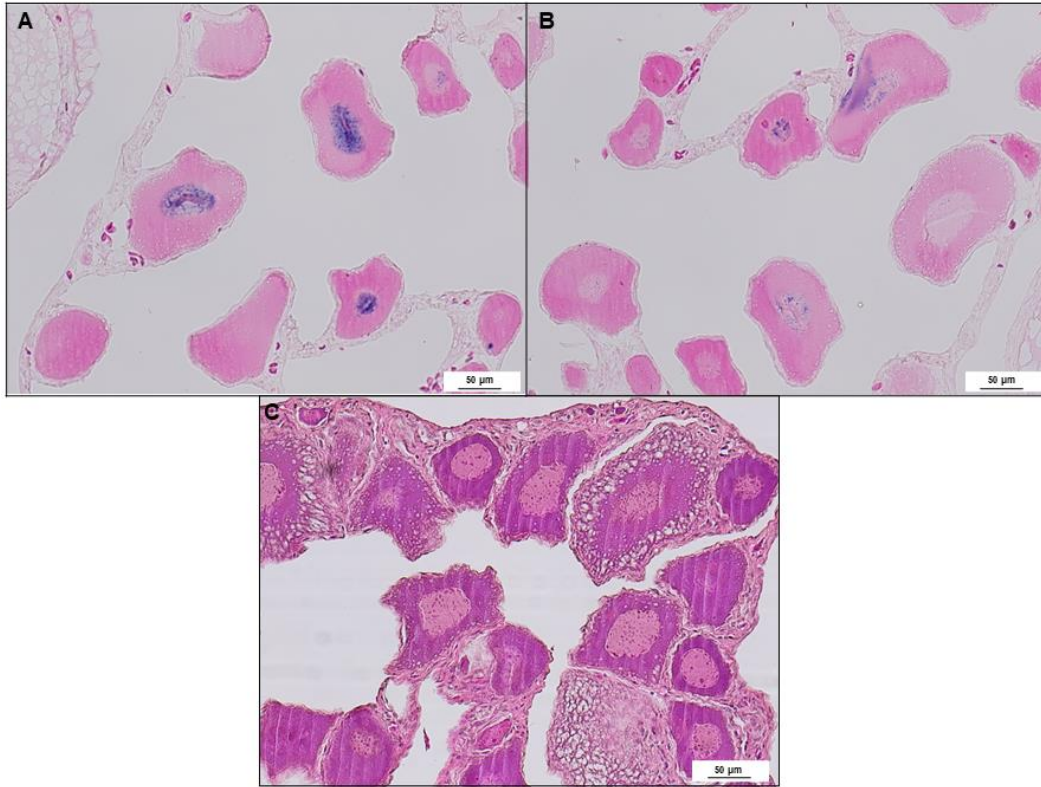


Figure 5.18 Photomicrographs of the *in situ* hybridization for *CYP19* mRNA of *H. rugulosus* ovary at 16 weeks after metamorphosis. *CYP19* mRNA localization in the ovary (A) hybridized with anti-sense probe showing false positive signals in some oocytes, (B) the tissue hybridized with sense probe showing false positive signals in some oocytes, (C) the tissue stained with H&E

5.3.4 *CYP17* and *CYP19* mRNA expressions in *H. rugulosus* gonad by quantitative real-time RT-PCR (qrt-RT-PCR)

During the developmental period, mRNA expression of *CYP17* and *CYP19* mRNA in the gonads of *H. rugulosus* was quantified by qrt-RT-PCR technique. The samples were divided into 7 groups according to the phase of gonadal development in chapter IV. The first group was stages 25-35 (n=82), the gonads were still in the undifferentiated phase. The second (stages 36-41, n=49) and the third (stages 42-46,

n=41) groups were developing ovary phases during metamorphosis which were defined by the shape of follicular cells. In group of stages 36-41, the follicular cells were oval shaped surrounding cyst of oogonia. In group of stages 42-46, the follicular cells were slightly flattened in shape surrounding cyst of oogonia and diplotene oocytes. The fourth group (1-3 weeks after metamorphosis, n=33) was developing ovary after complete metamorphosis. Then the last 3 groups were at 4-11 weeks after metamorphosis which could be distinguished the sex into 3 groups including female (n=54), intersex (n=11) and male (n=16).

The *CYP17* mRNA at stages 25-35, 36-41 and 42-46 were found to express at low level with no significant difference among groups. In 1-3 weeks after metamorphosis group, the level was significantly higher than those of stages 25-35 ($p=0.000$) and stages 36-41 ($p=0.002$). In female group at 4-11 weeks after metamorphosis, the mRNA expression of *CYP17* was significantly higher than the group at stages 25-35 ($p=0.000$), stages 36-41 ($p=0.000$), stages 42-46 ($p=0.003$), and 4-11 weeks after metamorphosis male ($p=0.022$). In intersex group at 4-11 weeks after metamorphosis the mRNA expression of *CYP17* was significantly higher than the group at stages 25-35 ($p=0.000$), stages 36-41 ($p=0.000$) and stages 42-46 ($p=0.000$). The level of expression in the intersex group was in between the female group and the male group, with no significant difference compared to either groups. *CYP17* mRNA expression in male group at 4-11 weeks after metamorphosis was significantly higher when compared to other groups ($p<0.05$), except the intersex group ($p=1.000$). At this period, seminiferous tubules were formed and the Leydig cells also presented between the tubules in both intersex and male groups (Figure 5.21).

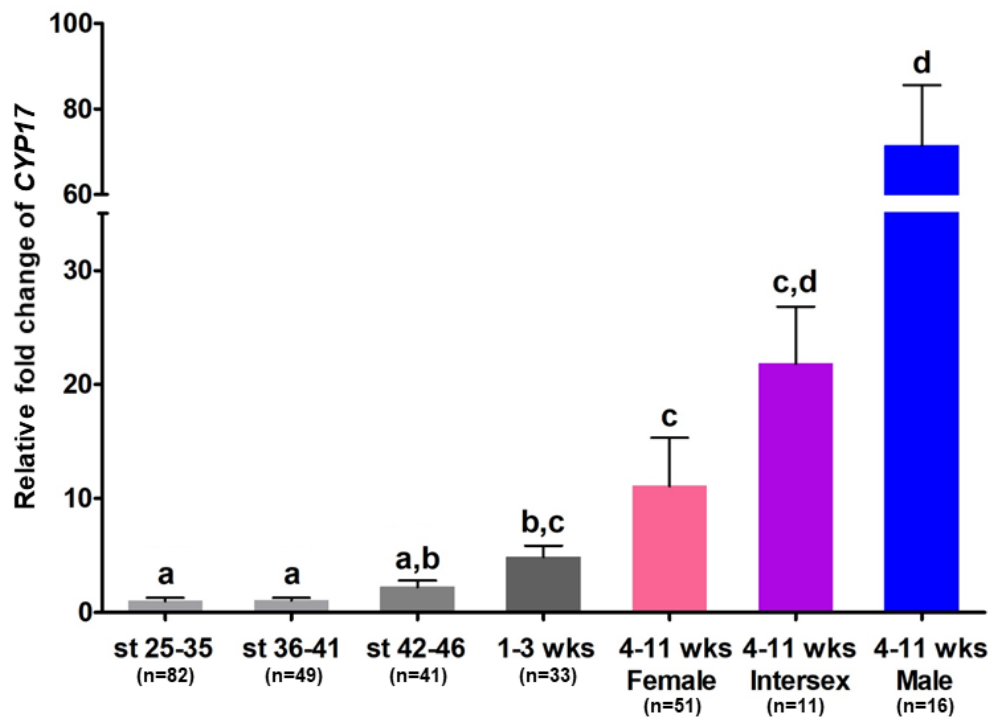


Figure 5.19 Quantification of *CYP17* mRNA in the *H. rugulosus* gonad during the gonadal development period (Gosner stages 25-46 and 1-11 weeks after metamorphosis) showing bar charts of fold changes in expression relative to st 25-35 group. Data were normalized with β -actin. Error bars represent SEM at each group. The different letters above each bar indicate significant differences between groups ($p < 0.05$). st: Gosner stage, wks: weeks after metamorphosis

The *CYP19* mRNA expression were detected consistently when observed in the group of stages 25-35, stages 36-41, and stages 42-46. Then the *CYP19* mRNA were gradually and significantly increased at 1-3 weeks after metamorphosis when compared to that of stages 25-35 ($p=0.037$) and stages 36-41 ($p=0.019$). In female group at 4-11 weeks after metamorphosis, the *CYP19* mRNA was expressed at higher level than other groups and significantly different from those of stages 25-35 ($p=0.000$), stages 36-41 ($p=0.000$), stages 42-46 ($p=0.000$), and 4-11 weeks after metamorphosis male ($p=0.004$) group. However, it was not significantly different from 1-3 weeks after metamorphosis and intersex group at 4-11 weeks after

metamorphosis. At this period, ovaries reached the fully developed stage (Figure 5.22).



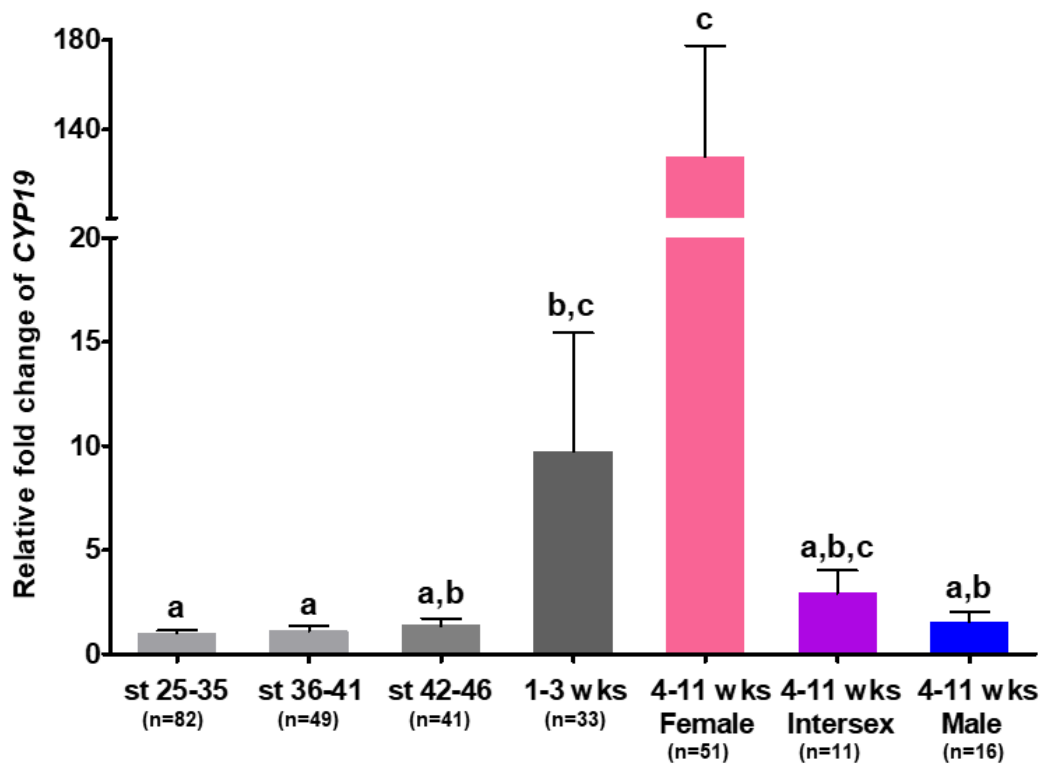


Figure 5.20 Quantification of *CYP19* mRNA in the *H. rugulosus* gonad during the gonadal development period (Gosner stages 25-46 and 1-11 weeks after metamorphosis) showing bar charts of fold changes in expression relative to st 25-35 group. Data were normalized with β -actin. Error bars represent SEM at each group. The different letters above each bar indicate significant differences between groups ($p < 0.05$). st: Gosner stage, wks: weeks after metamorphosis

According to the results in bar graph of relative fold change of *CYP17* and *CYP19* mRNA, score of expression could be provided using semi-quantitative scores. The scores were indicated based on mean of relative fold change of each gene as shown in Table 5.3.

Table 5.3 Semi-quantitative scores of relative fold change of *CYP17* and *CYP19* mRNA

Group	<i>CYP17</i> mRNA		<i>CYP19</i> mRNA	
	mean±SEM of relative fold change	score	mean±SEM of relative fold change	score
1	1.000±0.298	0	1.000±0.142	0
2	1.076±0.218	0	1.106±0.266	0
3	2.225±0.588	+1	1.366±0.344	0
4	4.857±0.986	+2	9.745±5.605	+3
5	11.087±4.243	+3	127.700±49.896	+6
6	21.827±4.993	+4	2.929±1.088	+1
7	71.466±14.124	+6	1.550±0.490	0

Score: (0) mean relative fold change = 1 to 2
 (+1) mean relative fold change = 2 to 4
 (+2) mean relative fold change = 4 to 8
 (+3) mean relative fold change = 8 to 16
 (+4) mean relative fold change = 16 to 32
 (+5) mean relative fold change = 32 to 64
 (+6) mean relative fold change = 64 to 128
 (+7) mean relative fold change more than 128

5.4 Discussion and conclusion

This is the first study isolated and reported the partial sequences of *CYP17* and *CYP19* cDNAs from *H. rugulosus* and investigated the mRNA levels of these two genes during gonadal development. In addition, this is the first report showing *CYP17* mRNA localization in the gonads during the developmental period of *H. rugulosus*. This study revealed that the chronological differences in mRNA level in the gonad of *H. rugulosus* could be detected by real-time RT-PCR. The results showed that the higher level of *CYP17* and *CYP19* mRNA was found at 1-3 weeks after metamorphosis compared to those of the earlier stages. This finding differs from other frog species. In *G. rugosa*, the differences in *CYP17* and *CYP19* mRNA were detected at the stage before morphological sex differentiation, at Gosner stages 25-26 (Maruo et al., 2008). In *X. laevis*, the differences in *CYP17* and *CYP19* mRNA were detected at the stage of morphological sex differentiation, at Gosner stages 28-31 (Mawaribuchi et al., 2014; Piprek et al., 2018). The localization of *CYP17* mRNA in *H. rugulosus* gonad was firstly detected at 4-5 weeks after metamorphosis which was later than the detection by the quantitative real-time RT-PCR. This may be because the amounts of *CYP17* mRNA at the earlier stages were too small to be detectable by the lesser sensitive technique such as the *in situ* hybridization. In contrast to *CYP17*, the localization of *CYP19* mRNA was undetectable in any stage of *H. rugulosus* gonad, possibly due to the low expression of *CYP19* mRNA. Unfortunately, the results from the immunohistochemical study revealed no positive signals of *CYP17* and *CYP19* enzymes in *H. rugulosus* testis and ovary. Even though the previous studies reported that anti-bovine *CYP17* antibodies cross-reacted to frog tissues such as *R. esculenta* (Do Rego et al., 2007), and *G. rugosa* (Sakurai et al., 2008), the epitope target of these antibodies may not cover the antigenic portion of the enzyme in this frog species. Further investigation should be carried out with other antibodies or other technique (such as immunofluorescence) to confirm results of the *in situ* hybridization and qrt-RT-PCR in the future.

The tissue quantification of *CYP17* mRNA in *H. rugulosus* showed that *CYP17* mRNA expressed in stage 25 and remained constant until stage 46 (complete metamorphosis). While the localization of *CYP17* mRNA was not detected at stages 42-46 by *in situ* hybridization. Previous study in *G. rugosa* revealed that the expression level of *CYP17* mRNA was higher in males than female tadpoles at stages 25, 26, 28, 30, and adult (Iwade et al., 2008; Sakurai et al., 2008). Localization of *CYP17* mRNA was detected in the indifferent gonad of male tadpole since stage 26 (Iwade et al., 2008). They found that in *G. rugosa*, *CYP17* mRNA expression in the indifferent gonad of male tadpole occurred before the onset of sex differentiation (Iwade et al., 2008). While in *H. rugulosus*, up to now, the sex of tadpoles could not be determined at the early stage of development by any technique. All their 13 pairs of chromosomes are homomorphic and there were no difference of each pair of chromosomes when compared between sexes (Ling et al., 1998; Chockchaichomnankit et al., 2001; Donsakul, 2009). These works suggested that sex chromosomes of *H. rugulosus* may have not yet developed (Chockchaichomnankit et al., 2001). In addition, the results in chapters III and IV revealed that during metamorphosis (stages 1-46), there were no distinct morphological and histological characteristics that can be used to distinguish the sex of *H. rugulosus*. Likewise, in this part, the quantities of *CYP17* and *CYP19* mRNA measured were related to the sex differentiation period and they were not different during metamorphosis (stages 25-46) in *H. rugulosus*. Therefore, based on the recent study, there were no detectable sexually dimorphic traits of gonad morphology, histology, and steroidogenic function during metamorphosis in this species.

The levels of mRNA were slightly higher in both *CYP17* and *CYP19* at 1-3 weeks after metamorphosis group. During 1-3 weeks after metamorphosis, histological study revealed that the gonad in *H. rugulosus* consisted of ovary and intersex gonad. At this period, the number of follicular cells were increased and well developed, consequently, these cells may produce high levels of *CYP19* mRNA. In

the intersex, conversely, the high level of *CYP17* mRNA may be due to the testicular formation and increasing number of Leydig cells in gonad of *H. rugulosus*. In addition, at this period, the gonads of some individual began to develop into testis and this sampling group may had high ratio of male frogs. It could be implied that the age of 1-3 weeks after metamorphosis was the beginning point of the sex differentiation in *H. rugulosus*. Moreover, the differentiation into male or female depended on the expression level of each mRNA. The expression level of *CYP19* mRNA could be used as a predictor of sex in *L. sylvaticus* and *S. tropicalis*). The presumptive female *L. sylvaticus* tadpole (Gosner stage 30) and presumptive female *S. tropicalis* tadpole (Gosnes stage 28) had a significantly higher level of *CYP19* mRNA than the presumptive male tadpole (Navarro-Martín et al., 2012).

At the age of 4-11 weeks after metamorphosis, the level of *CYP17* mRNA was much lower in the female group as compared to male group. This was in line with the *in situ* hybridization result. *CYP17* mRNA was not specifically detected in the ovary at 1-4 weeks after metamorphosis and the adult. The *CYP17* mRNA was at high level in the intersex and male group at 4-11 weeks after metamorphosis. This result corresponded to the localization study in which the *CYP17* mRNA signals were specifically detected at 4-16 weeks after metamorphosis in testicular tissue of both intersex gonad and testis. This finding could be implied that *CYP17* mRNA signals presented in some of somatic cells located in the intertubular space of developing testicular tissue whether it would be intersex gonad or testis. These results correlated with previous studies in *G. rugosa* in which *CYP17* enzyme was found in somatic cells of the indifferent gonad of male and the Leydig cells of the testis in adult male frog (Maruo et al., 2008; Sakurai et al., 2008; Nakamura, 2009). The expression of *CYP17* mRNA was also upregulated in ovotestis in ZW transgenic *G. rugosa* frog (Fujii et al., 2014). The expression trend was also similar to *L. sylvaticus* which *CYP17* mRNA was dominantly found in males than females (Navarro-Martín et al., 2012). It could be implied that *CYP17* enzyme may influence sperm structure and

function (Liu et al., 2005). However, in this study, the level of *CYP17* mRNA of the intersex group was much lower than the male group. It corresponded to the histological finding that some of the tissue areas in the intersex gonad were still ovarian tissue. As the function of ovary, the level of *CYP17* mRNA was expected to be much lower when compared to testis. At 4-5 weeks after metamorphosis, faint hybridization signals of *CYP17* mRNA were found in some intersex gonad (Figure 5.17A) while the signal was not found in some testes (Figure 5.17B). This period may be a key point that the level of *CYP17* mRNA was gradually changed and the different detection among individuals may be due to interindividual variation.

The expression of *CYP17* mRNA have been observed in several non-mammalian vertebrate species. In spotted sea bass *Lateolabrax maculatus*, *CYP17* mRNA presented in steroidogenic tissues and the strong signals were largely found in the area of Leydig cells of the testis when observed by *in situ* hybridization (Chi et al., 2019). In zebrafish, *CYP17A1* mRNA is prominently expressed in male gonad (Hinfray et al., 2011). The rice field eel *Monopterus albus*, a species with sex reversal process naturally occurred, *CYP17* enzyme expression showed prominent expression in the testis, less in the ovary and the least in the ovotestis. However, the expression patterns of the *CYP17* enzyme were consistent during the sex reversal process when observed by northern blot analysis (Yu et al., 2003). In stellate sturgeon *Acipenser stellatus*, *CYP17A1* and also *dmrt1*, and *sox9* gene expression were significantly higher in male gonads than in female gonads (Burcea et al., 2018). However, Yang et al. (2003) reported that *CYP17* enzyme activity was dominantly expressed in oocytes and other enzymes related to sex steroid production were also expressed in the follicular cells of frog *X. laevis* when observed by *CYP17* enzyme assay and steroid metabolism assay. They suggested that it possibly involved two-cell model in which follicular cells and oocytes played roles in *Xenopus* ovarian androgen production. The study in adult zebra finches, *CYP17* enzyme expressed in ovarian follicles especially in the theca cell layer which were higher than in the interstitial tissue of

testis (Freking et al., 2000). According to the steroidogenic pathway, CYP17 is an enzyme that converts pregnenolone into dehydroepiandrosterone (DHEA) and converts progesterone into androstenedione (AE). Both DHEA and AE are intermediate compounds that can be converted into testosterone via the activity of enzymes such as 17- β HSD (Norris and Carr, 2013). Thus, the expression of 17- β HSD is one of the key enzymes that should be considered during testicular formation.

In this study, the level of *CYP19* mRNA in gonad tissues was analyzed in tadpole and frog at each developmental period by the quantitative real-time RT-PCR. The level of *CYP19* mRNA was quite constant at stages 25-46. The expression level was high at 1-3 weeks after metamorphosis, the period that developing ovary reached the fully developed stage. Some follicular cells may be active and produce more *CYP19* enzyme. Then at 4-11 weeks after metamorphosis, the female group showed a higher level than other groups. Based on the gross morphology of the ovaries of this period, they were fully developed and enlarged in size. This finding corresponds with the histology at the same period which revealed that the number of oocytes and follicles were increased. Therefore, a large number of follicular cells may indicate fully steroidogenic function and *CYP19* mRNA and enzyme may be increased in the synthesis rate. In comparison, *CYP19* mRNA of intersex and male groups were lower than the female group. The quantitative result of *CYP19* mRNA in this study correlated with the study in *G. rugosa* that expression of *CYP19* mRNA was observed during ovarian differentiation and the level was much higher when observed in developing ovary which contained immature oocytes (Kato et al., 2004). In addition, the expression level of *CYP19* mRNA in *G. rugosa* females was higher than in males (Maruo et al., 2008). This expression trend was similar to *L. sylvaticus* which *CYP19* mRNA was dominantly expressed in females than males (Navarro-Martin et al., 2012). The ovarian differentiation and development in vertebrate species were potentially controlled by estrogens which were synthesized in the developing gonads after induction of *CYP19* gene expression so *CYP19* gene was dominantly expressed

in females (Nakamura, 2010). In rainbow trout *Oncorhynchus mykiss* and tilapia *Oreochromis niloticus*, *CYP19* mRNA was detected in females at the period of the first sign of sex differentiation, and the expression level was higher than males (Guiguen et al., 1999; Verneti et al., 2013). Likewise, in catfish *Clarias gariepinus*, *CYP19* mRNA was highly expressed in differentiating female gonads (Raghuveer et al., 2011). In adult zebra finches, *CYP19* mRNA was highly expressed in ovary but not in testis (Freking et al., 2000). In addition, the localization of CYP19 enzyme was detected in ovarian somatic cells at stage 46 in *G. rugosa* (Isomura et al., 2011). Kato et al (2004) reported that the ovarian somatic cells could be identified into 2 types based on electron microscopy including follicle cells with a heterochromatic nucleus, and theca cells with an attenuated dark nucleus. The positive signals of CYP19 enzyme were detected in the follicle cells. Based on the cell morphology and CYP19 enzyme activity, they suggested that follicle cells in *G. rugosa* were similar to the granulosa cells in other vertebrate species (Kato et al., 2004).

In case of the intersex gonad (at 4-11 weeks after metamorphosis), the level of *CYP17* mRNA was high, whereas the level of *CYP19* mRNA was quite low. The histology showed that the gonads at this period composed of both testicular tissue with developing testis cords/seminiferous tubules and testis-ova. Some oocytes presented a sign of degeneration. From the results of mRNA level, it could be suggested that the testicular tissue had developed and functioned. Therefore, it transcribed large amounts of *CYP17* mRNA. While at the area of ovarian tissue, the oocytes may not function. Therefore, it transcribed low level of *CYP19* mRNA. The regression of ovarian tissue was influenced by several factors. Lack of androgen synthesis resulted in accelerating ovarian development with numerous oocytes (Zaccanti et al., 1994). Lack of estrogen synthesis resulted in the transformation of ovary into testis (Hsü et al., 1979). Therefore, in this study, synthesizing small amounts of testosterone could influence the ovarian tissue to remain intact. In addition, anti-Müllerian hormone (AMH) is a hormone that blocks aromatization of testosterone to

estrogen and functions as a masculinizing factor. Kelly et al. (1996) suggested the hypothetical scheme of sex differentiation in *X. leavis* and considered that the ovarian differentiation was a default pathway. For the testicular differentiation, the pre-testis secreted AMH (masculinizing factor) to block the ovarian differentiation. Thus, in this study, remnant of oocytes in the intersex gonad of *H. rugulosus* may be because of low activity of AMH. However, study about factors involving oocytes degeneration in the intersex gonad should be further investigated.

CYP17 is one of key enzymes in intermediate steps for androgens and estrogens production. Overall results indicate that *CYP17* mRNA expressed at high level since 1-3 weeks after metamorphosis or a period sex differentiation. The increasing expression of *CYP17* mRNA may correlate with the increasing rate of androgen and estrogen production. At 4-11 weeks after metamorphosis, the testis transcribed *CYP17* mRNA at very high level which may result in a high rate of translation into CYP17 enzyme and a high rate of androgen synthesis. The intersex gonad also transcribed *CYP17* mRNA at high level possibly due to the functional testicular tissue in the gonad. *CYP17* mRNA synthesis of the testicular tissues was also detected spatially in Leydig cells during 4 to 16 weeks after metamorphosis. The ovary at 4-11 weeks after metamorphosis could also transcribe *CYP17* mRNA, albeit at a lower level than testis and intersex gonad. This may be because androgen were used as precursors for estrogen synthesis, or the CYP17 enzyme was used for other steroid synthesis of the ovary. CYP19 (aromatase) is a female specific enzyme that can convert androgen into estrogen. In this study *CYP19* mRNA expressed at high level since 1-3 weeks after metamorphosis and increased continuously when they reached at fully developed stage (4-11 weeks after metamorphosis). It could be implied that high expression level of *CYP19* mRNA may involve in a high rate of estrogen synthesis. The level of estrogen may be high during the ovarian development in order to stimulate the oogenesis until the complete development. The fact that testis and intersex gonad at 4-11 weeks after metamorphosis showed

high level of *CYP17* mRNA expression but low level of *CYP19* mRNA expression indicated that the sex steroid required for testicular development should be androgens, not estrogens. Based on the overall results, it can be concluded that sex-related differences in *CYP17* and *CYP19* mRNA expression after metamorphosis were evidenced. It confirms that steroidogenic potential of gonad after metamorphosis is different between sexes and it may indicate the roles of *CYP17* and *CYP19* in subsequent gonadal development in *H. rugulosus*.



Chapter VI

General Discussion and Conclusion

Amphibian is an excellent model to study embryonic development, sex determination, gonadal differentiation, and maturation according to many previous researches. *H. rugulosus*, the only species in the genus *Hoplobatrachus* that distribute in Thailand (Pansook et al., 2012), has been used as a model species in biological researches in Thailand. A previous study suggested that the pattern of gonadal sex differentiation in *H. rugulosus* seemed to be an undifferentiated type with the result of 100% females at complete metamorphosis (Traijitt et al., 2010). However, additional information of gonadal development after metamorphosis is still needed to confirm this finding and to examine process that occurs in order to develop the male. This study, therefore, aimed to further examine the chronology of somatic and gonadal development, pattern of gonadal sex differentiation, and steroidogenic potential of gonadal tissues during the development of *H. rugulosus*.

The phase in somatic development of *H. rugulosus* was reported in this study as follows: 1) the embryonic phase (stages 1-20) occurred in 13-21 haf, 2) the hatchling phase (stages 21-24), period of external gill development, occurred in 36-44 haf, 3) the tadpole phase (stages 25-41), period of external gill degeneration and hind limb development, occurred in 20-26 days post hatch (dph), and 4) the metamorph phase (stages 42-46), period of mouth development and tail degeneration, occurred in 25-33 dph. The evidence of gonadal development and their steroidogenic potential were described based on the stage and period of somatic development.

The chronology of gonadal sex differentiation in *H. rugulosus* was observed by morphology and histology, and summarized in Figure 6.1. Firstly, genital ridge formation began at stage 25 (1-2 dph). The genital ridge composed of primordial germ cells with yolk platelets inside cytoplasm and some somatic cells. The somatic development of stage 25 was simply identified by the external gill atrophy and

spiracle formation on the left side of the body. The onset of gonadal development, genital ridge formation at stage 25, is the same period as reported in several anuran species (Nakamura, 2009; Ogielska, 2009). Next, the development of indifferent gonads was found at stage 27 (3-5 dph). The indifferent gonad composed of 1-2 gonial cells per cross section and some somatic cells. The somatic development of stage 27 was identified by the length of the limb buds which was equal to or longer than half of its diameter ($L \geq \frac{1}{2}D$). Then, the gonad was firstly noticeable under a stereomicroscope at stage 33 (8-12 dph), when the gonadal tissues were still indifferent. The somatic development of stage 33 was identified by the second indentation of toe in which foot paddle showed indentation between the 5th - 4th and the 4th - 3rd toes. At stage 35 (11-17 dph) the indifferent gonad increased in size and the tissue could be identified as cortex and medulla. The somatic development of stage 35 was identified by the fourth indentation of the toe in which foot paddle margin showed indentation between all five toes. The steroidogenic potential in gonadal tissues of stages 25-35 group were detected at a low level as evidenced from both *CYP17* and *CYP19* mRNA expression. These stages were the tadpole phase that the gonad development initiated, and gonads were still in the indifferent form.

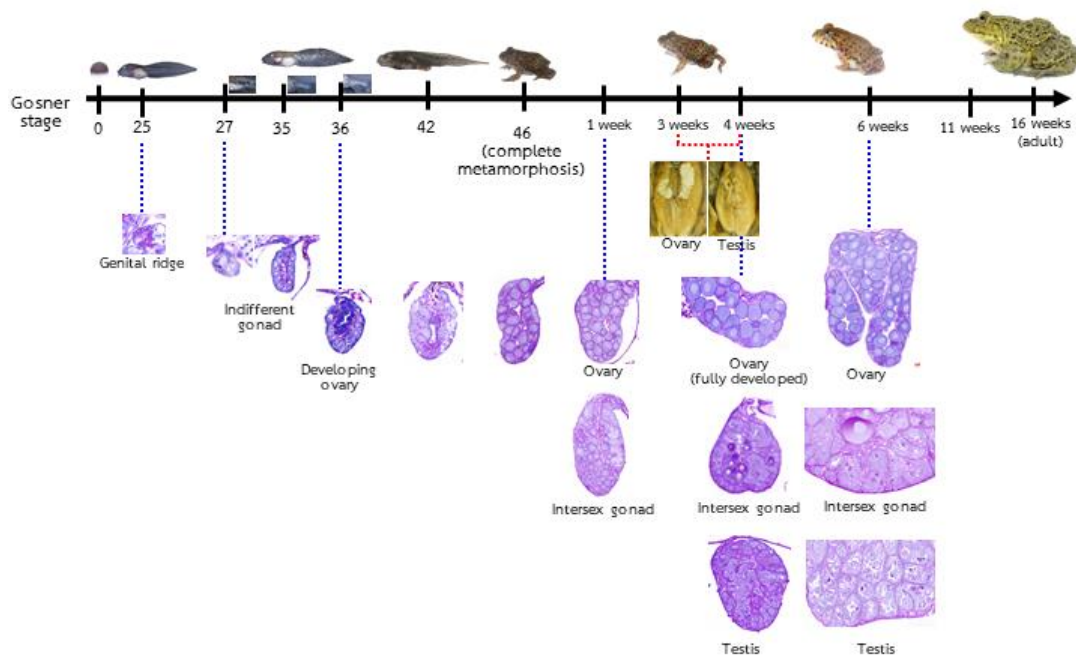


Figure 6.1 Summary diagram of somatic and gonadal development in *H. rugulosus*

Next, the ovarian differentiation began at stage 36 (12-20 dph). The developing ovary consisted of some gonocytes, medulla degenerated, and ovarian cavity developed. The somatic development of stage 36 was identified by the 3rd – 5th toes separation. All gonads developed through the same pattern (ovarian differentiation) until complete metamorphosis. At stage 46 (25-33 dph), the developing ovary composed of a number of diplotene oocytes protruding into the ovarian cavity. The somatic development of stage 46 was identified by tail completely reduced, indicating complete metamorphosis. The study of steroidogenic potential of the developing ovary was divided into 2 groups including 1) a group at stages 36-41, and 2) a group at stages 42-46. Stages 36-41 were in the phase of developing ovary with evidence of ovarian cavity formation (ovarian development stages IV-V). The expression levels of *CYP17* and *CYP19* mRNA in this group were not different from group of stages 25-35. Stages 42-46 were in the phase of developing ovary that composed of diplotene oocytes surrounding with follicular cells (ovarian development stages VI-VII). The expression of *CYP17* and *CYP19* mRNA were not

different from the previous group (stages 36-41). Although the follicular cells were developed, their steroidogenic activity might still be quiescent at this period.

The developmental period of *H. rugulosus* was 25-33 days from fertilization until complete metamorphosis. The rate of development was quite rapid when compared to other anuran species. The sexual dimorphism based on both somatic and gonadal characteristics was not found in *H. rugulosus* during metamorphosis. After metamorphosis, the criterion used to divide stage of somatic development in this study was the age of froglet shown as a number of weeks after metamorphosis.

At 1 week after metamorphosis, *H. rugulosus* gonads were separated into 2 groups including ovary and intersex gonad. The ovary at this period composed of mostly diplotene oocytes and some primary oogonia and nests of secondary oogonia in the outermost area (ovarian development stage VI-VII). The intersex gonad composed of both developing ovary and developing testis tissues. In the intersex gonad, the oocytes were usually found at the innermost area of cortex, some of them showed abnormal characters indicating degeneration. The testicular tissue was found at the outermost area of the cortex which composed of meiocytes and primary oogonia and cysts (testicular development stage iv). The study of steroidogenic potential in the gonad tissues was grouped as 1-3 weeks after metamorphosis because the gonad at this period could not be distinguished as intersex by their morphology. This group was in the phase of developing ovary (ovarian development stage VIII-IX) that numerous diplotene oocytes presented surrounding by a number of flattened follicular cells. The expression of *CYP17* and *CYP19* mRNA were slightly elevated. The levels of *CYP17* and *CYP19* mRNA expression were significantly higher than those of stages 25-35 (group of the indifferent gonad) and stage 36-41 (group of the early developing ovary). This may be because at 1-3 weeks old, follicular cells of the ovary were well developed and may produce high level of *CYP19* mRNA. Also, a number of Leydig cells in the intersex gonad were found to be active and may produce high level of *CYP17* mRNA.

Moreover, the higher level of *CYP17* mRNA may be due to some individual gonad began to develop into testis and this sampling group may have a high ratio of male frogs. It could be implied that the age of 1-3 weeks after metamorphosis was the onset of male sex differentiation in *H. rugulosus*.

The gonadal morphology can be distinguished into testis and ovary at 3–4 weeks after metamorphosis. At 4 weeks after metamorphosis, *H. rugulosus* gonads were separated into 3 groups including ovary, intersex gonad, and testis. The ovary reached at fully developed stage (ovarian development stage X). The testis consisted of developing seminiferous cords, and interstitial tissues (testicular development stage vii-viii). The intersex gonad consisted of developing testicular tissue at the same stage as the testis, some diplotene oocytes and degenerating oocytes were found at the innermost layer of the cortex. The fully developed testis was first identified at 6 weeks after metamorphosis. The result from this study suggested that testicular differentiation occurred via an intersex condition. The steroidogenic potential of gonad tissue was investigated in froglets at 4-11 weeks after metamorphosis, the sex could be differentiated into 3 groups including male, intersex, and female. Firstly, male group, the testis was at fully developed stage, the tissue composed of spermatogenic cells at every stage. The *CYP17* mRNA expression in this group was significantly elevated while *CYP19* mRNA expressed at a very low level. This maybe because the Leydig cells in the testis were active and transcribed *CYP17* mRNA at a high level. Secondly, intersex group, the gonad composed of both developing testicular tissue and fully developed testicular tissue with diplotene oocytes surrounding by follicular cells. The *CYP17* mRNA expression was high while the expression of *CYP19* was low. It could be implied that even the oocytes and follicular cells were well developed, they may not be fully functional. *CYP19* mRNA may be produced at a low level. Finally, female group, the ovary was fully developed and composed of fully functional follicular cells. *CYP19* mRNA expression of this group was relatively higher than every other groups, whereas *CYP17* mRNA

expressed at a low level. This was because *CYP19* mRNA encodes aromatase enzyme which converts androgens to estrogens (Norris and Carr, 2013). The *CYP19* activity increased after the ovary was fully developed with highly active follicular cells.

In addition, the hybridization signals of *CYP17* were detected in Leydig cells of testicular tissue in both intersex and testis groups since 4-5 weeks after metamorphosis until 16 weeks after metamorphosis. Therefore, it indicates that the steroidogenic functions of testicular tissue may start when the froglets are at the age of 4 weeks after metamorphosis, the first period that the testis could be identified by morphology and histology. They were at the testicular development stage viii which spermatogenesis began and the amount of interstitial tissue increases, however, testis-ova may be present.

The pattern of gonadal sex differentiation of *H. rugulosus* exhibited an undifferentiated type, in which the indifferent gonads develop into ovaries during metamorphosis. Testicular development occurs later, after the intersex gonads have differentiated. Comparing the times of gonadal differentiation and somatic development, it revealed that the testicular development exhibited a retarded rate (Traijitt et al., 2020). In anurans, the sex differentiation mostly occurred during metamorphosis while in *H. rugulosus* it occurred at 1 week after metamorphosis (33-41 days or 6 weeks after fertilization). It might be because *H. rugulosus* had a rapid rate of somatic development. At this point, comparing the rate of testicular differentiation with the tadpole age may be reasonable. The gonadal sex differentiation period in most anuran species occurred when tadpoles age is about 6 weeks (42 days) after fertilization (Ogielska, 2009), which is corresponded to the result in *H. rugulosus*. During the testicular development in *H. rugulosus*, intersex character and testes-ova were found until 16 weeks after metamorphosis. This finding correlated with a previous study in which the testis-ovum presented in the normal testis of 3-month-old frog (Sretarugsa et al., 1997). Therefore, the intersex

character (testis containing testis-ovum) is a normal character that can be found during testicular development of *H. rugulosus*.

Conclusion

In conclusion, this is the first study about somatic and gonadal development of *H. rugulosus* (bred type) under controlled laboratory conditions and demonstrates crucial evidence of gonadal sex differentiation pattern of *H. rugulosus*. The gonad developed primarily from the ovarian differentiation process then the testis developed from the intersex gonad. This study confirmed that the role of CYP17 and CYP19 in sex differentiation in *H. rugulosus* occurred after the gonadal sex differentiation and the steroidogenic potential of the gonads exhibited sexual dimorphic pattern. The important evidences in histological changes and steroidogenic potential were purposed as the ovarian and testicular development processes as follow:

1. Ovarian development process in *H. rugulosus* (Figure 6.2)

After the genital ridge formation (stages 25-26; 1-3 dph) and development of the indifferent gonad (stages 27-35; 3-15 dph), the ovarian differentiation began at stage 36 (13-17 dph) which could be identified by the presence of ovarian cavity and primary oogonia. At stage 42 (20-26 dph) the developing ovary increased in size and diplotene oocyte surrounding with follicular cells was firstly presented. Until complete metamorphosis (stage 46; 25-33 dph), the ovary composed of numerous diplotene oocytes surrounding with flattened follicular cells. The expression of both CYP17 and CYP19 mRNA during stages 25-46 was at low level. However, the level of CYP17 mRNA was slightly increased since stages 42-46 and may involve with the synthesis of precursors for androgen and estrogen production. At 1-3 weeks after complete metamorphosis, the ovary composed of numerous diplotene oocytes surrounding with follicular cells. The expression of CYP17 and CYP19 mRNA were slightly elevated. In this period, follicular cells may play roles in producing sex steroid hormones, especially estrogen. The ovary reached at fully developed stage since 4 weeks after metamorphosis. The ovary composed mostly of diplotene

oocytes surrounding with follicular cells. Some follicular cells were active and the expression level of *CYP19* mRNA was very high. This may indicate that at the period of fully developed ovary (4-11 weeks after metamorphosis), the high level of *CYP19* mRNA involved with *CYP19* enzyme (aromatase) and estrogen synthesis, and may correlate with the oogenesis and maintenance of the ovarian structure. The level of *CYP17* mRNA was also increased, possibly for providing androgen as a precursor for estrogen synthesis.



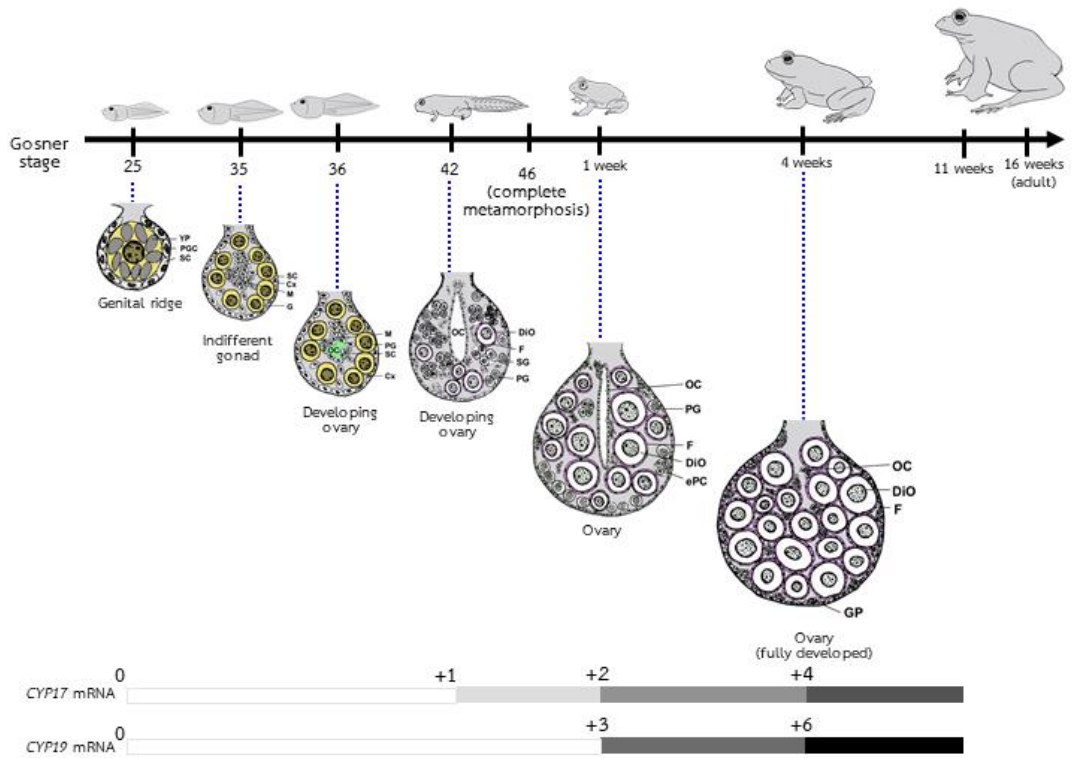


Figure 6.2 Schematic representation of ovarian development in *H. rugulosus* showing the developmental period with important histological evidences. *Stage 25, the genital ridge*: PGC with yolk platelet inside cytoplasm (yellow labeled cell). *Stage 35, the indifferent gonad*: numerous gonocytes (yellow labeled cells) in the cortex. *Stage 36, the developing ovary*: ovarian cavity formation (green labeled area). *Stage 42, the developing ovary*: diplotene oocytes surrounding by follicular cells (pink labeled cells). *One week after metamorphosis, ovary*: numerous diplotene oocytes and follicular cells (pink labeled cells). *Four weeks after metamorphosis, fully developed ovary*: mostly diplotene oocytes surrounding by follicular cells (pink labeled cells). The expression of *CYP17* and *CYP19* mRNA were represented as shaded bars at the bottom of figure. The score of gradient shade in the bar corresponded to the results in figure 5.21, 5.22. and Table 5.3 Cx: cortex, DiO: diplotene oocyte, ePC: early primary oocyte (leptotene-pachytene), F: follicle, G: gonocyte, GP: germ patch, M: medulla, OC: ovarian cavity, PG: primary oogonia, PGC: primordial germ cell, SC: somatic cell, SG: cyst with secondary oogonia, YP: yolk platelet.

2. Testicular development process in *H. rugulosus* (Figure 6.3)

The testicular development occurred through the process of intersex gonad formation. At 1-3 weeks after metamorphosis, some intersex gonads were found as the combined characteristics of the ovarian tissue at the innermost area and testicular tissue at the outermost area of the gonad. The ovarian tissue composed of diplotene oocytes and degenerating oocytes. The testicular tissue composed of cysts of spermatogonium which will develop into sex cords and, eventually, seminiferous tubules. At this period, the expression of *CYP17* and *CYP19* mRNA were slightly elevated. The level of *CYP19* mRNA was high, possibly due to the function of follicular cells in ovarian tissues. While the level of *CYP17* mRNA was high, possibly due to functions of both follicular cells and interstitial tissues for production of precursors of steroid hormones. The testicular tissues developed continuously until 6 weeks after metamorphosis. The seminiferous tubules composed of spermatogenic cells at every stage were found. The intersex condition was still found in some individuals until 16 weeks after metamorphosis. Some of the diplotene oocytes (testis-ovum) in the intersex gonad were degenerated. The expression level of *CYP17* mRNA during 4-11 weeks was high in the intersex group and very high in the male group. This may be because of the high level of androgen synthesis in the testicular tissues. The expression level of *CYP19* mRNA was decreased, possibly due to the fact that some of androgen were not further processed through the step of estrogen synthesis. Therefore, at this point, androgens may be presented at high level for stimulating spermatogenesis and maintenance of the testicular structure.

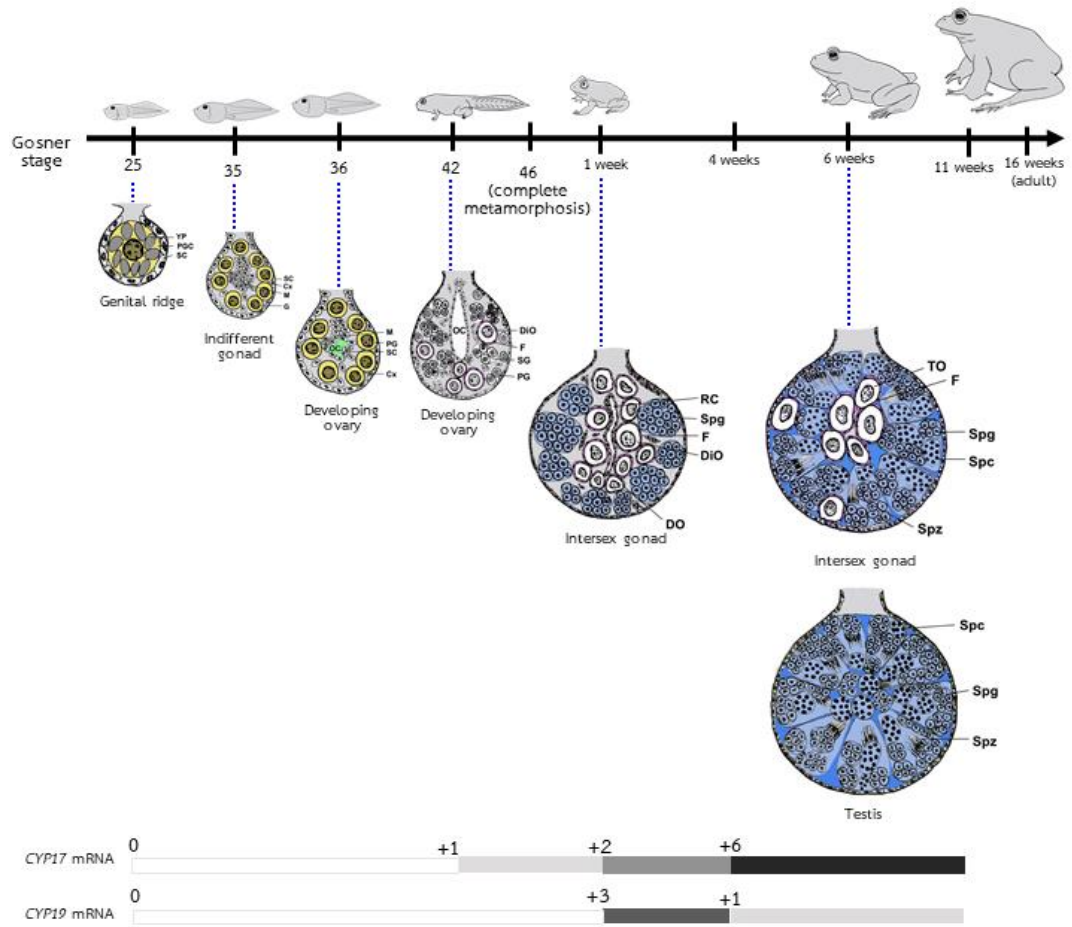


Figure 6.3 Schematic representation of testicular development in *H. rugulosus* showing the developmental period with important histological evidences. *Stage 25, the genital ridge*: PGC with yolk platelet inside cytoplasm (yellow labeled cell). *Stage 35, the indifferent gonad*: numerous gonocytes (yellow labeled cells) in the cortex. *Stage 36, the developing ovary*: ovarian cavity formation (green labeled area). *Stage 42, the developing ovary*: diplotene oocytes surrounding by follicular cells (pink labeled cells). *One week after metamorphosis, 1) intersex gonad*: group of spermatogonia at the outermost area (blue labeled area) and diplotene oocytes and degenerating oocyte at the innermost area. Six weeks after metamorphosis, intersex: seminiferous tubule containing spermatogonia, and spermatozoa at the outermost area (blue labeled area) and testis-ova at the innermost area, *2) testis*: seminiferous tubule containing spermatogonia, spermatocytes, and spermatozoa. The expression of *CYP17* and *CYP19* mRNA were represented as shaded bar at the bottom of figure. The score of gradient shade in the bar corresponded to the results in figure 5.21, 5.22. and Table 5.3. The *CYP17* mRNA was highly expressed since 4 weeks after metamorphosis and localized in the interstitial tissue of the testis and intersex gonad (dark blue labeled area). Cx: cortex, DiO: diplotene oocyte, DO: degenerating oocyte, F: follicle, G: gonocyte, M: medulla, OC: ovarian cavity, PG: primary oogonia, PGC: primordial germ cell, RC: regressed cavity, SC: somatic cell, SG: cyst with secondary oogonia, Spg: spermatogonia, Spc: spermatocyte, Spz: spermatozoa, TO: testis-ovum, YP: yolk platelet.



จุฬาลงกรณ์มหาวิทยาลัย
CHULALONGKORN UNIVERSITY

Recommendations

1. This study presented an overview of chronology and characteristics of somatic and gonadal development in *H. rugulosus*. It could be used as a crucial basic information to investigate abnormalities in their metamorphosis and organ development. All information in this study was obtained from the laboratory condition with natural light (12L: 12D) and temperature (27.5–28.1°C). It should be noted that some anuran species have plasticity in their development. So, the study in the different experimental conditions may possibly provide different somatic and gonadal development rate (Alvarez and Nicieza, 2002; Flament, 2016).
2. The abnormalities in development of reproductive organs of amphibians has been used as a biomarker in the assessment of endocrine disrupting effects for a long time. Since some amphibians have plasticity of gonadal development, several studies reported that abnormalities of gonad development, intersexes, and sex-reversed individuals are a results of endocrine disruptor treatment. Therefore, the knowledge of normal development of gonads is crucial in these kinds of studies. This study showed that the occurrence of the intersex character in *H. rugulosus* is an intermediate condition of testicular development, not the developmental anomaly. It raised concern on the validity of using the intersex condition as a biomarker for ecotoxicological research that should be further examined.
3. The knowledge of the sex transformation through the intersex condition in this species may lead to further research on studying the window of a sensitive period of sex differentiation. In this study, stage 42 to 1-3 weeks after metamorphosis has the potential to be a sensitive window in sex differentiation. Specific responses e.g. sex reversal, might be found when the tadpoles or froglets expose to some extrinsic factors. Hence, a novel protocol for developmental effect of xenobiotic or hormone-like chemical testing could be developed in this species.

4. This study demonstrated the steroidogenic potential in the gonad based on the expression of mRNA of the key enzymes in the steroidogenic pathway. However, the transcription of the mRNA may not always correspond to their translation. Therefore, studying the enzyme (protein) expression is still needed to confirm their activity. The other techniques for detected the protein expression such as fluorescence immunohistochemistry should be further examined. In addition, this study demonstrated the expression of only 2 key enzymes in the steroidogenic pathway. Other key enzymes in the pathway such as *3 β -HSD*, *17- β HSD*, and *5 α Red1* (Nakamura, 2009) should be observed and further examined. The overall results may help to understand the scenario of the steroidogenic activity during the gonadal sex differentiation in this species.
5. The information on sensitive windows may be useful in frog culture for commercial aspects in the future. Since the size of female is larger than male, there are higher market demand for the female. To investigate the factors and sensitive period that suitable for producing higher proportion of female frogs in population and the possibility to maintain the ovary development until they are fully mature are challenging and should be further pursued for agricultural applications.


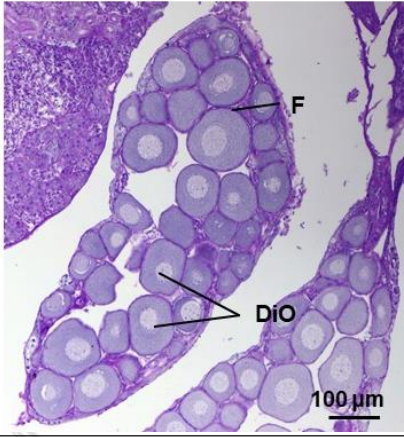

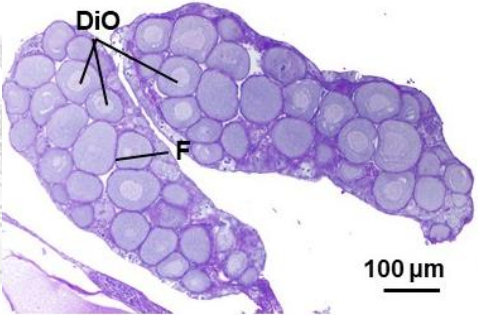

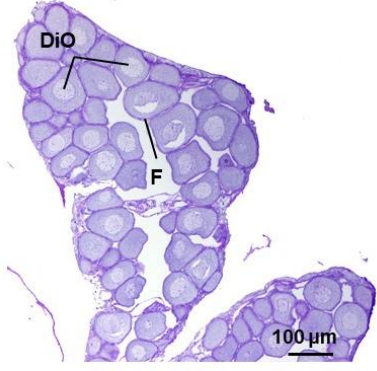



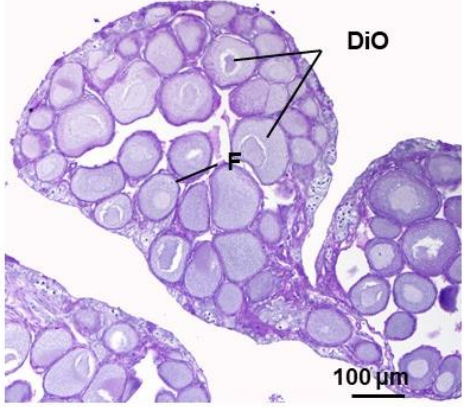
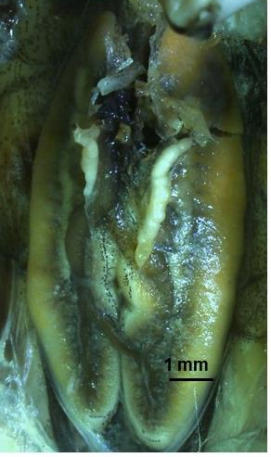
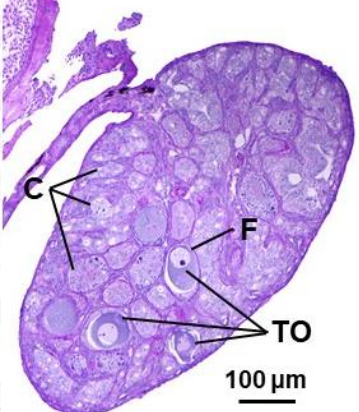

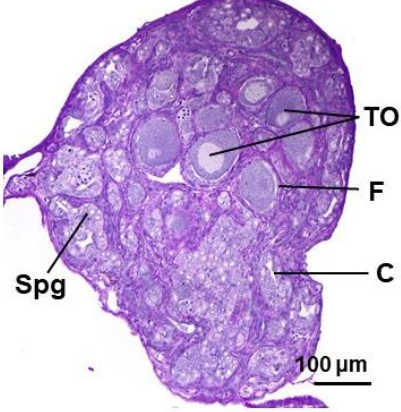
Appendix

Note on morphology and histology of gonad of *H. rugulosus* since the sex differentiation phase

จุฬาลงกรณ์มหาวิทยาลัย
CHULALONGKORN UNIVERSITY

Table 1 Morphological and histological characters of the *H. rugulosus* gonad at 4 weeks after metamorphosis. C: sex cord, DiO: diplotene oocyte, F: follicle, L: Leydig cell, Spg: spermatogonia, ST: seminiferous tubule, TO: testis-ovum

Sample	Morphology	Histology
4week_01		
4week_02		
4week_03		

Sample	Morphology	Histology
4week_04		
4week_05		
4week_06		


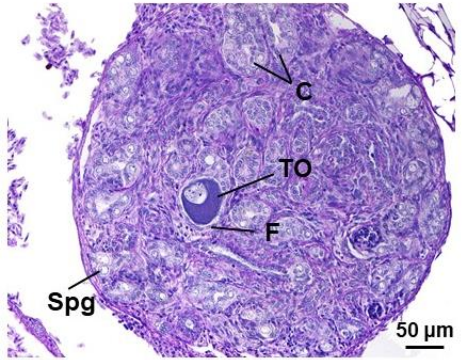

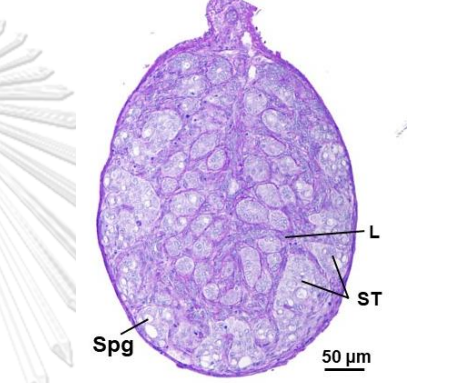

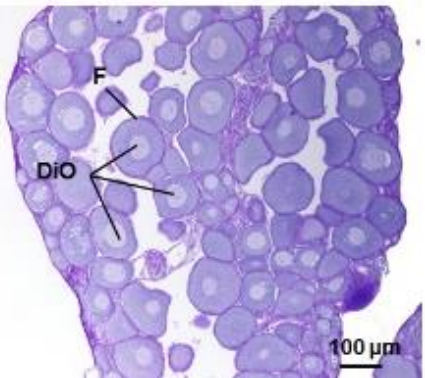

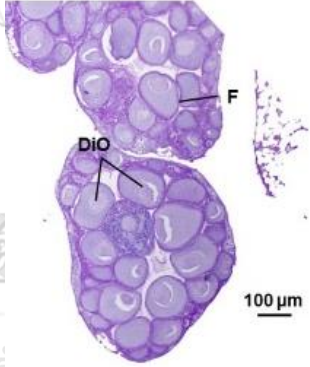

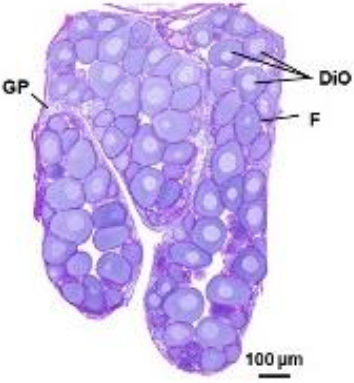

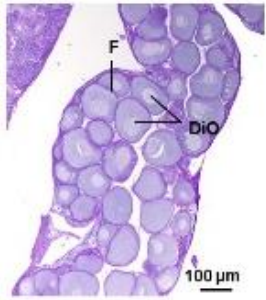

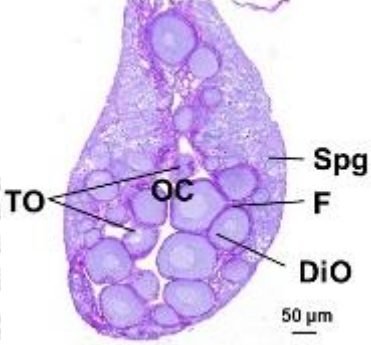

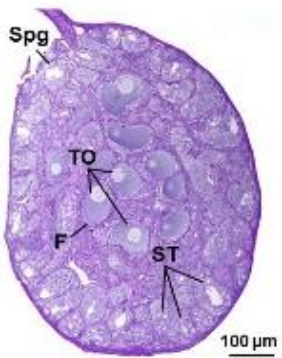

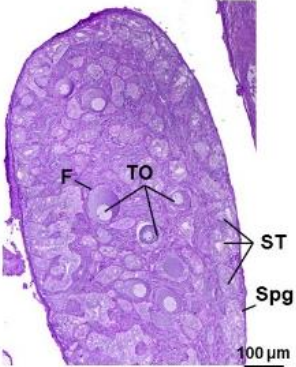

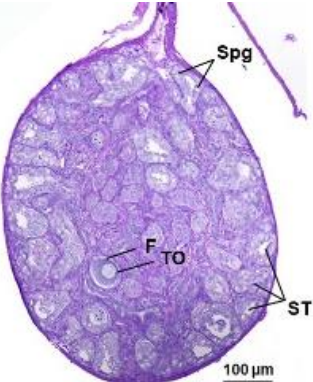

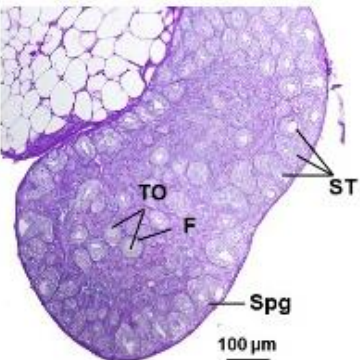
Sample	Morphology	Histology
4week_07		
4week_08		

Table 2 Morphological and histological character of the *H. rugulosus* gonad at 5 weeks after metamorphosis. C: sex cord, DiO: diplotene oocyte, F: follicle, GP: germ patch, L: Leydig cell, OC: ovarian cavity, Spg: spermatogonia, ST: seminiferous tubule, TO: testis-ovum

Sample	Morphology	Histology
5week_01		
5week_02		
5week_03		

Sample	Morphology	Histology
5week_04		
5week_05		
5week_06		

Sample	Morphology	Histology
5week_07		
5week_08		
5week_09		


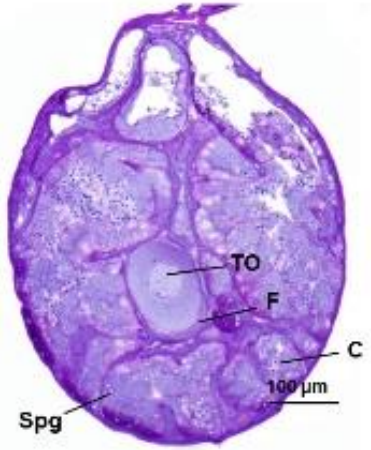

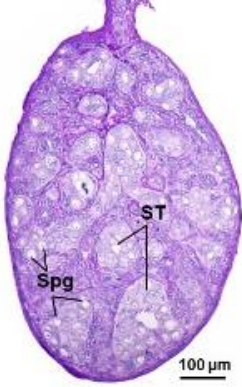

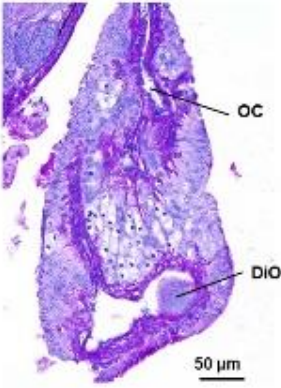

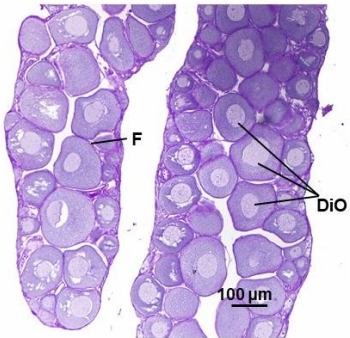

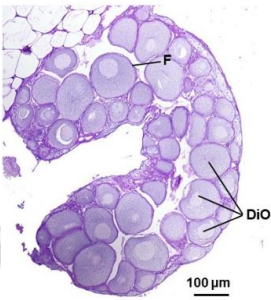



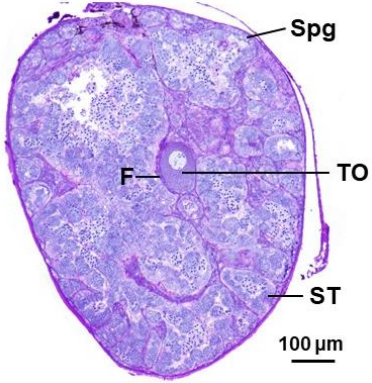

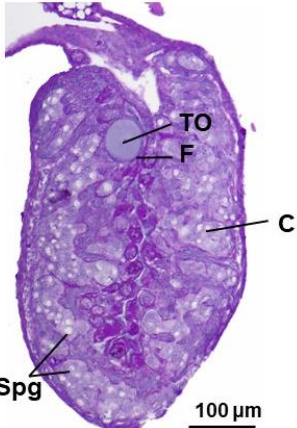

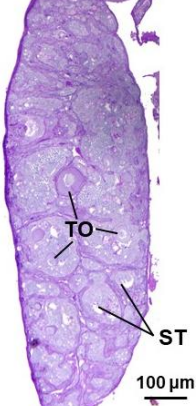
Sample	Morphology	Histology
5week_10		
5week_11		
5week_12		

Table 3 Morphological and histological character of the *H. rugulosus* gonad at 6 weeks after metamorphosis. C: sex cord, DiO: diplotene oocyte, F: follicle, L: Leydig cell, OC: ovarian cavity, RC: regressed cavity, Spc: spermatocyte, Spg: spermatogonium, Spz: spermatozoa, ST: seminiferous tubule, TO: testis-ovum

Sample	Morphology	Histology
6week_01	 A photograph showing the external morphology of the gonad for sample 6week_01. The gonad is elongated and yellowish, with a 1 mm scale bar at the bottom right.	 A histological section of the gonad for sample 6week_01, stained with H&E. It shows several follicles (F) and diplotene oocytes (DiO). A 100 µm scale bar is present at the bottom right.
6week_02	 A photograph showing the external morphology of the gonad for sample 6week_02. The gonad is yellowish and somewhat irregular, with a 1 mm scale bar at the bottom right.	 A histological section of the gonad for sample 6week_02, stained with H&E. It shows follicles (F) and diplotene oocytes (DiO). A 100 µm scale bar is present at the bottom right.
6week_03	 A photograph showing the external morphology of the gonad for sample 6week_03. The gonad is yellowish and elongated, with a 1 mm scale bar at the bottom right.	 A histological section of the gonad for sample 6week_03, stained with H&E. It shows follicles (F) and diplotene oocytes (DiO). A 100 µm scale bar is present at the bottom right.

Sample	Morphology	Histology
6week_04		
6week_05		
6week_06		


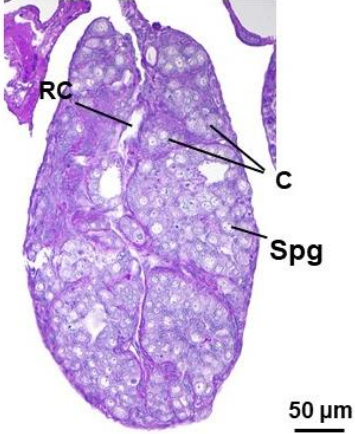

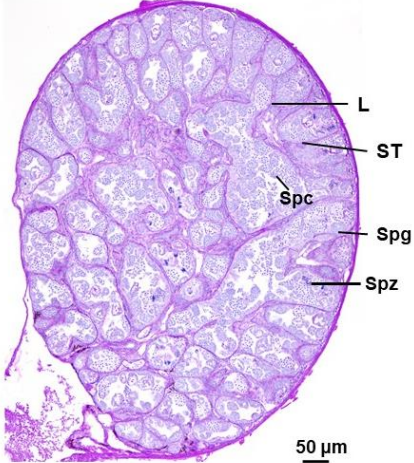

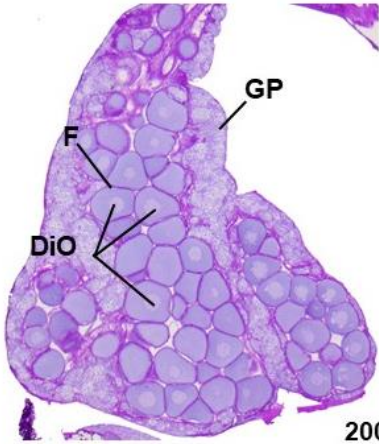

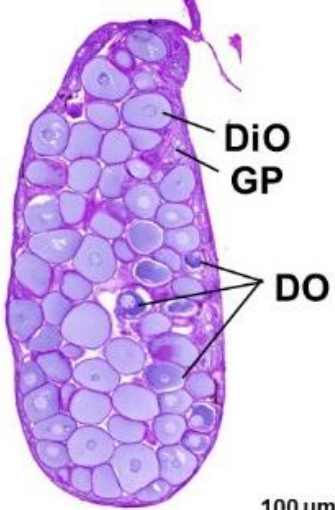

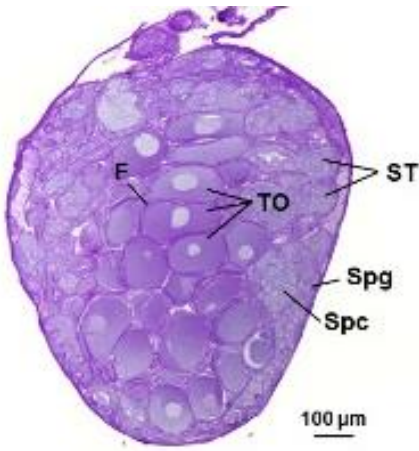

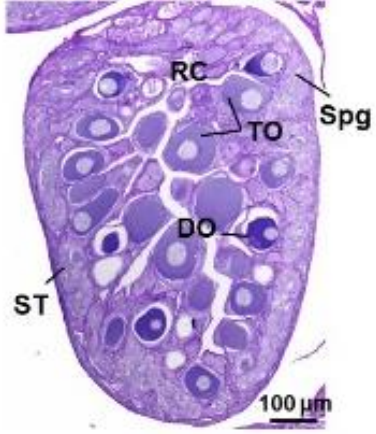

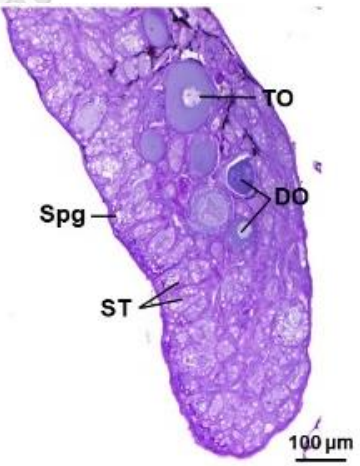

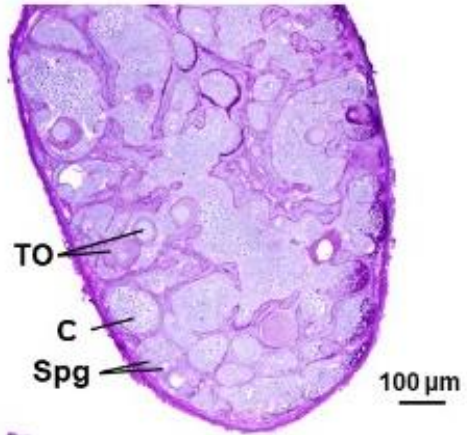

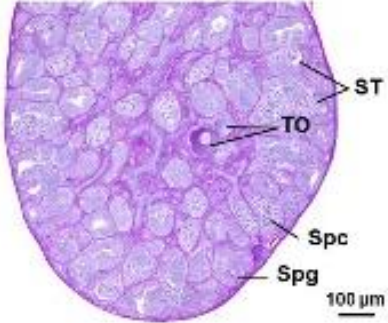

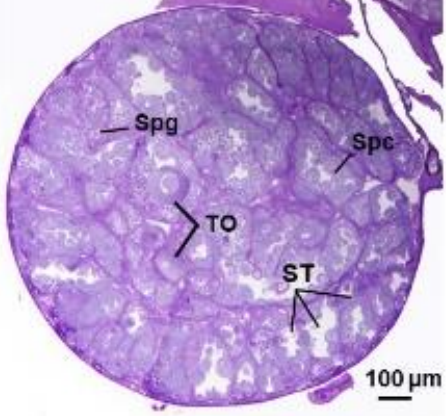

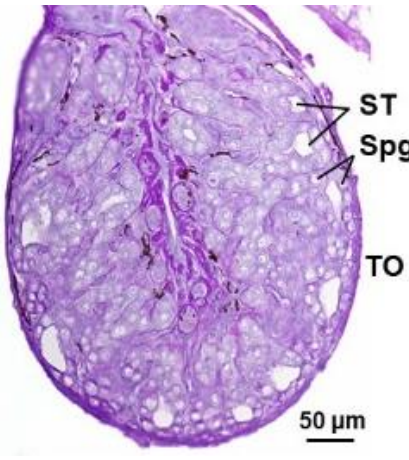

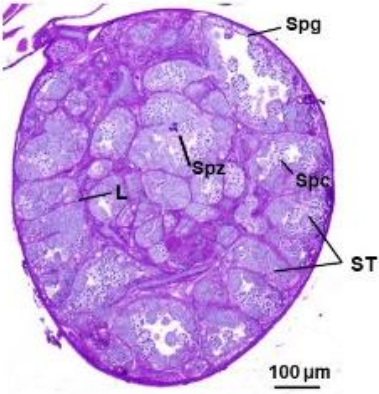
Sample	Morphology	Histology
6week_07		
6week_08		

Table 4 Morphological and histological character of the *H. rugulosus* gonad at 7 weeks after metamorphosis. C: sex cord, DO: degenerating oocyte, DiO: diplotene oocyte, F: follicle, GP: germ patch, L: Leydig cell, OC: ovarian cavity, RC: regressed cavity, Spc: spermatocyte, Spg: spermatogonium, Spz: spermatozoa, ST: seminiferous tubule, TO: testis-ovum

Sample	Morphology	Histology
7week_05		
7week_07		

Sample	Morphology	Histology
7week_08		
7week_09		
7week_10		

Sample	Morphology	Histology
7week_03		
7week_01		
7week_04		

Sample	Morphology	Histology
7week_06	 <p>A photograph showing the external morphology of the 7week_06 sample. It is a yellowish, elongated structure. A scale bar at the bottom right indicates 1 mm.</p>	 <p>A histological section of the 7week_06 sample stained with H&E. The structure is oval-shaped. Labels include ST (Spermatid), Spg (Spermatogonium), and TO (Testis Organ). A scale bar at the bottom right indicates 50 μm.</p>
7week_02	 <p>A photograph showing the external morphology of the 7week_02 sample. It is a yellowish, elongated structure with a more complex internal structure visible. A scale bar at the bottom right indicates 1 mm.</p>	 <p>A histological section of the 7week_02 sample stained with H&E. The structure is oval-shaped. Labels include Spg (Spermatogonium), Spz (Spermatid), Spc (Spermatocyte), and ST (Spermatid). A scale bar at the bottom right indicates 100 μm.</p>

REFERENCES

- Altig, R., and McDiarmid, R.W. 1999. Body plan: development and morphology. In McDiarmid, R.W. and Altig, R. (Eds.), Tadpole: The Biology of Anuran Larvae, pp. 24-51. Chicago, USA: University of Chicago Press.
- Altig, R., and McDiarmid, R.W. 2007. Morphological diversity and evolution of egg and clutch structure in amphibians. Herpetological Monographs 21: 1-32.
- Alvarez, D., and Nicieza, A. 2002. Effects of temperature and food quality on anuran larval growth and metamorphosis. Functional Ecology 16: 640-648.
- Aneesh, P.T., Sudha, K., Helna, A.K., and Anilkumar, G. 2018. *Agarna malayi* Tiwari 1952 (Crustacea: Isopoda: Cymothoidae) parasitising the marine fish, *Tenualosa toli* (Clupeidae) from India: re-description/description of parasite life cycle and patterns of occurrence. Zoological Studies 57: e25. doi: 10.6620/ZS.2018.57-25.
- Aran, S., Chuaynkern, C., Duengjai, S., and Chuaynkern, Y. 2012. Morphology of some tadpoles in Khon Kaen University, Khon Kaen Province. Journal of Wildlife in Thailand 19: 41-73.
- Bain, R.H., and Truong, N.Q. 2004. Herpetofaunal diversity of Ha Giang Province in northeastern Vietnam, with descriptions of two new species. American Museum Novitates 2004: 1-42.
- Banerjee, S.N., and Chakrabarti, S. 2003. Chromosomal sex determination in anuran amphibians. Hamadryad-Madras 27: 248-253.
- Bernardo, J. 1996. The particular maternal effect of propagule size, especially egg size: patterns, models, quality of evidence and interpretations. American Zoologist 36: 216-236.
- Burcea, A., Popa, G.O., Maereanu, M., Dudu, A., Georgescu, S.E., and Costache, M. 2018.

- Expression characterization of six genes possibly involved in gonad development for stellate sturgeon individuals (*Acipenser stellatus*, Pallas 1771). International Journal of Genomics 2018: 7835637. doi: 10.1155/2018/7835637.
- Burggren, W.W., and Warburton, S. 2007. Amphibians as animal models for laboratory research in physiology. ILAR Journal 48: 260-269.
- Burlibaşa, L., and Gavrilă, L. 2011. Amphibians as model organisms for study environmental genotoxicity. Applied Ecology and Environmental Research 9: 1-15.
- Calsbeek, R., and Kuchta, S. 2011. Predator mediated selection and the impact of developmental stage on viability in wood frog tadpoles (*Rana sylvatica*). BMC Evolutionary Biology 11: 353. doi: 10.1186/1471-2148-11-353.
- Chakravarty, P., Bordoloi, S., Grosjean, S., Ohler, A., and Borkotoki, A. 2011. Tadpole morphology and table of developmental stages of *Polypedates teraiensis* (Dubois, 1987). Alytes 27: 85-115.
- Chan-ard, T. 2003. A Photographic Guide to Amphibians in Thailand. Vol. 30. Bangkok, Thailand: Darnsutha Press.
- Chi, M., Ni, M., Jia, Y., Gu, Z., and Wen, H. 2019. Isolation of CYP17 I, 3 β -HSD and AR genes from Spotted sea bass (*Lateolabrax maculatus*) testis and their responses to hormones and salinity stimulations. Journal of Ocean University of China 18: 420-430.
- Chockchaichomnankit, P., Chulalaksananukul, W., and Pariyanonth, P. 2001. Sex chromosome identification of the frog *Rana rugulosa* by chromosome banding techniques. Proceedings of 5th BRT Annual Conference, Udon Thani, Thailand: 236.
- Del Pino, E.M., Avila, M.E., Perez, O.D., Benitez, M.S., Alarcon, I., Noboa, V., and Moya, I.M. 2004. Development of the dendrobatid frog *Colostethus machalilla*.

International Journal of Developmental Biology 48: 663-670.

- Diesmos, A., Van Dijk, P., Inger, R., Iskandar, D., Wai Neng Lau, M., Ermi, Z., Shunqing, L., Baorong, G., Kuangyang, L., and Zhigang, Y. 2004. *Hoplobatrachus rugulosus*. The IUCN Red List of Threatened Species [Online]. 2004: e.T58300A11760194. Available from: <https://dx.doi.org/10.2305/IUCN.UK.2004.RLTS.T58300A11760194.en>. [21 December 2020]
- Ding, G.H., Lin, Z.H., Fan, X.L., and Ji, X. 2015. The combined effects of food supply and larval density on survival, growth and metamorphosis of Chinese tiger frog (*Hoplobatrachus rugulosus*) tadpoles. Aquaculture 435: 398-402.
- Do Rego, J.L., Tremblay, Y., Luu The, V., Repetto, E., Castel, H., Vallarino, M., Bélanger, A., Pelletier, G., and Vaudry, H. 2007. Immunohistochemical localization and biological activity of the steroidogenic enzyme cytochrome P450 17 α -hydroxylase/C17, 20-lyase (P450C17) in the frog brain and pituitary. Journal of Neurochemistry 100: 251-268.
- Donsakul, T. 2009. Karyotype from liver cells of seven amphibians (Amphibia, Anura) from Thailand. Journal of Science and Technology Mahasarakham University 28: 162-170.
- Duarte, G.P., Langlois, V., Hodgkinson, K., Pauli, B., Cooke, G., Wade, M., and Trudeau, V. 2009. The aromatase inhibitor fadrozole and the 5-reductase inhibitor finasteride affect gonadal differentiation and gene expression in the frog *Silurana tropicalis*. Sexual Development 3: 333-341.
- Duellman, W., and Trueb, L. 1994. Biology of Amphibians. Baltimore, USA: The Johns Hopkins University Press.
- Eggert, C. 2004. Sex determination: the amphibian models. Reproduction Nutrition Development 44: 539-549.

- Flament, S. 2016. Sex reversal in amphibians. Sexual Development 10: 267-278.
- Flower, S. 1899. Notes on a second collection of batrachians made in the Malay Peninsula and Siam from November 1896 to September 1898, with a list of the species recorded from these countries. Proceedings of the Zoological Society of London: 885-916.
- Freking, F., Nazairians, T., and Schlinger, B.A. 2000. The expression of the sex steroid-synthesizing enzymes CYP11A1, 3 β -HSD, CYP17, and CYP19 in gonads and adrenals of adult and developing zebra finches. General and Comparative Endocrinology 119: 140-151.
- Frost, D.R., Grant, T., Faivovich, J., Bain, R.H., Haas, A., Haddad, C.F., De Sa, R.O., Channing, A., Wilkinson, M., and Donnellan, S.C. 2006. The amphibian tree of life. Bulletin of the American Museum of Natural History 2006: 1-291.
- Fujii, J., Kodama, M., Oike, A., Matsuo, Y., Min, M.-S., Hasebe, T., Ishizuya-Oka, A., Kawakami, K., and Nakamura, M. 2014. Involvement of androgen receptor in sex determination in an amphibian species. PLoS One 9: e93655. doi: 10.1371/journal.pone.0093655.
- Goldberg, J. 2015. Gonadal differentiation and development in the snouted treefrog, *Scinax fuscovarius* (Amphibia, Anura, Hylidae). Journal of Herpetology 49: 468-478.
- Gomez-Mestre, I., Kulkarni, S., and Buchholz, D.R. 2013. Mechanisms and consequences of developmental acceleration in tadpoles responding to pond drying. PLoS One 8: e84266. doi: 10.1371/journal.pone.0084266.
- Gosner, K.L. 1960. A simplified table for staging anuran embryos and larvae with notes on identification. Herpetologica 16: 183-190.
- Gramapurohit, N., Shanbhag, B., and Saidapur, S. 2000. Pattern of gonadal sex

- differentiation, development, and onset of steroidogenesis in the frog, *Rana curtipes*. General and Comparative Endocrinology 119: 256-264.
- Guiguen, Y., Baroiller, J.F., Ricordel, M.J., Iseki, K., McMeel, O., Martin, S.A.M., and Fostier, A. 1999. Involvement of estrogens in the process of sex differentiation in two fish species: the rainbow trout (*Oncorhynchus mykiss*) and a tilapia (*Oreochromis niloticus*). Molecular Reproduction and Development: Incorporating Gamete Research 54: 154-162.
- Hägström, M., and Richfield, D. 2014. Diagram of the pathways of human steroidogenesis. WikiJournal of Medicine 1. doi: 10.15347/WJM/2014.005.
- Haider, S.G. 1980. Histophysiological effects of an antiandrogen (cyproterone acetate) on the testis of the frog *Rana temporaria*. Cells Tissues Organs 106: 387-391.
- Hasan, M., Kuramoto, M., Islam, M.M., Alam, M.S., Khan, M.M.R., and Sumida, M. 2012. A new species of genus *Hoplobatrachus* (Anura, Dicroglossidae) from the coastal belt of Bangladesh. Zootaxa 3312: 45-58.
- Hayes, T.B. 1998. Sex determination and primary sex differentiation in amphibians: genetic and developmental mechanisms. Journal of Experimental Zoology 281: 373-399.
- Hinfray, N., Baudiffier, D., Leal, M.C., Porcher, J.-M., Ait-Aissa, S., Le Gac, F., Schulz, R.W., and Brion, F. 2011. Characterization of testicular expression of P450 17 α -hydroxylase, 17, 20-lyase in zebrafish and its perturbation by the pharmaceutical fungicide clotrimazole. General and Comparative Endocrinology 174: 309-317.
- Hsü, C.Y., Hsü, L.H., and Liang, H.M. 1979. The effect of cyproterone acetate on the activity of delta 5-3 beta-hydroxysteroid dehydrogenase in tadpole sex transformation. General and Comparative Endocrinology 39: 404-410.
- Isomura, T., Haraguchi, S., Miyamoto, K., Tsutsui, K., Nakamura, Y., and Nakamura, M.

2011. Estrogen biosynthesis in the gonad of the frog *Rana rugosa*. General and Comparative Endocrinology 170: 207-212.
- Iwade, R., Maruo, K., Okada, G., and Nakamura, M. 2008. Elevated expression of P450c17 (CYP17) during testicular formation in the frog. General and Comparative Endocrinology 155: 79-87.
- Iwasawa, H. 1969. Gonadal development in young frogs of *Rana ornativentris*, with special reference to sex differentiation and sex ratio. 日本動物学彙報 42: 183-192.
- Kakampuy, W., and Supanuam, P. 2018. Karyotype, standardized idiogram and meiotic cell division of rugose frog (*Hoplobatrachus rugulosus*, Dicroglossidae) by conventional staining. Journal of Fisheries Technology Research 12: 31-41.
- Katawutpoonphan, K. 2008. Effects of atrazine on the early development and gonad development of rice field frog *Hoplobatrachus rugulosus* (Wiegmann, 1834). Master's Thesis, Department of Biology, Faculty of Science, Chulalongkorn University.
- Kato, T., Matsui, K., Takase, M., Kobayashi, M., and Nakamura, M. 2004. Expression of P450 aromatase protein in developing and in sex-reversed gonads of the XX/XY type of the frog *Rana rugosa*. General and Comparative Endocrinology 137: 227-236.
- Kelley, D.B. 1996. The biology of *Xenopus*: Sexual differentiation in *Xenopus laevis*. In Tinsley, R.C. and Kobel, H.R. (Eds.), Symposia of the Zoological Society of London: 143.
- Khonsue, W., and Thirakhupt, K. 2001. A checklist of the amphibians in Thailand. Tropical Natural History 1: 69-82.
- Kiernan, J.A. 1999. Histological and Histochemical Methods: Theory and Practice. 3rd ed. Oxford, UK: Butterworth Heinemann.

- Kottarathil, H.A., and Kappalli, S. 2019. Reproductive system in the male phase of a parasitic isopod (crustacea)—morphological, histological and ultrastructural evidence for sequential protandrous hermaphroditic changes. Zoological Studies 58: e4. doi: 10.6620/ZS.2019.58-04.
- Liamtong, S., Saenphet, K., Chaiyapo, M., and Saenphet, S. 2019. Effect of water temperature on growth, survival and health status of East Asian Bullfrog (*Hoplobatrachus rugulosus*) larvae. Proceedings of International Conference on Biodiversity: 55-61.
- Limbaugh, B.A., and Volpe, E.P. 1957. Early Development of the Gulf Coast Toad, *Bufo valliceps* Wiegmann. New York, USA: American Museum of Natural History.
- Ling, F., Qiping, H., and Qinghua, L. 1998. The karyotype of *Rana tigrina rugulosa* Wiegmann. Journal of Guangxi Medical University 2. doi: CNKI:SUN: GXYD.0.1998-02-006.
- Liu, Y., Yao, Z.-X., Bendavid, C., Borgmeyer, C., Han, Z., Cavalli, L.R., Chan, W.-Y., Folmer, J., Zirkin, B.R., and Haddad, B.R. 2005. Haploinsufficiency of cytochrome P450 17 α -hydroxylase/17, 20 lyase (CYP17) causes infertility in male mice. Molecular Endocrinology 19: 2380-2389.
- Lopez, K. 1989. Sex differentiation and early gonadal development in *Bombina orientalis* (Anura: Discoglossidae). Journal of Morphology 199: 299-311.
- Manthey, U., and Grossmann, W. 1997. Amphibien & Reptilien Südostasiens. Münster, Germany: Natur und Tier Verlag.
- Maruo, K., Suda, M., Yokoyama, S., Oshima, Y., and Nakamura, M. 2008. Steroidogenic gene expression during sex determination in the frog *Rana rugosa*. General and Comparative Endocrinology 158: 87-94.
- Mawaribuchi, S., Ikeda, N., Fujitani, K., Ito, Y., Onuma, Y., Komiya, T., Takamatsu, N., and

- Ito, M. 2014. Cell-mass structures expressing the aromatase gene *Cyp19a1* lead to ovarian cavities in *Xenopus laevis*. *Endocrinology* 155: 3996-4005.
- Mayer, L.P., Overstreet, S.L., Dyer, C.A., and Propper, C.R. 2002. Sexually dimorphic expression of steroidogenic factor 1 (SF-1) in developing gonads of the American bullfrog, *Rana catesbeiana*. *General and Comparative Endocrinology* 127: 40-47.
- Miyata, S., and Kubo, T. 2000. In vitro effects of estradiol and aromatase inhibitor treatment on sex differentiation in *Xenopus laevis* gonads. *General and Comparative Endocrinology* 119: 105-110.
- Nakamura, M. 2009. Sex determination in amphibians. *Seminars in Cell & Developmental Biology* 20: 271-282.
- Nakamura, M. 2010. The mechanism of sex determination in vertebrates—are sex steroids the key-factor? *Journal of Experimental Zoology Part A: Ecological Genetics and Physiology* 313: 381-398.
- Nakamura, M. 2013. Is a sex-determining gene (s) necessary for sex-determination in amphibians? Steroid hormones may be the key factor. *Sexual Development* 7: 104-114.
- Nakkrasae, L.i., Phummisutthigoon, S., and Charoenphandhu, N. 2016. Low salinity increases survival, body weight and development in tadpoles of the Chinese edible frog *Hoplobatrachus rugulosus*. *Aquaculture Research* 47: 3109-3118.
- Narzary, J., and Bordoloi, S. 2013. Study of normal development and external morphology of tadpoles of *Microhyla ornata* and *Uperodon globulosus* of the family Microhylidae (Amphibia: Anura) from North East India. *International Journal of Advanced Biological and Biomedical Research* 3: 61-73.
- Navarro-Martín, L., Velasco-Santamaría, Y., Duarte-Guterman, P., Robertson, C., Lanctôt, C., Pauli, B., and Trudeau, V.L. 2012. Sexing frogs by real-time PCR: using aromatase (*cyp19*) as an early ovarian differentiation marker. *Sexual*

Development 6: 303-315.

- Nieuwkoop, P., and Faber, J. 1967. Normal Table of *Xenopus laevis* (Daudin): A Systematic and Chronological Survey of the Development from the Fertilized Egg till the End of Metamorphosis. Amsterdam, Netherlands: North-Holland.
- Nishioka, M., and Hanada, H. 1994. Sex of reciprocal hybrids between the Hamakita (XX-XY type) population and the Murakami (ZW-ZZ type) population of *Rana rugosa*. Scientific Report of the Laboratory for Amphibian Biology 13: 35-50.
- Norris, D.O., and Carr, J.A. 2013. Vertebrate Endocrinology. London, UK: Academic Press.
- Ogielska, M. 2009. Reproduction of Amphibians. Vol. 4. Enfield, USA: Science Publishers.
- Ogielska, M., and Kotusz, A. 2004. Pattern and rate of ovary differentiation with reference to somatic development in anuran amphibians. Journal of Morphology 259: 41-54.
- Ogielska, M., and Wagner, E. 1990. Oogenesis and development of the ovary in European green frog, *Rana ridibunda* (Pallas). I, Tadpole stages until metamorphosis. Zoologische Jahrbücher. Abteilung für Anatomie und Ontogenie der Tiere 120: 211-221.
- Pansook, A., Khonsue, W., Piyapattanakorn, S., and Pariyanonth, P. 2012. Phylogenetic relationships among *Hoplobatrachus rugulosus* in Thailand as inferred from mitochondrial DNA sequences of the cytochrome-b gene (Amphibia, Anura, Dicroglossidae). Zoological Science 29: 54-59.
- Pariyanonth, P., Chanpong, N., Watanasermkit, K., Meakwichai, V. and Rasmitta, A. 1985. Complete cycle of frog-farming. The Journal of Scientific Research Chulalongkorn University 1: 46-55.
- Pewphong, R., Kitana, J., and Kitana, N. 2020. Chronology of gonadal development in the Malayan snail-eating turtle *Malayemys macrocephala*. Zoological Studies

59: 16. doi: 10.6620/ZS.2020.59-20.

- Pfalzgraff, T., Hirschfeld, M., Barej, M.F., Dahmen, M., Gonwouo, L.N., Doherty-Bone, T.M., and Roedel, M.-O. 2015. The tadpoles of four Central Africa *Phrynobatrachus* species. *Salamandra* 51: 91-102.
- Phuge, S.K., and Gramapurohit, N.P. 2013. Gonadal sex differentiation, development up to sexual maturity and steroidogenesis in the skipper frog, *Euphlyctis cyanophlyctis*. *General and Comparative Endocrinology* 181: 65-71.
- Pinto Erazo, M.A., Goldberg, F.J., and Jerez, A. 2016. Gonadal development in the Neotropical high Andean frog *Dendropsophus labialis* (Amphibia: Hylidae). *Asociación Herpetológica Argentina; Cuadernos de Herpetología* 30: 55-68.
- Piprek, R.P., Damulewicz, M., Kloc, M., and Kubiak, J.Z. 2018. Transcriptome analysis identifies genes involved in sex determination and development of *Xenopus laevis* gonads. *Differentiation* 100: 46-56.
- Piprek, R.P., Pecio, A., Kubiak, J.Z., and Szymura, J.M. 2012. Differential effects of testosterone and 17-estradiol on gonadal development in five anuran species. *Reproduction* 144: 257-267.
- Piprek, R.P., Pecio, A., and Szymura, J.M. 2010. Differentiation and development of gonads in the yellow-bellied toad, *Bombina variegata* L., 1758 (Amphibia: Anura: Bombinatoridae). *Zoological Science* 27: 47-55.
- Raghuveer, K., Senthilkumaran, B., Sudhakumari, C., Sridevi, P., Rajakumar, A., Singh, R., Muruganankumar, R., and Majumdar, K. 2011. Dimorphic expression of various transcription factor and steroidogenic enzyme genes during gonadal ontogeny in the air-breathing catfish, *Clarias gariepinus*. *Sexual Development* 5: 213-223.
- Ratanasaeng, P., Chanchao, C., Pariyanonth, P., and Tanpraprutgul, P. 2008. Effects of 17 β -estradiol on liver vitellogenin gene expression in immature female frogs, *Hoplobatrachus rugulosus*. *Science Asia* 34: 377-384.

- Roco, Á.S., Olmstead, A.W., Degitz, S.J., Amano, T., Zimmerman, L.B., and Bullejos, M. 2015. Coexistence of Y, W, and Z sex chromosomes in *Xenopus tropicalis*. Proceedings of the National Academy of Sciences 112: E4752-E4761.
- Ruamthum, W., Visetson, S., Milne, J., and Bullangpoti, V. 2011. Effect of glyphosate-based herbicide on acetylcholinesterase activity in tadpoles, *Hoplobatrachus rugulosus*. Communications in Agricultural and Applied Biological Sciences 76: 923-930.
- Saha, B., and Gupta, B. 2011. The development and metamorphosis of an endangered frog, *Rana leptoglossa* (Cope, 1868). International Journal of Advanced Research 1: 67-76.
- Saidapur, S., Gramapurohit, N., and Shanbhag, B. 2001. Effect of sex steroids on gonadal differentiation and sex reversal in the frog, *Rana curtipes*. General and Comparative Endocrinology 124: 115-123.
- Sailasuta, A., Satetasit, J., and Chutmongkonkul, M. 2011. Pathological study of blood parasites in rice field frogs, *Hoplobatrachus rugulosus* (Wiegmann, 1834). Veterinary Medicine International 2011: 850568. doi: 10.4061/2011/850568.
- Sakurai, N., Maruo, K., Haraguchi, S., Uno, Y., Oshima, Y., Tsutsui, K., Matsuda, Y., Do Rego, J.-L., Pelletier, G., and Vaudry, H. 2008. Immunohistochemical detection and biological activities of CYP17 (P450c17) in the indifferent gonad of the frog *Rana rugosa*. The Journal of Steroid Biochemistry and Molecular Biology 112: 5-12.
- Satetasit, J., Chutmongkonkul, M., and Sailasuta, A. 2009. Blood parasites of the rice field frog, *Hoplobatrachus rugulosus* (Wiegmann, 1835), from Wang Nam Yen district, Sra-Kaew province, Thailand. Proceedings of the 8th Chulalongkorn University Veterinary Annual Conference: 84.
- Sayim, F., and Kaya, U. 2008. Embryonic development of the tree frog, *Hyla arborea*.

Biologia 63: 588-593.

- Schartl, M. 2015. Sex determination by multiple sex chromosomes in *Xenopus tropicalis*. Proceedings of the National Academy of Sciences 112: 10575-10576.
- Scheld, S., Bina Perl, R., Rauhaus, A., Karbe, D., Van der Straeten, K., Hauswaldt, S., Randrianania, R., Gawor, A., Vences, M., and Ziegler, T. 2013. Larval morphology and development of the Malagasy frog *Mantidactylus betsileanus*. Salamandra 49: 186-200.
- Schmalz, T.D., and Zug, G.R. 2002. Observations on geographic variation in the Asian frog, *Hoplobatrachus rugulosus* (Anura: Ranidae). Hamadryad 27: 90-98.
- Schmittgen, T.D., and Livak, K.J. 2008. Analyzing real-time PCR data by the comparative C T method. Nature Protocols 3: 1101-1108.
- Shimizu, S., and Ota, H. 2003. Normal development of *Microhyla ornata*: the first description of the complete embryonic and larval stages for the microhylid frogs (Amphibia: Anura). Current Herpetology 22: 73-90.
- Shirane, T. 1986. A new, early, morphological indication of sex differentiation in Anura, *Rana japonica* and *R. nigromaculata*. Journal of Experimental Zoology 240: 113-118.
- Shumway, W. 1940. Stages in the normal development of *Rana pipiens* I. External form. The Anatomical Record 78: 139-147.
- Simmons, A.M., and Horowitz, S.S. 2007. Plasticity in the auditory system across metamorphosis. In Narins, P.M., Feng, A.S., Fay, R.R., and Popper, A.N. (Eds.), Hearing and Sound Communication in Amphibians, pp. 291-322. New York, USA: Springer.
- Somsueb, P., and Boonyaratpalin, M. 2001. Optimum protein and energy levels for the Thai native frog, *Rana rugulosa* Weigmann. Aquaculture Research 32: 33-38.

- Sretarugsa, P., Nakiem, V., Sobhon, P., Chavadej, J., Kruatrachue, M., and Upatham, E.S. 1997. Structure of the testis of *Rana tigerina* and its changes during development and seasonal variation. Journal of The Science Society of Thailand 23: 75-86.
- Sretarugsa, P., Weerachayanukul, W., Chavadej, J., Kruatrachue, M., and Sobhon, P. 2001. Classification of developing oocytes, ovarian development and seasonal variation in *Rana tigerina*. ScienceAsia 27: 1-14.
- Storrs-Méndez, S.I., and Semlitsch, R.D. 2010. Intersex gonads in frogs: understanding the time course of natural development and role of endocrine disruptors. Journal of Experimental Zoology Part B: Molecular and Developmental Evolution 314: 57-66.
- Swingle, W. 1925. Sex differentiation in the bullfrog (*Rana catesbeiana*). The American Naturalist 59: 154-176.
- Tang, Y., Chen, Z.Q., Lin, Y.F., Chen, J.Y., Ding, G.H., and Ji, X. 2020. The combined effects of temperature and aromatase inhibitor on metamorphosis, growth, locomotion, and sex ratio of tiger frog (*Hoplobatrachus rugulosus*) tadpoles. PeerJ 8: e8834. doi: 10.7717/peerj.8834.
- Tanimura, A., and Iwasawa, H. 1987. Germ cell kinetics in gonadal development in the toad *Bufo japonicus formosus*. Zoological Science 4: 657-664.
- Tanimura, A., and Iwasawa, H. 1989. Origin of somatic cells and histogenesis in the primordial gonad of the Japanese tree frog *Rhacophorus arboreus*. Anatomy and Embryology 180: 165-173.
- Tokur, B., Gürbüz, R.D., and Özyurt, G. 2008. Nutritional composition of frog (*Rana esculanta*) waste meal. Bioresource Technology 99: 1332-1338.
- Trachantong, W., Promya, J., Saenphet, S., and Saenphet, K. 2013. Effects of atrazine

herbicide on metamorphosis and gonadal development of *Hoplobatrachus rugulosus*. Maejo International Journal of Science and Technology 7: 60-71.

Traijitt, T., Khonsue, W., and Kitana, J. 2010. Chronology of gonadal development in rice field frog *Hoplobatrachus rugulosus* embryo. Senior project, Department of Biology, Faculty of Science, Chulalongkorn University.

Traijitt, T., Kitana, N., and Kitana, J. 2020. Pattern of gonadal sex differentiation in the rice field frog *Hoplobatrachus rugulosus* (Anura: Dicroglossidae). Zoological Studies 59: 51. doi: 10.6620/ZS.2020.59-51.

Trueb, L., and Hanken, J. 1992. Skeletal development in *Xenopus laevis* (Anura: Pipidae). Journal of Morphology 214: 1-41.

Tsai, Y.J., Lee, M.F., Chen, C.Y., and Chang, C.F. 2011. Development of gonadal tissue and aromatase function in the protogynous orange-spotted grouper *Epinephelus coioides*. Zoological Studies 50: 693-704.

Vernetti, C.H.M.M., Rodrigues, M.D.N., Gutierrez, H.J.P., Calabuig, C.P., Moreira, C.G.Á., Nlewadim, A.A., and Moreira, H.L.M. 2013. Genes involved in sex determination and the influence of temperature during the sexual differentiation process in fish: a review. African Journal of Biotechnology 12: 2129-2146.

Viertel, B., and Richter, S. 1999. Anatomy: viscera and endocrines. In McDiarmid, R. and Altig, R. (Eds.), Tadpoles: The Biology of Anuran Larvae. Chicago, USA: University of Chicago Press.

Warne, R.W., Crespi, E.J., and Brunner, J.L. 2011. Escape from the pond: stress and developmental responses to ranavirus infection in wood frog tadpoles. Functional Ecology 25: 139-146.

Wei, L., Lin, Z.H., Ma, X.M., Zhao, L.H., and Ma, X.H. 2011. Acoustic characteristics of the tiger frog, *Hoplobatrachus rugulosus*, during the breeding season. Zoological Research 32: 456-460.

- Wei, L., Shao, W., Ding, G., Fan, X., and Lin, Z. 2014. Density but not kinship regulates the growth and developmental traits of Chinese tiger frog (*Hoplobatrachus chinensis*) tadpoles. Asian Herpetological Research 5: 113-118.
- West, J. 2018. Importance of Amphibians: A Synthesis of Their Environmental Functions, Benefits to Humans, and Need for Conservation. BSU Honors Program Theses and Projects, Department of Biological Sciences, Bridgewater State University.
- Witschi, E. 1921. Development of gonads and transformation of sex in the frog. The American Naturalist 55: 529-538.
- Witschi, E. 1929a. Studies on sex differentiation and sex determination in amphibians. I. Development and sexual differentiation of the gonads of *Rana sylvatica*. Journal of Experimental Zoology 52: 235-265.
- Witschi, E. 1929b. Studies on sex differentiation and sex determination in amphibians. III. Rudimentary hermaphroditism and Y chromosome in *Rana temporaria*. Journal of Experimental Zoology 54: 157-223.
- Yang, W.-H., Lutz, L.B., and Hammes, S.R. 2003. *Xenopus laevis* ovarian cyp17 is a highly potent enzyme expressed exclusively in oocytes evidence that oocytes play a critical role in xenopus ovarian androgen production. Journal of Biological Chemistry 278: 9552-9559.
- Yu, D., Zhang, J., Li, P., Zheng, R., and Shao, C. 2015. Do cryptic species exist in *Hoplobatrachus rugulosus*? An examination using four nuclear genes, the Cyt b gene and the complete MT genome. PloS One 10: e0124825. doi: 10.1371/journal.pone.0124825.
- Yu, H., Cheng, H., Guo, Y., Xia, L., and Zhou, R. 2003. Alternative splicing and differential expression of P450c17 (CYP17) in gonads during sex transformation in the rice field eel. Biochemical and Biophysical Research Communications 307: 165-171.

Yu, N.W., Hsu, C.Y., Ku, H.H., Chang, L.T., and Liu, H.W. 1993. Gonadal differentiation and secretions of estradiol and testosterone of the ovaries of *Rana catesbeiana* tadpoles treated with 4-hydroxyandrostenedione. Journal of Experimental Zoology 265: 252-257.

Zaccanti, F., Petrini, S., Rubatta, M.L., Stagni, A.M., and Giorgi, P.P. 1994. Accelerated female differentiation of the gonad by inhibition of steroidogenesis in amphibia. Comparative Biochemistry and Physiology Part A: Physiology 107: 171-179.





จุฬาลงกรณ์มหาวิทยาลัย
CHULALONGKORN UNIVERSITY

VITA

NAME Thrissawan Traijitt

DATE OF BIRTH 16 May 1989

PLACE OF BIRTH Lopburi Province, Thailand

INSTITUTIONS ATTENDED B.Sc. (Biology), Department of Biology, Faculty of Science, Chulalongkorn University, 2010
M.Sc. (Anatomy), Department of Anatomy, Faculty of Medicine Siriraj Hospital, Mahidol University, 2014

HOME ADDRESS 55 Moo 8 Patan Sub-district, Mueang District, Lopburi Province 15000

PUBLICATION JOURNAL ARTICLES:
Traijitt, T., Kitana, N., Kitana, J. 2020. Pattern of gonadal sex differentiation in the rice field frog *Hoplobatrachus rugulosus* (Anura: Dicroglossidae). *Zoological Studies*, 59:51 (2020). [JCR Impact Factor 2019=1.257]
Traijitt, T., Kitana, N., Khonsue, W., Kitana, J. 2020. Chronological changes in somatic development of *Hoplobatrachus rugulosus* (Wiegmann, 1834) (Anura: Dicroglossidae). (submitted to *Tropical Natural History*, SJR Q2)

ABSTRACTS:
Traijitt, T., Kitana, N., Kitana, J. 2015. Chronology of morphological changes during metamorphosis of *Hoplobatrachus rugulosus* embryo. The 5th International Symposium on Asian Vertebrate Species Diversity. December 16-18, 2015, Chulalongkorn University, Bangkok and Saraburi, Thailand. (Poster presentation)
Traijitt, T., Kitana, N., Kitana, J. 2016. Chronology of morphological changes during metamorphosis of *Hoplobatrachus rugulosus* embryo. The 21st Biological science Graduate. December 15-16, 2016, Institute of Biological Science, Malaysia. (Oral presentation)

Traijitt, T., Kitana, N., Nagasawa, K., Osada, M., Kitana, J. 2018. Chronology of gonadal sex differentiation and steroidogenic potential in the rice field frog *Hoplobatrachus rugulosus*. The 8th Intercongress Asian and Oceanic Society for Comparative Endocrinology. July 8-12, 2018, University of Sydney, Sydney, Australia. (Oral presentation)

Traijitt, T., Kitana, N. and Kitana, J. 2018. Chronology of gonadal development in rice field frog *Hoplobatrachus rugulosus*. The 23rd Biological science Graduate. December 18-20, 2018, Chulalongkorn University, Bangkok, Thailand. (Oral presentation)

Traijitt, T., Kitana, N. and Kitana, J. 2019. Anatomical assessment for mode of sex differentiation in the rice field frog *Hoplobatrachus rugulosus* (Anura: Dicroglossidae). The 19th Congress of The International Federation of Associations of Anatomists. August 9-11, 2019, London, The United Kingdom (Poster presentation)

AWARD RECEIVED

2014-2019: The Development and Promotion of Science and Technology Talents Project (DPST)

2019: The 90th Anniversary of Chulalongkorn University
Scholarship from the Graduate School, Chulalongkorn University

2019: Overseas Academic Presentation Scholarship for Graduate Students from the Graduate School, Chulalongkorn University